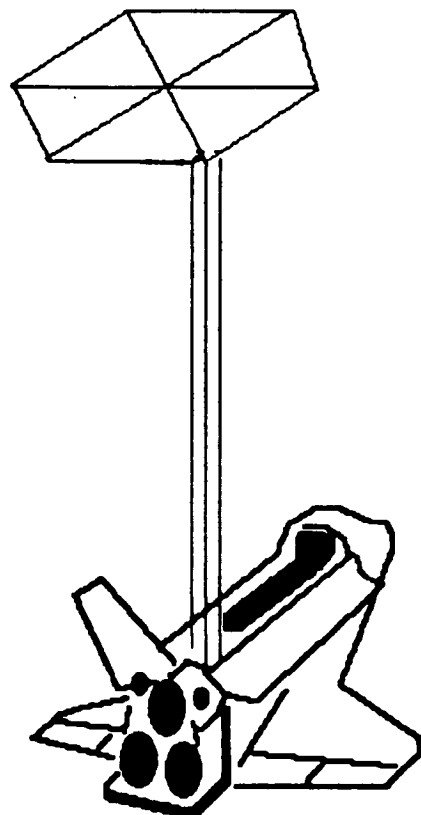


2nd Annual

**SCOLE<sup>\*</sup> Workshop**



**1985**

Proceedings of a Workshop  
Concerning the .....

**NASA  
DESIGN CHALLENGE**

*Held at  
NASA Langley Research Center  
Hampton, Virginia 23665  
December 9-10, 1985*



National Aeronautics and  
Space Administration

Langley Research Center  
Hampton, Virginia 23665

*Compiled by Larry Taylor*

(NASA-TM-89048) PROCEEDINGS OF THE 2ND  
ANNUAL SCOLE WORKSHOP (NASA) 268 p CSCL 22B

N87-10945

G3/18 43975  
Unclass

**\*Spacecraft Control Laboratory Experiment**

**The 2nd Annual SCOLE Workshop**  
at the NASA Langley Research Center, Hampton, Virginia  
Building 1192C, Room 124

**Monday, December 9**

8:30 Welcoming Remarks.....	John Dibattista
8:45 Definition of the SCOLE Design Challenge.....	Larry Taylor
9:00 Panel on Issues in Modeling the SCOLE Configuration.....	A.V. Balakrishnan Peter Bainum Jer-nan Juang Leonard Meirovitch Yogendra Kakad Tony Hotz Larry Taylor
12:00 Lunch	

1:00 Guest Investigators Role in the COFS Program.....	Tony Fontana
1:15 Panel on Issues in Controlling the SCOLE Configuration.....	A.V. Balakrishnan Peter Bainum Shalom Fisher Dan Minnick Gene Lin Sahjendra Singh Steve Yurkovich Mike Barret
5:00 Attitude Adjustment	
6:00 Supper Without Speeches	

**Tuesday, December 10**

8:30 Laboratory Tour in Building 1232	
SCOLE Experiment Demonstration.....	Jeff Williams
Grid Experiment Demonstration.....	Ray Montgomery
Optical Sensing Demonstration.....	Bob Bullock

12:00 Lunch

1:00 Laboratory Tour in Building 1293B	
Flexible Beam Experiment Demonstration.....	Lucas Horta
15 Meter Hoop/Column Antenna Structural Tests.....	Keith Belvin
2:30 End of Workshop	

# Table of Contents

	Page
The SCOLE Design Challenge - An Overview..... Larry Taylor	1
SCOLE Equations of Motion - A New Formulation..... Suresh Joshi	14
Dynamics of Flexible Spacecraft (SCOLE) During Slewing Maneuvers..... Yogendra Kakad	26
Functional Analysis of the SCOLE Problem..... A. V. Balakrishnan	38
Maneuvering of Flexible Spacecraft..... Leonard Meirovitch	50
Model Reference Control of the SCOLE..... Dan Minnick and Howard Kaufman	62
Rapid Pointing and Vibration Control of the SCOLE Configuration..... Jiguan Gene Lin	82
A Perspective on the Control of Flexible Spacecraft..... Mike Barrett and K. W. Lips	86
Equations du Mouvement d'une poutre Flexible en Rotation Autour d'un Axe Lionel R. Passeron	102
Flexible Beam Simulation..... Shalom Fisher and Tom Posbergh	113
Issues in Modeling and Controlling the SCOLE Configuration..... Peter Bainum, A.S.S.R. Reddy and Cheick Modibo Diarra	132
Decentralized Control Experiments on a Flexible Grid..... U. Ozguner and S. Yurkovich	217
A Mathematical Problem and a Spacecraft Control Laboratory Experiment (SCOLE) Used to Evaluate Control Laws for Flexible Spacecraft (Reprint) L. W. Taylor, Jr. and A. V. Balakrishnan	236
List of Attendees.....	263

# **The SCOLE Design Challenge**

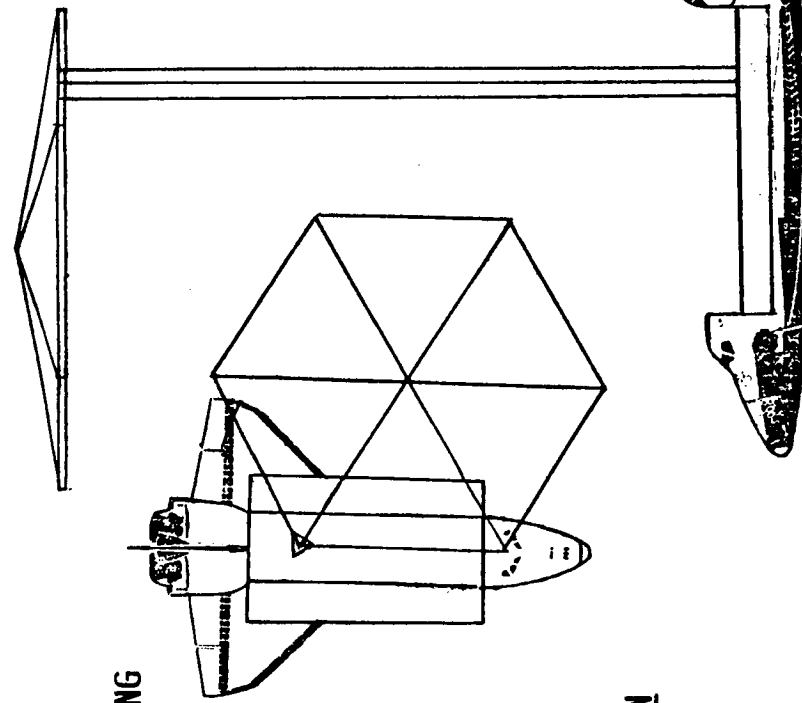
**by**

**Larry Taylor  
NASA Langley  
Research Center**

SPACECRAFT CONTROL LAB EXPERIMENT  
(SCOLE)

ANALYTIC MODELING  
MODEL REDUCTION  
CONTROL-DRIVE MODELING

SYSTEMS IDENTIFICATION  
COMPLEX MODAL METHODS  
PHYSICAL/PDE PARAMETER  
NONLINEAR  
INPUT OPTIMIZATION



CONTROL-LAW DESIGN  
LARGE MOTION  
NONLINEAR  
MULTI-AXIS  
HIGH ORDER

INTEGRATED DESIGN  
MULTIDISCIPLINARY  
DESIGN TOOLS

## **Benefits of the SCELE Program**

- O Comparison of Design Approaches**
- O Novel Control Techniques**
- O Validation of Design Methods**
- O Precursor to Co-Investigators for Flight Experiments**

## **Objectives of the Scole Program**

- O To Validate Methodologies for the Control  
of Flexible Antenna Structures**
- O Identify Advantages and Disadvantages of  
Various Systems Identification Techniques**
- O Identify Advantages and Disadvantages of  
Various Control Synthesis Techniques**
- O Identify Outstanding Identification and  
Control Candidates for the COFS II Flight  
Experiments**

# EQUATIONS OF MOTION

$$\begin{aligned}\ddot{\omega}_1 &= -\bar{I}_1 (\tilde{\omega}_1 \bar{I}_1 \omega_1 + M_1 + M_D + M_{B,1}) \\ \ddot{v}_1 &= F_{B,1}/m_1 \\ \dot{\bar{T}}_1^T &= -\tilde{\omega}_1 \bar{T}_1^T\end{aligned}$$

} SHUTTLE BODY

(SIMILARLY FOR REFLECTOR BODY)

## ROLL BEAM BENDING:

$$PA \frac{\partial^2 u_\phi}{\partial t^2} + 2\zeta_\phi \sqrt{PA EI_\phi} \frac{\partial^3 u_\phi}{\partial s^2 \partial t} + EI_\phi \frac{\partial^4 u_\phi}{\partial s^4} = \sum_{n=1}^4 [f_{\phi,n} \delta(s-s_n) + g_{\phi,n} \frac{\partial \delta}{\partial s}(s-s_n)]$$

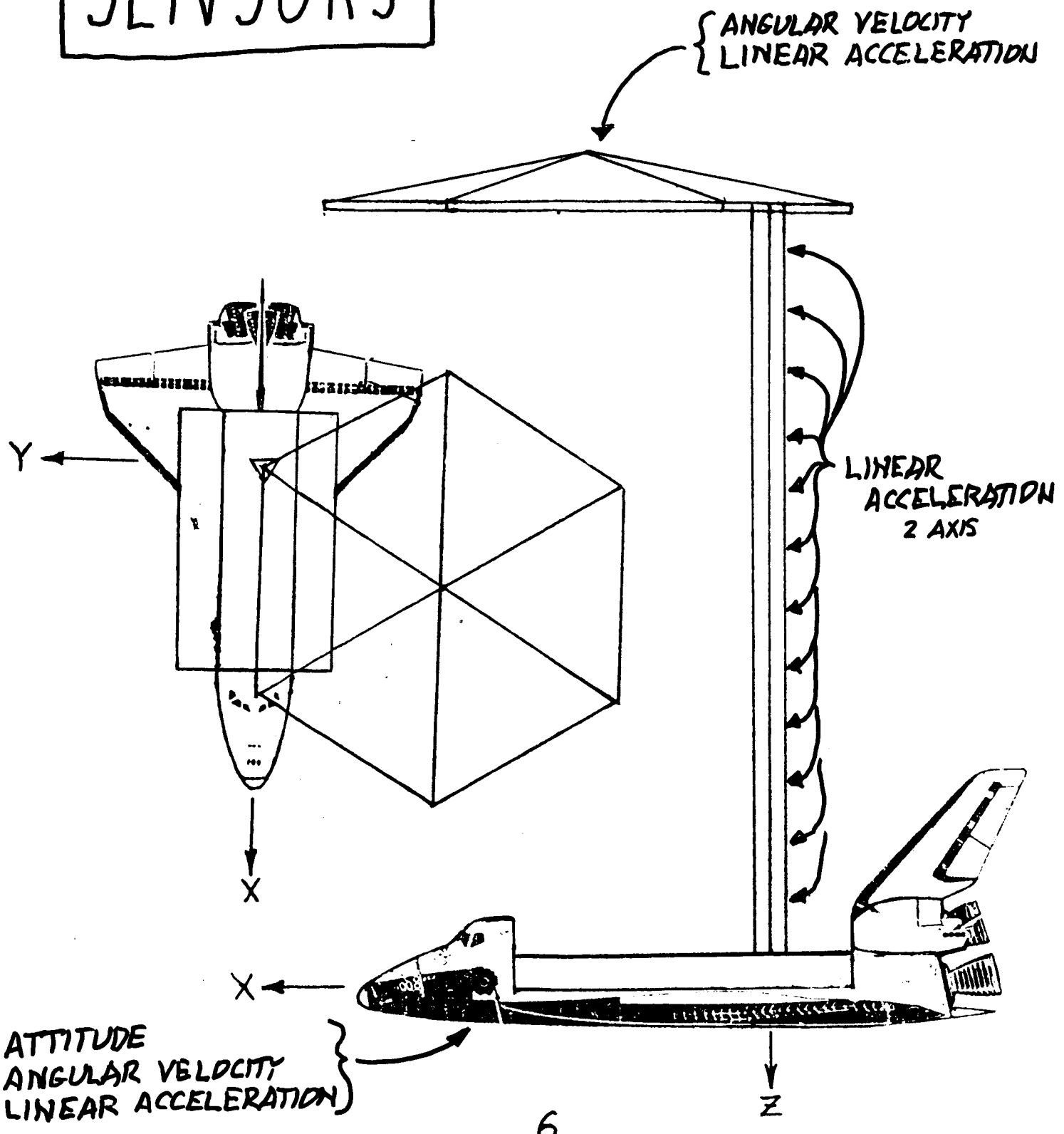
## PITCH BEAM BENDING:

$$PA \frac{\partial^2 u_\theta}{\partial t^2} + 2\zeta_\theta \sqrt{PA EI_\theta} \frac{\partial^3 u_\theta}{\partial s^2 \partial t} + EI_\theta \frac{\partial^4 u_\theta}{\partial s^4} = \sum_{n=1}^4 [f_{\theta,n} \delta(s-s_n) + g_{\theta,n} \frac{\partial \delta}{\partial s}(s-s_n)]$$

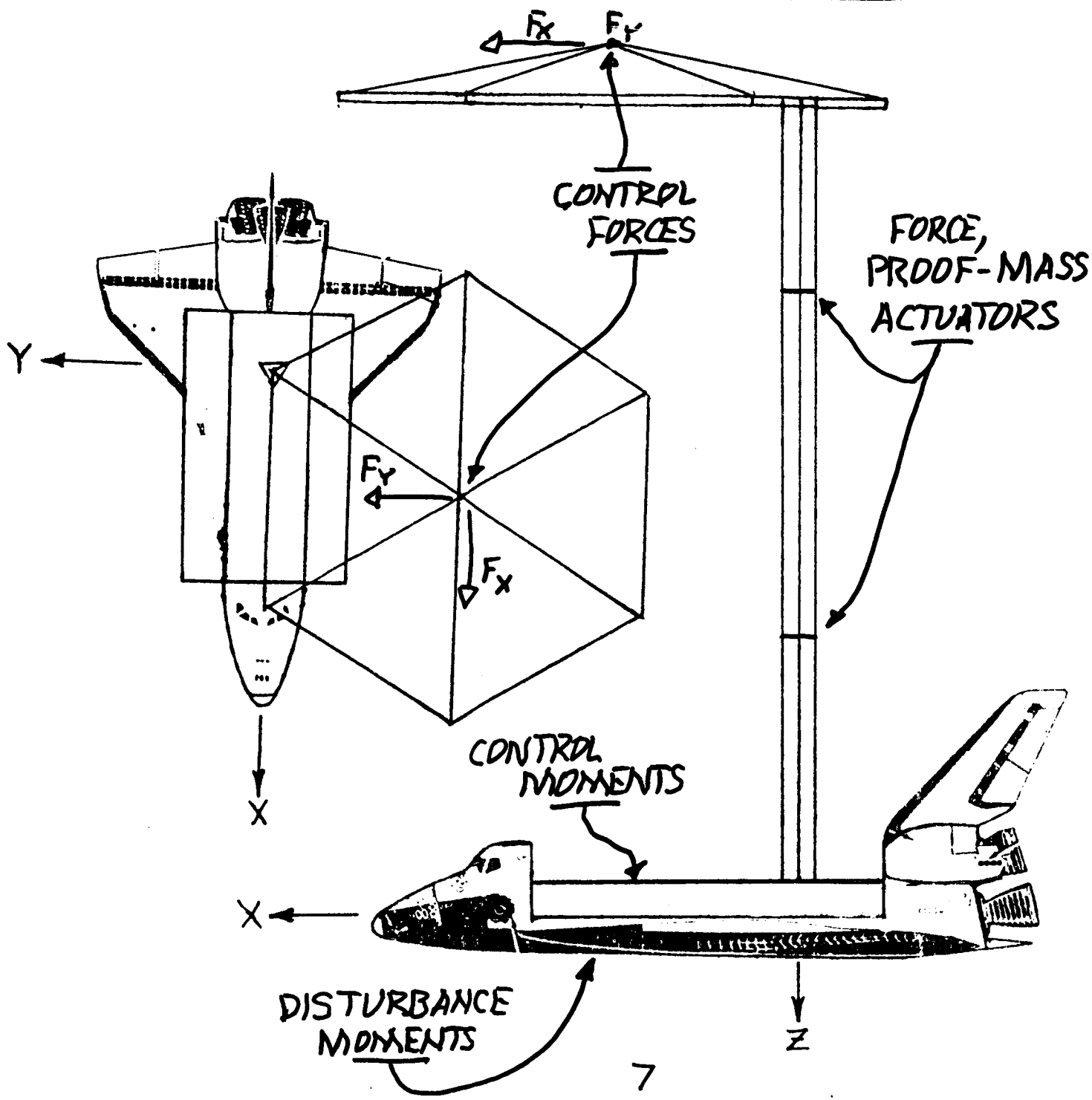
## YAW BEAM TORSION:

$$PI_\psi \frac{\partial^2 u_\psi}{\partial t^2} + 2\zeta_\psi I_\psi \sqrt{GP} \frac{\partial^3 u_\psi}{\partial s \partial t} + GI_\psi \frac{\partial^2 u_\psi}{\partial s^2} = \sum_{n=1}^4 g_{\psi,n} \delta(s-s_n)$$

# SENSORS



# CONTROLLERS AND DISTURBANCES



# CONTROL TASK

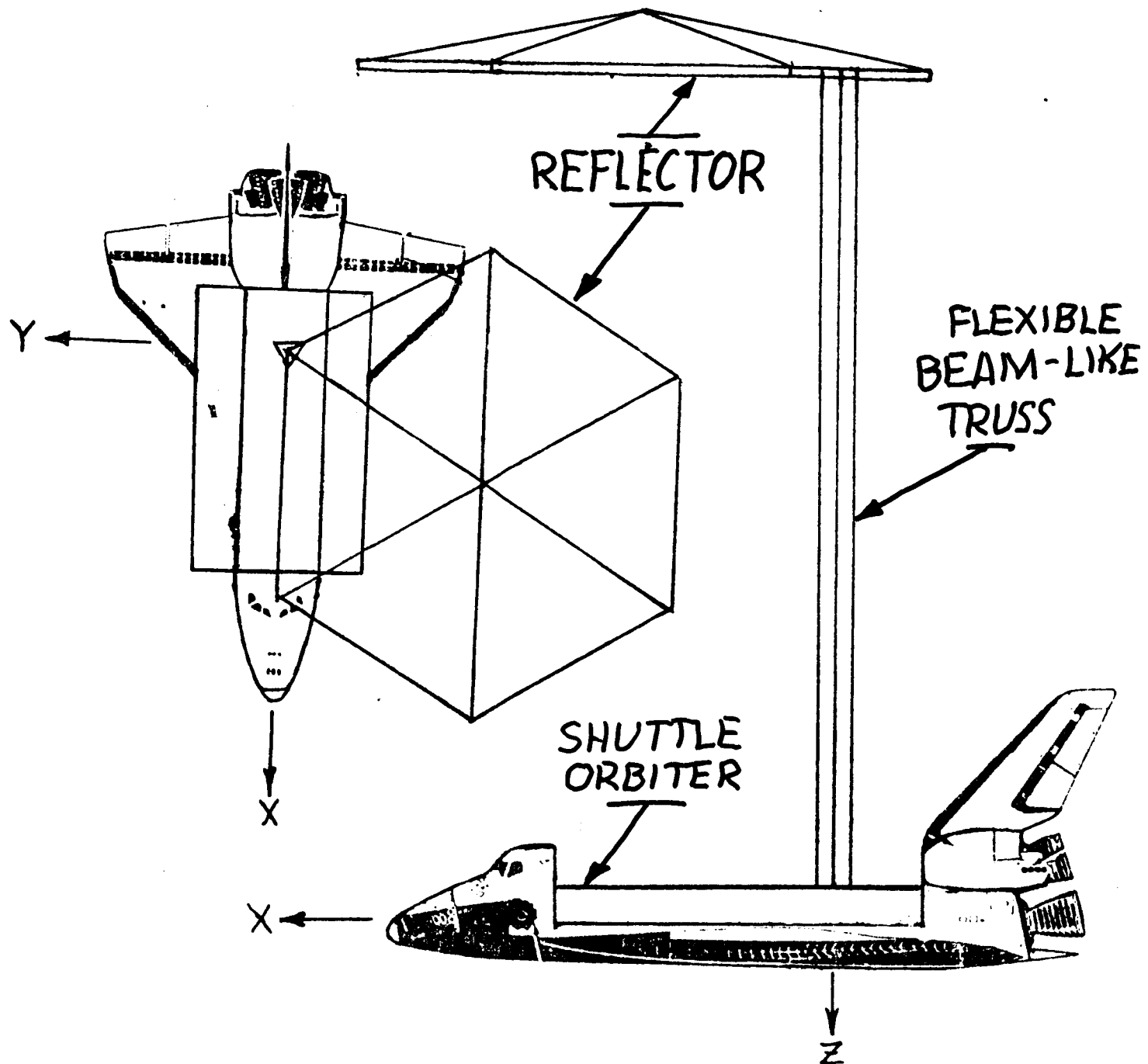
## PRIMARY

- SLEW  $20^\circ$
- STABILIZE AND
- POINT ... IN MINIMUM TIME

## SECONDARY

- ROTATE  $90^\circ$  ABOUT LINE-OF-SIGHT

# CONFIGURATION



Justification for the

# SCOPE Program

- Methodologies for Control of Flexible Spacecraft Have Not Yet Been Validated
- Methodologies for On-Orbit Modelling of Structural Dynamics of Flexible Spacecraft Have Not Been Validated
- The High Cost of On-Orbit Testing Needed to Support Initial Validation May be Alleviated by Using Hi-Fidelity Ground Based Experiments
- A Direct Comparison of Different Design Approaches for the Control of Flexible Spacecraft is Needed
- On-Orbit Systems Identification Techniques Need to be Compared in Preparation for Actual Flight Application

## **Timeliness of the SCOLE Program**

- O Ground Demonstrations on Two Dimensional Structures are Nearing Completion - A 3-Dimensional Problem is Needed to Advance Our Active Structural Control Capability**
- O The Planned COFS Flight Tests Demand Development of Our Most Sophisticated Flexible Structure Control Capability - This Can Only be Accomplished by Ground Testing on Structures with 3-Dimensional Characteristics and Large Numbers of Inertial Sensors and Actuators**

# **Results of the SCOLE Program**

- O NASA-IEEE Design Challenge**  
June '83
- O Eight Grants/Contracts Underway**  
Feb '84
- O SCOLE Workshop**  
Dec '84
- O Experimental Apparatus Ready**  
July '85

Milestones of the  
**SCOLE Program**

FY      1985      1986      1987      1988

**MATH SOLUTIONS**

**EXP. FAC. DEV.**

< IDENTIFICATION > **CONTROL** >  
**EXP. IMPLEMENTATION**

**EVALUATION**

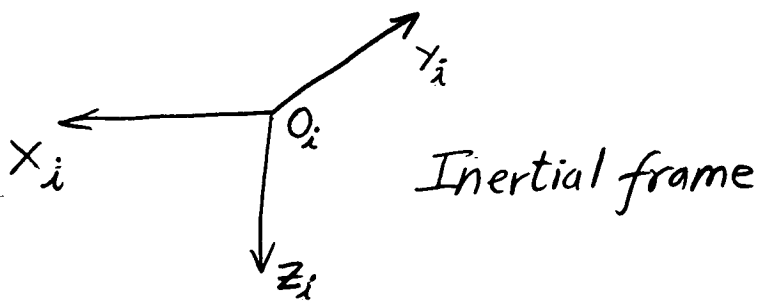
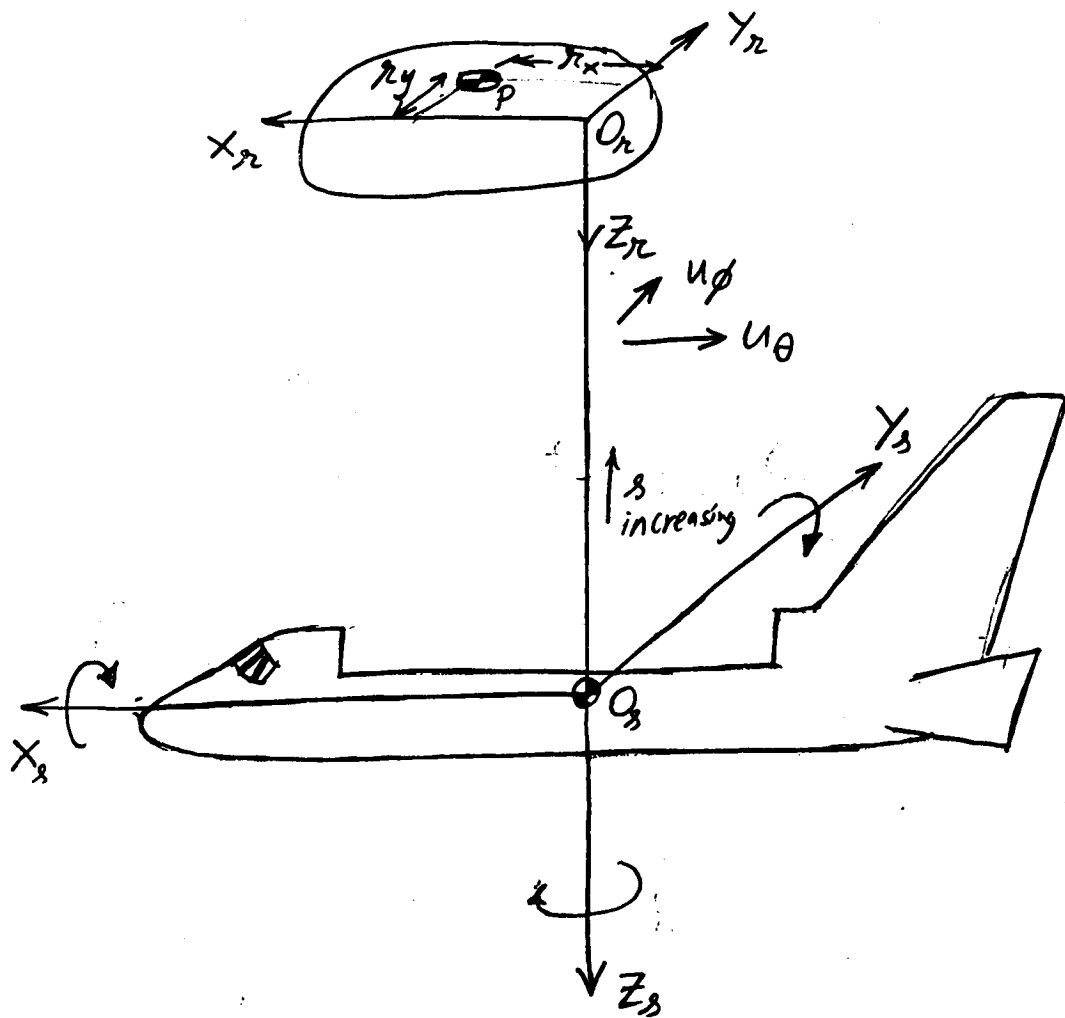
# **SCOLE Equations of Motion A New Formulation**

**by**

**Suresh Joshi  
NASA Langley  
Research Center**

**SCOLE equations of motion are derived  
in the Shuttle-fixed coordinate system  
using a Newtonian formulation.**

## Coordinate Systems



$-u_\theta(s)$  = beam defl. in  $x_s$ -direction

$i$ : Inertial system

$s$ : Shuttle-fixed "

$r$ : reflector-fixed"  
(w/origin at beam tip)

$u_\phi(s) =$  " " "  $y_s$  "

$u'_\phi =$  beam angular defl. about  $x_s$ -axis

$u'_\theta =$  " " " "  $y_s$  "

$u_y =$  " " " " "  $z_s$  "

Let  $\alpha_i = (\phi_i, \theta_i, \psi_i)^T$  = shuttle Euler angles  
 (1-2-3 rotation) w.r.t. inertial ( $i$ -) frame.

Let  $\mathcal{I}_i = (I_{x_i}, I_{y_i}, I_{z_i})^T$   
 = moment acting on beam at shuttle interface  
 $I_4 = " " " " " \text{ reflector } "$

$f_i = (f_{x_i}, f_{y_i}, f_{z_i})^T$   
 = force acting on beam at shuttle interface  
 $f_4 = " " " " " \text{ at reflector } "$

Assume  $f_i, \mathcal{I}_i, f_4, I_4$  to be defined in the  $-s$ -frame.

## Shuttle Center of mass (c.m.) translation

$$m_1 a_1 = -f_1 \quad (1)$$

where  $a_1 = \begin{matrix} \text{inertial} \\ \text{acceleration of } O_s \end{matrix}$ , expressed in  $s$ -system

If  $R_1 = \text{position of } O_s \text{ in } i\text{-system}$ , then

$$m_1 \ddot{R}_1 = -T_1 f_1 \quad (2)$$

where  $T_1^T = \text{transformation matrix from inertial to shuttle frame (function of } \phi_1, \theta_1, \psi_1 \text{)}$

## Shuttle rotation

$$I_1 \ddot{\omega}_1 + \tilde{\omega}_1 I_1 \omega_1 = M_1 + M_D - g_1 \quad (3)$$

$$\text{where } \omega_1 = \begin{bmatrix} \omega_x_1 \\ \omega_y_1 \\ \omega_z_1 \end{bmatrix} = \begin{bmatrix} \cos \theta_1 \cos \psi_1 & \sin \psi_1 & 0 \\ -\cos \theta_1 \sin \psi_1 & \cos \psi_1 & 0 \\ \sin \theta_1 & 0 & 1 \end{bmatrix} \begin{bmatrix} \dot{\phi}_1 \\ \dot{\theta}_1 \\ \dot{\psi}_1 \end{bmatrix} \quad (4)$$

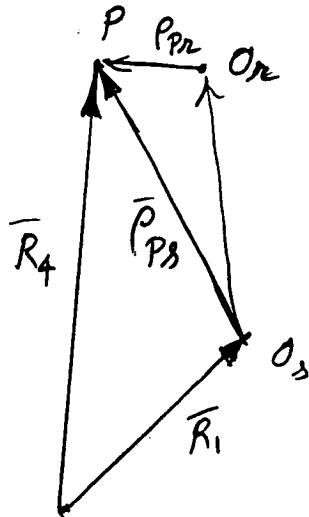
$I_1 = \text{shuttle inertia about } s\text{-axes}$

$M_1 = \text{control moment applied to shuttle}$

$M_D = \text{disturbance } "$

$g_1 = \text{interface moment}$

### Reflector center of mass (c.m.) translation



Let  $R_4$  = position of reflector c.m. ( $P$ )  
in  $i$ -system

In vector notation,

$$\bar{R}_4 = \bar{R}_1 + \bar{P}_{Ps} \quad (5)$$

$O_i$

where  $\bar{P}_{Ps}$  is position vector of  $P$  w.r.t.  $O_3$ .

$$\ddot{\bar{R}}_4 = \ddot{\bar{R}}_1 + \ddot{\bar{P}}_{Ps} \quad (6)$$

$$= \ddot{\bar{R}}_1 + (\ddot{\bar{P}}_{Ps})_r + \ddot{\bar{\omega}}_1 \times \bar{P}_{Ps} + \bar{\omega}_1 \times (\bar{\omega}_1 \times \bar{P}_{Ps}) \\ + 2\bar{\omega}_1 \times (\dot{\bar{P}}_{Ps})_r \quad (7)$$

where  $(\bar{P}_{Ps})_r$  = pos. of  $P$  w.r.t.  $O_3$   
 $(\dot{\bar{P}}_{Ps})_r$  = net. of " "

Expressing in  $s$ -system,

$$T_1^T \ddot{\bar{R}}_4 = T_1^T \ddot{\bar{R}}_1 + (\ddot{\bar{P}}_{Ps})_r + \ddot{\bar{\omega}}_1 (\bar{P}_{Ps})_r + \ddot{\bar{\omega}}_1^2 (\bar{P}_{Ps})_r \\ + 2\ddot{\bar{\omega}}_1 (\dot{\bar{P}}_{Ps})_r \quad (8)$$

But

$$(\bar{P}_{Ps})_r = \bar{r}_c + d \quad (9)$$

where  $\bar{r}_c = \begin{bmatrix} r_{cx} \\ r_{cy} \\ -L \end{bmatrix} =$  nominal pos. of refl. c.m. in  $s$ -system

- - - (10)

and

$$d = \begin{bmatrix} -u_\theta(L) - r_y u_\phi(L) \\ u_\phi(L) + r_x u_\theta(L) \\ -r_y u'_\phi(L) + r_x u'_\theta(L) \end{bmatrix} \quad (11)$$

Therefore,

$$\begin{aligned} T_1 \ddot{R}_4 &= T_1 \ddot{R}_1 + \ddot{d} + (\dot{\tilde{\omega}}_1 + \tilde{\omega}_1^2)(r+d) \\ &\quad + 2\tilde{\omega}_1 \dot{d} \end{aligned} \quad (12)$$

Since  $m_4 \ddot{R}_4 = T_1 (F - f_4)$  (13)

where  $F = \begin{bmatrix} F_x \\ F_y \\ 0 \end{bmatrix}$  = force applied at reflector c.m.  
(in S-system) (14)

$$\begin{aligned} m_4 [T_1 \ddot{R}_1 + \ddot{d} + (\dot{\tilde{\omega}}_1 + \tilde{\omega}_1^2)(r+d) + 2\tilde{\omega}_1 \dot{d}] \\ = F - f_4 \end{aligned} \quad (14)$$

## Reflector rotation

Let  $\Omega_{rs}$  be the angular velocity of reflector relative to the shuttle. Then absolute angular velocity of reflector

$$\bar{\omega}_4 = \bar{\omega}_1 + \bar{\Omega}_{rs} \quad (15)$$

If  $\bar{\Omega}_{rs}$  is expressed in the  $S$ -system, we can replace vector addition by straight addition:

$$\omega_4 = \omega_1 + \bar{\Omega}_{rs} \quad (16)$$

where

$$\bar{\Omega}_{rs} = \begin{bmatrix} \bar{\Omega}_{rsx} \\ \bar{\Omega}_{rsy} \\ \bar{\Omega}_{rsz} \end{bmatrix} = \begin{bmatrix} Cu'_\theta(L)Cu_\phi(L) & Su'_\theta(L) & 0 \\ -Cu'_\theta(L)Su_\phi(L) & Cu_\phi(L) & 0 \\ Su'_\theta(L) & 0 & 1 \end{bmatrix} \begin{bmatrix} \dot{u}'_\phi(L) \\ \dot{u}'_\theta(L) \\ \dot{u}_4(L) \end{bmatrix} \quad (17)$$

where "S" and "C" represent sine and cosine.

The angular momentum of the reflector w.r.t. P (the c.m.)

$$H_{C4} = I_4' \omega_4 \quad (18)$$

$$\text{where } I_4' = T_2^T I_4 T_2 \quad (19)$$

where  $T_2$  is the transformation matrix from  $S$ -system to  $s$ -system.  $T_2$  is a function of  $u'_\phi(L)$ ,  $u'_\theta(L)$ ,  $u_4(L)$ .

Then

$$\dot{I}_4' = \dot{T}_2^T I_4 T_2 + T_2^T I_4 \dot{T}_2$$

Therefore,

$$\begin{aligned}\dot{H}_{C4} &= \dot{I}'_4(\ddot{\omega}_1 + \dot{\omega}_{rs}) + \dot{I}'_4(\omega_1 + \omega_{rs}) \\ &\quad + \tilde{\omega}_1 [ \dot{I}'_4(\omega_1 + \omega_{rs}) ] \\ &= -g_4 - \tilde{\omega}_1 f_4 \quad \dots \quad (20)\end{aligned}$$

where  $\omega_1 = \begin{pmatrix} \omega_x \\ \omega_y \\ 0 \end{pmatrix}$  (21)

Substituting for  $f_4$  from (14),

$$\begin{aligned}& \dot{I}'_4(\ddot{\omega}_1 + \dot{\omega}_{rs}) + \dot{I}'_4(\omega_1 + \omega_{rs}) + \tilde{\omega}_1 [ \dot{I}'_4(\omega_1 + \omega_{rs}) ] \\ & - \tilde{\omega}_1 [ F - m_4 \{ T_1^T \ddot{R}_1 + \ddot{d} + (\tilde{\omega}_1 + \tilde{\omega}_1^2)(r+d) + 2\tilde{\omega}_1 \dot{d} \} ] \\ & = -g_4 \quad (22)\end{aligned}$$

Small-deflection approximation:

Let  $h = \begin{bmatrix} u'_\phi(L) \\ u'_\theta(L) \\ u_4(L) \end{bmatrix}$  (23)

If  $h$  is small, then instead of (17), we have

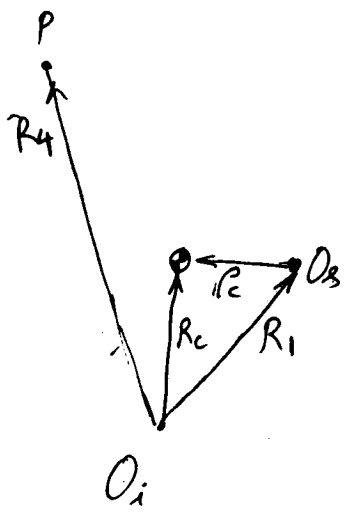
$$-\omega_{rs} = h \quad (24)$$

in eq. (22).

Combined translation eq.

Let  $R_c$  = position of combined C.M. in  $i$ -system

Then



$$m \bar{R}_c = m_1 \bar{R}_1 + m_4 \bar{R}_4 \quad (25)$$

$$\text{where } m = m_1 + m_4$$

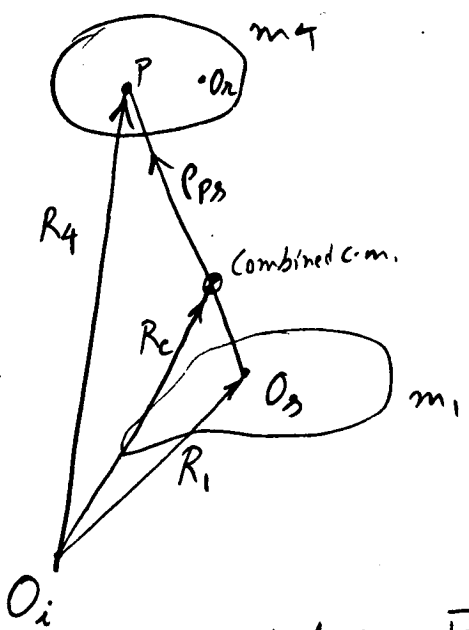
$$m \ddot{\bar{R}}_c = m_1 \ddot{\bar{R}}_1 + m_4 \ddot{\bar{R}}_4 = \bar{F} \quad (26)$$

Working in the  $s$ -system, and using (12),

$$m_1 T_1 \ddot{\bar{R}}_1 + m_4 [ T_1 \ddot{\bar{R}}_1 + d \ddot{\dot{d}} + (\ddot{\omega}_1 + \ddot{\omega}_1^2)(r+d) + 2\ddot{\omega}_1 \dot{d} ] = F$$

$$\Rightarrow m T_1 \ddot{\bar{R}}_1 + m_4 [ \ddot{\dot{d}} + (\ddot{\omega}_1 + \ddot{\omega}_1^2)(r+d) + 2\ddot{\omega}_1 \dot{d} ] = F \quad (27)$$

## Combined rotation eqs.



Let  $\bar{H}_1, \bar{H}_4$  be angular momenta of shuttle & reflector about  $O_i$  (origin of inertial frame).

Then

$$\dot{\bar{H}}_1 = \bar{H}_{c1} + \bar{R}_1 \times m_1 \ddot{\bar{R}}_1 \quad (28)$$

and

$$\dot{\bar{H}}_4 = \bar{H}_{c4} + \bar{R}_4 \times m_4 \ddot{\bar{R}}_4 \quad (29)$$

where  $\bar{H}_{c1}, \bar{H}_{c4}$  represent angular momenta w.r.t. the centers of mass.

The combined rotation eq. is:

$$\dot{\bar{H}}_1 + \dot{\bar{H}}_4 = \bar{M}_1 + \bar{M}_D + \bar{R}_4 \times \bar{F} \quad (30)$$

i.e.,  $\dot{\bar{H}}_{c1} + \dot{\bar{H}}_{c2} + \bar{R}_1 \times m_1 \ddot{\bar{R}}_1 + \bar{R}_4 \times m_4 \ddot{\bar{R}}_4 = \bar{M}_1 + \bar{M}_D + \bar{R}_4 \times \bar{F}$

Since  $\bar{R}_1 = \bar{R}_4 - \bar{P}_{PS}$ ,

$$\begin{aligned} \dot{\bar{H}}_{c1} + \dot{\bar{H}}_{c2} + \bar{R}_4 \times [m_1 \ddot{\bar{R}}_1 + m_4 \ddot{\bar{R}}_4] - \bar{P}_{PS} \times m_1 \ddot{\bar{R}}_1 \\ = \bar{M}_1 + \bar{M}_D + \bar{R}_4 \times \bar{F} \end{aligned}$$

But  $m_1 \ddot{\bar{R}}_1 + m_4 \ddot{\bar{R}}_4 = m \ddot{\bar{R}}_c = \bar{F}$

$$\therefore \dot{\bar{H}}_{c1} + \dot{\bar{H}}_{c2} - \bar{P}_{PS} \times m_1 \ddot{\bar{R}}_1 = \bar{M}_1 + \bar{M}_D \quad (31)$$

Working in the 8-system,

$$\begin{aligned} I_1 \ddot{\omega}_1 + \tilde{c} \dot{\omega}_1 I_1 \omega_1 + I_4' (\ddot{\omega}_1 + \tilde{\omega}_{rs}) + \dot{I}_4' (\omega_1 + \omega_{rs}) \\ + \tilde{\omega}_1 [I_4' (\omega_1 + \omega_{rs})] - m_1 (\tilde{r} + d) T_1^T \ddot{R} \\ = M_1 + M_D \quad \dots \quad (32) \end{aligned}$$

Complete eqs. of motion are given by (27), (32),

beam PDE's, and (2), (3), (14), (22)

These are presented on the next page.

Complete Eqn. of motion:

$$m T_1^T \ddot{R}_1 + m_4 [ \ddot{d} + (\ddot{\tilde{\omega}}_1 + \ddot{\tilde{\omega}}_{12})(r+d) + 2\ddot{\tilde{\omega}}_1 \dot{d} ] = F \quad (33)$$

where  $d = \begin{bmatrix} -u_\theta(L) - r_y u_\phi(L) \\ u_\phi(L) + r_x u_\theta(L) \\ -r_y u'_\phi(L) + r_x u'_\theta(L) \end{bmatrix}, \quad r = \begin{bmatrix} r_x \\ r_y \\ -L \end{bmatrix}$

$$(I_1 + I_4') \ddot{\omega}_1 + I_4' \ddot{r}_{rs} + \ddot{\tilde{\omega}}_1 (I_1 + I_4') \omega_1 + I_4' (\omega_1 + r_{rs}) \\ + \ddot{\tilde{\omega}}_1 I_4' r_{rs} - m_1 (r \ddot{d}) T_1^T \ddot{R}_1 = M_1 + M_D \quad (34)$$

Beam PDE's:

$$PA \ddot{u}'_\phi + EI_\phi \ddot{u}'''_\phi = f_{1y} \delta(s) + f_{4y} \delta(s-L) + g_{1y} \frac{\partial \delta(s)}{\partial s} + g_{4y} \frac{\partial \delta(s-L)}{\partial s} \quad (35)$$

$$PA \ddot{u}'_\theta + EI_\theta \ddot{u}''''_\theta = f_{1x} \delta(s) + f_{4x} \delta(s-L) + g_{1x} \frac{\partial \delta(s)}{\partial s} + g_{4x} \frac{\partial \delta(s-L)}{\partial s} \quad (36)$$

$$PI_4 \ddot{u}_y - GI_4 \ddot{u}''_\phi = g_{31} \delta(s) + g_{34} \delta(s-L) \quad (37)$$

$$u_\phi(0) = u_\theta(0) = u_\phi'(0) = u_\theta'(0) = 0 \quad (38)$$

(Cantilever conditions)

In (35) - (38),  $f_1, g_1, f_4, g_4$  are given by:

$$f_1 = \begin{bmatrix} f_{x1} \\ f_{y1} \\ f_{z1} \end{bmatrix} = -m_1 T_1^T \ddot{R}_1 \quad (\ddot{R}_1 \text{ given by (33)}) \quad (39)$$

$$f_4 = F - m_4 [ T_1^T \ddot{R}_1 + \ddot{d} + (\ddot{\tilde{\omega}}_1 + \ddot{\tilde{\omega}}_{12})(r+d) + 2\ddot{\tilde{\omega}}_1 \dot{d} ] \quad (40)$$

$$g_1 = -I_1 \ddot{\omega}_1 - \ddot{\tilde{\omega}}_1 I_1 \omega_1 + M_1 + M_D \quad (41)$$

$$g_4 = -I_4' (\ddot{\omega}_1 + \ddot{r}_{rs}) - I_4' (\omega_1 + r_{rs}) + \ddot{\tilde{\omega}}_1 [ I_4' (\omega_1 + r_{rs}) ] \\ + \ddot{\tilde{\omega}}_1 [ F - m_4 \{ T_1^T \ddot{R}_1 + (\ddot{\tilde{\omega}}_1 + \ddot{\tilde{\omega}}_{12})(r+d) + 2\ddot{\tilde{\omega}}_1 \dot{d} \} ] \quad (42)$$

# **Dynamics of Flexible Spacecraft (SCOLE) During Slewing Maneuvers**

**by**

**Yogendra P. Kakad**  
**University of N.C.**<sup>at</sup>  
**Charlotte, N. Carolina**

$$T_e = \begin{bmatrix} \cos\theta_2 \cos\theta_3 & -\cos\theta_2 \sin\theta_3 & \sin\theta_2 \\ (\sin\theta_1 \sin\theta_2 \cos\theta_3 + \sin\theta_3 \cos\theta_1) & (-\sin\theta_1 \sin\theta_2 \sin\theta_3 + \cos\theta_3 \cos\theta_1) & -\sin\theta_1 \cos\theta_2 \\ (-\cos\theta_1 \sin\theta_2 \cos\theta_3 + \sin\theta_3 \sin\theta_1) & (\cos\theta_1 \sin\theta_2 \sin\theta_3 + \cos\theta_3 \sin\theta_1) & \cos\theta_1 \cos\theta_2 \end{bmatrix}$$

$$M^T = \begin{bmatrix} \cos\theta_2 \cos\theta_3 & \sin\theta_3 & 0 \\ -\cos\theta_2 \sin\theta_3 & \cos\theta_3 & 0 \\ \sin\theta_2 & 0 & 1 \end{bmatrix}$$

$$\underline{\omega} = M^T \dot{\underline{\theta}}$$

R the position vector of the mass center in the inertial frame is

$$\underline{R} = \begin{bmatrix} R_x \\ R_y \\ R_z \end{bmatrix}$$

The velocity of mass center in the inertial frame is

$$\underline{v}^I(t) = \begin{bmatrix} \dot{R}_x \\ \dot{R}_y \\ \dot{R}_z \end{bmatrix}$$

The velocity in the body frame is

$$\underline{v}(t) = \underline{T}_t \begin{bmatrix} \dot{R}_x \\ \dot{R}_y \\ \dot{R}_z \end{bmatrix}$$

The velocity of the point of attachment in the body frame is

$$\underline{v}_o = \underline{v} + \underline{\omega} \times \underline{r}$$

where  $\underline{r}$  is the vector from mass center to the point of attachment.

If the body-fixed frame is located at the point of attachment,  $\underline{a}$  is the position vector of a mass element on the beam from the point of origin before deformation.

The displacement vector is

$$\underline{d}(z, t) = \begin{bmatrix} u_x(z, t) \\ u_y(z, t) \\ 0 \end{bmatrix}$$

The position vector after deflection is

$$\underline{r} + \underline{d}$$

The kinetic energy in the beam is

$$T_1 = \frac{1}{2} m \underline{v}_0^T \underline{v}_0 + \frac{1}{2} \underline{\omega}^T [\underline{J}] \underline{\omega} - m \underline{v}_0^T [\tilde{\underline{c}}] \underline{\omega} + \frac{1}{2} \int \underline{\dot{a}}^T \underline{\dot{a}} dm + \underline{v}_0^T \int \underline{\dot{a}} dm + \underline{\omega}^T \int \tilde{\underline{a}} \underline{\dot{a}} dm$$

where

$$\underline{c} = \frac{1}{m} \int \underline{a} dm = \begin{bmatrix} 0 \\ 0 \\ L/2 \end{bmatrix}$$

$$\tilde{\underline{c}} = \begin{bmatrix} 0 & -c_3 & c_2 \\ c_3 & 0 & -c_1 \\ -c_2 & c_1 & 0 \end{bmatrix}$$

$$\underline{a} = \begin{bmatrix} 0 \\ 0 \\ 3 \end{bmatrix}$$

$$\underline{J} = \frac{1}{3} S L^3 \begin{bmatrix} 1 & 0 & 0 \\ 0 & 1 & 0 \\ 0 & 0 & 0 \end{bmatrix}$$

$$T_1 = \frac{1}{2} g L \underline{v}_0^T \underline{v}_0 + \frac{1}{6} g L^3 (\omega_1^2 + \omega_2^2) - g L \underline{v}_0^T \tilde{\underline{\omega}} \\ + g L \sum_{i=1}^n \dot{q}_i^2 + \underline{v}_0^T \dot{\underline{q}} + \underline{\omega}^T \dot{\underline{\beta}}$$

where

$$u_x = \sum_{i=1}^n \Phi_{x_i}(s) q_i(t)$$

$$u_y = \sum_{i=1}^n \Phi_{y_i}(s) q_i(t)$$

$$p_{1i} = \int_0^L \Phi_{x_i}(s) ds$$

$$p_{2i} = \int_0^L \Phi_{y_i}(s) ds$$

$$p_{3i} = \int_0^L s \Phi_{x_i}(s) ds$$

$$p_{4i} = \int_0^L s \Phi_{y_i}(s) ds$$

$$\dot{\underline{\alpha}}(t) = g \begin{bmatrix} \sum_{i=1}^n p_{1i} \dot{q}_i \\ \sum_{i=1}^n p_{2i} \dot{q}_i \\ 0 \end{bmatrix}$$

$$\dot{\underline{\beta}}(t) = g \begin{bmatrix} \sum_{i=1}^n p_{4i} \dot{q}_i \\ \sum_{i=1}^n p_{3i} \dot{q}_i \\ 0 \end{bmatrix}$$

The kinetic energy of the reflector is

$$T_2 = \frac{1}{2} m_2 \underline{v}_0^T \underline{v}_0 - m_2 \underline{v}_0^T \tilde{\underline{a}}(L) \underline{\omega} + m_2 \underline{v}_0^T \dot{\underline{d}}(L) \\ - \frac{1}{2} m_2 \underline{\omega}^T \tilde{\underline{a}}(L) \tilde{\underline{a}}(L) \underline{\omega} + m_2 \underline{\omega}^T \tilde{\underline{a}}(L) \dot{\underline{d}}(L) \\ + \frac{1}{2} m_2 \dot{\underline{d}}^T(L) \dot{\underline{d}}(L) + \frac{1}{2} \underline{\Omega}^T I_2 \underline{\Omega}$$

where

$$\underline{\Omega} = \underline{\omega} + \begin{bmatrix} \dot{u}'_x \\ \dot{u}'_y \\ \dot{u}'_z \end{bmatrix} \Big|_L$$

$$T_2 = \frac{1}{2} m_2 \underline{v}_0^T \underline{v}_0 - m_2 \underline{v}_0^T \tilde{\underline{a}}(L) \underline{\omega} + m_2 \underline{v}_0^T \dot{\underline{d}}(L) + \\ \frac{1}{2} m_2 L^2 (\omega_1^2 + \omega_2^2) + m_2 \underline{\omega}^T \tilde{\underline{a}}(L) \dot{\underline{d}}(L) \\ + m_2 \sum_{i=1}^n \dot{q}_i^2 + \frac{1}{2} \dot{\underline{P}}^T I_2 \dot{\underline{P}}$$

The kinetic energy of the shuttle,  $T_0$ , is given as

$$T_0 = \frac{1}{2} m_1 \underline{v}^T \underline{v} + \frac{1}{2} \underline{\omega}^T [I_1] \underline{\omega}$$

The total kinetic energy is

$$T = T_0 + T_1 + T_2$$

$$T = \frac{1}{2} m_0 \underline{v}^T \underline{v} + \underline{\omega}^T [H] \underline{v} + \frac{1}{2} \underline{\omega}^T [I_0] \underline{\omega} + g L \sum_{i=1}^n \dot{q}_i^2 \\ + \underline{v}^T \dot{\underline{a}} + \underline{\omega}^T \dot{\underline{P}} \dot{\underline{a}} + \underline{\omega}^T \dot{\underline{P}} + m_2 \underline{v}^T \dot{\underline{d}}(L) + \\ m_2 \underline{\omega}^T \dot{\underline{P}} \dot{\underline{d}}(L) + m_2 \underline{\omega}^T \tilde{\underline{a}}(L) \dot{\underline{d}}(L) + m_2 \sum_{i=1}^n \dot{q}_i^2 \\ + \frac{1}{2} \dot{\underline{P}}^T I_2 \dot{\underline{P}}$$

where

$$m_0 = m_1 + \beta L + m_2$$

$$H = (\beta L + m_2) \ddot{x} + m_2 \ddot{a}(L) + \beta L \dot{\tilde{c}}$$

$$I_0 = I_1 + \frac{1}{3} \beta L^3 \begin{bmatrix} 1 & 0 & 0 \\ 0 & 1 & 0 \\ 0 & 0 & 0 \end{bmatrix} + m_2 L^2 \begin{bmatrix} 1 & 0 & 0 \\ 0 & 1 & 0 \\ 0 & 0 & 0 \end{bmatrix}$$

$$- \beta L \ddot{x} \ddot{x} - \beta L \ddot{x} \dot{\tilde{c}} - m_2 \ddot{x} \ddot{x} - m_2 \ddot{x} \ddot{a}(L)$$

$$\begin{aligned} T = & \frac{1}{2} m_0 \dot{v}^T \dot{v} + \underline{\omega}^T [H] \dot{v} + \frac{1}{2} \underline{\omega}^T [I_0] \underline{\omega} + \dot{v}^T [A_1] \dot{q} \\ & + \underline{\omega}^T [A_2] \dot{q} + \frac{1}{2} \dot{q}^T [A_3] \dot{q} \end{aligned}$$

where

$$[A_1] \dot{q} = \dot{q} + m_2 \dot{a}(L)$$

$$[A_2] \dot{q} = \ddot{x} \dot{q} + \dot{\beta} + m_2 \ddot{x} \dot{a}(L) + m_2 \ddot{a}(L) \dot{a}(L)$$

### Equations of Motion

Lagrange's Equations

$$\frac{d}{dt} \frac{\partial T}{\partial \dot{q}_k} - \frac{\partial T}{\partial q_k} = Q_k - \frac{\partial V}{\partial q_k} \quad (k=1, 2, 3, \dots)$$

$$\underline{q}^T = [x, y, z, \theta_1, \theta_2, \theta_3, q_1, q_2, \dots]$$

### Translational Equation

In terms of  $\underline{v}$ ,  $\underline{\omega}$  (non-generalized) and  $\underline{q}$  (generalized),

$$\frac{d}{dt} \left( \frac{\partial T}{\partial \underline{v}} \right) + \underline{T}^T \dot{\underline{t}} \left( \frac{\partial T}{\partial \underline{v}} \right) = \underline{F}(t)$$

where  $\underline{F}(t) = \underline{F}_0(t) + \underline{F}_2(t)$

From the total energy expression

$$\frac{\partial T}{\partial \underline{v}} = m_0 \underline{v} - H \underline{\omega} + A_1 \dot{\underline{q}}$$

$$m_0 \dot{\underline{v}} - H \dot{\underline{\omega}} + A_1 \ddot{\underline{q}} = - \underline{T}^T \dot{\underline{t}} \left( m_0 \underline{v} - H \underline{\omega} + A_1 \dot{\underline{q}} \right) + \underline{F}(t)$$

$$= \underline{N}_1 + \underline{F}(t)$$

$$\begin{aligned} \underline{N}_1 &= - \underline{T}^T \dot{\underline{t}} \left( m_0 \underline{v} - H \underline{\omega} + A_1 \dot{\underline{q}} \right) \\ &= \tilde{\underline{\omega}} (m \underline{v} - H \underline{\omega} + A_1 \dot{\underline{q}}) \end{aligned}$$

### Rotational Equation

$$\frac{d}{dt} \left( \frac{\partial T}{\partial \underline{\omega}} \right) - \frac{\partial T}{\partial \underline{\omega}} = M \underline{G}$$

where  $\underline{G} = \underline{G}_0 + (\underline{r} + \underline{\alpha}) \times \underline{F}_2$

$$\left( \frac{\partial T}{\partial \underline{\omega}} \right) = H \underline{v} + I_0 \underline{\omega} + A_2 \dot{\underline{q}}$$

$$\begin{aligned} \dot{\Sigma}_2 &= \dot{\Sigma}_1^{-1} \left[ \begin{matrix} \ddot{v}^T T_{\theta\theta_1}^T & T_{\theta_1}^T \\ \ddot{v}^T T_{\theta\theta_2}^T & T_{\theta_2}^T \\ \ddot{v}^T T_{\theta\theta_3}^T & T_{\theta_3}^T \end{matrix} \right] \left( \frac{\partial T}{\partial v} \right) + \\ &\quad \left\{ \left[ \begin{matrix} \ddot{w}^T \dot{\Sigma}_1^{-1} \frac{\partial M}{\partial \theta_1} \\ \ddot{w}^T \dot{\Sigma}_1^{-1} \frac{\partial M}{\partial \theta_2} \\ \ddot{w}^T \dot{\Sigma}_1^{-1} \frac{\partial M}{\partial \theta_3} \end{matrix} \right] - \dot{\Sigma}_1 \right\} \left( \frac{\partial T}{\partial w} \right) \end{aligned}$$

$$H\dot{\underline{v}} + I_0\dot{\underline{\omega}} + A_2\dot{\underline{q}} = \underline{G} + \underline{N}$$

Vibration Equation

$$\left( \frac{\partial T}{\partial \dot{\underline{q}}} \right) = A_1^T \underline{v} + A_2^T \underline{\omega} + A_3 \dot{\underline{q}}$$

$$V = \frac{1}{2} \underline{q}^T [K] \underline{q}$$

$$\left( \frac{\partial V}{\partial \underline{q}} \right) = [K] \underline{q}$$

Using Lagrangian Equations

$$A_1^T \dot{\underline{v}} + A_2^T \dot{\underline{\omega}} + A_3 \ddot{\underline{q}} = -[K] \underline{q}$$

## Slewing

$\underline{\lambda}$  - vector representing the axis of rotation

$\theta$  - Angle of rotation

Euler Parameters:

$$\underline{\xi} = \begin{bmatrix} \epsilon_1 \\ \epsilon_2 \\ \epsilon_3 \end{bmatrix} \triangleq \underline{\lambda} \sin \frac{\theta}{2}$$

$$\epsilon_4 \triangleq \cos \frac{\theta}{2}$$

$$\frac{d\underline{\xi}}{dt} = \frac{1}{2} (\epsilon_4 \underline{\omega} + \underline{\xi} \times \underline{\omega})$$

$$\frac{d\epsilon_4}{dt} = -\frac{1}{2} \underline{\omega} \cdot \underline{\xi}$$

## Summary of Equations:

$$m_0 \ddot{v} - H \dot{\omega} + A_1 \dot{q}_1 = N_1 + F(t)$$

$$H \ddot{v} + I_0 \dot{\omega} + A_2 \dot{q}_2 = N_2 + G(t)$$

$$A_1^T \ddot{v} + A_2^T \dot{\omega} + A_3 \ddot{q}_2 = -[K] q_2$$

$$\frac{d\epsilon}{dt} = \frac{1}{2} (\epsilon_+ \underline{\omega} + \underline{\epsilon} \times \underline{\omega})$$

$$\frac{dt_4}{dt} = -\frac{1}{2} \underline{\omega} \cdot \underline{\epsilon}$$

# **Functional Analysis of the SCOLE Problem**

**by**

**A. V. Balakrishnan**

**U. C. L. A.**

**Los Angeles, California**

X - STATE

$u_\phi(s)$	$b$	$u_\phi'''(s)$	$0 < s < L$
$u_\theta(s)$		$u_\theta'''(s)$	$0 < s < L$
$u_\psi(s)$		$-u_\psi''(s)$	$0 < s < L$
$u_\phi(0)$		$u_\phi'''(0)$	
$u_\theta(0)$		$u_\theta'''(0)$	
$u_\phi(L)$		$-u_\phi'''(L)$	
$u_\theta(L)$		$-u_\theta'''(L)$	
$u'_\phi(0)$		$-u_\phi''(0)$	
$\omega_1 = \dot{\Omega}_1$		$-u_\theta''(0)$	
$u'_\theta(0)$		$-u'_\psi(0)$	
$u'_\psi(0)$		$u_\phi''(L)$	
$u'_\phi(L)$		$u_\theta''(L)$	
$\Omega_4$		$u_\psi''(L)$	
$u'_\theta(L)$		$u_\phi'''(s_1+) - u_\phi'''(s_1-)$	
$u_\psi(L)$		$u_\theta'''(s_2+) - u_\theta'''(s_2-)$	
$u_\phi(s_2)$		$u_\phi'''(s_3+) - u_\phi'''(s_3-)$	
$u_\theta(s_2)$		$u_\theta'''(s_4+) - u_\theta'''(s_4-)$	
$u_\phi(s_3)$			
$u_\theta(s_3)$			

Ax

$u_\phi'''(s)$	$0 < s < L$
$u_\theta'''(s)$	$0 < s < L$
$-u_\psi''(s)$	$0 < s < L$
$u_\phi'''(0)$	
$u_\theta'''(0)$	
$-u_\phi'''(L)$	
$-u_\theta'''(L)$	
$-u_\phi''(0)$	
$-u_\theta''(0)$	
$u_\phi''(L)$	
$u_\theta''(L)$	
$u_\psi''(L)$	
$u_\phi'''(s_1+) - u_\phi'''(s_1-)$	
$u_\theta'''(s_2+) - u_\theta'''(s_2-)$	
$u_\phi'''(s_3+) - u_\phi'''(s_3-)$	
$u_\theta'''(s_4+) - u_\theta'''(s_4-)$	

$$H = L_2(0, L)^3 * R^{14}$$

M - INERTIA MATRIX

$M > 0$ ;  $M^{-1}$  BOUNDED

CONTROL:

$$B_{u(t)} = \begin{matrix} 0 \\ 0 \\ 0 \\ u(t) \end{matrix}$$

: FINITE DIMENSIONAL

$$u(t) = b(t)$$

$$M\ddot{x} + Ax + K(\dot{x}) + B_{u(t)} = 0$$

ENERGY  
NORM

$$E(t) = \frac{1}{2} \left\{ [M\dot{x}, \dot{x}] + [Ax, x] \right\}$$

$$[\dot{x}(t), K(\dot{x}(t))] = 0$$

$$\frac{d}{dt} E(t) = - [B_{u(t)}, \dot{x}(t)]$$

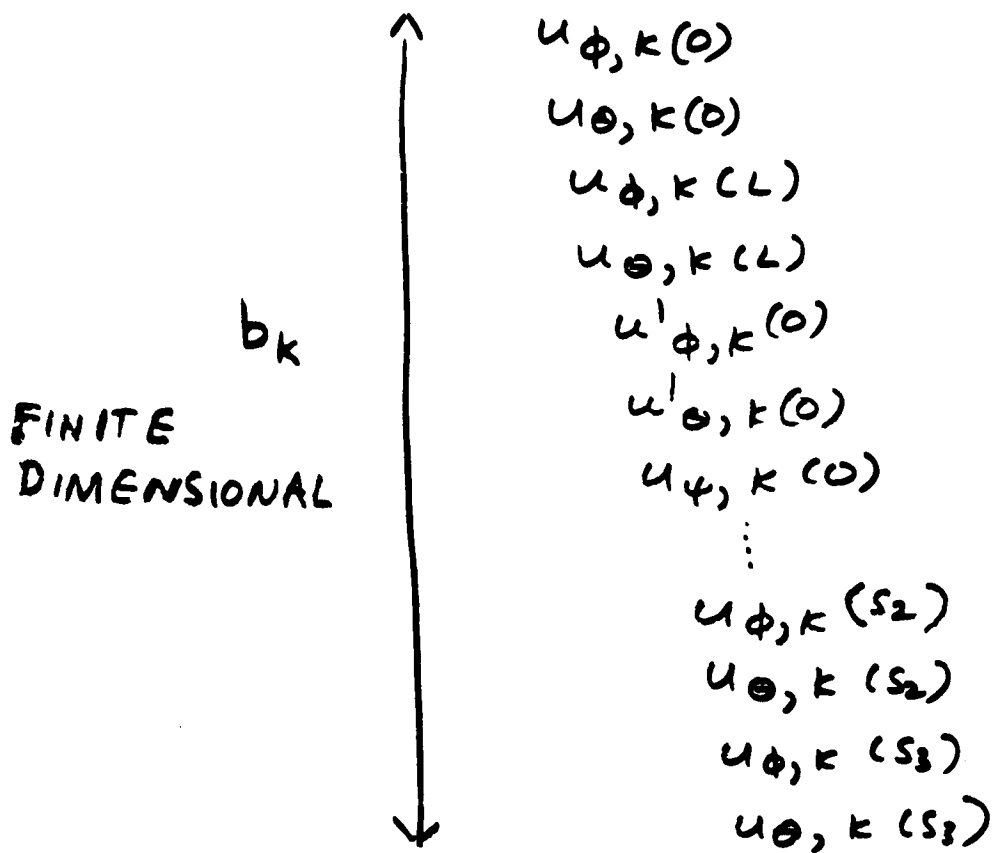
A SELF-ADJOINT  $\geq 0$

HAS M-ORTHOGONAL  
COMPLETE  
EIGEN- VECTORS

$$A \phi_k = \mu_k^2 M \phi_k$$

$$\begin{cases} [M \phi_k, \phi_j] = 0 & k \neq j \\ = 1 & k = j \end{cases}$$

$$\phi_k \sim \begin{array}{ll} u_{\phi, k}(s) & 0 < s < L \\ u_{\theta, k}(s) & 0 < s < L \\ u_{\psi, k}(s) & 0 < s < L \end{array}$$



THE  $b_k \rightarrow 0$  as  $k \rightarrow \infty$   
 $\mu_k = 0 \rightarrow$  ~'CLAMPED'

BEAM IS NOT

'EXPONENTIALLY' STABILIZABLE

IT IS

ST-AUGMENTABLE

"STRONGLY STABILIZABLE" / WHP?

— LESS AND LESS CONTROL  
EFFECT AS MODE FREQUENCY  
INCREASES —

THERE IS A CANONICAL  
ROBUST <sup>(DET.) F.B</sup> CONTROL WHICH  
DOES NOT DESTABILIZE  
HIGHER ORDER MODES  
(IGNORING SENSOR NOISE)

## DAMPING MODELS

### PROPORTIONAL DAMPING

'ROLL' BEAM BENDING:

$$PA \frac{\partial^2 u_\phi}{\partial t^2} + 2\zeta \sqrt{PAEI_\phi} \left( -\frac{\partial^3 u_\phi}{\partial t \partial s^2} \right) + EI_\phi \frac{\partial^4 u_\phi}{\partial s^4} = \sum f \delta + \sum g \delta'$$

SIMILARLY FOR PITCH.

YAW BEAM TORSION

$$PI_\psi \frac{\partial^2 u_\psi}{\partial t^2} + 2\zeta \sqrt{GPI_\psi} \frac{\partial}{\partial t} H[u_\psi] - GI_\psi \frac{\partial^2}{\partial s^2} u_\psi(t, s) = \sum g \delta'$$

$H(u(\cdot)) \sim$  HILBERT  
TRANSFORM

$$\frac{\partial}{\partial t} H(u_\psi(t, \cdot))$$

$$\doteq \frac{\partial}{\partial t} \frac{1}{\pi} \int_0^L \frac{u_\psi(t, \sigma)}{s - \sigma} d\sigma$$

'CAUCHY' INTEGRAL

$$= \frac{\partial}{\partial t} \frac{1}{\pi} \int_{-e}^e \frac{u_\psi(t, \sigma + e)}{s - e - \sigma} d\sigma$$

$2e = L$  'LARGE'

# STOCHASTICS

## 1. STATE NOISE

$$M\ddot{x} + Ax + Bu(t) + K(\dot{x}(t)) \\ + FN(t) = 0$$

$$F N(t) = \begin{pmatrix} 0 & 0 & 0 \\ 0 & 0 & 0 \\ 0 & 0 & 0 \end{pmatrix} N(t) \quad 3 \times 1 \quad [= M_D]$$

F IS FINITE DIMENSIONAL

## SENSOR (OBSERVATION) MODEL

$$v(t) = c_1 b(t) + N_o(t) \\ + c_2 \dot{b}(t)$$

$$x(t) = \begin{matrix} 0 \\ 0 \\ 0 \\ b(t) \end{matrix} + \begin{matrix} u_\phi(t, \cdot) \\ u_\theta(t, \cdot) \\ u_\psi(t, \cdot) \\ 0 \end{matrix}$$

$$Y(t) = \begin{matrix} x(t) \\ \dot{x}(t) \end{matrix}$$

$$c_1 b(t) + c_2 \dot{b}(t) = C Y(t)$$

C : FINITE DIMENSIONAL

→ KALMAN FILTER  
IMPLICATIONS

# CONTROL

## BEAM STABILITY AUGMENT.

→ STABILIZABILITY  
 THEORY ~ HILBERT SPACE

$$\dot{Y} = AY + BU \quad \begin{cases} Y = \begin{pmatrix} x \\ \dot{x} \end{pmatrix} \\ A = \begin{bmatrix} 0 & I \\ -m^2 & 0 \end{bmatrix} \end{cases}$$

## BENCHIMOL

(i)  $(A, B)$  (APPROX.)  
 CONTROLLABLE

(ii)  $A$  HAS COMPACT RESOLVENT

(iii)  $[AY, Y] \leq 0$

$\Rightarrow (A - B B^*)$   
 STRONGLY STABLE

$$\dot{Y}(t) = A Y(t) + B u(t) \\ + K(Y(t))$$

$$\frac{d}{dt} E(t) = \frac{d}{dt} \left( \frac{1}{2} [M \dot{x}, \dot{x}] + \frac{1}{2} [A x, x] \right) \\ = - [B^* Y, B^* Y] \\ = - \|\dot{b}(t)\|^2$$

$$\dot{b}(t) = P \begin{pmatrix} \dot{u}_\phi(0) \\ \vdots \\ \dot{u}_\phi(s_1) \\ \omega_1(t) \\ \omega_4(t) \\ \dot{u}_\phi(t, s_2) \\ \vdots \\ \dot{u}_\phi(t, s_3) \end{pmatrix}$$

$$P \geq 0$$

→

$$u = -B^*Y$$

YIELDS ROBUST CONTROLLER

(i) CONTROL DOES NOT NEED  
'QUANTITATIVE' A:

NO NEED TO KNOW  
WHAT DAMPING IS- ETC

(ii) CONTROL DOES NOT  
DESTABILIZE ANY  
MODE

IN OUR CASE

$$Y(t) = \begin{vmatrix} x(t) \\ \dot{x}(t) \end{vmatrix}$$

→

$$B^*Y = \begin{matrix} 0 \\ 0 \\ 0 \\ b(t) \end{matrix}$$

~ RATE FEED-BACK

**Maneuvering of  
Flexible Spacecraft**  
by  
**Leonard Meirovitch**  
**Virginia Polytechnic  
Institute and State U.**  
**Blacksburg, Virginia**

MANEUVERING OF FLEXIBLE SPACECRAFT

LEONARD MEIROVITCH

DEPARTMENT OF ENGINEERING SCIENCE AND MECHANICS  
VIRGINIA POLYTECHNIC INSTITUTE AND STATE UNIVERSITY  
BLACKSBURG, VA 24061

PRESENTED AT THE 2ND ANNUAL SCOLE WORKSHOP  
NASA Langley Research Center  
December 9-10, 1985

## MANEUVERING OF FLEXIBLE SPACECRAFT

**Objectives:** 1) Simultaneous maneuvering and vibration suppression of LS  
2) Minimum-time rotational maneuver.

**Strategy:** Use a perturbation approach with the rigid-body maneuvering as the unperturbed solution (zero-order) and the vibration suppression as the perturbation (first-order). The first represents control of a nonlinear system, which can be open loop, and the second represents feedback control of a large-order, time-varying linear system.

**Advantage:** It obviates the need for solving a two-point boundary-value problem.

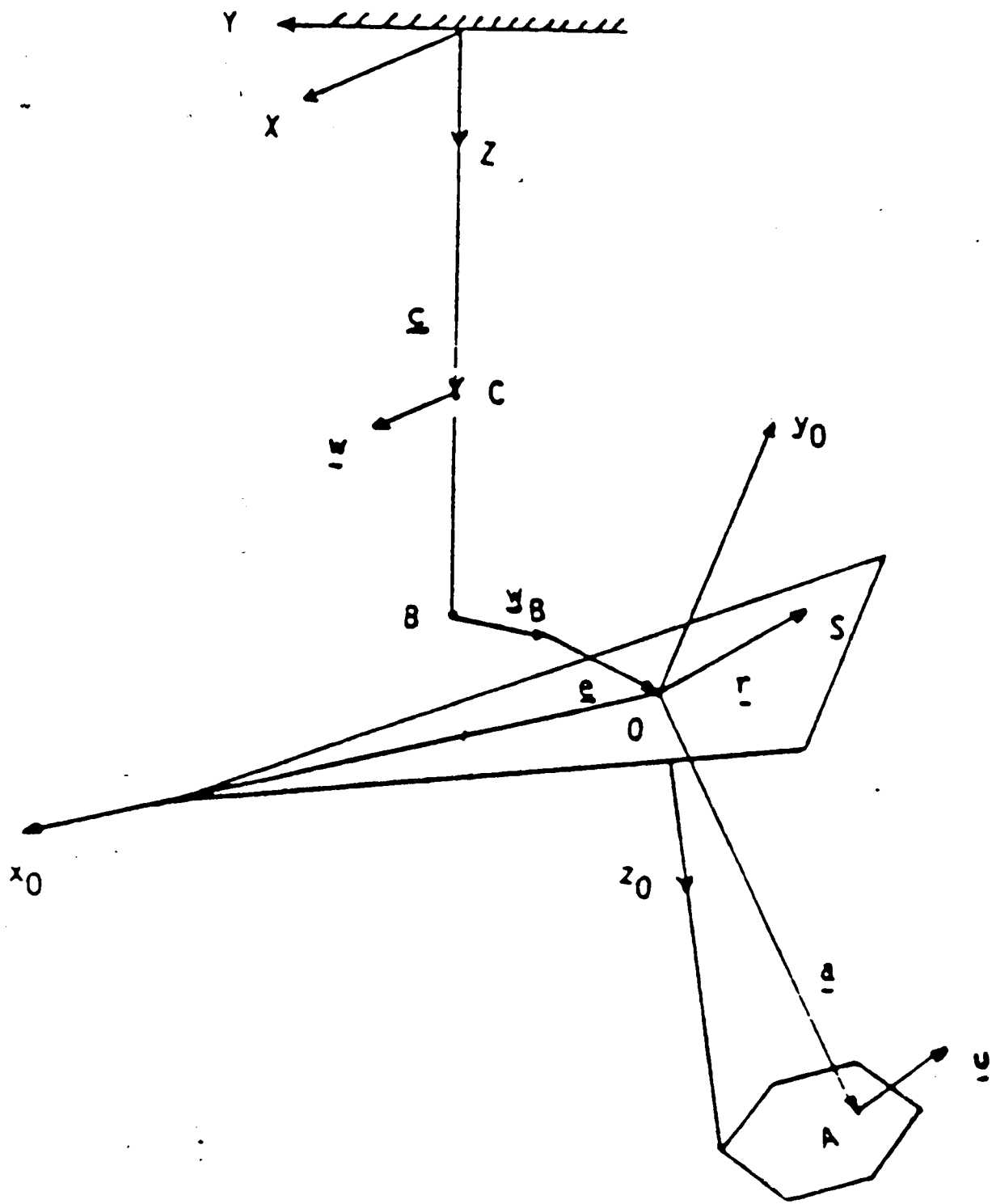


Figure 2.2 SCOLE configuration

## NOMENCLATURE

Position of a point on the cable:  $\underline{R}_C = \underline{c} + \underline{w}$

Position of a point on the shuttle:  $\underline{R}_S = \underline{c}_B + \underline{w}_B + \underline{e} + \underline{r}$

Position of a point on the appendage:  $\underline{R}_A = \underline{c}_B + \underline{w}_B + \underline{e} + \underline{a} + \underline{u}$

$\underline{w}$  = elastic displacement of a point on the cable

$\underline{u}$  = elastic displacement of a point on the appendage

Discretization in space:  $\underline{w} = \psi \underline{\eta}$ ,  $\underline{u} = \phi \underline{q}$

$\psi$  = matrix of admissible functions for the cable

$\phi$  = matrix of admissible functions for the appendage

## PERTURBATION SCHEME

Angular velocity of reference frame:  $\tilde{\omega}(t) = \omega_0(t) + \omega_1(t)$

$\omega_0(t)$  = angular velocity of rigid frame

$\omega_1(t)$  - first-order perturbation angular velocity

Perturbation angular velocity in terms of small angles  $\beta_1, \beta_2, \beta_3$

about the rigid frame

$$\omega_1(t) = \tilde{\omega}_0^T \tilde{B} + \dot{\tilde{B}}$$

## ZERO-ORDER AND FIRST-ORDER EQUATIONS OF MOTION

Zero-order equations:  $\dot{I}_B \ddot{\omega}_0 + \tilde{\omega}_0^T I_B \tilde{\omega}_0 = \tilde{M}_0$

First-order equations:  $\ddot{M}_{\tilde{x}} + G_{\tilde{x}} + (K_S + K_NS)_{\tilde{x}} = F^*$

Perturbations vector:  $\tilde{x}^T = [\eta^T \quad \beta^T \quad q^T]$

Perturbing force vector:  $F^* = [F_0^T + \psi_B F_1^T \quad M_0^T + M_1^T \quad Q_0^T + Q_1^T]$

$$M = \begin{bmatrix} \tilde{M}_C & \tilde{S}_B^T \psi_B & I_B \\ \tilde{S}_B \psi_B & \tilde{\Phi}^T & \tilde{\Phi} \\ \tilde{\Phi}^T & \tilde{\Phi} & M_A \end{bmatrix}$$

ZERO-ORDER AND FIRST-ORDER EQUATIONS OF MOTION (CONT'D)

$$\text{Gyroscopic Matrix: } G = \begin{bmatrix} \tilde{L}_C & 2\tilde{\psi}_B \tilde{\omega}_0 S_B & 2\tilde{\psi}_B \tilde{\omega}_0 \tilde{T} \\ -2(\tilde{\psi}_B \tilde{\omega}_0 T_S_B)^T & I_B \tilde{\omega}_0^T + \tilde{\omega}_0^T I_B + [I_B \tilde{\omega}_0] & \tilde{\omega}_0^T \tilde{\phi} + J_0 \\ -2(\tilde{\psi}_B \tilde{\omega}_0 \tilde{\Phi}) & -[\tilde{\omega}_0^T \tilde{\Phi}] + J_0^T & 2L_A \end{bmatrix}$$

$$\text{Symmetric Stiffness Matrix: } K_S = \begin{bmatrix} \tilde{L}_C + K_C & \tilde{\psi}_B \tilde{\omega}_0^2 S_B & \tilde{\psi}_B \tilde{\omega}_0 \tilde{T} \\ S_B \tilde{\omega}_0^2 \psi_B & \tilde{\omega}_0^T I_B \tilde{\omega}_0 & \tilde{\omega}_0^T J_0 + [C_0 g]^T \\ -\tilde{\omega}_0^2 \psi_B & J_0 \tilde{\omega}_0 + \tilde{\Phi}^T [C_0 g]^T & \tilde{L}_A + K_A \end{bmatrix}$$

$$\text{Nonsymmetric Stiffness Matrix: } K_{NS} = \begin{bmatrix} \tilde{L}_C & \tilde{\psi}_B \tilde{\omega}_0 S_B & \tilde{\psi}_B \tilde{\omega}_0 \tilde{T} \\ -(\tilde{\psi}_B \tilde{\omega}_0 T_S_B)^T & I_B \tilde{\omega}_0^T + [\tilde{I}_B \tilde{\omega}_0] \tilde{\omega}_0^T + \tilde{S}_B [C_0 g]^T & J_0 \\ -(\tilde{\psi}_B \tilde{\omega}_0 \tilde{\Phi})^T & \tilde{\Phi} \tilde{\omega}_0^T & \tilde{L}_A \end{bmatrix}$$

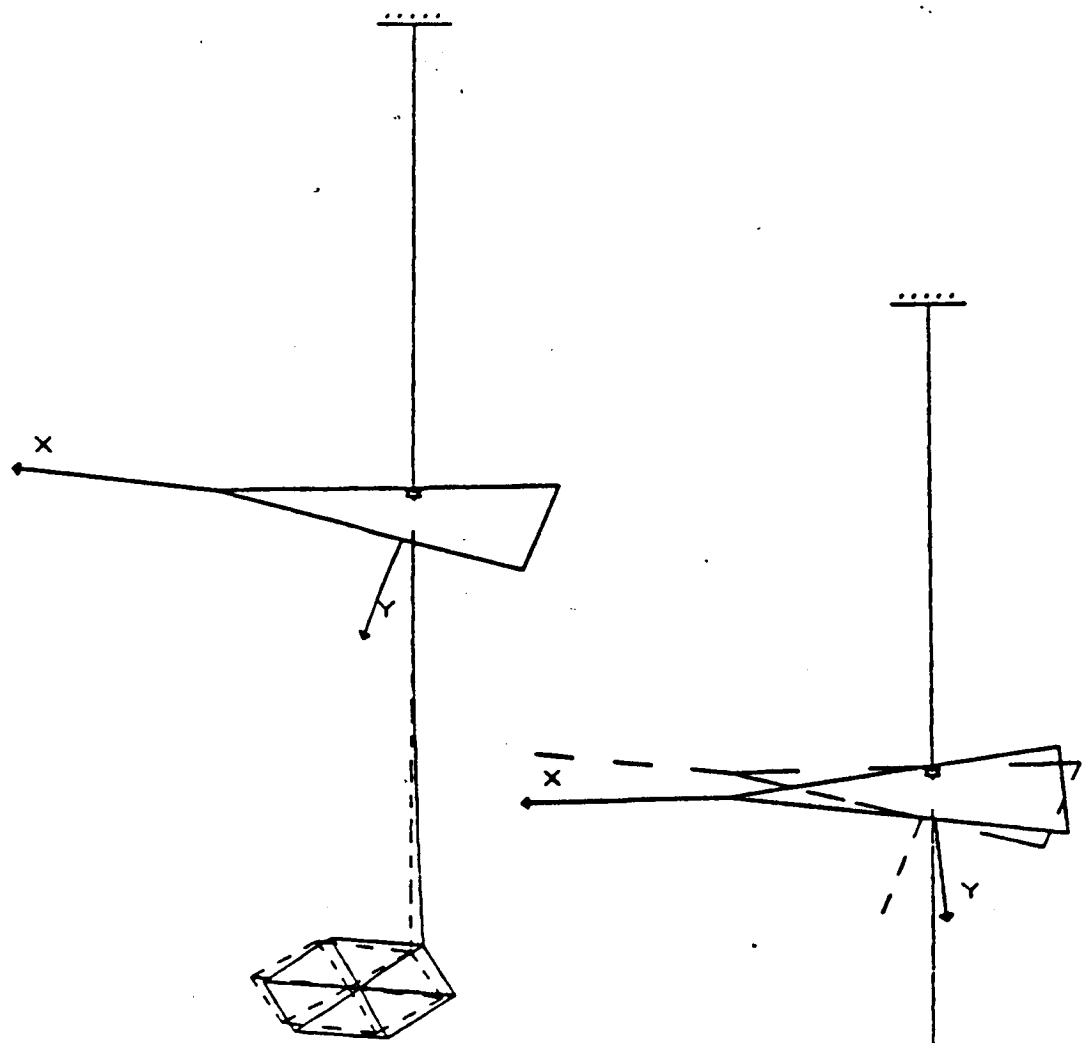


Figure 8.2 Static deflection,  
FACT = 2.5

Figure 8.3 Mode 1, FACT = 0.25,  
0.000001 Hz

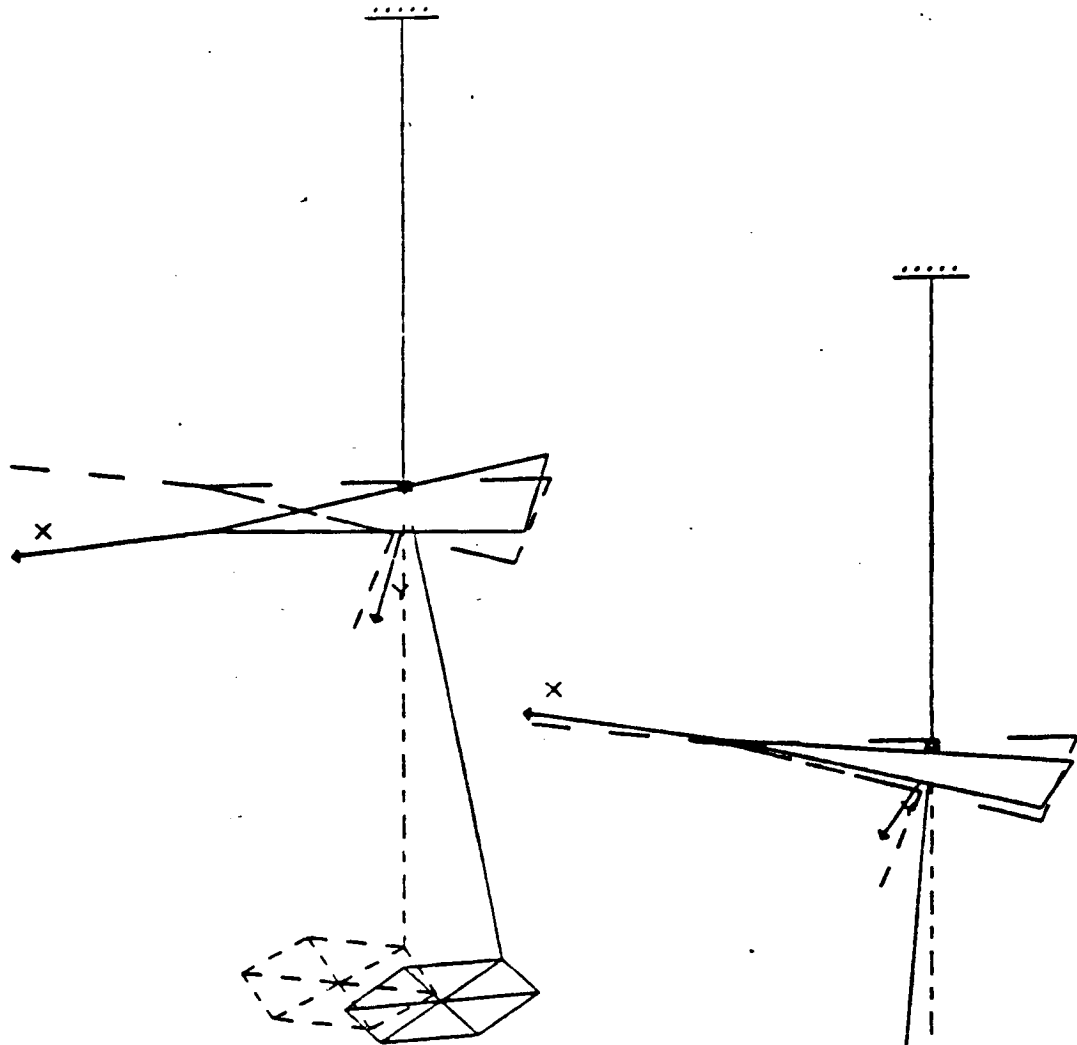


Figure 8.4 Mode 2, FACT = 0.25,  
0.026618 Hz



Figure 8.5 Mode 3, FACT = 0.25,  
0.033353 Hz

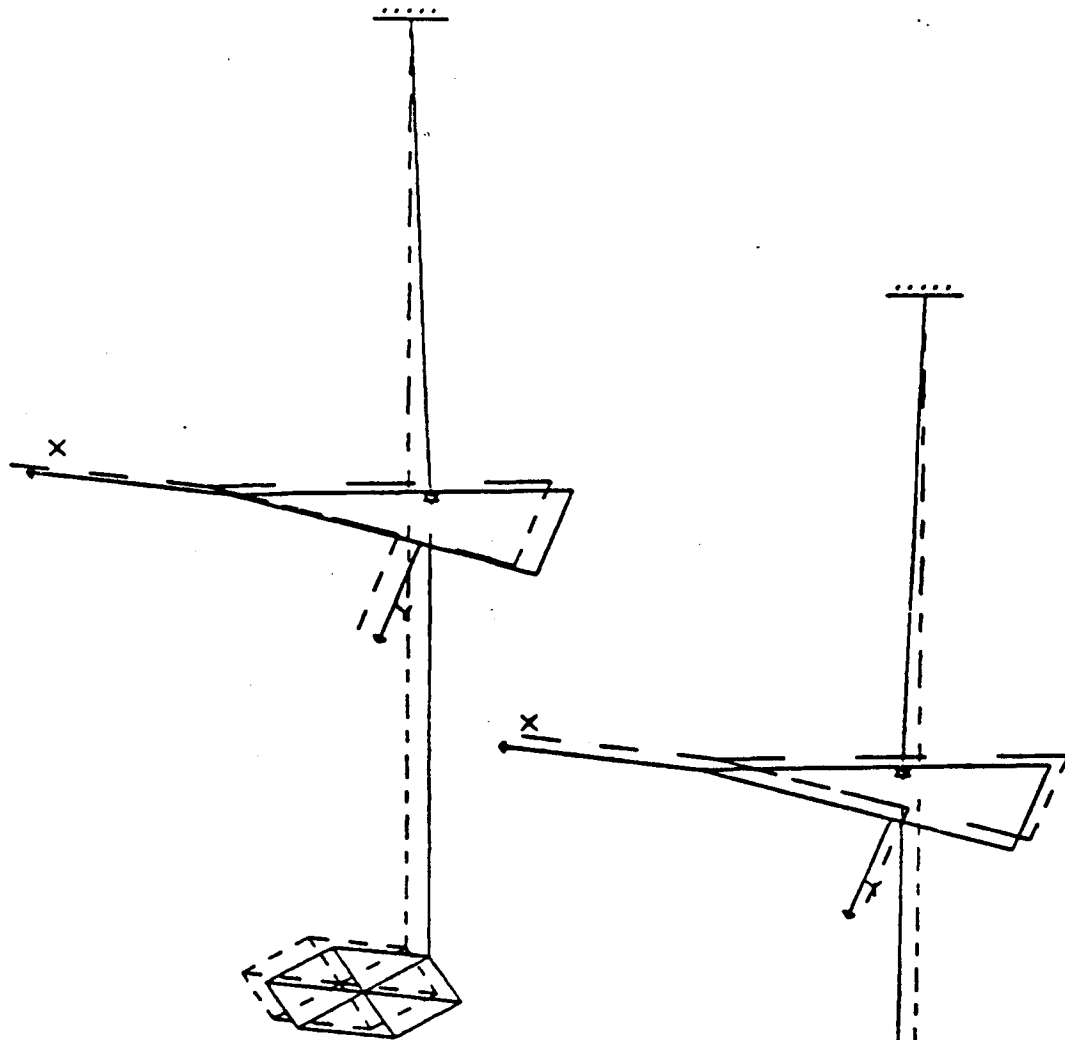


Figure 8.6 Mode 4, FACT = 0.50,  
0.275272 Hz



Figure 8.7 Mode 5, FACT = 0.50,  
0.275282 Hz

Table 8.4 Natural Frequencies (Hz)

Mode	Equilibrium Position		Zero Gravity (Space)	
	Actual	Massless Cable	Actual	Rigid Antenna
1	0.0	0.0	0.0	0.0
2	0.02661800	0.02661800	0.0	0.0
3	0.03335345	0.03335345	0.0	0.0
4	0.27527161	0.27550803	0.0	0.0
5	0.27528201	0.27551848	0.0	0.0
6	1.02135153	1.02136222	0.95626111	0.95781737
7	1.09274338	1.09275532	1.02205468	1.02304393
8	2.86993771	2.86993909	2.85798288	2.91078995
9	4.14099978	4.14100682	4.12238565	4.77249201
10	7.21202381	7.21203514	7.13573328	7.53400307
11	11.8888566	11.8892693	11.8067296	14.3285908
12	11.9975825	-----	-----	-----
13	11.9979985	-----	-----	-----
14	14.5271386	14.5271319	14.4703039	18.0655372
15	17.8807340	17.8965361	0.0	0.0
16	23.9951935	-----	-----	-----
17	23.9951971	-----	-----	-----
18	29.4618566	29.4618689	29.3765971	
19	31.9790379	31.9790406	31.8650183	
20	35.6083428	35.6083908	35.5681068	

Table 8.5 Cantilever Natural Frequencies (Hz)

Mode	Roll Angle (Deg)	
	0	180
1	0.90329379	0.74059481
2	0.92231250	0.74130235
3	2.85838001	2.84157907
4	4.11631152	4.06401370
5	7.18829155	7.03295932
6	11.8569533	11.6900310
7	14.5078152	14.3982264
8	29.4282394	29.2763643
9	31.9410827	31.7363829

# **Model Reference Control of the SCOLE**

**by**

**Dan Minnick  
Howard Kaufman  
Rensselaer Polytech. In.  
Troy, New York**

OUTLINE

- INTRODUCTION
- MODEL REFERENCE CONTROL OF LUMPED LINEAR SYSTEMS
  - THEORY
  - SCOPE APPLICATION
- MODEL REFERENCE CONTROL OF DPS
  - THEORY
  - SCOPE APPLICATION
- PLANNED ACTIVITIES

## INTRODUCTION

### SCOLE MODELS

LUMPED: 16th ORDER WITH 5 FLEXIBLE AND 3 RIGID BODY MODES

DISTRIBUTED: 3 PARTIAL DIFFERENTIAL EQUATIONS FOR ROLL,  
PITCH, YAW BEAM BENDING

LUMPED MODEL

$$\dot{x} = Ax + Bu$$

$$y = Cx$$

$$x^T = (\underline{u}_1^T, \dots, \underline{u}_r^T, \underline{\phi}_{RB}^T, \underline{\theta}_{RB}^T, \underline{\psi}_{RB}^T)$$

$$y_F^T = (\underline{\phi}_s^T, \underline{\theta}_s^T, \underline{\psi}_s^T, \underline{\phi}_r^T, \underline{\theta}_r^T, \underline{\psi}_r^T, \zeta_x, \zeta_y)$$

$$y^T = y_F^T + (\underline{\phi}_{RB}^T, \underline{\theta}_{RB}^T, \underline{\psi}_{RB}^T, \underline{\phi}_{RB}^T, \underline{\theta}_{RB}^T, \underline{\psi}_{RB}^T, 0, 0)$$

$$\underline{u}^T = (\underline{I}_s, f_r, I_r)$$

OBJECTIVE: IF  $\phi_{RB}(0) = 20^\circ$

$\phi_{RB} \rightarrow 0$  IN ABOUT 10 SEC.

$$|T| \leq 10,000$$

$$|f| \leq 800$$

DISTRIBUTED MODEL

ROLL BEAM BENDING:

$$PA \frac{\partial^2 u_\phi}{\partial t^2} + 2\zeta_\phi \sqrt{PA/EI_\phi} \frac{\partial^3 u_\phi}{\partial s^2 \partial t} + EI_\phi \frac{\partial^4 u_\phi}{\partial s^4} = \sum_{n=1}^4 [f_{\phi,n} \delta(s-s_n) + g_{\phi,n} \frac{\partial \delta}{\partial s}(s-s_n)]$$

PITCH BEAM BENDING:

$$PA \frac{\partial^2 u_\theta}{\partial t^2} + 2\zeta_\theta \sqrt{PA/EI_\theta} \frac{\partial^3 u_\theta}{\partial s^2 \partial t} + EI_\theta \frac{\partial^4 u_\theta}{\partial s^4} = \sum_{n=1}^4 [f_{\theta,n} \delta(s-s_n) + g_{\theta,n} \frac{\partial \delta}{\partial s}(s-s_n)]$$

YAW BEAM TORSION:

$$PI_\psi \frac{\partial^2 u_\psi}{\partial t^2} + 2\zeta_\psi I_\psi \sqrt{}$$

MODEL REFERENCE CONTROL OF LUMPED LINEAR SYSTEMS

THEORY

$$\left. \begin{array}{l} \dot{x}_p = A_p x_p + B_p u_p \\ y_p = C_p x_p \end{array} \right\} \text{PROCESS}$$

$$\left. \begin{array}{l} \dot{x}_m = A_m x_m + B_m u_m \\ y_m = C_m x_m \end{array} \right\} \text{REFERENCE MODEL}$$

DESIRE

$$y_p \rightarrow y_m$$

SPECIAL CASE (PMF)

$$x_p \rightarrow x_m$$

$$\text{OR } C_p = C_m = I$$

$$u_p = S_{21} x_m + S_{22} u_m + K(x_m - x_p)$$

$$B_p S_{21} = A_m - A_p$$

$$B_m = B_p S_{22}$$

$$(A_p - B_p K) \text{ STABLE}$$

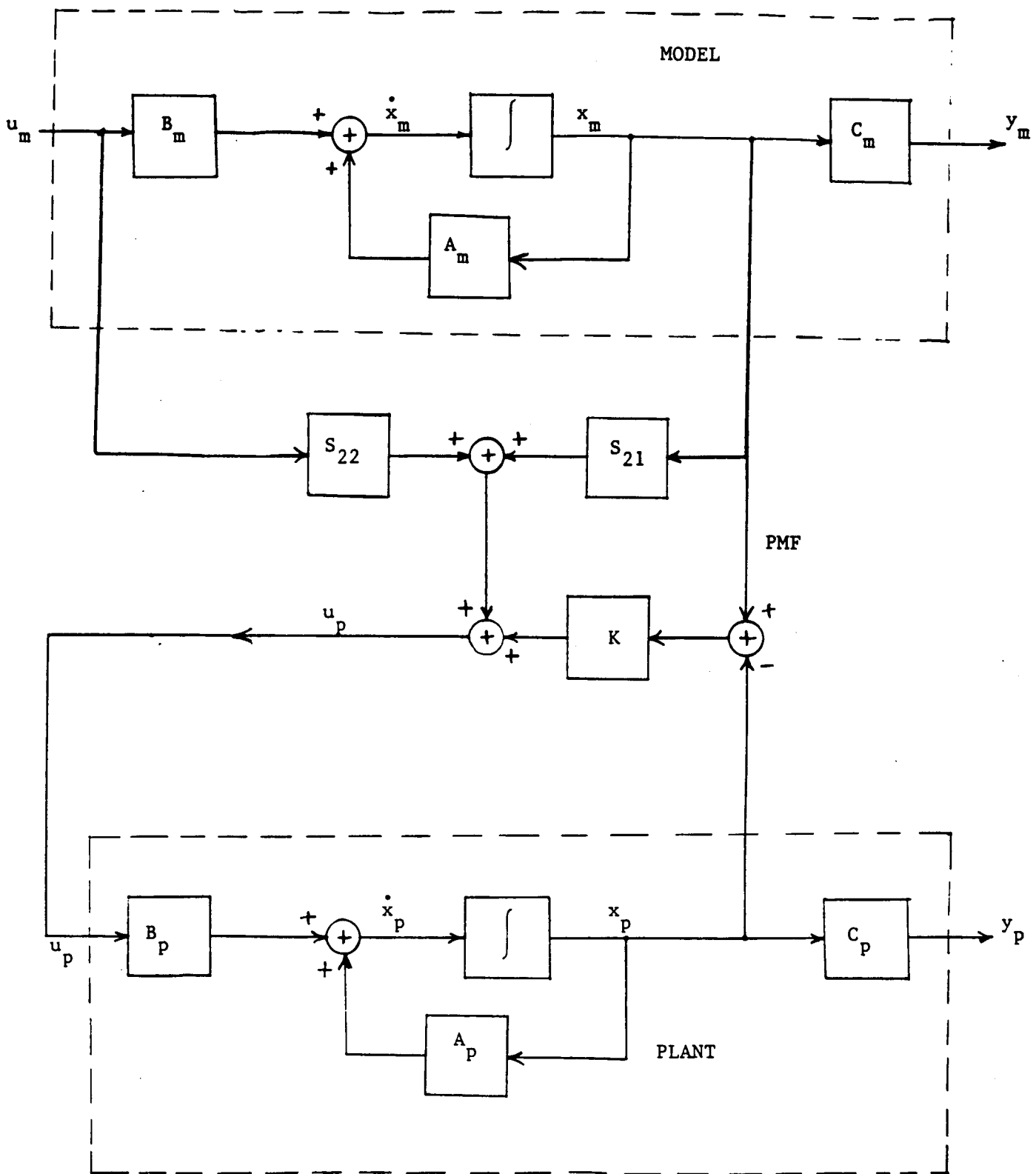


Figure 1: System block diagram.

SCOPE APPLICATION OF LUMPED MODEL FOLLOWING

OBSERVATIONS

- EIGHT CONTROLS
- EIGHT OUTPUT MODES TO BE CONTROLLED

PROCEDURES

- PMF  
 $x_p \rightarrow x_m$
- OUTPUT FOLLOWING  
 $y_p \rightarrow y_m$

MODEL REFERENCE CONTROL OF DISTRIBUTED SYSTEMS

$$m(x)u_{tt}(x,t) + D_0 u_t(x,t) + A_0 u(x,t) = f(x,t)$$

$$v_1 = u(x,t)$$

$$\text{BC} \quad v_1'''(0) = v_1'''(L) = 0$$

$$v_2 = \frac{\partial}{\partial t} u(x,t)$$

$$\text{and } v_2'''(0) = v_2'''(L) = 0$$

$$\dot{y} = Ay + Bf(x,t)$$

$$A = \begin{bmatrix} 0 & 1 \\ -A_0 & \frac{-D_0}{m(x)} \end{bmatrix}$$

$$B = \begin{bmatrix} 0 \\ \frac{1}{m(x)} \end{bmatrix}$$

$$y = Cv$$

### CONTROL PROBLEM FORMULATION

GIVEN THE DPS, IT IS DESIRED TO FIND A FINITE DIMENSIONAL CONTROLLER

SO THAT THE OUTPUT  $y(t)$  "FOLLOWS" A DESIRABLE OUTPUT TRAJECTORY  $y_m(t)$ .

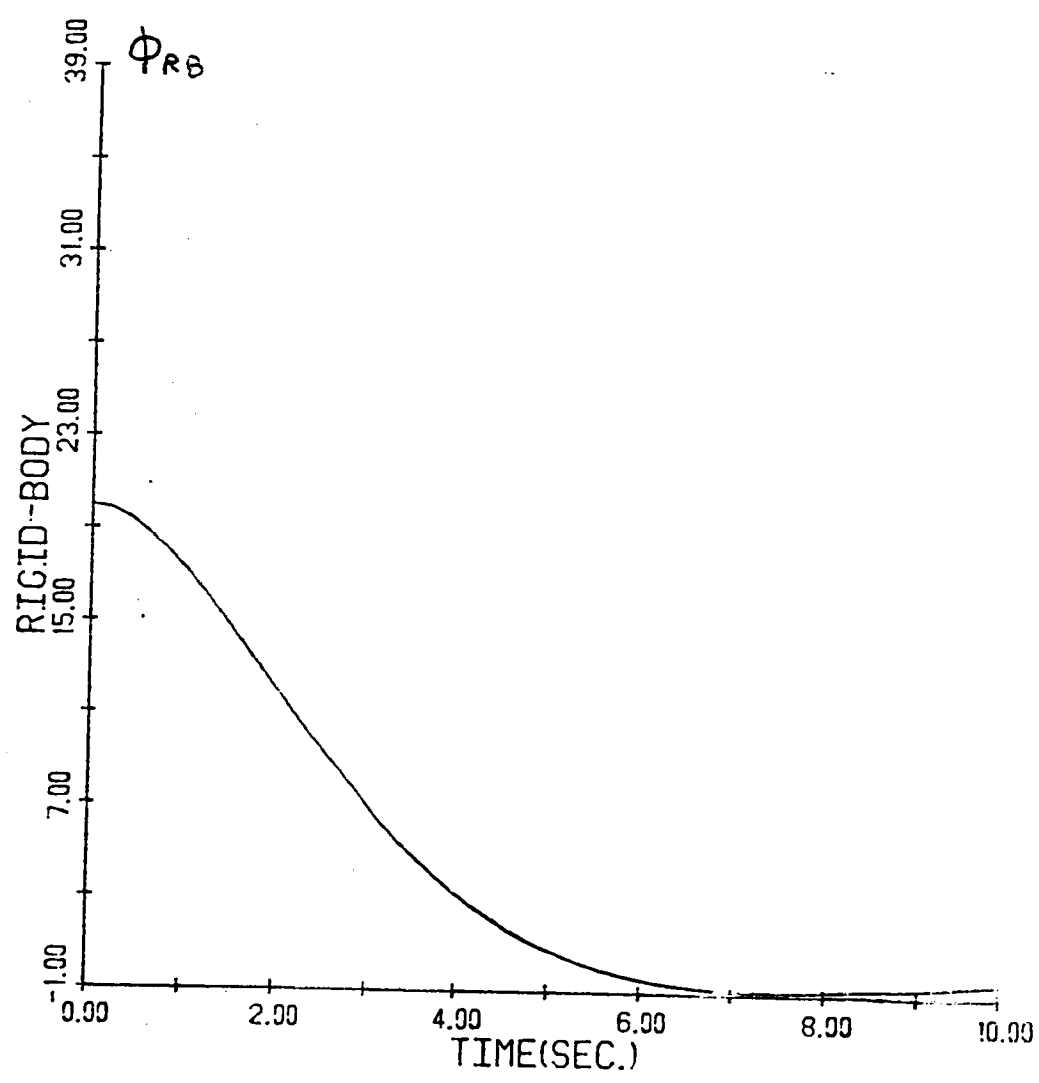
$$\dot{q} = A_m q + B_m u_m$$

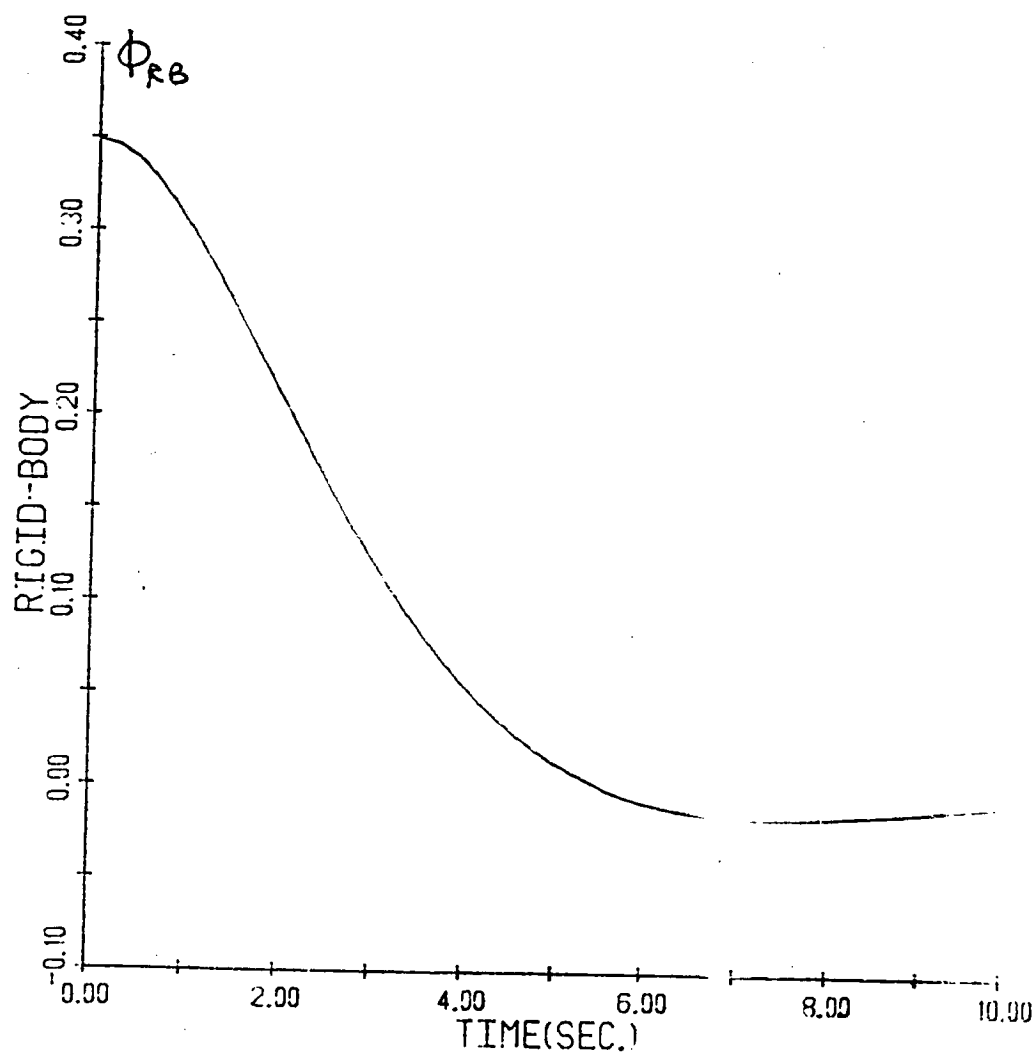
$$y_m = C_m q$$

### CONTROLLER STRUCTURE

$$f = S_{21}q + S_{22}u_m + G(y_m - y_p)$$

$$\dot{e} = (A - BG)e$$





ILLUSTRATIVE APPLICATION TO SCOLE ROLL

BEAM BENDING EQUATION

ASSUMPTIONS: PROOF MASSES NEGIGIBLE

DAMPING NEGIGIBLE

$$PA \ddot{v}(t,s) + EI v'''(t,s) =$$

$$\begin{aligned} m_1 \ddot{v}(t,s) + f_1 \delta(s-L) \\ + f_2 \delta'(s) + f_3 \delta'(s-L) \end{aligned}$$

FOR ILLUSTRATIVE PURPOSES WE WILL CONTROL

$$\omega_1 = \dot{v}(t, 0)$$

$$\omega_4 = \dot{v}(t, L)$$

AND

$$y = v(t, s_0) + \alpha \dot{v}(t, s_0)$$

WHERE

$$0 < s_0 < L$$

THUS

$$C = \begin{bmatrix} 0 & \frac{\partial}{\partial s} \delta(s) \\ 0 & \partial/\partial s [\delta(s-L)] \\ \delta(s-s_0) & \alpha \delta(s-s_0) \end{bmatrix}$$

## REFERENCE MODEL

$$\dot{q} = a_m q + b_m u_m$$

$$y_{m1} = c_1 q$$

$$y_{m2} = c_2 q$$

$$y_{m3} = c_3 q$$

$$\begin{aligned}
S_{11}^{-1}(s) = & \sum \frac{m_1 a_m c_1 x_k(0)}{K \frac{L}{4} (PA a_m^2 + EI K^4) x_k^2(L)} x_k(s) \\
& + S_{21}^{-1} \sum_k \frac{x_k(L)}{\frac{1}{4} (PA a_m^2 + EI K^4) x_k^2(L)} x_k(s) \\
& + S_{21}^{-2} \sum_k \frac{-x_k'(0)}{\frac{1}{4} (PA a_m^2 + EI K^4) x_k^2(L)} x_k(s) \\
& + S_{21}^{-3} \sum_k \frac{-x_k'(L)}{\frac{1}{4} (PA a_m^2 + EI K^4) x_k^2(L)} x_k(s)
\end{aligned}$$

WHERE  $x_k(s) = \left[ \begin{array}{c} \left( \frac{\sinh(KL)}{\cosh(KL)} - \frac{\sin(KL)}{\cosh(KL)} \right) (\cosh ks + \cos ks) \\ + \sinh(ks) + \sin(ks) \end{array} \right]$

RECALL THAT FOR TRUE STABILITY WE NEED

$$f = f^* + G(y_m - y) = f^* + GC(v^* - v)$$

THIS SYSTEM WILL BE STABLE FOR

$$G = \begin{vmatrix} 0 & 0 \\ G_1 & 0 \\ 0 & 0 \end{vmatrix}$$

WHERE  $G_1 > 0$ .

CURRENT EFFORTS

- SIMULATION OF ROLL BEAM PDE
- COMPUTATION OF TRUNCATED SERIES EXPANSIONS FOR  $f^*$
- EVALUATION OF THE MODEL REFERENCE CONTROLLER FOR  
VARIOUS MODELS AND OUTPUTS.

PLANNED ACTIVITIES

LUMPED SYSTEM

OUTPUT MODEL FOLLOWING

ROBUSTNESS STUDIES

ADAPTIVE MODEL FOLLOWING

DISTRIBUTED SYSTEM

MODEL FOLLOWING CONTROL OF ALL THREE BEAM MODES

ROBUSTNESS STUDY

ADAPTIVE CONTROL

# **Rapid Pointing and Vibration Control of the SCOLE Configuration**

**by**

**Jiguan Gene Lin  
Control Research Corp.  
Lexington, MA**

## STRUCTURAL VIBRATIONS

- o 10-MODE ABC-MODEL (DR. JOSHI)
  - o LINEARIZED DYNAMICS
    - DECOUPLED WITH RB MOTIONS
    - EXCITATION BY THE BPB LOS POINGING SLEW
  - o "SMALL" VIBRATIONS
    - OUTPUT AT BOTH ENDS OF MAST
  - o NEED OUTPUT FROM THE 12 SENSORS ALONG THE MAST
    - ACTUAL VIBRATIONS OF THE MAST
  - o NEED COMPLETE DYNAMICS (RB & EB)
    - CORIOLIS COUPLING COULD FURTHER EXCITE VIBRATIONS DUE TO RESULTING MOMENT SPILLOVER.

## RAPID LOS POINTING

o INITIAL ALIGNMENT AND BPB POINTING SLEW

o CORIOLIS COUPLING (w X)

-- MOVING SHUTTLE-BODY-FIXED COORDINATES

o DIRECT TORQUE/FORCE SPILLOVER

--SINGLE AXIS BB OR BPB

$$T_4 = T_1 T_{\text{DEFLECT}}$$

$$\text{i.e., } T_4^T = T_{\text{DEFLECT}}^T T_1^T$$

## VIBRATION CONTROL

### o CONTROL INFLUENCES

- ACTUATORS AT ENDS OF MAST ONLY
- HIGH FEEDBACK GAINS
- HENCE, HIGH ADDITIONAL TORQUES AND FORCES

### o NEED ACTUATION ALONG THE MAST.

# **A Perspective on the Control of Flexible Spacecraft**

**by**

**Mike Barrett  
K. W. Lips  
Honeywell  
Minneapolis, MN**

1. STRUCTURAL DYNAMICS  
EXPERIMENT

## PURPOSE

PREDICT MODE FREQUENCIES, MODE SHAPES  
AND MODAL DAMPING FOR JOINT - DOMINATED  
STRUCTURES ON GROUND AND IN-DESSIT

## PROBLEM AREAS

- JOINT CHARACTERIZATION
  - /linear? non/linear? effect of location?
- DAMPING
  - /linear viscous? hysteretic? visco elastic?
- ENVIRONMENTAL
  - gravity? solar pressure? thermal? vacuum? aerodynamic?
- IN-ORBIT DYNAMIC LOADING (contracks-needed, experiment-induced)
  - orbit rate? spin/slew maneuvers? deployment / retraction?

## OVERVIEW

### STRUCTURAL DYNAMICS EXPERIMENT

#### (I) GROUND - BASED

- DEVELOP GROUND - BASED STRUCTURAL MODELS OF MAST BOOM ANTENNA ...  
assume mast type models are also available from contractor)
- CALCULATE MODAL DATA FOR EACH STRUCTURE
- CONDUCT MODEL SURVEY TESTS ON GROUND
- CORRELATE CALCULATED WITH MEASURED DATA

## OVERVIEW (cont'd.)

### (II) IN-ORBIT

- DEVELOP IN-ORBIT SYSTEM MODEL  
CORBITER + MAST + BOOM --- ANTENNA ... )
- USE BEST STRUCTURAL MODELS FROM (I)
- TREETOPS SYSTEM MODEL = ORBITER + MAST + ...
- CALCULATE SYSTEM MODEL BEHAVIOR IN-ORBIT
- CONDUCT MODAL SURVEY TESTS IN-ORBIT
- CORRELATE CALCULATED WITH MEASURED DATA

### (III)

### ASSESS MODELING, ESTIMATION TOOLS

**2. SYSTEMS IDENTIFICATION EXPERIMENTS**

## PURPOSE

Maximum likelihood identification of control-relevant modal properties for joint-dominated structures on ground and in orbit

## IDENTIFICATION PROBLEM ISSUES

- Identification Objectives (driven by control requirements)
- Initial Conditions/Convergence
- Test Signals
- Sensor/Actuator Placement (Control Related)
- Control Hardware Limitations
- Realistic Disturbances/Noise Characteristics
- Closely Spaced Modes
- Computational Complexity

## SYSTEMS IDENTIFICATION EXPERIMENTS

### (1) GROUND-BASED

- Start with ground-based structural model from structural dynamics experiment
- Conduct analyses of identification issues (control related)
- Select and place sensors and actuators (control related)
- Excite structure and measure responses
- Process data with batch MLE algorithm and identify modal parameters (frequencies, dampings, shapes) for critical modes
- Correlate identified model with apriori model and refine

## SYSTEMS IDENTIFICATION EXPERIMENTS (CONTINUED)

### (II) IN-ORBIT

- Start with in-orbit structural model from structural dynamics experiment
- Refine analyses of identification issues (control related)
- Select and place sensors and actuators (control related)
- Excite structure and measure responses
- Process data with batch MLE algorithm and identify modal parameters (frequencies, dampings, shapes) for critical modes
- Correlate identified model with apriori model and identified ground-based model and refine
- Assess adequacy of MLE identification methodology for providing reliable structural models for control design

**3. ROBUST CONTROL EXPERIMENTS**

## PURPOSE

Robust control of joint-dominated structures on  
ground and in orbit

## Control Problem Issues

- Control Objectives
- Disturbance Characteristics vs. Control Requirements
- Sensor/Actuator Placement
- Control Hardware Limitations
- Robustness to model uncertainty: Apriori vs. identified model
- Computational complexity

## **Robust Control Experiments**

### **(I) Ground-Based**

- Start with ground-based structural model from structural dynamics or systems identification experiments
- Conduct analyses of control issues (driven by control requirements)
- Select and place sensors and actuators
- Design control laws that are robust to model uncertainty
- Verify closed-loop stability and performance robustness
- Correlate actual results with analyses

## Robust Control Experiments (Continued)

### (III) IN-ORBIT

- Start with in-orbit structural model from structural dynamics or systems identification experiments
- Refine analyses of control issues (driven by control requirements)
- Select and place sensors and actuators
- Design control laws that are robust to model uncertainty
- Verify closed-loop stability and robustness
- Correlate actual results with analyses
- Assess adequacy of control design methodology for meeting control objectives

**Equations du Mouvement  
d'une poutre Flexible  
en Rotation Autour  
d'un Axe**

by

**Lionel R. Passeron  
Aerospatiale  
Cannes, France**

EQUATIONS DU MOUVEMENT D'UNE POUTRE  
FLEXIBLE EN ROTATION AUTOUR D'UN AXE

On détermine, dans ce qui suit, les équations du mouvement d'une poutre flexible encastrée à sa base sur un axe vertical en rotation.

On néglige la flexion verticale pour ne s'intéresser qu'aux mouvements de traction-compression et de flexion horizontale : autrement dit, la poutre est supposée se déplacer dans un plan horizontal.

### 2.1 - NOTATIONS ET HYPOTHESES

#### 2.1.1 - Notations

On dénote respectivement :

- par  $I = (O, \vec{i}, \vec{j}, \vec{k})$  un repère inertiel, le vecteur  $\vec{k}$  étant dirigé suivant la verticale,
- par  $R = (O, \vec{i}, \vec{j}, \vec{k})$  un repère lié à la barre considérée comme rigide,
- par  $\theta$  l'angle de la rotation autour de  $\vec{k}$  permettant de passer du repère  $I$  au repère  $R$ .

La ligne moyenne de la poutre à l'équilibre est dirigée suivant l'axe  $\vec{i}$ .

On désigne respectivement :

- par  $G(x)$  le point courant de la ligne moyenne,
- par  $\rho(x)$  la masse volumique de la poutre
- par  $S(x)$  la surface de la section droite de la poutre
- par  $I_z(x)$  le moment quadratique de  $S(x)$  par rapport à l'axe  $Gz$  (la dimension de  $I_z$  est celle d'une longueur à la puissance quatre).

#### 2.1.2 - Hypothèses

En sus des hypothèses classiques :

- (H.1) - les déformations restent petites,

(H.2) - chaque section droite reste plane au cours de la déformation.

on suppose que :

(H.3) - l'axe Gz (parallèle à l'axe de rotation  $\vec{K}$ ) est un axe principal d'inertie pour la section droite S.

## 2.2 - CALCUL DU LAGRANGIEN DU SYSTEME

### 2.2.1 - Préliminaires

- Poutre non déformée : le point G occupe la position  $G_0$  de composantes  $(x, 0, 0)$  dans le repère R.

- Poutre déformée : le point G occupe la position définie par les composantes  $(x+u, v, 0)$  dans le repère R. Si  $\alpha(x)$  désigne l'angle que fait la tangente à la ligne moyenne de la poutre avec l'axe i, l'hypothèse H.3 permet d'écrire

$$\alpha(x) = \frac{\partial v}{\partial x}$$

### 2.2.2 - Calcul de l'énergie cinétique d'un élément de la poutre

Considérons une tranche élémentaire de poutre, comprise entre les sections droites voisines  $S(x)$  et  $S(x + dx)$ .

L'énergie cinétique de cette tranche s'écrit comme somme :

- de son énergie cinétique de translation :

$$dT_t = \frac{1}{2} \rho S v_G^2 dx$$

- et de son énergie cinétique de rotation qui (cf. hypothèse H.3) s'exprime sous la forme :

$$dT_r = \frac{1}{2} \rho I_z \omega^2 dx$$

$\omega$  désignant la vitesse de rotation de cette tranche.

#### 2.2.2.1 - Energie cinétique de translation

La vitesse absolue  $\vec{v}_G$  du point G est égale à la somme de sa vitesse d'entraînement  $\vec{v}_{Ge}$  par rapport au repère inertiel I et de sa vitesse relative  $\vec{v}_{Gr}$  par rapport au repère R.

En désignant par :

$$\vec{\omega}_e = \dot{\theta} \vec{K}$$

la vitesse de rotation d'entraînement du repère R par rapport au repère I, il vient :

$$\vec{v}_{Ge} = \vec{\omega}_e \wedge \vec{OG}$$

Projetons cette relation sur le repère R. On obtient :

$$\begin{array}{c|c|c|c} \vec{\omega}_e & \begin{matrix} 0 \\ 0 \\ \dot{\theta} \end{matrix} & \vec{OG} & \begin{matrix} x + u \\ v \\ 0 \end{matrix} & \vec{v}_{Ge} & \begin{matrix} -\dot{\theta} v \\ \dot{\theta}(x + u) \\ 0 \end{matrix} \end{array}$$

De même, dans le repère R :

$$\vec{v}_{Gr} \begin{vmatrix} \dot{u} \\ \dot{v} \\ 0 \end{vmatrix}$$

Il en résulte l'expression de  $\vec{v}_G$  dans le repère R :

$$\begin{array}{c|c} \vec{v}_G & \begin{matrix} \dot{u} - \dot{\theta}v \\ \dot{v} + \dot{\theta}(x + u) \\ 0 \end{matrix} \end{array}$$

et finalement :

$$(1) \quad dT_t = \frac{1}{2} \rho S \{ [\dot{u} - \dot{\theta}v]^2 + [\dot{v} + \dot{\theta}(x + u)]^2 \} dx$$

#### 2.2.2.2 - Energie cinétique de rotation

Soit  $\vec{\omega}_r$  la vitesse de rotation relative de S par rapport au repère R :

$$\vec{\omega}_r = \dot{\alpha} \vec{K}$$

Il vient :

$$\vec{\omega} = \vec{\omega}_e + \vec{\omega}_r$$

soit :

$$\vec{\omega} = (\dot{\theta} + \dot{\alpha}) \vec{K}$$

ce qui, puisque (cf. § 2.2.1) :

$$\alpha = v'$$

fournit :

$$\vec{\omega} = (\dot{\theta} + \dot{v}') \vec{K}$$

Ainsi :

$$(2) \quad dT_r = \frac{1}{2} \rho I_z (\dot{\theta} + \dot{v}')^2 dx$$

### 2.2.3 - Calcul de l'énergie potentielle d'un élément de poutre

Cette énergie potentielle est égale à la somme de l'énergie potentielle de traction-compression et de l'énergie potentielle de flexion.

#### 2.2.3.1 - Energie potentielle de traction-compression

Elle s'écrit (cf. référence (1), tome 2, page 35) :

$$dV_c = \frac{1}{2} \frac{N^2}{ES} dx$$

avec :

N : contrainte normale

E : module d'Young du matériau

Comme (cf. référence (1), tome 3, page 125) :

$$N = ES \frac{\partial u}{\partial x}$$

il vient :

(3)

$$dV_C = \frac{1}{2} ES (u')^2 dx$$

#### 2.2.3.2 - Energie potentielle de flexion

Elle s'écrit (cf. référence (1), tome 2, page 61) :

$$dV_f = \frac{1}{2} \frac{M_z^2}{EI_z}$$

où  $M_z$  est la contrainte de flexion.

Comme (cf. référence (1), tome 3, page 125) :

$$M_z = EI_z \frac{\partial \alpha}{\partial x}$$

il vient :

$$dV_f = \frac{1}{2} EI_z (\alpha')^2$$

ou encore (cf. § 2.2.1) :

(4)

$$dV_f = \frac{1}{2} EI_z (v'')^2$$

#### 2.2.4 - Lagrangien du système

Ce Lagrangien s'écrit sous la forme :

$$L = \int_0^L \hat{L} dx$$

avec :

$$\hat{L} = \hat{T} - \hat{V}$$

et (cf. § 2.2.2) :

$$\hat{T} = \frac{1}{2} \rho S \{ [\dot{u} - \dot{\theta}v]^2 + [\dot{v} + \dot{\theta}(x + u)]^2 \} + \frac{1}{2} \rho I_z (\dot{\theta} + \dot{v}')^2$$

et (cf. § 2.2.3) :

$$\hat{V} = \frac{1}{2} ES (u')^2 + \frac{1}{2} EI_z (v'')^2$$

D'où l'expression de  $\hat{L}$  :

(5)

$$\begin{aligned} \hat{L} = & \frac{1}{2} \rho S \{ [\dot{u} - \dot{\theta}v]^2 + [\dot{v} + \dot{\theta}(x + u)]^2 \} + \frac{1}{2} \rho I_z (\dot{\theta} + \dot{v}')^2 \\ & - \frac{1}{2} ES (u')^2 - \frac{1}{2} EI_z (v'')^2 \end{aligned}$$

### 2.3 - OBTENTION DES EQUATIONS DU MOUVEMENT

#### 2.3.1 - Formulation générale

La poutre est soumise à un couple :

$$\vec{M}(t) = M(t) \vec{k}$$

au point O.

Les forces de pesanteur ne travaillent pas (car perpendiculaires à tout déplacement virtuel ( $\delta u, \delta v, \delta \theta$ )), n'interviennent pas.

Les équations du mouvement s'écrivent donc sous la forme (cf. référence (2), page 233) :

$$(e.1) \quad \frac{\partial \hat{L}}{\partial u} - \frac{\partial}{\partial x} \left( \frac{\partial \hat{L}}{\partial u''} \right) + \frac{\partial^2}{\partial x^2} \left( \frac{\partial \hat{L}}{\partial u''} \right) - \frac{\partial}{\partial t} \left( \frac{\partial \hat{L}}{\partial \dot{u}} \right) + \frac{\partial^2}{\partial x \partial t} \left( \frac{\partial \hat{L}}{\partial \dot{u}'} \right) = 0$$

$$(e.2) \quad \frac{\partial \hat{L}}{\partial v} - \frac{\partial}{\partial x} \left( \frac{\partial \hat{L}}{\partial v'} \right) + \frac{\partial^2}{\partial x^2} \left( \frac{\partial \hat{L}}{\partial v''} \right) - \frac{\partial}{\partial t} \left( \frac{\partial \hat{L}}{\partial \dot{v}} \right) + \frac{\partial^2}{\partial x \partial t} \left( \frac{\partial \hat{L}}{\partial \dot{v}'} \right) = 0$$

$$(e.3) \quad \frac{d}{dt} \left[ \frac{\partial \hat{L}}{\partial \theta} \right] - \frac{\partial \hat{L}}{\partial \dot{\theta}} = M$$

avec les conditions aux limites :

$$(cl.1) \quad \left[ \frac{\partial \hat{L}}{\partial u} - \frac{\partial}{\partial x} \left( \frac{\partial \hat{L}}{\partial u''} \right) - \frac{\partial}{\partial t} \left( \frac{\partial \hat{L}}{\partial \dot{u}'} \right) \right] \delta u = 0 \quad \text{pour } x = 0 \text{ et } x = L$$

$$(cl.2) \quad \frac{\partial \hat{L}}{\partial u''} \delta u' = 0 \quad \text{pour } x = 0 \text{ et } x = L$$

$$(cl.3) \quad \left[ \frac{\partial \hat{L}}{\partial v'} - \frac{\partial}{\partial x} \left( \frac{\partial \hat{L}}{\partial v''} \right) - \frac{\partial}{\partial t} \left( \frac{\partial \hat{L}}{\partial \dot{v}'} \right) \right] \delta v = 0 \quad \text{pour } x = 0 \text{ et } x = L$$

$$(cl.4) \quad \frac{\partial \hat{L}}{\partial v''} \delta v' = 0 \quad \text{pour } x = 0 \text{ et } x = L$$

### 2.3.2 - Formulation explicite

Tous calculs faits, les relation (e.1) et (e.2) s'expriment sous la forme :

$$(e'.1) \quad \rho S \dot{\theta} [\ddot{v} + \dot{\theta}(x + u)] + \frac{\partial}{\partial x} (\rho S u') + \rho S (-\ddot{u} + \ddot{\theta}v + \dot{\theta}\dot{v}) = 0$$

$$(e'.2) \quad -\rho S \dot{\theta} (\dot{u} - \dot{\theta}v) - \frac{\partial^2}{\partial x^2} (\rho I_z v'') - \rho S [\ddot{v} + \ddot{\theta}(x + u) + \dot{\theta}\dot{u}] + \frac{\partial}{\partial x} (\rho I_z \ddot{v}') = 0$$

Sachant que :

$$\frac{\partial L}{\partial \dot{\theta}} = 0$$

la relation (e.3) s'écrit sous forme intégrale :

$$(e'.3) \quad \left[ \frac{\partial L}{\partial \dot{\theta}} \right]_{t_0}^t = \int_{t_0}^t M(y) dy$$

avec :

$$\begin{aligned} \frac{\partial L}{\partial \dot{\theta}} &= \left[ \int_0^L \{ I_z + S [(x + u)^2 + v^2] \} \rho dx \right] \dot{\theta} \\ &\quad + \int_0^L \{ I_z \dot{v}' + S [\dot{v} (x + u) - \dot{u}v] \} \rho dx \end{aligned}$$

En ce qui concerne les conditions aux limites (cl.1) et (cl.2), on obtient respectivement :

$$\frac{\partial \hat{L}}{\partial u'} - \frac{\partial}{\partial x} \left( \frac{\partial \hat{L}}{\partial u''} \right) - \frac{\partial}{\partial t} \left( \frac{\partial \hat{L}}{\partial \dot{u}'} \right) = - E S u'$$

$$\frac{\partial \hat{L}}{\partial u''} = 0$$

En ce qui concerne les conditions aux limites (cl.3) et (cl.4), on obtient respectivement :

$$\frac{\partial \hat{L}}{\partial v'} - \frac{\partial}{\partial x} \left( \frac{\partial \hat{L}}{\partial v''} \right) - \frac{\partial}{\partial t} \left( \frac{\partial \hat{L}}{\partial \dot{v}'} \right) = \frac{\partial}{\partial x} (E I_z v'') - \rho I_z (\ddot{\theta} + \ddot{v}')$$

$$\frac{\partial \hat{L}}{\partial v''} = - E I_z v''$$

a) conditions aux limites en  $x = 0$  :

En  $x = 0$ , la poutre est encastrée. Elle satisfait donc les conditions géométriques :

$$u(0, t) = 0$$

$$v(0, t) = 0$$

$$v'(0, t) = 0$$

On a alors :

$$\delta u|_{x=0} = 0 \quad \delta v|_{x=0} = 0 \quad \delta v'|_{x=0} = 0$$

et les conditions aux limites (cl.1) à (cl.4) sont satisfaites.

b) conditions aux limites en  $x = L$  :

En  $x = L$ , la poutre est libre. Elle ne satisfait donc aucune condition géométrique, ce qui permet de choisir des déplacements virtuels non nuls :

$$\delta u|_{x=L} \neq 0 \quad \delta v|_{x=L} \neq 0 \quad \delta v'|_{x=L} \neq 0$$

Les conditions aux limites (cl.1) à (cl.4) fournissent alors respectivement :

$$- E S u' \Big|_{x=L} = 0 \implies u'(L, t) = 0$$

$$\left[ \frac{\partial}{\partial x} (E I_z v'') - \rho I_z (\ddot{\theta} + \ddot{v}') \right] \Big|_{x=L} = 0$$

$$- E I_z v'' \Big|_{x=L} = 0 \implies v''(L, t) = 0$$

///

## CONCLUSION

Les équations du mouvement d'une poutre flexible encastrée à sa base sur un axe vertical en rotation s'écrivent :

- . équation de traction-compression

$$\left\{ \frac{\partial}{\partial x} (E S u') - \rho S \ddot{u} \right\} + \rho S [\ddot{\theta} v + 2 \dot{\theta} \dot{v} + \dot{\theta}^2 (x + u)] = 0$$

- . équation de flexion

$$\begin{aligned} \left\{ \frac{\partial}{\partial x} (\rho I_z \ddot{v}') - \frac{\partial^2}{\partial x^2} (E I_z v'') - \rho S \ddot{v} \right\} \\ - \rho S [\ddot{\theta}(x + u) + 2 \dot{\theta} \dot{u} - \dot{\theta}^2 v] = 0 \end{aligned}$$

- . équation de rotation d'ensemble

$$\frac{\partial L}{\partial \dot{\theta}} \Big|_t - \frac{\partial L}{\partial \dot{\theta}} \Big|_{t=t_0} = \int_{t_0}^t M(y) dy$$

avec :

$$\begin{aligned} \frac{\partial L}{\partial \dot{\theta}} = & \left[ \int_0^L \{I_z + S [(x + u)^2 + v^2]\} \rho dx \right] \dot{\theta} \\ & + \int_0^L \{I_z \dot{v}' + S [\dot{v}(x + u) - \dot{u}v]\} \rho dx \end{aligned}$$

Les conditions aux limites s'expriment sous la forme :

- . en  $x = 0$

$$u(0, t) = 0$$

$$v(0, t) = 0$$

$$v'(0, t) = 0$$

- . en  $x = L$

$$u'(L, t) = 0$$

$$\frac{\partial}{\partial x} (E I_z v'') - \rho I_z (\ddot{\theta} + \ddot{v}') = 0 \quad \text{pour } x = L$$

$$v''(L, t) = 0$$

# **Flexible Beam Simulation**

**by**

**Shalom Fisher  
Tom Posbergh  
Naval Research Lab  
Washington, D. C.**

## Flexible Beam Model, Nonlinear Slew Simulation

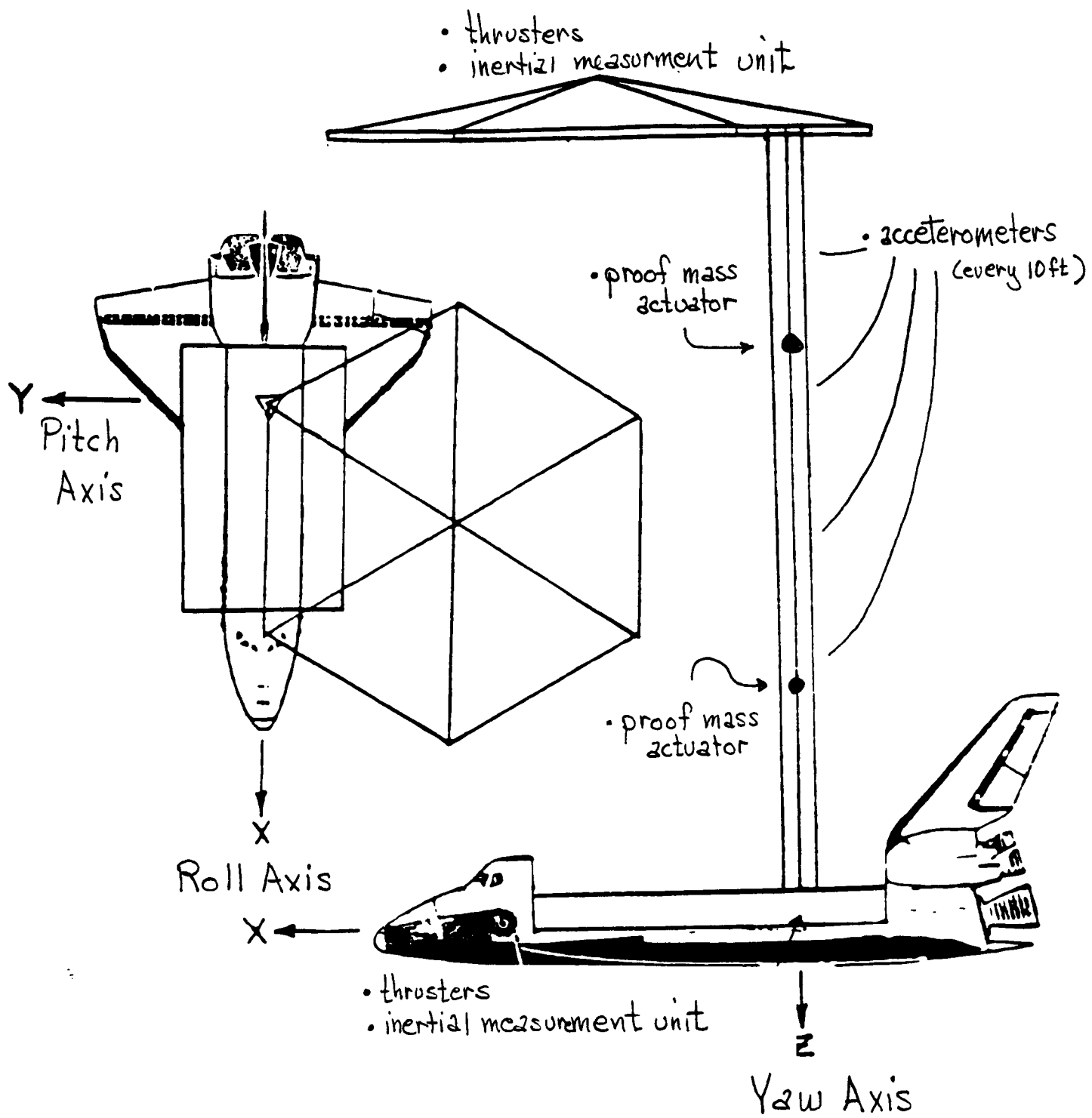
- DISCOS simulation of nonlinear slew of SCOLE configuration with a flexible beam.
- NASTRAN finite-element program provides modal frequencies and displacements of beam.
- Open loop commanded roll only slew of 20 degrees Bang-bang control of torque thrusters.
- Regulator design is based upon linear quadratic theory, with a deterministic SCOLE model, to calculate the feedback forces used to suppress beam oscillations during the slew.

## DISCOS CHARACTERISTICS

- Treats systems of rigid or flexible interconnected bodies.
- Points of contact between bodies are hinges with 6 degrees of freedom. They can be locked or treated as springs along any or all of the 6 degrees of freedom.
- Location of hinges and sensors with respect to body cm and body reference points are user-defined.
- Can evaluate non-linear dynamics, as well as linear oscillations of system.
- External torques and forces can be added by the user.

# SCOLE CONFIGURATION

## Sensors and Actuators



## COMPARISON OF MODEL FIDELITY

Mode Number	Type	Defined Frequency	3 Rigid Body Model	NASTRAN/ DISCOS
7	PITCH BENDING	0.29	$H_3$	0.28 $H_2$
8	ROLL BENDING	0.32	$H_3$	0.31
9	TORSION	0.53		0.81
10	ROLL BENDING	1.29	1.14	1.18
11	PITCH BENDING	1.65	2.30	2.045
12	ROLL BENDING	4.80		4.68
13	PITCH BENDING	4.97		5.45
14	ROLL BENDING	12.3		11.88
15	PITCH BENDING	12.4		12.55
:				
20	TORSION		45.1	

## Regulator Design

- Full-state feedback, no sensor or actuator time delays, or noise disturbances.
- Linear quadratic regulator theory is used to determine the feedback to suppress beam oscillations during the entire slew.
- The shuttle-reflector-beam system is modelled by deterministic methods.

## Regulator for flexible beam

- Purpose: To maintain the flexible beam in a nominally unbent position during the large angle slew.
- Model: Obtained from DISCOS and linearized about unbent position of the beam.  
(This is a modal model of the beam.)

$$\dot{\hat{x}}(t) = A\hat{x}(t) + Bu(t)$$

where  $\hat{x}(t) = x(t) - x_o$

$x_o$  = rest configuration of beam

$$A = \frac{\partial f}{\partial x} \Big|_{x=x_o}$$

- Method: The method used to compute controls is linear quadratic regulator theory.  
Gain matrix, computed via ORACLS.
- Assumptions: Full state feedback with  $B = I$   
No disturbances or time delays.
- The cost functional to be minimized will be:

$$J = \int_0^\infty [\hat{x}^T(s) Q x(s) + u^T(s) R u(s)] ds$$

we assume  $Q \geq 0, R > 0$ .

- The optimal control will be:

$$u(t) = -P B^T R^{-1} \hat{x}(t)$$

## Implementation of regulator in DISCOS

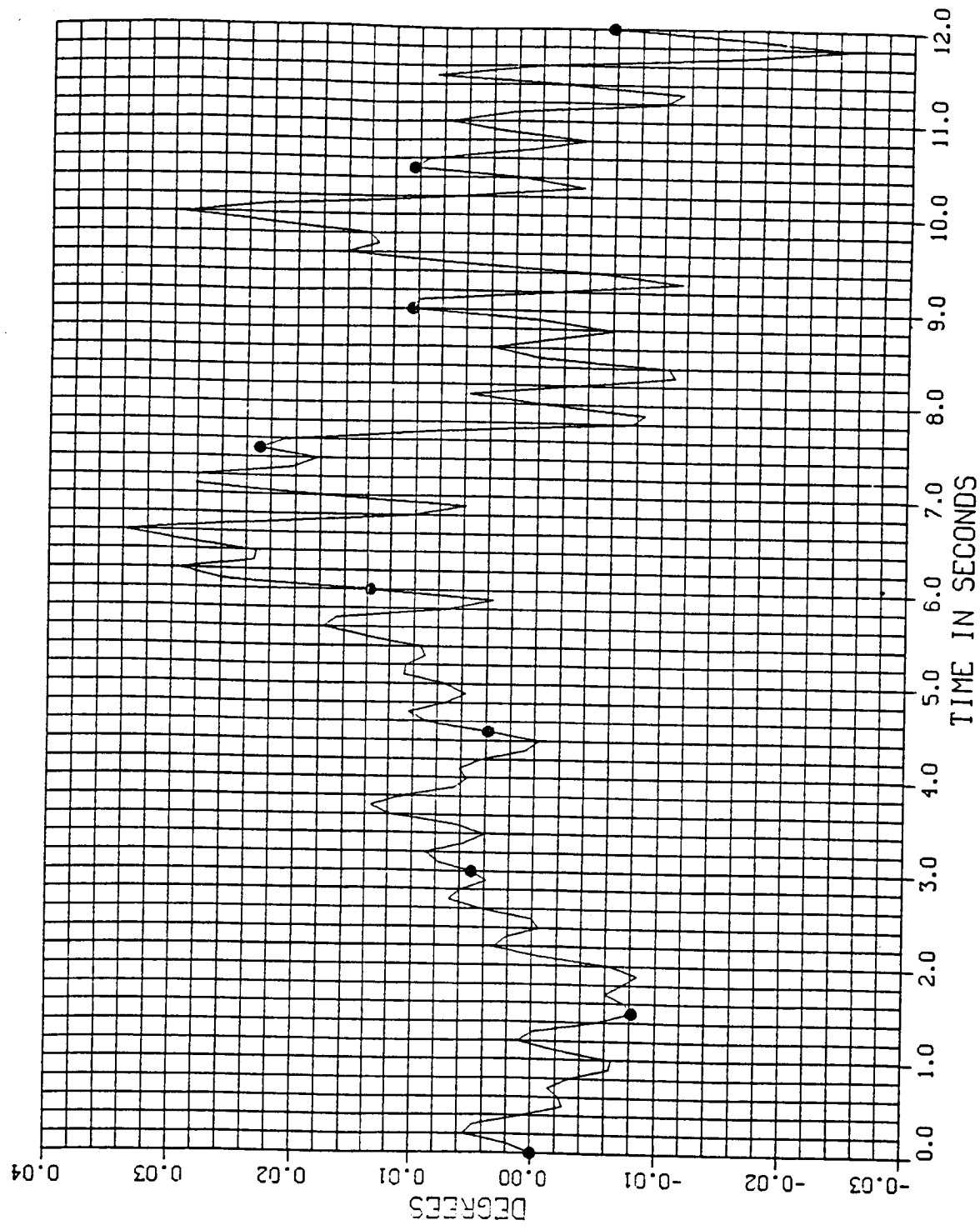
- $PB^T R^{-1}$  matrix is time independent.
- P is calculated by ORACLS.
- B is unit matrix, at present time.
- R equals  $10^{-3} \cdot I$  with all modes controlled. The components of R can be changed to see the effects of regulation of some modes.
- DISCOS solves the state equation:

$$\dot{x}(t) = Ax(t) - B P B^T R^{-1} x(t)$$

# Closed loop damping and frequency shift Eigenvalues of closed loop system

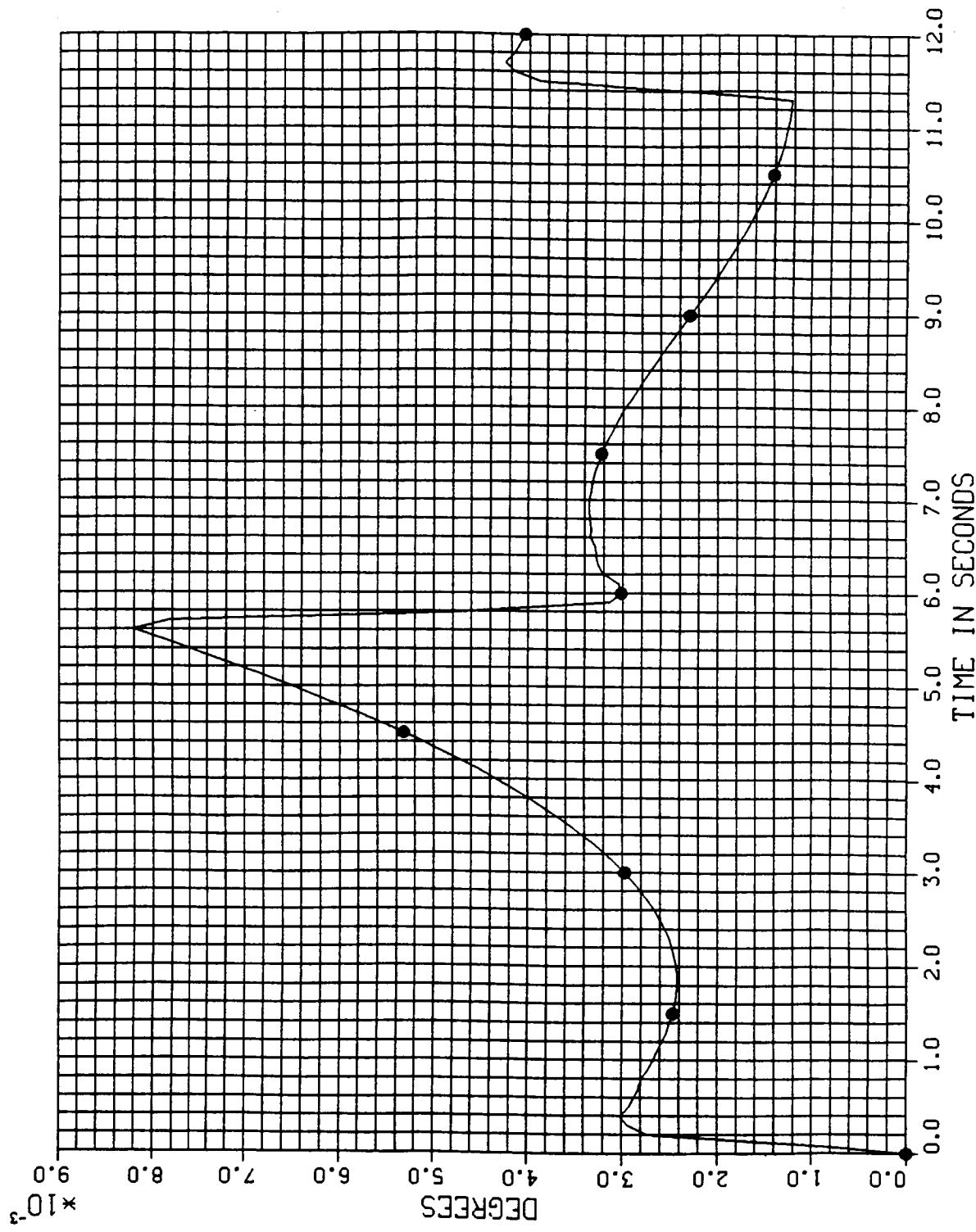
Defined modal frequency in rads/sec	Closed loop eigenvalues in rads/sec	Closed loop damping
1.746	2.02	-31.53
1.97	2.44	-31.54
5.10	12.7	-33.61
7.41	23.01	-38.37
12.85	47.37	-55.46
29.46	116.9	-117.5
34.76	136.6	-136.0
74.67	300.8	-293.1
78.9	317.9	-309.6
106.3	428.8	-416.6
142.5	575.1	-558.1
145.6	587.8	-570.4

ROLL OF ANTENNA RELATIVE TO SHUTTLE VERSUS TIME  
(REGULATOR OFF)

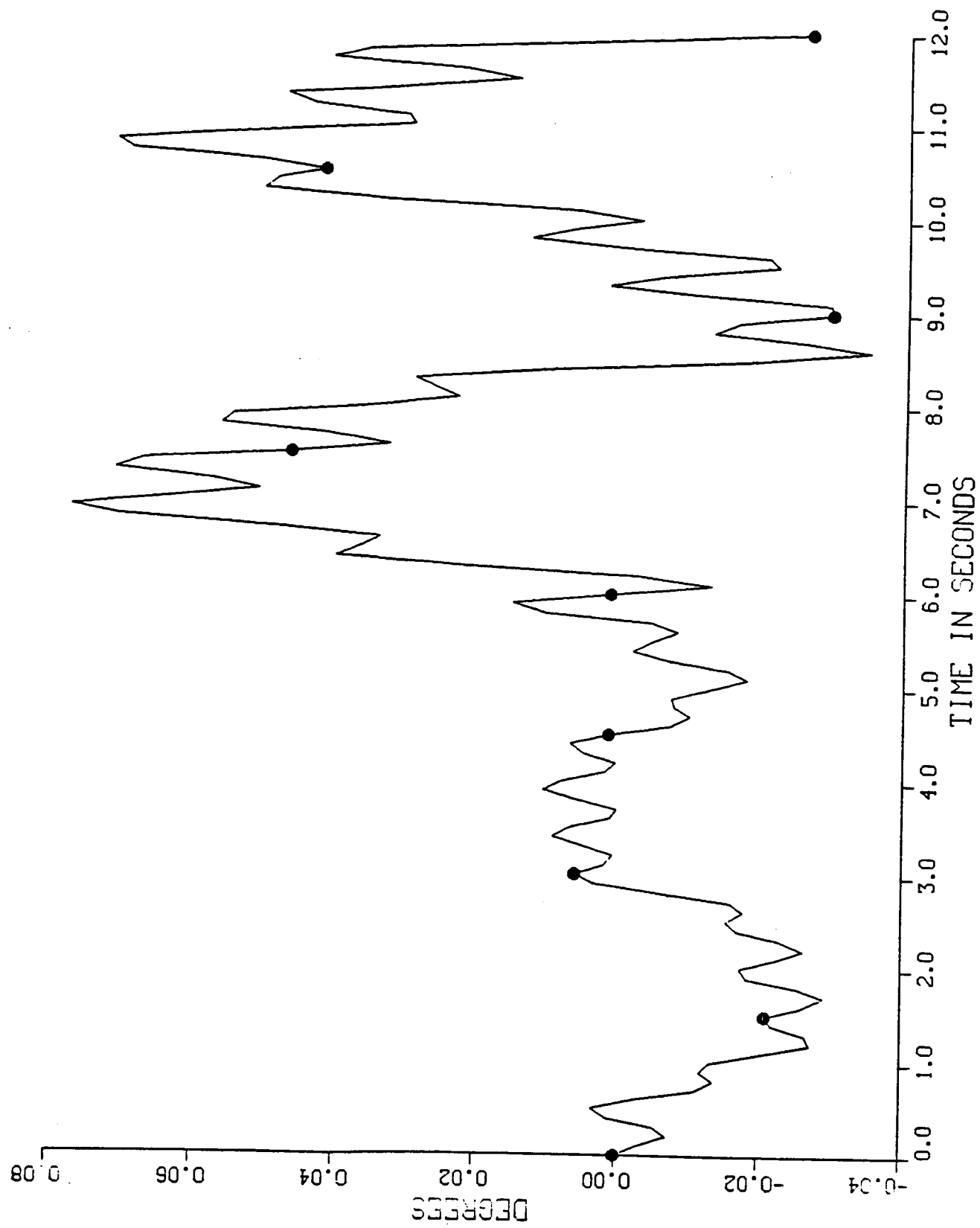


123

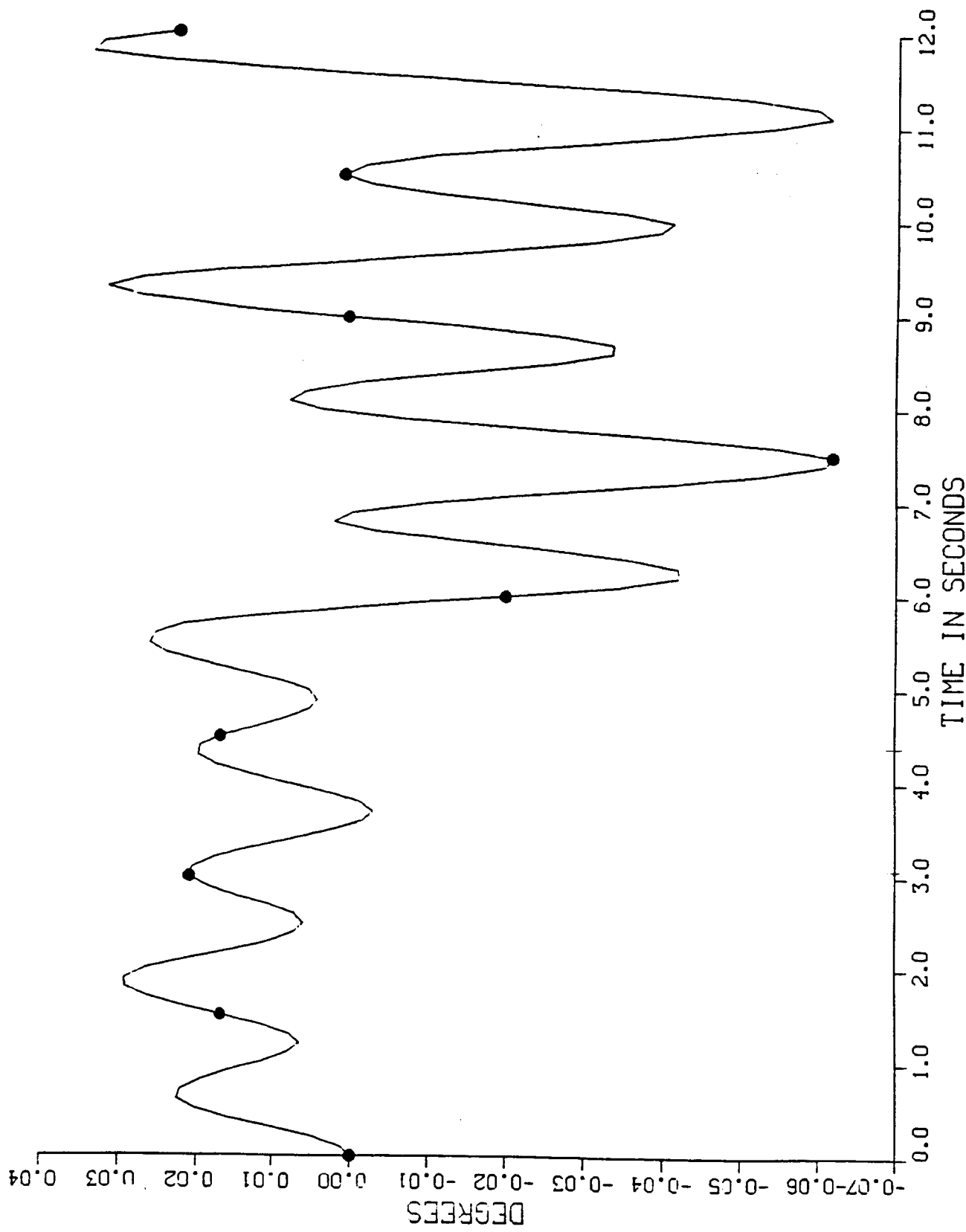
ROLL OF ANTENNA RELATIVE TO SHUTTLE VERSUS TIME  
(Regulator On)



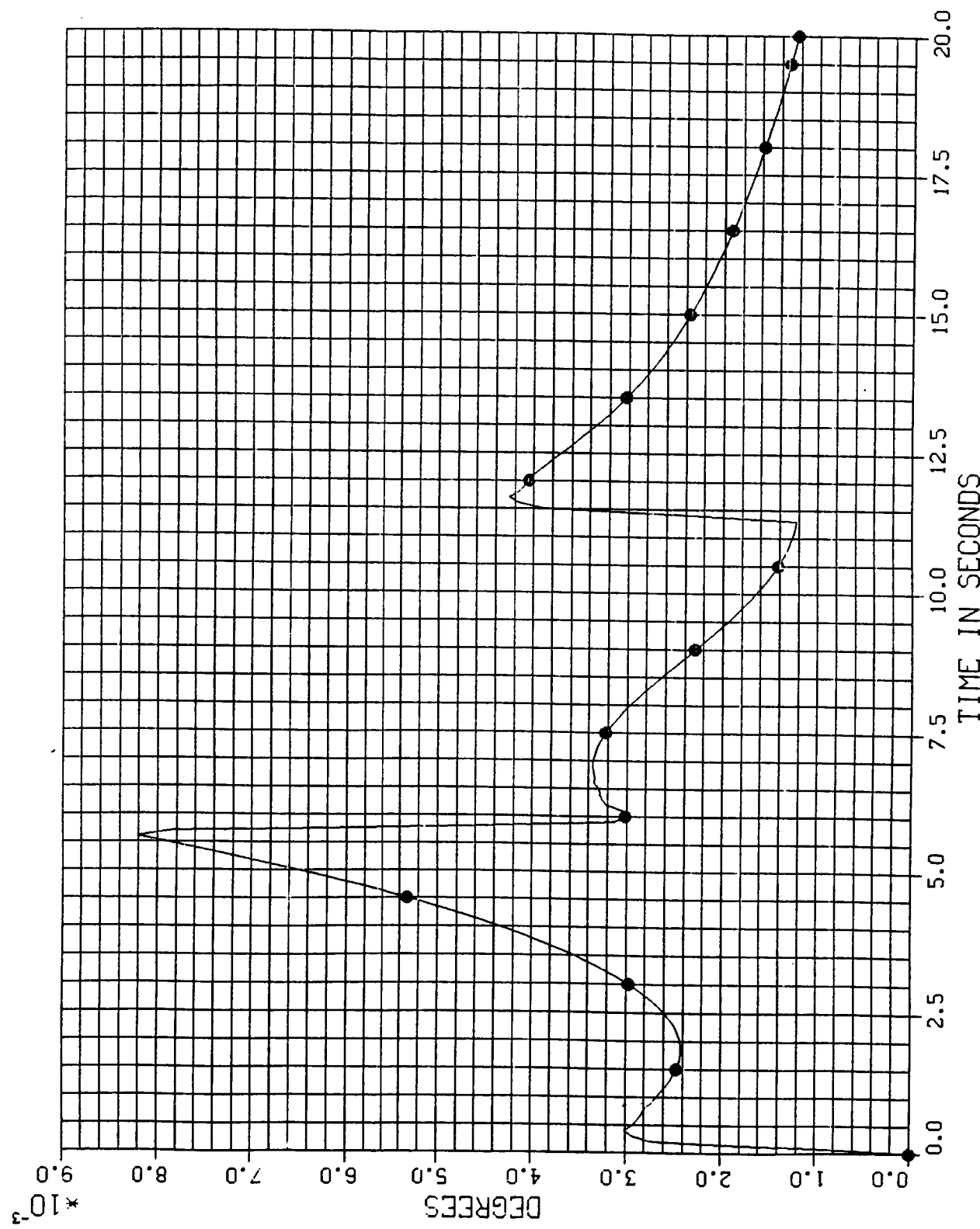
(REGULATOR OFF)



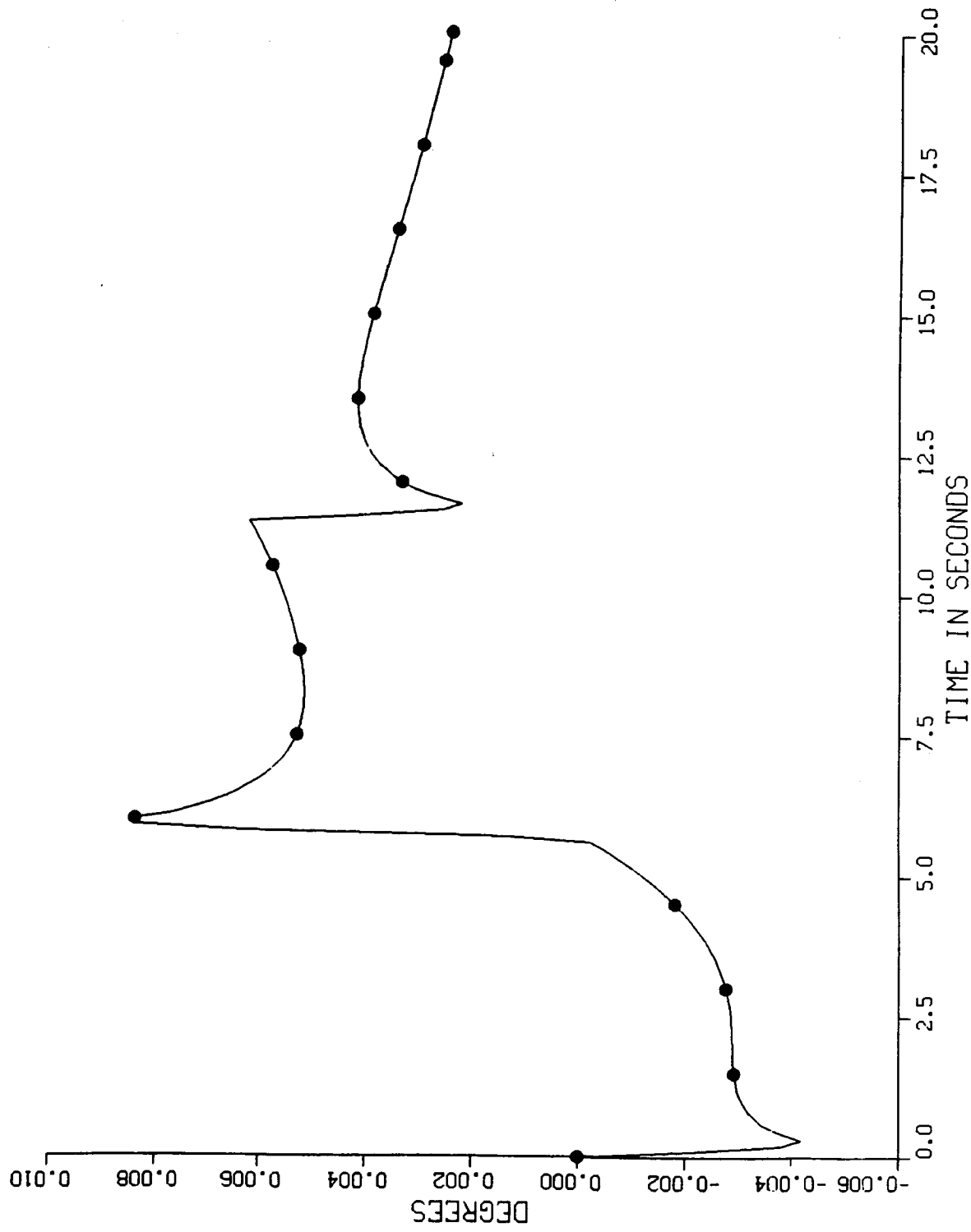
(REGULATOR OFF)



ROLL OF ANTENNA RELATIVE TO SHUTTLE VERSUS TIME

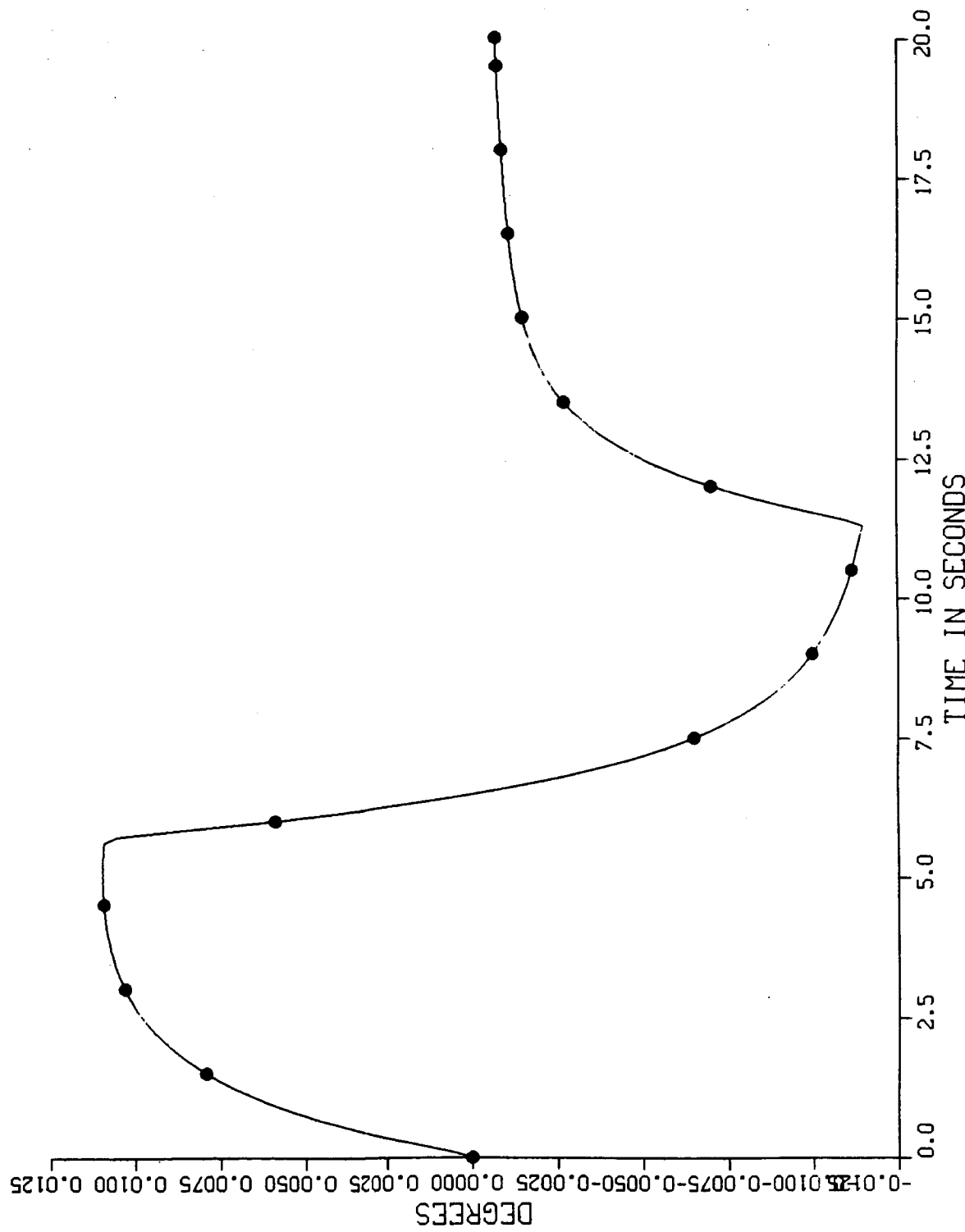


PITCH OF ANTENNA RELATIVE TO SHUTTLE VERSUS TIME



128

YAW OF ANTENNA RELATIVE TO SHUTTLE VERSUS TIME



129

## RESULTS

Maximum relative deflections of reflector

	<u>roll</u>	<u>pitch</u>	<u>yaw</u>
regulator off	.034 deg.	.08 deg.	.06 deg.
regulator on	.008	.015	.013

Note: Final deflections are much less than above.

## CONCLUSIONS

- DISCOS simulation is a useful test bed for control and regulator design.
- Feasibility of design challenge (.02 degree pointing error) is not ruled out.
- Need to incorporate sensor noise as well as sensor and actuator time delay.
- Actuator placement considerations also need to be addressed.

# **Issues in Modeling and Controlling the SCOLE Configuration**

**by**

**Peter M. Bainum**

**A.S.S.R. Reddy**

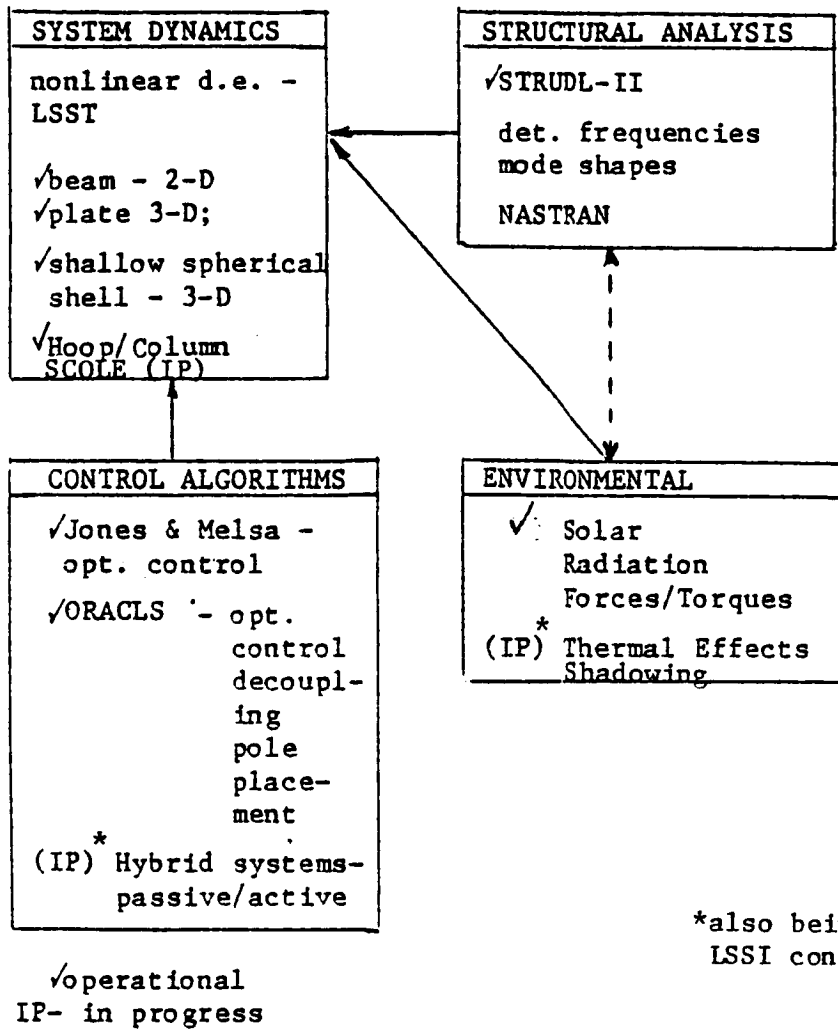
**Cheick Modibo Diarra**

**Howard University**

**Washington, D. C.**

## I. ISSUES IN MODELING THE SCOLE CONFIGURATION

- REVIEW HU DEVELOPMENT OF SYSTEM SOFTWARE FOR LSST DYNAMICS ANALYSIS.
- OPEN-LOOP SYSTEM DYNAMICS WITH RELATED STRUCTURAL ANALYSIS REPRESENTS FUNDAMENTAL STEP.
- FORMULATION METHODS.
- WHAT CAN WE LEARN ABOUT THE OPEN-LOOP SYSTEM?



\*also being studied in NASA/HU LSSI contract

Fig. 1 Development of system software for LSST dynamics analysis

## FORMULATION TECHNIQUES

- (1) Eulerian vs. La Grangian
- ✓ (2) Modeling of the Flexible Appendage (Mast)  
with Offset Inertial Masses at Both Ends
- (2a) Initial 2-D Vibration Analysis
  - (i) P.D.E. approach
  - (ii) Finite element methods
  - (iii) Treatment of boundary conditions
    - Mast as cantilever
    - Mast as a uniform beam with end bodies  
having inertia
  - (iv) Separate treatment of lateral and torsional  
modes.
- (2b) 3-D Vibration Analysis
  - D.K. Robertson, Sept. 1985
  - Harris Corp. Dec. 1984
- (3) Linearization of 2-D Equations
- (4) Formulation of 3-D Equations Based on 3-D Vibration  
Analysis

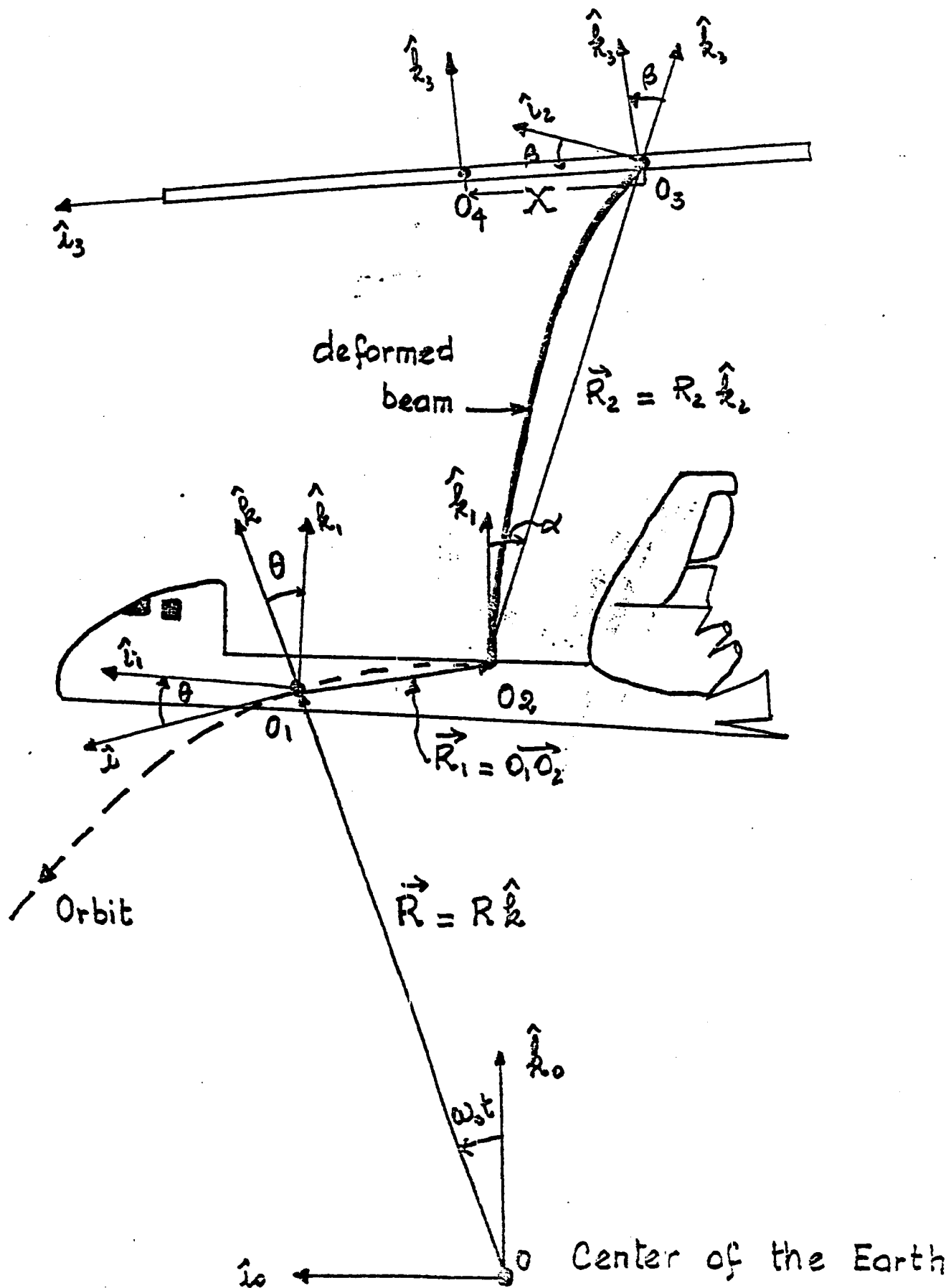


Fig. 2.1. SCOLE System Geometry in the Deformed State (2-D)

## II. A Development of the Two Dimensional Model - (Eulerian Moment Equations)

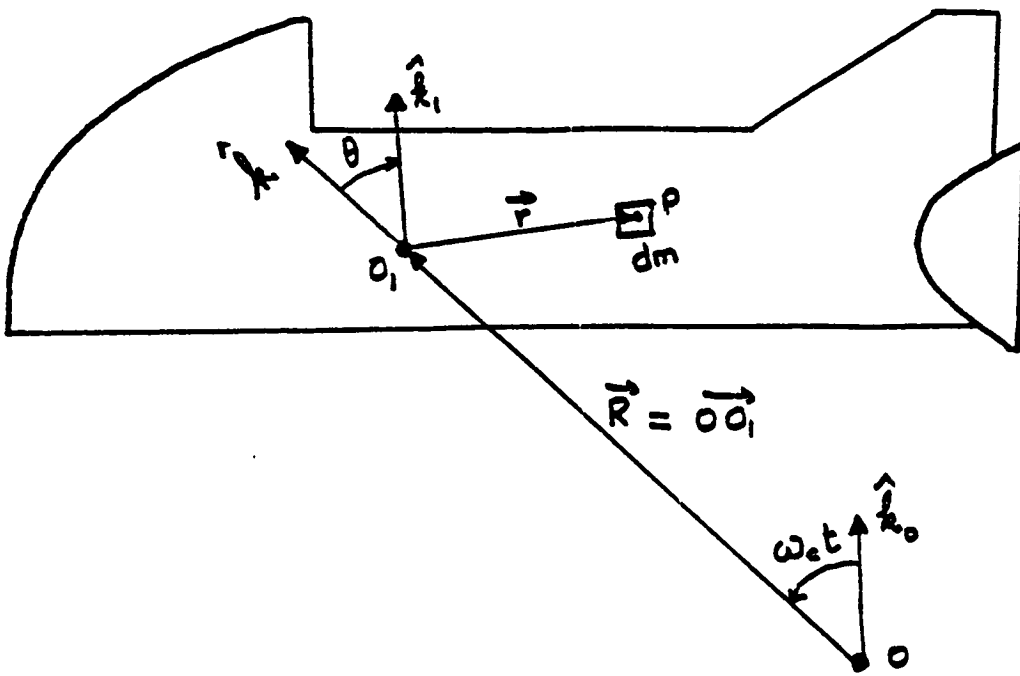
The SCOLE system is assumed to be comprised of three main parts (Fig. 2.1):

- i) the Space Shuttle Orbiter with its center of mass located at point  $O_1$ ;
- ii) the mast, treated as a 130 ft long beam, connected to the Shuttle at  $O_2$  and to the reflector at  $O_3$ ;
- iii) the reflector, considered to be a flat plate with its center of mass at  $O_4$ .

The preliminary analysis presented here started before it was specified<sup>8</sup> that the interface point between the mast and the Shuttle is at  $O_1$ .<sup>8</sup> Therefore, in what follows, a position vector  $\vec{R}_1$  appears which defines  $O_1O_2$ , where  $O_2$  is the assumed interface point.

In the following analysis, the angular momentum of the entire system is evaluated at point  $O_1$  and the dynamics include the lateral displacements of the beam.

### II. A.1 Angular Momentum of the Shuttle with Respect to Point $O_1$



Consider a point, P, of mass,  $dm$ , at an arbitrary position in the Shuttle such that  $\vec{O}_1P = \vec{r}$ . The elemental angular momentum of the mass,  $dm$ , is given by:

$$d\vec{H}_{O_1} = \vec{r} \times \frac{d}{dt} \vec{OP}|_{R_0} dm = \vec{r} \times \frac{d}{dt} (\vec{R} + \vec{r})|_{R_0} dm \\ = \vec{r} \times \{ \dot{\vec{R}} \hat{k} + R \omega_c \hat{i} \times \vec{r} + (\omega_c - \dot{\theta}) \hat{j} \times \vec{r} \} dm \quad (2.1)$$

The total angular momentum for the Shuttle is obtained by integrating Eq. (2.1) over the entire mass of Shuttle as:

$$\vec{H}_{S/O_1} = - \dot{\vec{R}} \hat{k} \times \int_{M_S} \vec{r} dm - R \omega_c \hat{i} \times \int_{M_S} \vec{r} dm + \int_{M_S} \vec{r} \times \{ (\omega_c - \dot{\theta}) \hat{j} \times \vec{r} \} dm \quad (2.2)$$

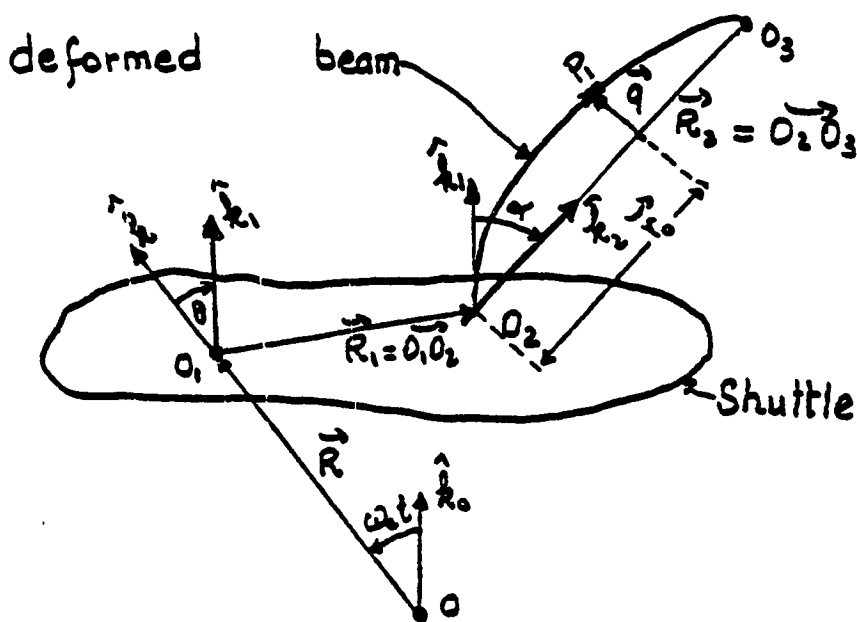
The first and second integrals appearing in the right side of Eq. (2.2) vanish because the center of mass of the Shuttle is at point  $O_1$ .

Since  $\vec{r} \cdot \hat{j} = 0$ , Eq. (2.2) takes the form:

$$\vec{H}_{S/O_1} = (\omega_c - \dot{\theta}) \hat{j} \int_{M_S} r^2 dm = I_S \vec{\omega}_{R_1/R_0} \quad (2.3)$$

where  $I_S$  is the Inertia tensor of the Shuttle at point  $O_1$  and  $\vec{\omega}_{R_1/R_0} = (\omega_c - \dot{\theta}) \hat{j}$ .

### III. A.2 Angular Momentum of the Mast with Respect to Point $O_1$



Consider here an element of the mast located at point,  $P_1$ , with mass,  $dm$ . The elemental angular momentum of such an element is given by:

$$\frac{d\vec{H}_{M/0_i}}{dt} = \left\{ \vec{O}_i \vec{P}_i \times \frac{d}{dt} \vec{Q} \vec{P}_i / R_o \right\} dm \quad (2.4)$$

if one notes that

$$\begin{aligned}\vec{O}_i \vec{P}_i &= \vec{r}_o + \vec{q} \\ \vec{O} \vec{P}_i &= \vec{R} + \vec{r}_o + \vec{q}\end{aligned} \quad (2.5)$$

then, Eq. (2.4) may be expanded according to:

$$\vec{H}_{M/0_i} = - \frac{d\vec{R}}{dt} / R_o \times \int_{M_m} (\vec{r}_o \hat{k}_z + \vec{q} \hat{i}_z) dm + \int_{M_m} (\vec{r}_o \hat{k}_z + \vec{q} \hat{i}_z) \times (\dot{\vec{r}}_o \hat{k}_z + \dot{\vec{q}} \hat{i}_z) dm \quad (2.6)$$

$\frac{d\vec{R}}{dt} / R_o$  is expressed using the relationship between the rate of change of a vector,  $\vec{w}$ , in an inertial ( $R_o$ ) and rotating ( $R_i$ ) frames, i.e.

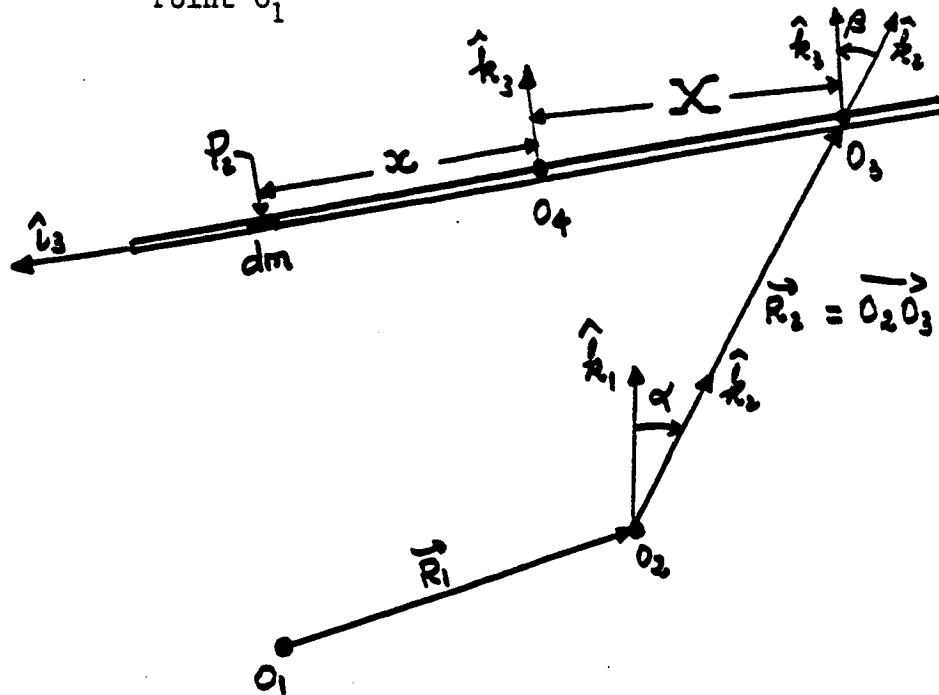
$$\frac{d}{dt} \vec{w} / R_o = \frac{d}{dt} \vec{w} / R_i + \vec{\Omega} R_i / R_o \times \vec{w} \quad (2.7)$$

After substitution of Eq. (2.7) into Eq. (2.6) and integration term by term, one can develop:

$$\begin{aligned}\vec{H}_{M/0_i} &= Mm \int w_c R \left[ \cos(\alpha + \theta) \frac{l}{2} + \sin(\alpha + \theta) \int \frac{\alpha l}{2} \right. \\ &\quad \left. - \frac{1}{\beta l} \cos(wt + \phi) (A \sin \beta l - B \cos \beta l + C \sinh \beta l + D \cosh \beta l + E - F) \right] \\ &\quad + \dot{\alpha} \frac{l^2}{3} + \omega \sin(wt + \phi) \int \frac{1}{\beta} (A \sin \beta l - B \cos \beta l + C \sinh \beta l + D \cosh \beta l) \\ &\quad + \frac{1}{\beta^2 l} (A \cos \beta l + B \sin \beta l - C \cosh \beta l - D \sinh \beta l - E + F) \left. + \frac{l^2}{3} (w_c - \dot{\theta} - \dot{\alpha}) \right] \int\end{aligned} \quad (2.8)$$

If  $Q(z, t)$  is assumed =  $A \cos \beta z + B \sin \beta z + C \cosh \beta z + D \sinh \beta z$

II. A.3 Angular Momentum of the Rigid Reflector with Respect to Point  $O_1$



Let  $O_4$  be the center of mass of the reflector, and  $O_3$  the interface point between the reflector and the mast. The distance,  $X$ , between  $O_3$  and  $O_4$  is constant since the reflector is assumed to be rigid, at least for this analysis.

Let us now consider an element of mass,  $dm$ , of the reflector located at an arbitrary point,  $P_2$ . The elemental angular momentum of that element of mass can be expressed as:

$$d\vec{H}_{r/O_1} = \overrightarrow{O_1P_2} \times \frac{d}{dt} (\overrightarrow{OP_2})|_{R_0} dm \quad (2.9)$$

$\overrightarrow{O_1P_2}$  and  $\overrightarrow{O_2P_2}$  can be expressed as:

$$\left. \begin{aligned} \overrightarrow{O_1P_2} &= \overrightarrow{R_1} + \overrightarrow{R_2} + X \hat{i}_3 + z \hat{i}_3 \\ \overrightarrow{OP_2} &= \overrightarrow{R} + \overrightarrow{O_1P_2} \end{aligned} \right\} (2.10)$$

Eq. (2.9) may be expanded according to

$$d\vec{H}_{r/0} = (\vec{R}_1 + (x+z)\hat{i}_3) \times \frac{d}{dt} (\vec{R}_1 + \vec{R}_2 + (x+z)\hat{i}_3) / R_0 \quad (2.11)$$

Once more,  $\frac{d}{dt} [\vec{R}_1 + \vec{R}_2 + (x+z)\hat{i}_3] / R_0$  is

expressed using Eq. (2.7):

$$\frac{d}{dt} \vec{w}/R_0 = \frac{d}{dt} \vec{w}/R_0 + \vec{\Omega}_{Ri}/R_0 \times \vec{w}$$

After substitution of Eq. (2.7) into Eq. (2.11) and integration term by term over the entire mass of the reflector, one arrives at

$$\begin{aligned} \vec{H}_{r/0} = & \left\{ M_r R R_2 \omega_c \cos(\alpha+\theta) + M_r X R \omega_c \times \right. \\ & \left. \sin(\alpha+\theta) + (\omega_c - \dot{\theta} - \dot{\alpha}) [I_{2r} + M_r (X^2 + R_2^2)] \right\} \hat{j} \end{aligned}$$

(2.12)

where  $I_{2r}$  is the moment of inertia of the reflector about the  $\hat{j}$  axis taken at point  $O_4$ .

## II. B.1 Moment Equation

The angular momentum of the entire system about  $O_1$  is obtained by summing the angular momentum of each part about  $O_1$ , i.e.

$$\vec{H}_{T/O_1} = \sum_{i=1}^3 \vec{H}_{i/O_1} \quad (2.13)$$

The moment equation

$$\frac{d}{dt} \vec{H}_{T/O_1}/R_0 = \vec{N} \quad (2.14)$$

where  $N$  is the sum of all the external torques, acting on the entire system, about an axis through point  $O_1$ .

At this stage of the analysis, it is assumed that the center of mass of the Shuttle moves in a circular orbit, i.e.

$$\frac{d}{dt} \vec{R}/R = \dot{\vec{R}}/R = \vec{\omega} \quad (2.15)$$

Taking into consideration the coincidence between points  $O_1$  and  $O_2$ , Eq. (2.14) is expanded using once more Eq. (2.7) and the following result is obtained:

$$\begin{aligned} \frac{d}{dt} \vec{H}_{T/O_1}/R_0 \cdot \hat{j} &= \vec{N} \cdot \hat{j} = N_y = \\ -\ddot{\theta} \left( I_{2s} + M_m \frac{\ell^2}{3} + I_{sr} + M_r (x^2 + R_s^2) \right) \\ -\ddot{\alpha} (I_{sr} + M_r (x^2 + R_s^2)) + (\alpha + \dot{\theta}) \dot{x} \frac{\ell}{2} M_m w_c R \\ + (\dot{\theta} + \dot{\alpha}) \int M_m [w_c R] \{(\theta + \alpha) \frac{\ell}{2} + \frac{x\ell}{2} - \frac{1}{\beta\ell} \cos(\omega t + \phi)\} x \end{aligned}$$

$$\begin{aligned}
& \left( A \sin \beta l - B \cos \beta l + C \sinh \beta l + D \cosh \beta l + B - D \right) \} \\
& - M_r (R R_z w_c (\theta + \alpha) + X R w_c) \} \\
& + M_m w_c R \left[ (\alpha + \theta) \frac{\omega}{\beta l} \sin(\omega t + \phi) (A \sin \beta l \right. \\
& \left. - B \cos \beta l + C \sinh \beta l + D \cosh \beta l + B - D) \right] \\
& + M_m \omega^2 \cos(\omega t + \phi) \left\{ \frac{1}{\beta l} (A \sin \beta l + C \sinh \beta l - B \cos \beta l \right. \\
& \left. + D \cosh \beta l) + \frac{1}{\beta^2 l} (A \cos \beta l + B \sin \beta l - C \cosh \beta l \right. \\
& \left. - D \sinh \beta l - A + C) \right\}
\end{aligned}$$

Point

$$\alpha = \frac{1}{l} \cos(\omega t + \phi) \psi(l)$$

$$\dot{\alpha} = -\frac{\omega}{l} \sin(\omega t + \phi) \psi(l)$$

$$\ddot{\alpha} = -\frac{\omega^2}{l} \cos(\omega t + \phi) \psi(l)$$

(2.16)

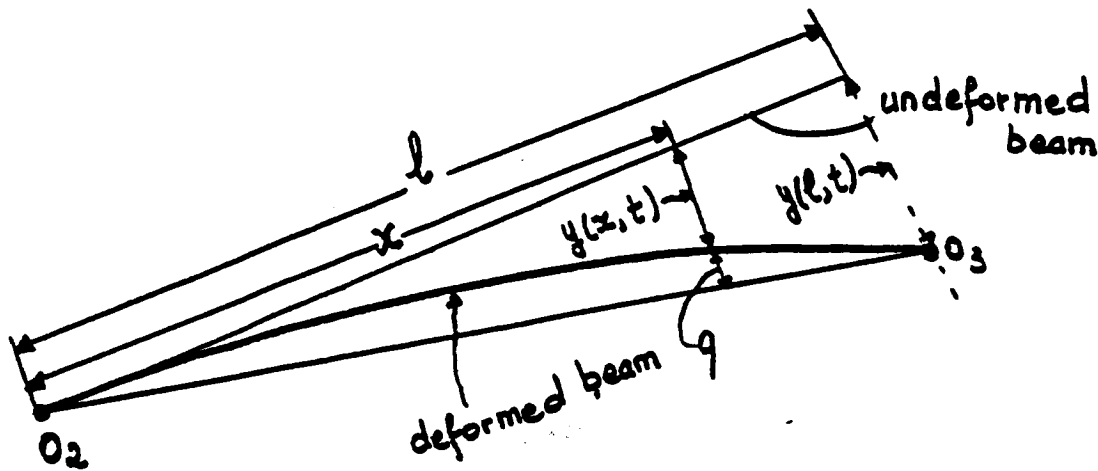
## FORMULATION TECHNIQUES

- (1) Eulerian vs. La Grangian
- (2) Modeling of the Flexible Appendage (Mast)  
with Offset Inertial Masses at Both Ends
- ✓ (2a) Initial 2-D Vibration Analysis
  - (i) P.D.E. approach
  - (ii) Finite element methods
  - (iii) Treatment of boundary conditions
    - Mast as cantilever
    - Mast as a uniform beam with end bodies  
having inertia
  - (iv) Separate treatment of lateral and torsional  
modes.
- (2b) 3-D Vibration Analysis
  - D.K. Robertson, Sept. 1985
  - Harris Corp. Dec. 1984
- (3) Linearization of 2-D Equations
- (4) Formulation of 3-D Equations Based on 3-D Vibration  
Analysis

### III. B.2 Expression for $\vec{q}$

In the moment equation, Eq. (2.16), one notices integrals involving  $\vec{q}$ , the transverse displacement vector, and its first and second derivatives with respect to time. It is, therefore, necessary to develop an expression for  $\vec{q}$ .

#### II.B.2.i Relation between $q(x,t)$ and $y(x,t)$



Consider the beam in its deflected configuration.  $y(l,t)$  is the deflection of the reflector-end of the mast at an arbitrary time,  $t$ ;  $y(x,t)$ , the deflection of an arbitrary point on the mast at the same time.

$$\text{From Fig. (2.1), } \hat{k}_1 \cdot \hat{k}_2 = \cos \alpha \quad (2.17)$$

Assuming  $\alpha$  small,  $\tan \alpha$  can be expressed as

$$\tan \alpha = \frac{y(l,t)}{l} \approx \alpha = \frac{y(x,t) + q(x,t)}{x} \quad (2.18)$$

From Eq. (2.18) one derives

$$q(x,t) = \frac{x}{l} y(l,t) - y(x,t) \quad (2.19)$$

or

$$q(x,t) = \alpha x - y(x,t) \quad (2.20)$$

### II.B.2.ii Evaluation of $y(x,t)$

Assuming separability of the variables, the beam equation,

$$+ \frac{EI}{\delta A} \frac{\partial^4 y(x,t)}{\partial x^4} + \frac{\partial^2 y(x,t)}{\partial t^2} = 0 \quad (2.21)$$

is solved to yield solutions of the form:

$$y(x,t) = f(t) \phi(x) \quad (2.22)$$

where

$f(t) = E \sin \omega t + F \cos \omega t$  with  $\omega$  = frequency of the vibration

and  $\phi(x) = A \cos \beta x + B \sin \beta x + C \cosh \beta x + D \sinh \beta x$  (2.23)

When the following boundary conditions are assumed:

- a)  $y(0,t) = 0$  ; b)  $y'(0,t) = 0$
- c)  $EI y'''(l,t) = -M_r y(l,t)$ ; d)  $EI y''(l,t) = 0$  (2.24)

where  $y' = \frac{\partial y}{\partial x}$  and  $y'' = \frac{\partial^2 y}{\partial t^2}$  (2.25)

these can be expressed in the form:

$$\left. \begin{array}{l} \alpha A + \gamma B = 0 \\ \gamma A + \tau B = 0 \end{array} \right\} \Leftrightarrow \underbrace{\begin{bmatrix} \alpha & \gamma \\ \gamma & \tau \end{bmatrix}}_C \begin{bmatrix} A \\ B \end{bmatrix} = \begin{bmatrix} 0 \\ 0 \end{bmatrix} \quad (2.26)$$

where

$$\alpha = \sin\beta l - \sinh\beta l - \frac{M_r}{\rho A'} \beta (\cos\beta l - \cosh\beta l)$$
$$\delta = -\cos\beta l - \cosh\beta l - \frac{M_r}{\rho A'} \beta (\sin\beta l - \sinh\beta l) \quad (2.26)$$

$$\gamma = \cos\beta l + \cosh\beta l$$

$$\sigma = \sin\beta l + \sinh\beta l$$

$$\beta^2 = \omega \sqrt{\frac{\rho A'}{EI}} \quad (2.28)$$

For the SCOLE system, the following parameters have been supplied<sup>8</sup>:

$$\rho A' = 0.09556 \text{ slugs/ft}$$

$$EI = 4.0 \times 10^7 \text{ lb-ft}^2$$

$$M_r = (400/32.2) \text{ slugs}$$

$$l = 130 \text{ ft.}$$

For non-trivial solutions for A and B,  $\det C$  must vanish. The values of  $\beta$  for which  $\det C = 0$  are computed and substituted back into Eq. (2.28) to obtain the frequencies of the different vibrational modes (Table 2.1).

The same values of  $\beta$  are substituted into  $\phi(x)$ , (Eq. 2.23), which is normalized with respect to its maximum value and the normalized mode shapes plotted (see Table 2.1 and Figs. 2.2 - 2.6). Note that the ranges of frequencies obtained in Table 2.1 are higher than those previously presented in the April 13, 1984 oral presentation due to previous inconsistencies in dimensional analysis of some physical units.

TABLE 2.1

Values of  $\beta$  and Natural Frequencies (Hz)  
for the First 8 In-Plane (Pitch) Bending Modes

<u><math>\beta</math></u>	<u><math>\omega</math>(Hz)</u>
1.874599	.677828
4.6929	4.245
7.8519	11.884
10.997	23.3128
14.1309	38.4933
17.276	57.5283
20.4229	80.4045
23.555	106.958

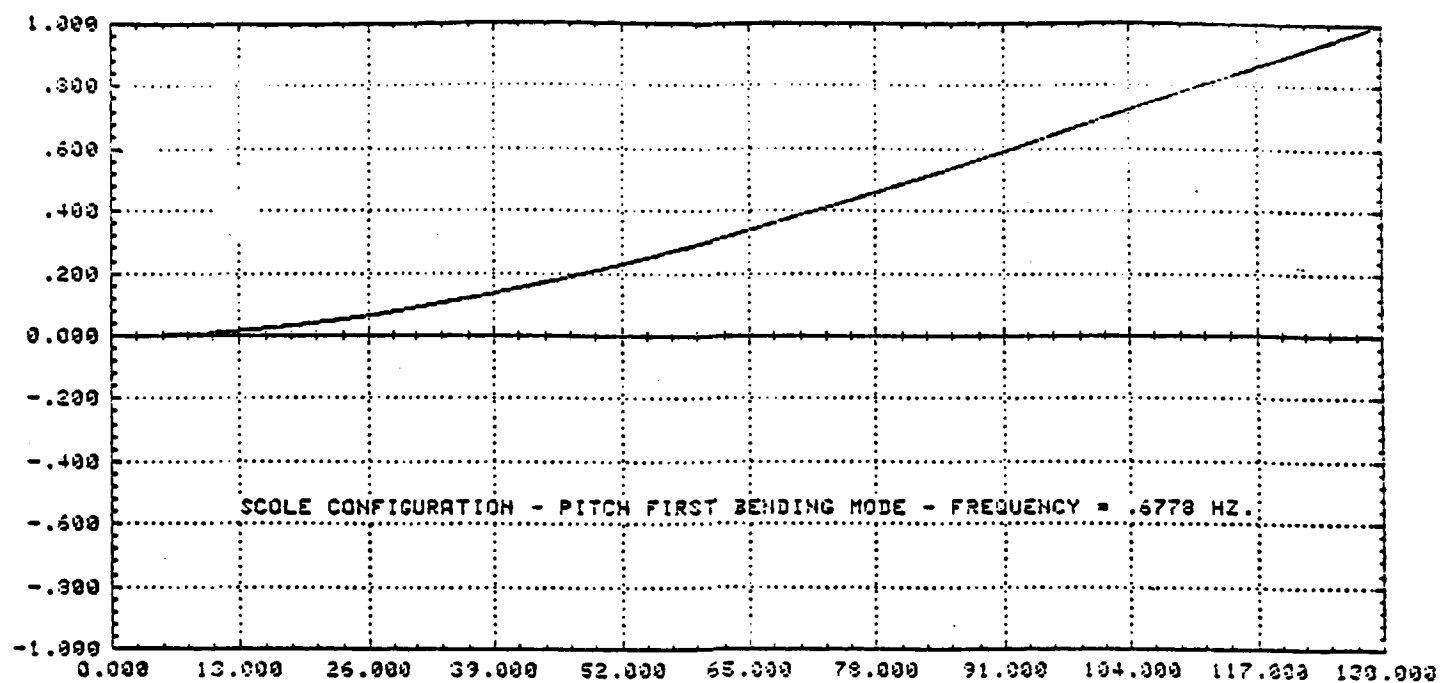


Fig. 2.2

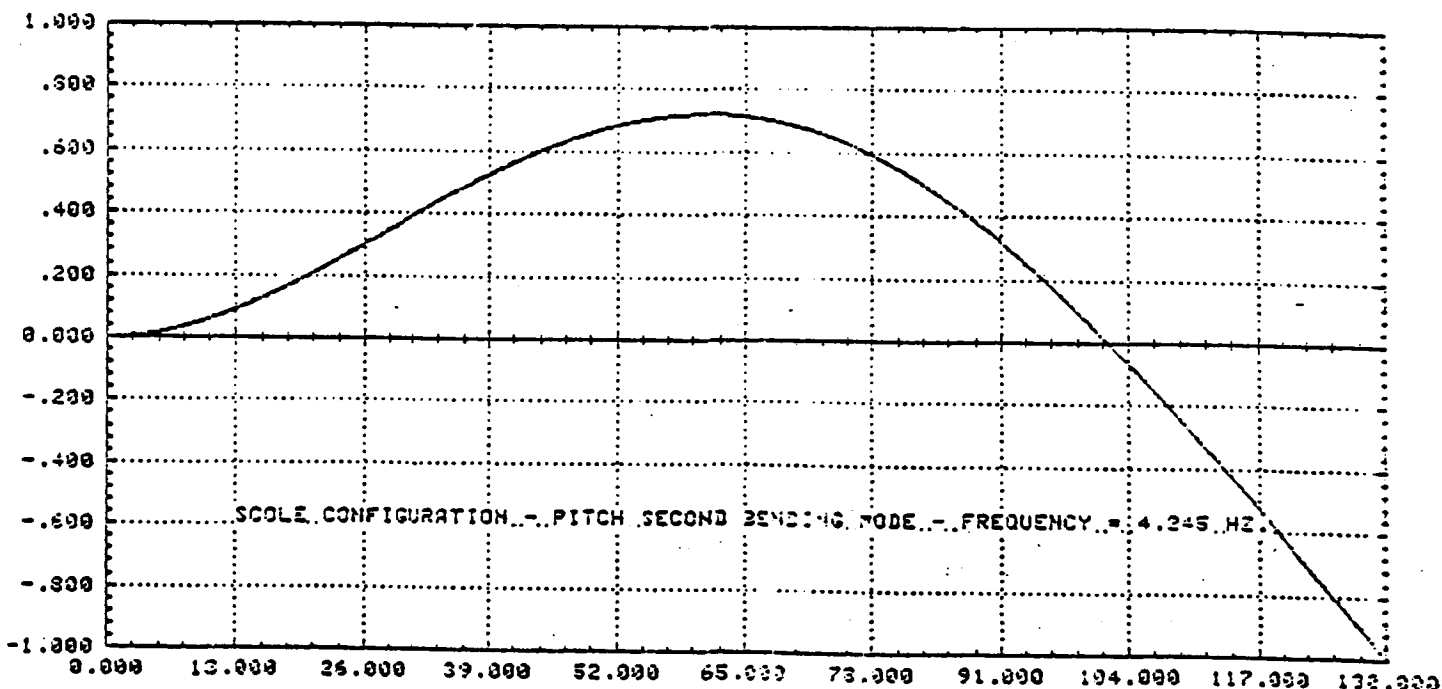


Fig. 2.3

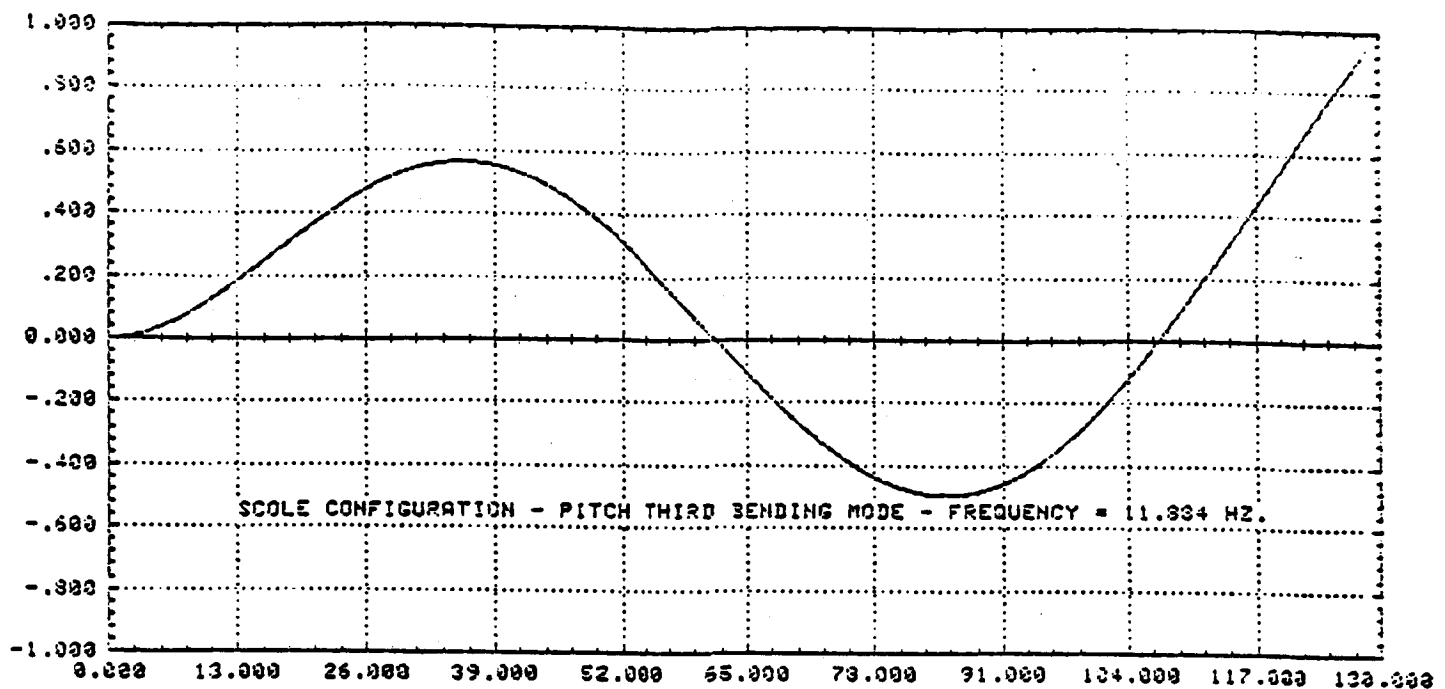


Fig. 2.4

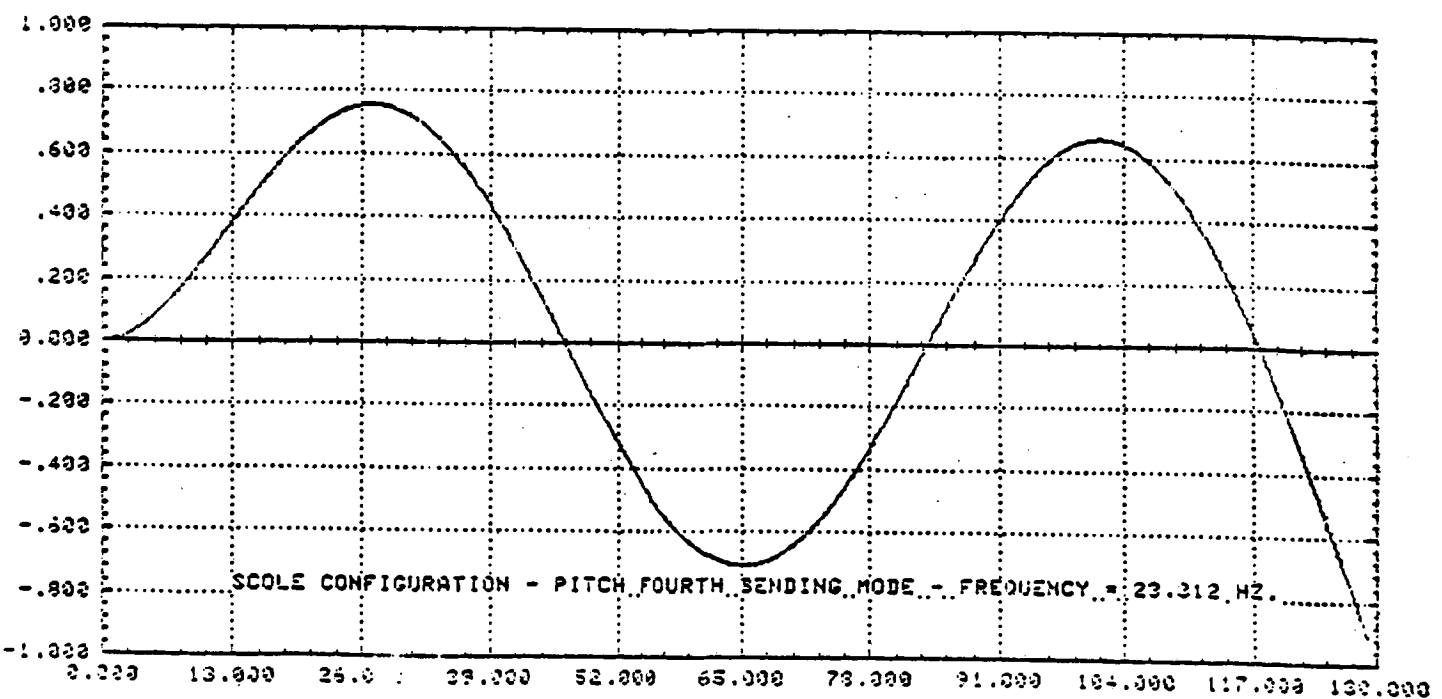


Fig. 2.5

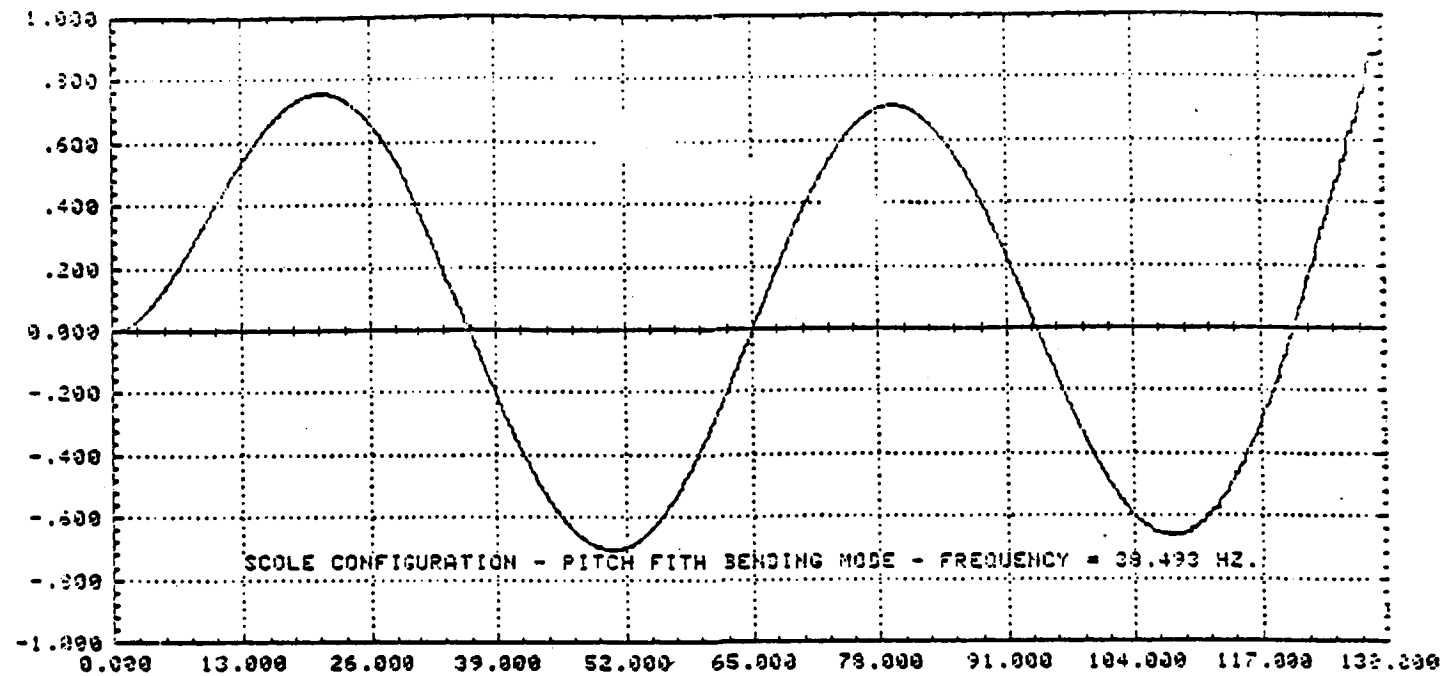


Fig. 2.6

II.C Frequencies of the Lateral Vibrational Modes when the SCOLE System is Modelled as a Free-Free Beam with End Bodies having Inertia

The solution to the beam equation (2.21) is again considered and the following boundary conditions assumed:

1. The shear force at either end is equal to the mass located at that end multiplied by the acceleration of the interface point at that end.

This boundary condition combined with the equilibrium conditions yields

$$-EI \frac{\partial^3 y(x,t)}{\partial x^3} = M_i \frac{\partial^2 y(x,t)}{\partial t^2}$$

at the Shuttle end,

$$-EI \frac{\partial^3 y(x,t)}{\partial x^3} \Big|_{x=0} = M_s \frac{\partial^2 y(x,t)}{\partial t^2} \Big|_{x=0} = -M_s \omega^2 y(x,t) \Big|_{x=0} \quad (2.29)$$

at the reflector end

$$EI \frac{\partial^3 y(x,t)}{\partial x^3} \Big|_{x=130} = M_r \frac{\partial^2 y(x,t)}{\partial t^2} \Big|_{x=130} = -M_r \omega^2 y(x,t) \Big|_{x=130} \quad (2.30)$$

where

$$\omega^2 = \beta^4 \frac{EI}{\rho A'}$$

2. Next, expressing the equality between the moment at an end point and the product of the inertia of the mass at that end by the angular acceleration of the interface point results in:

$$I_s \ddot{\theta}(x, t) = EI \frac{\partial^2 y(x, t)}{\partial x^2}$$

$$\text{where } \theta(x, t) = \frac{\partial(y(x, t))}{\partial x}$$

At the Shuttle end:  $x = 0$ , this is expressed as:

$$\begin{aligned} I_s \frac{\partial^2}{\partial t^2} \left[ \frac{\partial y(x, t)}{\partial x} \right]_{x=0} &= EI \frac{\partial^2 y(x, t)}{\partial x^2} \Big|_{x=0} \\ -\omega^2 I_s \frac{\partial y(x, t)}{\partial x} \Big|_{x=0} &= EI \frac{\partial^2 y(x, t)}{\partial x^2} \Big|_{x=0} \quad (2.31) \end{aligned}$$

the same boundary condition at the reflector end translates as:

$$-\omega^2 I_r \frac{\partial y(x, t)}{\partial x} \Big|_{x=130} = -EI \frac{\partial^2 y(x, t)}{\partial x^2} \Big|_{x=130} \quad (2.32)$$

After performing the required differentiation of the assumed solution of the beam equation (Eq. 2.23), one arrives at the following system of four equations with 4 unknowns, A, B, C, and D,

$$\text{Eq. (2.29)} \Rightarrow \frac{M_r \beta}{\rho A'} A + B + \frac{M_r \beta}{\rho A'} C - D = 0 \quad (2.33)$$

Eq. (2.30)  $\Rightarrow$

$$\begin{aligned} &\left[ \frac{M_r \beta}{\rho A'} \cos \beta l + \sinh \beta l \right] A + \left[ \frac{M_r \beta}{\rho A'} \sin \beta l - \cosh \beta l \right] B \\ &+ \left[ \frac{M_r \beta}{\rho A'} \cosh \beta l + \sinh \beta l \right] C + \left[ \frac{M_r \beta}{\rho A'} \sinh \beta l + \cosh \beta l \right] D = 0 \quad (2.34) \end{aligned}$$

$$\text{Eq. (2.31)} \Rightarrow -A + \frac{I_s \beta^3}{\rho A'} B + C + \frac{I_s \beta^3}{\rho A'} D = 0 \quad (2.35)$$

and Eq. (2.32)  $\Rightarrow$

$$\left[ \frac{I_r \beta^3}{\rho A'} \sin \beta l - \cos \beta l \right] A - \left[ \frac{I_r \beta^3}{\rho A'} \cos \beta l + \sin \beta l \right] B \\ + \left[ \cosh \beta l - \frac{I_r \beta^3}{\rho A'} \sinh \beta l \right] C + \left[ \sinh \beta l - \frac{I_r \beta^3}{\rho A'} \cosh \beta l \right] = 0 \quad (2.36)$$

Equations (2.33) - (2.36) can be recast in the matrix format as

$$\begin{bmatrix} M(\beta) \end{bmatrix} \begin{bmatrix} A \\ B \\ C \\ D \end{bmatrix} = \begin{bmatrix} 0 \\ 0 \\ 0 \\ 0 \end{bmatrix} \quad (2.37)$$

For non-trivial solution of  $\phi(x)$  (Eq. 2.23) the determinant of  $M(\beta)$  must be zero. A computer program was written, and the values of  $\beta$ , solutions of the nonlinear equation  $\det [M(\beta)] = 0$ , obtained.

These values of  $\beta$  were substituted into

$$\omega = \beta^2 \sqrt{\frac{EI}{\rho A'}}$$

to derive the frequencies of the inplane and out-of-plane lateral vibrational modes. The results are given in Tables (2.2) and (2.3).

Table 2.2 Values of  $\beta$  and Natural  
 Frequencies ( $H_z$ ) for the first 9  
 In-plane (Pitch) Bending Modes

<u><math>\beta</math></u>	<u><math>\omega(H_z)</math></u>
0.0097	0.3065
0.0310	3.1308
0.0549	9.81922
0.0789	20.2809
0.1030	34.562
0.1271	52.6288
0.1512	74.4794
0.1754	100.229
0.1995	129.664

**Table 2.3 Values of  $\beta$  and Natural  
Frequencies ( $\omega_z$ ) for the First 9  
Out-Plane (Roll) Bending Modes**

<u><math>\beta</math></u>	<u><math>\omega(\text{H}_z)</math></u>
0.0103	0.3456
0.0310	3.1308
0.0549	9.81922
0.0789	20.2809
0.1030	34.562
0.1271	52.6288
0.1512	74.4794
0.1754	100.229
0.1995	129.664

II. D. Derivation of the Frequencies of the Torsional Vibration,  
SCOLE Configuration.

Assuming the mast to be a circular shaft, the torque at any point on the shaft is given by

$$T = GI \frac{\partial y(x,t)}{\partial x}$$

where  $G$  is the modulus of rigidity and  $I$  the polar moment of inertia of the cross sectional area of the beam. This torque is opposed by the inertial torque

$$I\rho \frac{\partial^2 (y(x,t))}{\partial t^2}$$

where  $\rho$  is the density of the beam. For equilibrium,

$$GI \frac{\partial y(x,t)}{\partial x} - I\rho \frac{\partial^2 y(x,t)}{\partial t^2} = 0 \quad (2.38)$$

Assuming the separability of the variables, Equation (2.38) is solved to yield, solutions of the form

$$y(x,t) = f(t) \phi(x)$$

where

$$f(t) = \alpha \cos(\omega t) + \beta \sin(\omega t)$$

$$\phi(x) = A \sin \omega \sqrt{\rho/G} x + B \cos \omega \sqrt{\rho/G} x$$

} (2.39)

### Boundary Conditions

Writing that the torque,  $T$ , at either end of the beam equals the moment of inertia times the angular acceleration of the interface point yields:

$$GI \frac{\partial y(x,t)}{\partial x} = I_s \frac{\partial^2 y(x,t)}{\partial t^2} \quad (2.40)$$

Equation (2.40) along with the equilibrium of the shaft gives:

for the Shuttle end:  $x = 0$

$$GI \left. \frac{\partial y(x,t)}{\partial x} \right|_{x=0} = - I_s \omega^2 y(x,t) \Big|_{x=0} \quad (2.41)$$

for the reflector end:  $x = l = 130$

$$- GI \left. \frac{\partial y(x,t)}{\partial x} \right|_{x=130} = - I_r \omega^2 y(x,t) \Big|_{x=130} \quad (2.42)$$

After substitution of equation (2.39) into equations (2.41) and (2.42), one arrives at:

$$\text{Eq. (2.41)} \Rightarrow A GI \sqrt{\frac{\rho}{G}} + B I_s \omega = 0 \quad (2.43)$$

Eq. (2.42)  $\Rightarrow$

$$\begin{aligned} & \left[ GI \sqrt{\frac{\rho}{G}} \cos \omega l \sqrt{\frac{\rho}{G}} - I_r \omega \sin \omega l \sqrt{\frac{\rho}{G}} \right] A \\ & - \left[ GI \sqrt{\frac{\rho}{G}} \sin \omega l \sqrt{\frac{\rho}{G}} + I_r \omega \cos \omega l \sqrt{\frac{\rho}{G}} \right] B = 0 \quad (2.44) \end{aligned}$$

Equations (2.43) and (2.44) can be recast in matrix format

as 
$$\begin{bmatrix} P(\omega) \end{bmatrix} \begin{bmatrix} A \\ B \end{bmatrix} = \begin{bmatrix} 0 \\ 0 \end{bmatrix} \quad (2.45)$$

For non-trivial solution of equation (2.39) one must insure that the determinant  $[P(\omega)]$  is equal to zero.

The values of  $\omega$  for which  $\det [P(\omega)] = 0$  correspond to the frequencies of the torsional vibration. A computer program was written to solve this determinental equation and the frequencies for the torsional modes are listed in Table 2.4.

Table 2.4 Values of Natural  
Frequencies ( $\text{Hz}$ ) for the First 9  
Torsional Vibration Modes

$\omega(\text{Hz})$

0.0305

39.99

79.98

119.97

157.97

199.96

239.55

279.94

319.939

## II.E Preliminary Calculation of the SCOLE Appendage Frequencies based on Finite Element Techniques

For this application both the reflector and the mast are assumed to be a single flexible body. This body is considered to be comprised of two types of elements: (1) beam elements; and (2) triangular plate elements. The actual finite element model (FEM) is described as follows:

### Mass distribution

Space Shuttle	6,366.46 slug
---------------	---------------

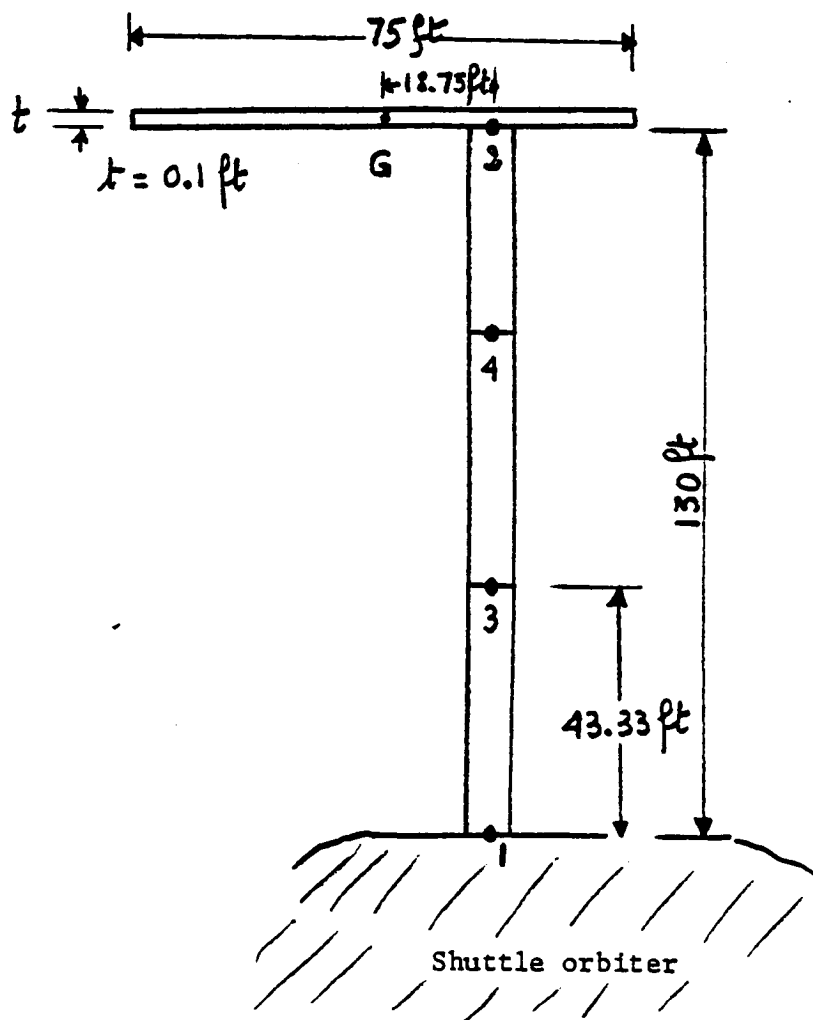
Mast	12.42 slug
------	------------

Reflector	12.42 slug
-----------	------------

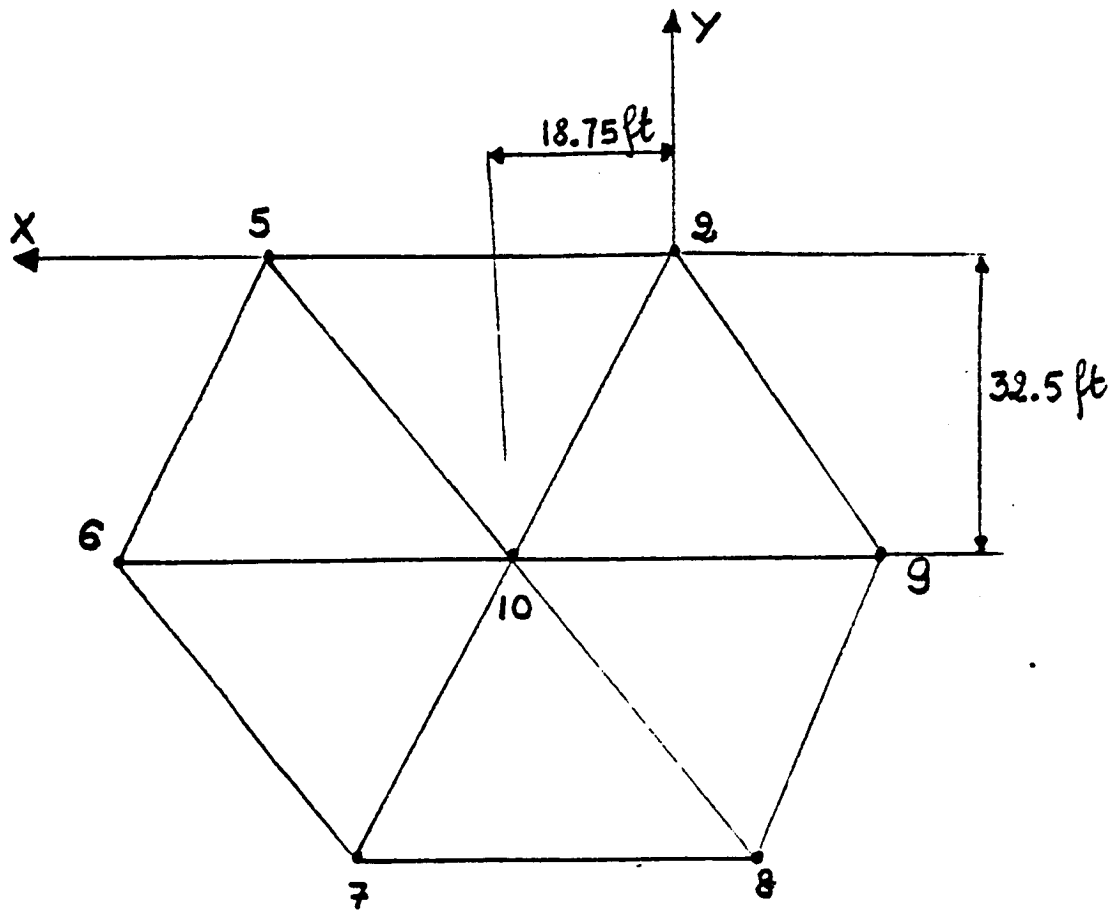
The masses of the reflector and the mast being so small (.39%) as compared with the mass of the orbiter, which in this analysis is assumed rigid, the system could be modelled as a cantilever beam (mast) with a mass with inertia (reflector) at its end. Also, the reflector in this section is going to be assumed flat with a constant thickness small as compared with its characteristic dimensions.

The dynamics analysis of the STRUDL software package, which uses a physical analysis to solve the equations of dynamic equilibrium, is used to generate the eigenvalues, the frequencies, and the periods of the system.

System Geometry (Model)



The beam (mast) will be divided into 3 beam elements (each of 43.33ft length) having a mass of 4.14 slug to be lumped at the ends of the elements.



Coordinates of nodes for the System

Node No.	X	Y	Z	in ft.
1.	0.0	0.0	0.0	
2.	0.0	0.0	-130.0	
3.	0.0	0.0	-43.33	
4.	0.0	0.0	-86.66	
5.	37.50	0.0	-130.00	
6.	56.25	-32.50	-130.00	
7.	37.50	-65.00	-130.00	
8.	00.00	-65.00	-130.00	
9.	-18.75	-32.50	-130.00	
10.	18.75	-32.50	-130.00	

### Results - Conclusions

The following results have been obtained (Table 2.5). They show that the system is less stiff in this model as compared with previously developed NASA<sup>8</sup> and Howard University continuum models and also that recently described by the Harris Corporation.<sup>9</sup>

Table 2.5 - Modal Frequencies ( $\text{Hz}$ )  
Obtained by Implementing a FEM  
of the Preliminary Model of SCOLE  
(Poisson's ratio = 0.3 assumed)

0.157
0.275
0.782
1.083
1.232
<u>1.386</u>
80.09
107.24
107.24
265.99
421.50

## FORMULATION TECHNIQUES

- (1) Eulerian vs. La Grangian
- (2) Modeling of the Flexible Appendage (Mast)  
with Offset Inertial Masses at Both Ends
- (2a) Initial 2-D Vibration Analysis
  - (i) P.D.E. approach
  - (ii) Finite element methods
  - (iii) Treatment of boundary conditions
    - Mast as cantilever
    - Mast as a uniform beam with end bodies having inertia
  - (iv) Separate treatment of lateral and torsional modes.
- (2b) 3-D Vibration Analysis
  - D.K. Robertson, Sept. 1985
  - Harris Corp. Dec. 1984
- ✓ (3) Linearization of 2-D Equations
- (4) Formulation of 3-D Equations Based on 3-D Vibration Analysis

## II.F Linearization of the Equation of Motion-Floquet Analysis

Let  $\tau$  the dimensionless time be equal to  $\omega_c t$ ;  $\frac{d}{dt} = \omega_c \frac{d}{d\tau}$  ;  
 $\frac{d^2}{d\tau^2} = \omega_c^2 \frac{d^2}{d\tau^2}$

Dividing each term of Eq. (2.16) by  $M_m l$  yields

$$\begin{aligned}
 & -\ddot{\theta} \left\{ I_{zs}/M_m l + \ell/3 + I_{er}/M_m l + \frac{Mr}{M_m l} X + \frac{Mr}{M_m} R_2 \right\} \\
 & + \left\{ \left( \frac{R}{l} - \frac{Mr}{M_m l} \right) \omega_c \psi(l) - \omega_c \frac{R}{\beta l^2} \psi_1(l) \right\} (\dot{\theta} \cos(\omega t + \phi) - \theta \omega \sin(\omega t + \phi)) \\
 & - \frac{Mr}{M_m l} X R \omega_c \dot{\theta} \cos(\omega t + \phi) + \omega^2 \cos(\omega t + \phi) \left\{ \left( I_{er}/M_m l^2 + \frac{Mr}{M_m} + \frac{Mr}{M_m} \frac{X^2}{l^2} \right) \psi(l) \right. \\
 & \left. + \frac{1}{\beta l} \psi_2(l) + \frac{1}{\beta^2 l^2} \psi_3(l) \right\} - \omega \sin(\omega t + \phi) \cos(\omega t + \phi) [\psi^2(l)] \left\{ \frac{3}{2} \frac{R}{l^2} \omega_c \right. \\
 & \left. - \frac{Mr}{M_m} \frac{R}{l^2} \omega_c \right\} - \omega \sin(\omega t + \phi) \psi(l) \frac{Mr}{M_m l} \frac{X}{l} \frac{R}{l} \omega_c = 0 \quad (2.46)
 \end{aligned}$$

Let now  $c_1 = \left\{ I_{zs}/M_m l + \ell/3 + I_{er}/M_m l + \mu \lambda X + \mu R_2 \right\}$

where  $\mu = \frac{Mr}{M_m}$ ;  $\lambda = \frac{X}{l}$

$$c_2 = \left( \frac{R}{l} - \mu \frac{R}{l} \right) \psi(l) - \frac{R}{\beta l^2} \psi_1(l)$$

where  $\psi(l) = A \cos \beta l + B \sin \beta l + C \cosh \beta l + D \sinh \beta l$

$$\psi_1(l) = A \sin \beta l - B \cos \beta l + C \sinh \beta l + D \cosh \beta l + B - D$$

$$c_3 = \left( I_{er}/M_m l^2 + \mu + \mu \lambda^2 \right) \psi(l) + \psi_2(l)/\beta l + \psi_3(l)/\beta^2 l^2$$

where  $\psi_2(l) = A \sin \beta l - B \cos \beta l + C \sinh \beta l + D \cosh \beta l$

$$\psi_3(l) = A \cos \beta l + B \sin \beta l - C \cosh \beta l - D \sinh \beta l - A + C$$

$$c_4 = \left(4(\ell)\right)^2 \left\{ \frac{3}{2} \frac{R}{I^2} - \mu \frac{R}{I^2} \right\}$$

$$c_5 = \mu \lambda R$$

$$\text{and } c_6 = 4(\ell) \mu \lambda \frac{R}{I}$$

Eq. (2.46) can be written as

$$\begin{aligned} & -C_1 \ddot{\theta} + \omega_c c_2 \frac{d}{dt} (\theta \cos(\omega t + \phi)) - \omega_c c_5 \dot{\theta} + \omega^2 c_3 \cos(\omega t + \phi) \\ & - \omega_c \omega c_4 \sin(\omega t + \phi) \cos(\omega t + \phi) - \omega \omega_c c_6 \sin(\omega t + \phi) - 3\omega_c^2 (I_{11} - I_{33}) \dot{\theta} = 0 \end{aligned} \quad (2.47)$$

Introducing the dimensionless time  $\tau = \omega_c t$  and dividing Eq. (2.47)

by  $\omega_c^2$  one arrives at

$$\begin{aligned} & -\omega_c^2 C_1 \ddot{\theta}'' + \omega_c^2 C_2 \frac{d}{d\tau} (\theta \cos(\omega t + \phi)) - \omega_c^2 C_5 \frac{d}{d\tau} \theta - 3\omega_c^2 (I_{11} - I_{33}) \theta \\ & + \omega^2 C_3 \cos(\omega t + \phi) - \omega_c \omega C_4 \sin(\omega t + \phi) \cos(\omega t + \phi) - \omega \omega_c C_6 \sin(\omega t + \phi) = 0 \end{aligned} \quad (2.48)$$

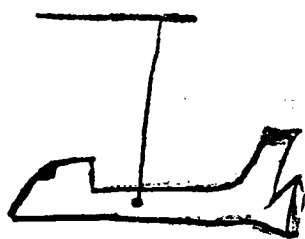
Introducing now the new parameter  $\Omega = \frac{\omega}{\omega_c}$  yields

$$\begin{aligned} & -C_1 \ddot{\theta}'' + C_2 \frac{d}{d\tau} [\theta \cos(\Omega \tau + \phi)] - C_5 \frac{d}{d\tau} \theta \\ & + \Omega^2 C_3 \cos(\Omega \tau + \phi) - \frac{\Omega C_4}{2} \sin[2(\Omega \tau + \phi)] \\ & - \Omega C_6 \sin(\Omega \tau + \phi) - 3(I_{11} - I_{33}) \theta = 0 \end{aligned} \quad (2.49)$$

## FORMULATION TECHNIQUES

- (1) Eulerian vs. La Grangian
- (2) Modeling of the Flexible Appendage (Mast)  
with Offset Inertial Masses at Both Ends
- (2a) Initial 2-D Vibration Analysis
  - (i) P.D.E. approach
  - (ii) Finite element methods
  - (iii) Treatment of boundary conditions
    - Mast as cantilever
    - Mast as a uniform beam with end bodies  
having inertia
  - (iv) Separate treatment of lateral and torsional  
modes.
- (2b) 3-D Vibration Analysis
  - D.K. Robertson, Sept. 1985
  - Harris Corp. Dec. 1984
- (3) Linearization of 2-D Equations
- ✓ (4) Formulation of 3-D Equations Based on 3-D Vibration  
Analysis

## 3-D Formulation (SCOLE)



Consider an elemental mass of the system,  $dm$ , located at  $\vec{r}$  in the body frame,  $R_i$ , moving with the shuttle.

The equations of motion (Newton's second law) of  $dm$  are expressed as:  $\vec{a} dm = \sum \vec{F} = \vec{f} dm + L(\vec{q}) \frac{\vec{q}}{g} dm + \vec{e} dm \quad (1)$

Where :  $\vec{a}$  = inertial acceleration of  $dm$

$\vec{f}$  = gravitational force per unit mass

$\vec{e}$  = external force per unit mass (including control)

$\vec{q}$  = transverse elastic displacement of  $dm$

$L$  = linear operator which when applied to

$\vec{q}$  and divided by  $g$  yields the elastic forces acting on  $dm$

$g$  = Mass per unit volume.

Equation (1) is rewritten as

$$\vec{a} = \vec{f} + L(\vec{q})/\rho + \vec{e} \quad (2)$$

In  $(R_1)$  moving with the shuttle,

$$\vec{a} = \vec{a}_0 + \ddot{\vec{r}} + 2\vec{\omega} \times \dot{\vec{r}} + \dot{\vec{\omega}} \times \vec{r} + \vec{\omega} \times (\vec{\omega} \times \vec{r}) \quad (3)$$

The expression for  $\vec{f}$  contains terms due to gravity at the system center of mass,  $\vec{f}_0$ , and the gravity gradient  $M(\vec{r})$

$$\vec{f} = \vec{f}_0 + M(\vec{r}) \quad (4)$$

Equation (2) can therefore be rewritten as

$$\vec{a}_0 + \ddot{\vec{r}} + 2\vec{\omega} \times \dot{\vec{r}} + \dot{\vec{\omega}} \times \vec{r} + \vec{\omega} \times (\vec{\omega} \times \vec{r}) - \vec{f}_0 - M(\vec{r}) - L(\vec{q})/\rho - \vec{e} = \vec{0} \quad (5)$$

The translational equations of motion are obtained by integrating equation (5) over the entire system.  $\Rightarrow$

$$\int_{\text{Shuttle}}^{(5)} + \int_{\text{Mast}}^{(5)} + \int_{\text{Reflector}}^{(5)} = \vec{0}$$

The rotational equations of motion are obtained by writing the moment equation:

$$\int_{\text{System}} (\vec{r} \times \vec{a}) dm = \int_{\text{System}} \vec{r} \times \vec{f} dm + \int_{\text{System}} \vec{r} \times L(\vec{q})/\rho dm + \int_{\text{System}} \vec{r} \times \vec{e} dm$$

Expressed in R.

$$\vec{\omega}_{\text{shuttle}/R_0} = \left[ \dot{\phi} \cos \theta \cos \psi + \dot{\theta} \sin \psi + \omega_c (\omega_c \psi \sin \theta \sin \phi + \sin \psi \cos \phi) \right] \hat{i}_1 \\ + \left[ -\dot{\phi} \cos \theta \sin \psi + \dot{\theta} \cos \psi + \omega_c (\cos \psi \cos \phi - \sin \psi \sin \theta \sin \phi) \right] \hat{j}_1 \\ + \left[ \dot{\phi} \sin \theta - \omega_c \cos \theta \sin \phi + \dot{\psi} \right] \hat{k}_1 = \omega_x \hat{i}_1 + \omega_y \hat{j}_1 + \omega_z \hat{k}_1$$

$$M = \frac{\rho a^2}{R_0^3} T_1 B_0 T_1^{-1} \quad \text{where}$$

$$T_1 = \begin{bmatrix} \cos \psi \cos \theta & \cos \psi \sin \theta \sin \phi + \sin \psi \cos \phi & -\cos \psi \sin \theta \cos \phi + \sin \psi \sin \phi \\ -\sin \psi \cos \theta & -\sin \psi \sin \theta \sin \phi + \cos \psi \cos \phi & \sin \psi \sin \theta \cos \phi + \sin \phi \cos \psi \\ \sin \theta & -\cos \theta \sin \phi & \cos \theta \cos \phi \end{bmatrix}$$

$$B_0 = \begin{bmatrix} -1 & 0 & 0 \\ 0 & -1 & 0 \\ 0 & 0 & 2 \end{bmatrix}$$

$$T_1^{-1} = \begin{bmatrix} \cos \theta \cos \phi & -\cos \theta \sin \phi & \sin \theta \\ \cos \phi \sin \theta + \sin \phi \sin \theta \cos \phi & \cos \phi \cos \theta - \sin \phi \sin \theta \sin \phi & -\sin \theta \cos \phi \\ \sin \phi \sin \theta - \cos \phi \sin \theta \cos \phi & \sin \phi \cos \theta + \sin \theta \cos \phi \sin \phi & \cos \theta \cos \phi \end{bmatrix}$$

$$M = \frac{\rho a^2}{R_0^3} [M_{ij}]$$

## WHAT CAN WE LEARN ABOUT THE OPEN-LOOP SYSTEM?

- (1) Linearization of 2-D Equations (Torque-Free)
- ✓ (2) Stability Analysis -
  - (2a) Assume appendage is vibrating at only one of its flexible modes
  - (2b) System can be described by periodic coefficients
  - (2c) Floquet analysis can be used to determine system parametric instabilities - quasi-analytic results obtained for cases of (i) No gravity-gradient, no offset of mast interface point on reflector, (ii) with offset of mast interface point, but not gravity-gradient.
  - (2d) For general case, a numerical implementation of the Floquet analysis is required.
- (3) Relation between this system and other systems involving geometric offset
  - (3a) The dynamics of orbiting tethered platform systems  
2-D analysis, Stanley Woodard LSSI  
3-D analysis (in-progress), Fan Ruying - Visiting Scholar, Beijing Inst. of Control Engineering
  - (3b) The dynamics of the Wrap-Rib Antenna system - any published results?

### Parametric Study of the System

Let us assume that the interface point between the reflector and the mast is at the center of mass of the reflector

$$\rightarrow x = 0 \rightarrow \lambda = 0 = c_5 = c_6$$

Under this assumption, the equation becomes

$$\begin{aligned} -\theta'' + \frac{c_2}{c_1} \frac{d}{dt} [\theta \cos(\Omega t + \phi)] + \Omega^2 \frac{c_3}{c_1} \cos(\Omega t + \phi) \\ - \frac{c_4}{2c_1} \Omega \sin[2(\Omega t + \phi)] - \frac{3}{c_1} (I_{11} - I_{33}) \theta = 0 \end{aligned} \quad (2.50)$$

which yields the following first integral

$$\begin{aligned} -\theta' + \frac{c_2}{c_1} [\theta \cos(\Omega t + \phi)] + \Omega^2 \frac{c_3}{c_1} \sin(\Omega t + \phi) \\ + \frac{c_4}{c_1} \cos[2(\Omega t + \phi)] - \frac{3}{c_1} (I_{11} - I_{33}) \int \theta dt = K \end{aligned} \quad (2.51)$$

This equation can be plotted in the phase plane  $(\theta', \theta)$  for different values of  $\mu$  and  $\Omega$ .

### Floquet Analysis

The angular motion about an axis perpendicular to the orbit plane is described by:

$$\theta'' = \left[ -\frac{c_3}{c_1} + \frac{c_2}{c_1} \cos \Omega t \right] \theta' - \left[ \frac{c_2}{c_1} \Omega \sin \Omega t + \frac{3}{c_1} (I_{33} - I_{11}) \right] \theta \quad (2.52)$$

This equation can be recast into the following matrix format

$$\begin{bmatrix} \theta' \\ \theta'' \end{bmatrix} = \begin{bmatrix} P_{11} & P_{12} \\ P_{21} & P_{22} \end{bmatrix} \begin{bmatrix} \theta \\ \theta' \end{bmatrix} \quad (2.53)$$

where

$$[P(\tau)] = \begin{bmatrix} -\frac{C_5}{C_1} + \frac{C_2}{C_1} \cos \Omega \tau & -\left[\frac{C_2}{C_1} \Omega \sin(\Omega \tau) + \frac{3}{C_1} (I_{11} - I_{33})\right] \\ 1 & 0 \end{bmatrix}$$

Since  $P(\tau)$  is a matrix with periodic coefficients, the stability of the motion will be analyzed in what follows using the Floquet theorem.

Case 1. No gravity gradient, No offset

$$P(\tau) = \begin{bmatrix} \frac{C_2}{C_1} \cos \Omega \tau & -\frac{C_2}{C_1} \Omega \sin \Omega \tau \\ 1 & 0 \end{bmatrix}$$

$$[Z(\tau)] = [P(\tau)] [Z(\tau)]$$

## 2. Floquet theorem

Equation (2.53) can be written as

$$\phi'' + p(\tau)\phi = 0 \quad (4.3)$$

where  $p(\tau)$  is a periodic function with period  $T = 2\pi/\Omega$ .

By setting  $y_1 = \phi$ ;  $y_2 = \phi' = y'_1$ , one could recast equation (4.3) in the following state variable form.

$$\begin{bmatrix} y'_1 \\ y'_2 \\ \vdots \\ y' \end{bmatrix} = \begin{bmatrix} 0 & 1 \\ -p(\tau) & 0 \\ \vdots & \vdots \\ E(\tau) \end{bmatrix} \begin{bmatrix} y_1 \\ y_2 \\ \vdots \\ y \end{bmatrix} \quad (4.4)$$

Assuming that the quantities  $z_{11}(T)$ ,  $z_{12}(T)$ ,  $z_{21}(T)$ , and  $z_{22}(T)$  are known (where the  $z_{ij}(T)$  are the elements of the matrix  $[Z(T)]$ ) which satisfies the matrix equation  $[Z(\tau)]' = [E(\tau)][Z(\tau)]$  and which, when  $\tau=0$ , equals the identity matrix( $I$ ); one can derive the stability conditions applying the Floquet theorem<sup>14</sup> which states:

- (i) if for any  $j$ ,  $||s_j|| > 1$ , (where  $||s_j||$  represents the modulus of the eigenvalue,  $s_j$ ), the zero solution of equation (4.3) is unstable;
- (ii) if for all  $j$ ,  $||s_j|| < 1$ , the zero

solution of equation (4.3) is asymptotically stable;

(iii) if for all  $j$ ,  $\|s_j\|$  is not greater than 1, but for some  $j$ ,  $\|s_j\| = 1$ , and each  $s_j$  of modulus 1 is distinct from the others, then the zero solution is stable but not asymptotically stable,

(iv) if for all  $j$ ,  $\|s_j\|$  is not greater than 1, and there exist some  $s_j$  with  $\|s_j\| = 1$  in multiplicity  $n$ , the zero solution of equation (4.3) is unstable unless  $n = k$  where the  $s_j$  are the eigenvalues of  $[Z(T)]$ ,  $s_n$  = repeated eigenvalues, and  $k = \text{nullity of } [Z(T) - s_n I] = (\text{order of } [Z(T) - s_n I]) - \text{minus rank of } [Z(T) - s_n I]$ .

$$\dot{z}_{11} = p_{11}z_{11} + p_{12}z_{21} \quad (1)$$

$$\dot{z}_{12} = p_{11}z_{12} + p_{12}z_{22} \quad (2)$$

$$\dot{z}_{21} = p_{21}z_{11} + p_{22}z_{21} \quad (3) \text{ which becomes } \dot{z}_{21} = z_{11} \text{ since } p_{21} = 1 \text{ and } p_{22} = 0$$

$$\dot{z}_{22} = p_{21}z_{12} + p_{22}z_{22} \quad (4) \text{ which becomes } \dot{z}_{22} = z_{12}$$

from (3)  $\ddot{z}_{21} = \dot{z}_{11}$  substituted into 1 yields

$$\ddot{z}_{21} = p_{11}\dot{z}_{21} + p_{12}z_{21}$$

Similarly from (4)  $\ddot{z}_{22} = \dot{z}_{12}$  which substituted into (2) yields

$$\ddot{z}_{22} = p_{11}\dot{z}_{22} + p_{12}z_{22}$$

If one notices that  $p_{12} = \frac{d}{dt} p_{11}$

then  $\ddot{z}_{21} = p_{11}\dot{z}_{21} + \dot{p}_{11}z_{21} = \frac{d}{dt} (p_{11}z_{21})$

and  $\ddot{z}_{22} = p_{11}\dot{z}_{22} + \dot{p}_{11}z_{22} = \frac{d}{dt} (p_{11}z_{22})$

These two last equations are integrated and the following result for  $z_{21}$  and  $z_{22}$  obtained

$$\dot{z}_{21} = p_{11}z_{21} + K_1$$

$$\dot{z}_{22} = p_{11}z_{22} + K_2$$

but from (3),  $\dot{z}_{21} = z_{11}(\tau)$  and

from (4),  $\dot{z}_{22} = z_{12}(\tau)$

$$\text{therefore, } \dot{z}_{21}(0) = z_{11}(0) = 1 = p_{11}(0)z_{21}(0) + K_1$$

or for  $\phi = 0 \quad 1 = K_1 \quad \text{since } z_{21}(0) = 0$

$$\Rightarrow K_1 = 1$$

$$\dot{z}_{22}(0) = z_{12}(0) = 0 = p_{11}(0)z_{22}(0) + K_2$$

or for  $\phi = 0$   $\frac{c_2}{c_1} = -k_2$  since  $z_{22}(0) = 1$

$$\dot{z}_{21} = p_{11} z_{21} + 1$$

$$\dot{z}_{22} = p_{11} z_{22} - \frac{c_2}{c_1}$$

Solution of the linear first order equation

$$\frac{dz_{22}}{d\tau} - p_{11} z_{22} = -\frac{c_2}{c_1} \quad (1)$$

The presence of  $\frac{dz_{22}}{d\tau}$  and  $p_{11} z_{22}$  in the equation suggests a product of the type  $\phi(\tau) z_{22}(\tau)$

$$\text{but } \frac{d}{d\tau}(\phi z_{22}) = \frac{d\phi}{d\tau} z_{22} + \phi \frac{d}{d\tau} z_{22} \quad (2)$$

Multiplying (1) by  $\phi(\tau)$  yields

$$\phi \frac{d}{d\tau}(\phi z_{22}) - \phi p_{11} z_{22} = -\frac{c_2}{c_1} \phi \quad (3)$$

which can become

$$\frac{d}{d\tau}(\phi z_{22}) = -\frac{c_2}{c_1} \phi \quad (4)$$

if one can find  $\phi(\tau)$  (the integrating factor) such that

$$\frac{d\phi}{d\tau} = -\phi p_{11} \quad (5)$$

$$\Rightarrow \ln \phi(\tau) = \int -\rho_{11} d\tau = \int -\frac{c_2}{c_1} \cos \Omega \tau d\tau$$

$$\ln \phi(\tau) = -\frac{c_2}{c_1 \Omega} \sin \Omega \tau + K \quad \text{or}$$

$$\phi(\tau) = \exp \left[ -\frac{c_2}{c_1 \Omega} \sin \Omega \tau + K \right]$$

from  $\frac{d}{d\tau} (\phi z_{22}) = -\frac{c_2}{c_1} \phi(\tau)$  one arrives at

$$\phi z_{22} = \int -\frac{c_2}{c_1} \phi(\tau) d\tau$$

or  $z_{22} = \frac{1}{\phi(\tau)} \int -\frac{c_2}{c_1} \phi(\tau) d\tau$

$$z_{11}(\tau) = \exp \left[ \frac{c_2}{c_1 \Omega} \sin \Omega \tau + K \right] \left\{ -\frac{c_2}{c_1} \int \exp \left[ -\frac{c_2}{c_1 \Omega} \sin \Omega \tau + K \right] d\tau \right\}$$

According to Taylor's series development of a function

$$e^k \exp \left[ -\frac{c_2}{c_1 \Omega} \sin \Omega \tau \right] = e^k \left\{ 1 - \frac{c_2}{c_1} \tau + \left( \frac{c_2}{c_1} \right)^2 \frac{\tau^2}{2} - \left( \left( \frac{c_2}{c_1} \right)^3 - \Omega^2 \frac{c_2}{c_1} \right) \frac{\tau^3}{6} + \dots \right\}$$

which is integrated term by term to give

$$z_{22} = -\frac{c_2}{c_1} \exp \left[ \frac{c_2}{c_1 \Omega} \sin \Omega \tau - K \right] \left\{ \tau - \frac{c_2}{c_1} \frac{\tau^2}{2} + \frac{c_2^2}{6c_1^2} \tau^3 - \left( \left( \frac{c_2}{c_1} \right)^3 - \Omega^2 \frac{c_2}{c_1} \right) \frac{\tau^4}{24} + K \right\}$$

since  $z_{22}(0) = 1 \Rightarrow K_1 = -\frac{c_1}{c_2}$

$$z_{22} = -\frac{c_2}{c_1} \exp \left\{ \frac{c_2}{\Omega c_1} \sin \Omega \tau \right\} \left[ -\frac{c_1}{c_2} + \tau - \frac{c_2}{c_1} \frac{\tau^2}{2} + \frac{c_2^2}{6c_1^2} \tau^3 + \dots \right]$$

Solution of  $\dot{z}_{21} = p_{11} z_{21} + 1$  where  $p_{11} = \frac{C_2}{C_1} \cos \Omega \tau$

$$\Rightarrow \frac{d}{d\tau} (\phi' z_{21}) = \frac{d}{d\tau} \phi' z_{21} + \phi' \frac{d}{d\tau} z_{21} \quad (1)$$

and  $\phi' \frac{d}{d\tau} z_{21} - \phi' p_{11} z_{21} = \phi'$  (2)

$$(1) = (2) \Rightarrow \frac{d\phi'}{d\tau} = -\phi' p_{11}$$

$$\Rightarrow \ln \phi'(\tau) = -\frac{C_2}{\Omega C_1} \sin \Omega \tau + K' \text{ or}$$

$$\phi'(\tau) = \exp \left[ -\frac{C_2}{C_1 \Omega} \sin \Omega \tau + K' \right]$$

from

$$\frac{d}{d\tau} (\phi' z_{21}) = \phi' \Rightarrow \phi' z_{21} = \int \phi' d\tau$$

$$z_{21} = \frac{1}{\phi'} \int \phi' d\tau = \exp \left[ \frac{C_2}{C_1 \Omega} \sin \Omega \tau - K' \right] \int \phi' d\tau$$

According to Taylor's series

$$\phi'(\tau) = \exp \left[ -\frac{C_2}{\Omega C_1} \sin \Omega \tau \right] e^{K'} = e^{K'} \left\{ 1 - \frac{C_2}{C_1} \tau + \frac{C_2^2}{C_1^2} \frac{\tau^2}{2} + \left[ -\left( \frac{C_2}{C_1} \right)^3 + \left( \frac{C_2}{C_1} \Omega^2 \right) \right] \right\}$$

which is integrated term by term to yield

$$Z_{21}(\tau) = \exp\left[\frac{C_2}{\Omega C_1} \sin \Omega \tau\right] \left\{ \tau - \frac{C_2}{2C_1} \tau^2 + \frac{C_2^2}{6C_1^2} \tau^3 + \dots + K'_1 \right\}$$

$$Z_{21}(0) = 0 \Rightarrow K'_1 = 0$$

$$\dot{Z}_{11}(\tau) = \dot{Z}_{21}(\tau) \Rightarrow$$

$$Z_{11}(\tau) = \exp\left[\frac{C_2}{\Omega C_1} \sin \Omega \tau\right] \left[ \frac{C_2}{C_1} \tau - \left(\frac{C_2}{C_1}\right)^2 \frac{\tau^2}{2} + \dots \right] (\cos \Omega \tau - 1) \\ + \exp\left[\frac{C_2}{\Omega C_1} \sin \Omega \tau\right]$$

It can easily be verified that  $Z_{11}(0) = \exp\left\{\frac{C_2}{C_1 \Omega} \sin 0\right\} = 1$   
and finally

$$\dot{Z}_{22} = Z_{12}(\tau)$$

$$\Rightarrow Z_{12}(\tau) = -\left(\frac{C_2}{C_1}\right)^2 \exp\left\{\frac{C_2}{\Omega C_1} \sin \Omega \tau\right\} \left[ \tau - \frac{C_2}{C_1} \frac{\tau^2}{2} + \left(\frac{C_2}{C_1}\right)^2 \frac{\tau^3}{6} + \dots \right] \times \\ (\cos \Omega \tau - 1) + \left(\frac{C_2}{C_1} \cos \Omega \tau - \frac{C_2}{C_1}\right) \exp\left\{\frac{C_2}{\Omega C_1} \sin \Omega \tau\right\}$$

With the use of a computer program, the eigenvalues of the  $[Z(\tau)]$  matrix are computed for  $\tau = \text{a period}$  and their modulus compared with 1 to determine the values of the parameters for which the system is stable. The results of such parametric study are shown in the following stability diagram, Fig. 2.7. The large number of unstable points in the parametric space ( $\Omega, MU$ ) are thought to be attributed to the absence of the gravity-gradient torque in the model. Future plans call for the extension of the Floquet analysis for the cases where a non-zero reflector attachment offset is considered and also where both a non-zero offset and the effects of gravity-gradient are included.

$$\Omega = \frac{\omega}{\omega_0}$$

to be multiplied  
by 10<sup>3</sup>

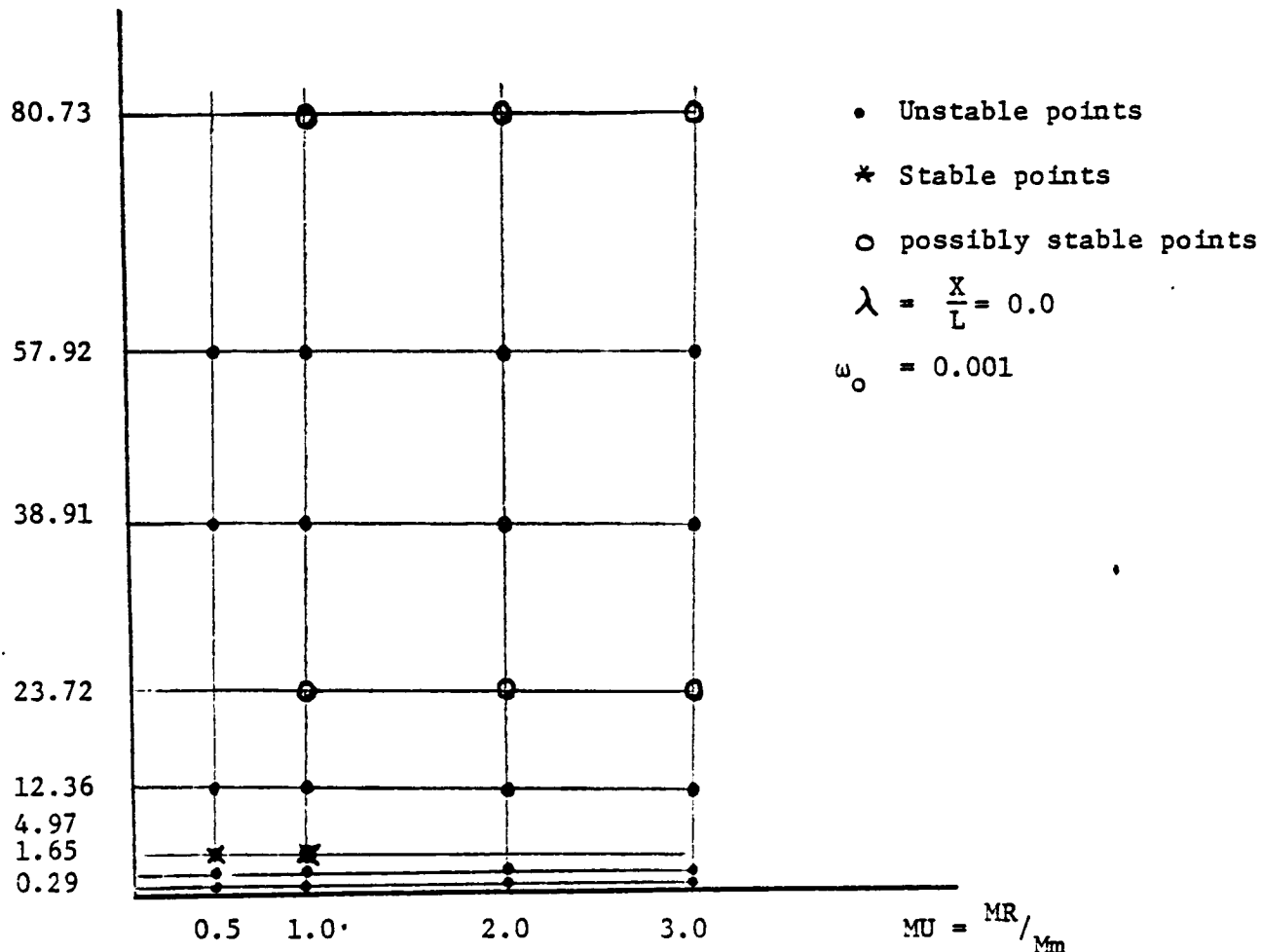


Fig. 2.7 Floquet Stability Diagram - SCOLE Configuration-No Offset  
No Gravity Gradient.

Case 2. No gravity gradient, but offset.

$$p(z) = \begin{bmatrix} \frac{c_2}{c_1} \cos \omega t - \frac{c_5}{c_1} & -\frac{c_2 \omega}{c_1} \sin \omega t \\ 1 & 0 \end{bmatrix}$$

$$[\dot{z}(t)] = [P(t)][z(t)]$$

$$\dot{z}_{11} = P_{11} z_{11} + P_{12} z_{21} \quad (1)$$

$$\dot{z}_{12} = P_{11} z_{12} + P_{12} z_{22} \quad (2)$$

$$\dot{z}_{21} = P_{21} z_{11} + P_{22} z_{21} \quad (3) \text{ which becomes}$$

$$\dot{z}_{21} = z_{11} \text{ since } P_{21} = 1 \text{ and } P_{22} = 0$$

$$\dot{z}_{22} = P_{21} z_{12} + P_{22} z_{22} \quad (4) \text{ which becomes}$$

$$\dot{z}_{22} = z_{12}$$

from (3)  $\ddot{z}_{21} = \dot{z}_{11}$  substituted into (1) yields

$$\ddot{z}_{21} = P_{11} \dot{z}_{21} + P_{12} z_{21}$$

Similarly from (4)  $\ddot{z}_{22} = \dot{z}_{12}$  substituted into (2) yields

$$\ddot{z}_{22} = P_{11} \dot{z}_{22} + P_{12} z_{22}$$

Since  $\frac{c_5}{c_1} = \text{constant}$   $\frac{d}{dt} P_{11} = P_{12}$

Then

$$\ddot{z}_{21} = P_{11} \dot{z}_{21} + \dot{P}_{11} z_{21} = \frac{d}{dt} (P_{11} z_{21})$$

and  $\ddot{z}_{22} = P_{11} \dot{z}_{22} + \dot{P}_{11} z_{22} = \frac{d}{dt} (P_{11} z_{22})$

These two last equations are integrated and the following results for  $z_{21}$  and  $z_{22}$  obtained.

$$\dot{z}_{21} = P_{11} z_{21} + k_1$$

$$\dot{z}_{22} = P_{11} z_{22} + k_2$$

but from (3)  $\dot{z}_{21}(t) = z_{11}(t)$  and from (4)

$$\dot{z}_{22}(t) = z_{12}(t)$$

Therefore,  $\dot{z}_{21}(0) = z_{11}(0) = P_{11}(0) z_{21}(0) + k_1 \Rightarrow k_1 = 1$

Since  $z_{11}(0) = 1$  and  $z_{21}(0) = 0$

$$\dot{z}_{22}(0) = z_{12}(0) = 0 = P_{11}(0) z_{22}(0) + k_2$$

$$\Rightarrow \frac{C_5}{C_1} + \frac{C_2}{C_1} + k_2 = 0 \quad \text{or} \quad k_2 = -\frac{C_2}{C_1} + \frac{C_5}{C_1}$$

The two last equations integrated once, yield

$$\dot{z}_{21} = P_{11} z_{21} + 1$$

$$\dot{z}_{22} = P_{11} z_{22} - \frac{(C_2 - C_5)}{C_1}$$

## Solution of the first order equations

$$\frac{dZ_{22}}{d\tau} - P_{11} Z_{22} = -\frac{(C_2 - C_5)}{C_1} \quad (1)$$

The presence of  $\frac{dZ_{22}}{d\tau}$  and  $P_{11} Z_{22}$  in the equation suggest a product of the type  $\Phi(\tau) Z_{22}(\tau)$

$$\text{but } \frac{d}{d\tau}(\Phi Z_{22}) = \frac{d\Phi}{d\tau} Z_{22} + \Phi \frac{d}{d\tau} Z_{22} \quad (2)$$

Multiplying (1) by  $\Phi(\tau)$  yields

$$\Phi \frac{dZ_{22}}{d\tau} - \Phi P_{11} Z_{22} = -\Phi \frac{(C_2 - C_5)}{C_1}$$

which can become

$$\frac{d}{d\tau}(\Phi Z_{22}) = -\Phi \frac{(C_2 - C_5)}{C_1}$$

if one can find  $\Phi(\tau)$  (integrating factor) such that

$$\frac{d\Phi}{d\tau} = -\Phi P_{11}$$

$$\Rightarrow \ln \Phi(\tau) = \int -P_{11} d\tau = \int -\frac{C_2}{C_1} \cos \Omega \tau d\tau + \int \frac{C_5}{C_1} d\tau$$

$$\ln \Phi(\tau) = -\frac{C_2}{C_1 \Omega} \sin \Omega \tau + \frac{C_5}{C_1} \tau + K$$

$$\text{or } \Phi(\tau) = \exp \left[ -\frac{C_2}{C_1 \Omega} \sin \Omega \tau \right] \cdot e^{\left( \frac{C_5}{C_1} \tau + K \right)}$$

$$\text{from } \frac{d(\bar{\alpha}_{22}\phi)}{d\tau} = -\phi \left( \frac{c_2 - c_5}{c_1} \right)$$

$$\bar{\alpha}_{22} = \frac{1}{\phi} \int \phi \left( \frac{c_5 - c_2}{c_1} \right) d\tau$$

$$\text{or } \bar{\alpha}_{22} = \exp \left[ \frac{c_2}{c_1 \Omega} \sin \Omega \tau - \frac{c_5}{c_1} \tau - K \right] \left( \frac{c_5 - c_2}{c_1} \right) \int \exp \left[ -\frac{c_2}{c_1 \Omega} \sin \Omega \tau + \frac{c_5}{c_1} \tau + K \right] d\tau$$

$$\exp \left[ -\frac{c_2}{\Omega c_1} \sin \Omega \tau \right] \approx 1 - \frac{c_2}{c_1} \tau + \frac{c_2^2}{c_1^2} \frac{\tau^2}{2} - \left\{ \left( \frac{c_2}{c_1} \right)^2 - \Omega^2 \frac{c_2}{c_1} \right\} \frac{\tau^3}{6} + \dots$$

$$\exp \left[ \frac{c_5}{c_1} \tau \right] \approx 1 + \frac{c_5}{c_1} \tau + \left( \frac{c_5}{c_1} \right)^2 \frac{\tau^2}{2} + \dots$$

$$\text{Therefore, } \exp \left[ \frac{c_2}{\Omega c_1} \sin \Omega \tau + \frac{c_5}{c_1} \tau \right] \approx 1 + \left( \frac{c_5 - c_2}{c_1} \right) \tau + \left( \frac{c_5 - c_2}{c_1} \right)^2 \frac{\tau^2}{2} + \dots$$

$$\bar{\alpha}_{22} = \exp \left[ \frac{c_2}{\Omega c_1} \sin \Omega \tau - \frac{c_5}{c_1} \tau - K \right] \left( \frac{c_5 - c_2}{c_1} \right) e^K \left( \tau + \left( \frac{c_5 - c_2}{c_1} \right) \frac{\tau^2}{2} + \left( \frac{c_5 - c_2}{c_1} \right)^2 \frac{\tau^3}{6} + \dots \right)$$

$$\bar{\alpha}_{22}(0) = 1 \Rightarrow \left( \frac{c_5 - c_2}{c_1} \right) K' = 1 \Rightarrow K' = \frac{c_1}{c_5 - c_2}$$

$$\boxed{\bar{\alpha}_{22} = \exp \left[ \frac{c_2}{c_1 \Omega} \sin \Omega \tau - \frac{c_5}{c_1} \tau \right] \left\{ 1 + \left( \frac{c_5 - c_2}{c_1} \right) \tau + \left( \frac{c_5 - c_2}{c_1} \right)^2 \frac{\tau^2}{2} + \left( \frac{c_5 - c_2}{c_1} \right)^3 \frac{\tau^3}{6} + \dots \right\}}$$

$$\text{Since } \dot{\bar{\alpha}}_{22} = \bar{\alpha}_{22}(\tau) = \exp \left[ \frac{c_2}{c_1 \Omega} \sin \Omega \tau - \frac{c_5}{c_1} \tau \right] \left\{ \left( \frac{c_5 - c_2}{c_1} \right) \tau + \left( \frac{c_5 - c_2}{c_1} \right)^2 \frac{\tau^2}{2} + \left( \frac{c_5 - c_2}{c_1} \right)^3 \frac{\tau^3}{6} + \dots \right\}$$

$$+ \left( \frac{c_2}{c_1} \cos \Omega \tau - \frac{c_5}{c_1} \right) \exp \left[ \frac{c_2}{c_1 \Omega} \sin \Omega \tau - \frac{c_5}{c_1} \tau \right] \left\{ 1 + \left( \frac{c_5 - c_2}{c_1} \right) \tau + \left( \frac{c_5 - c_2}{c_1} \right)^2 \frac{\tau^2}{2} + \dots \right\}$$

$$Z_{12} = \exp \left[ \frac{C_2}{C_1 \Omega} \sin \Omega \tau - \frac{C_5}{C_1} \tau \right] \left\{ \frac{-C_2 + C_5 - C_5 + C_2 \cos \Omega \tau}{C_1} \right. \\ \left. + \left[ \left( \frac{C_2 \cos \Omega \tau - C_5}{C_1} \right) \left( \frac{C_5 - C_2}{C_1} \right) + \left( \frac{C_5 - C_2}{C_1} \right)^2 \right] \tau + \left[ \left( \frac{C_2 \cos \Omega \tau - C_5}{C_1} \right) \left( \frac{C_5 - C_2}{C_1} \right)^2 + \right. \right. \\ \left. \left. \left( \frac{C_5 - C_2}{C_1} \right)^3 \right] \frac{\tau^2}{2} + \dots \right\}$$

$$Z_{12}(\tau) = \exp \left[ \frac{C_2}{C_1 \Omega} \sin \Omega \tau - \frac{C_5}{C_1} \tau \right] \left\{ \frac{C_2 (1 + \cos \Omega \tau)}{C_1} + \left( \frac{C_5 - C_2}{C_1} \right) \left( \frac{C_2 \cos \Omega \tau - C_5 + C_5 - C_2}{C_1} \right) \right. \\ \left. + \dots \right\}$$

$$Z_{12}(\tau) = \exp \left[ \frac{C_2}{C_1 \Omega} \sin \Omega \tau - \frac{C_5}{C_1} \tau \right] \left[ C_2 \left( \frac{\cos \Omega \tau - 1}{C_1} \right) \right] \left[ 1 + \frac{C_5 - C_2}{C_1} \tau + \left( \frac{C_5 - C_2}{C_1} \right)^2 \frac{\tau^2}{2} \right]$$

$$\frac{dZ_{21}}{d\tau} = P_{11} Z_{21} + 1 \quad \text{where } P_{11} = \frac{C_2}{C_1} \cos \Omega \tau - \frac{C_5}{C_1}$$

Integrating factor  $\phi$ ;  $\frac{d\phi}{d\tau} = -\phi' P_{11}$

$$\Rightarrow \phi = \exp \left[ -\frac{C_2}{\Omega C_1} \sin \Omega \tau + \frac{C_5}{C_1} \tau + K \right] \text{ and}$$

$$Z_{21} = \frac{1}{\phi} \int \phi d\tau = \exp \left[ +\frac{C_2}{\Omega C_1} \sin \Omega \tau - \frac{C_5}{C_1} \tau - K \right] \int \phi d\tau$$

$$\exp \left[ -\frac{C_2}{\Omega C_1} \sin \Omega \tau + \frac{C_5}{C_1} \tau \right] \approx 1 + \left( \frac{C_5 - C_2}{C_1} \right) \tau + \left( \frac{C_5 - C_2}{C_1} \right)^2 \frac{\tau^2}{2} + \dots$$

Integrating term by term yields,

$$Z_{21} = \exp \left[ \frac{C_2}{\Omega C_1} \sin \Omega \tau - \frac{C_5}{C_1} \tau \right] \left[ \tau + \left( \frac{C_5 - C_2}{C_1} \right) \frac{\tau^2}{2} + \left( \frac{C_5 - C_2}{C_1} \right)^2 \frac{\tau^3}{6} + \dots + K' \right]$$

$$\text{Since } Z_{21}(0) = K' = 0$$

$$Z_{21}(\tau) = \exp \left[ \frac{C_2}{\Omega C_1} \sin \Omega \tau - \frac{C_5}{C_1} \tau \right] \left[ \tau + \left( \frac{C_5 - C_2}{C_1} \right) \frac{\tau^2}{2} + \left( \frac{C_5 - C_2}{C_1} \right)^2 \frac{\tau^3}{6} + \dots \right]$$

$$\dot{Z}_{21} = Z_{11}(\tau) = \exp \left[ \frac{C_2}{\Omega C_1} \sin \Omega \tau - \frac{C_5}{C_1} \tau \right] \left\{ 1 + \left( \frac{C_5 - C_2}{C_1} \right) \tau + \left( \frac{C_5 - C_2}{C_1} \right)^2 \frac{\tau^2}{2} + \dots \right.$$

$$\left. + \left[ \frac{C_2}{C_1} \cos \Omega \tau - \frac{C_5}{C_1} \right] \exp \left[ \frac{C_2}{\Omega C_1} \sin \Omega \tau - \frac{C_5}{C_1} \tau \right] \left[ \tau + \left( \frac{C_5 - C_2}{C_1} \right) \frac{\tau^2}{2} + \left( \frac{C_5 - C_2}{C_1} \right)^2 \frac{\tau^3}{6} + \dots \right] \right)$$

$$Z_{11}(\tau) = \exp \left[ \frac{C_2}{\Omega C_1} \sin \Omega \tau - \frac{C_5}{C_1} \tau \right] \left[ 1 + \left( \frac{C_5 - C_2 + C_2 \cos \Omega \tau - C_5}{C_1} \right) \tau + \dots \right]$$

$$\bar{Z}_{11}(\tau) = \exp \left[ \frac{C_2}{\Omega C_1} \sin \Omega \tau - \frac{C_5}{C_1} \tau \right] \left[ 1 + \frac{C_2}{C_1} (\cos \Omega \tau - 1) \tau + \frac{C_2}{C_1} (C_5 - C_2) (\omega \Omega \tau)^2 \frac{1}{2} \right. \\ \left. + \dots \right]$$

It is seen that  $Z_{11}(0) = 1$

$$\Omega = \frac{\omega}{\omega_0}$$

to be multiplied  
by  $10^3$

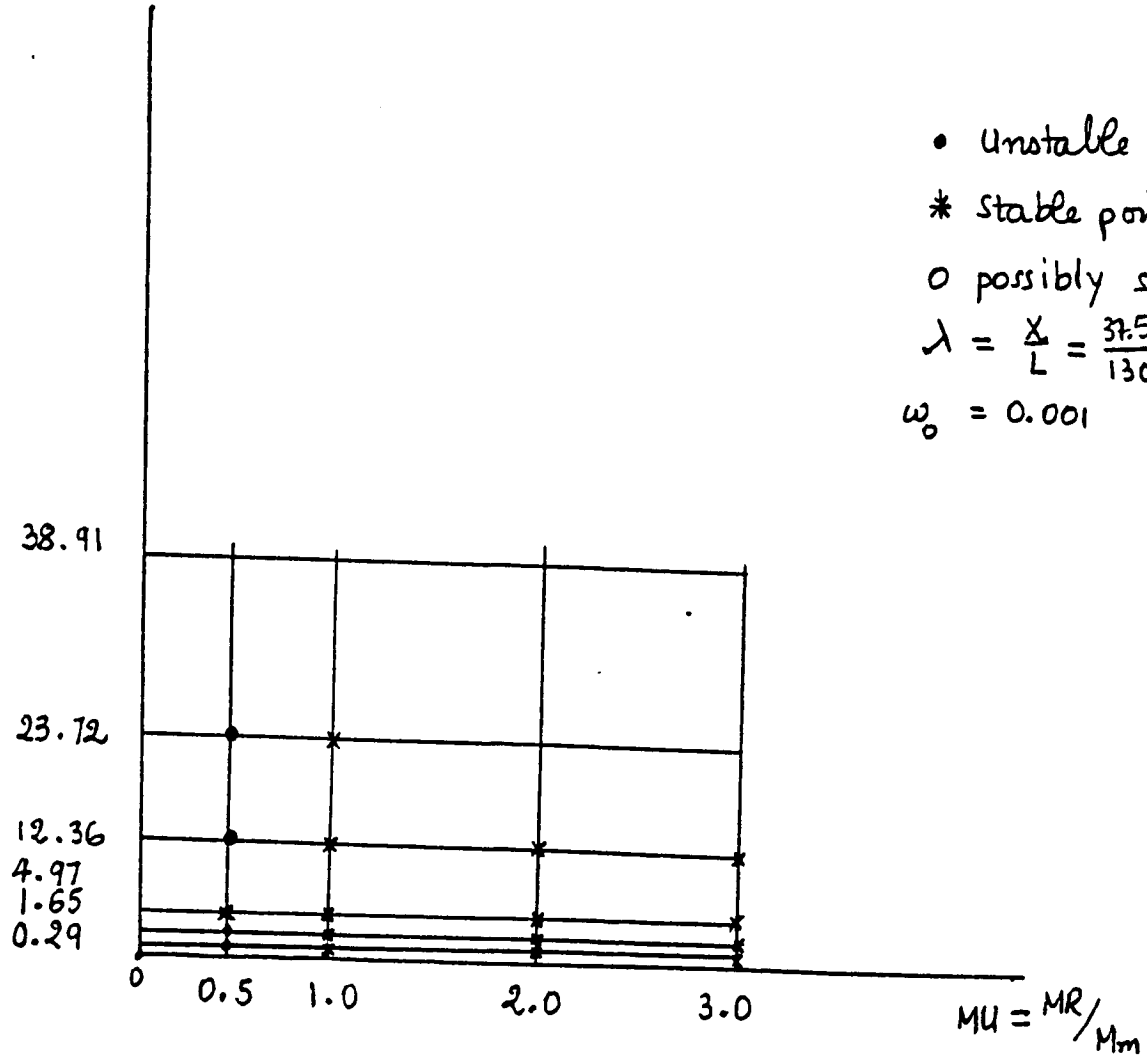


Fig 2.8 Floquet Stability diagram - SCOLE Configuration  
No Gravity Gradient.

$$\Omega = \frac{\omega}{\omega_0}$$

to be multiplied  
by  $10^3$

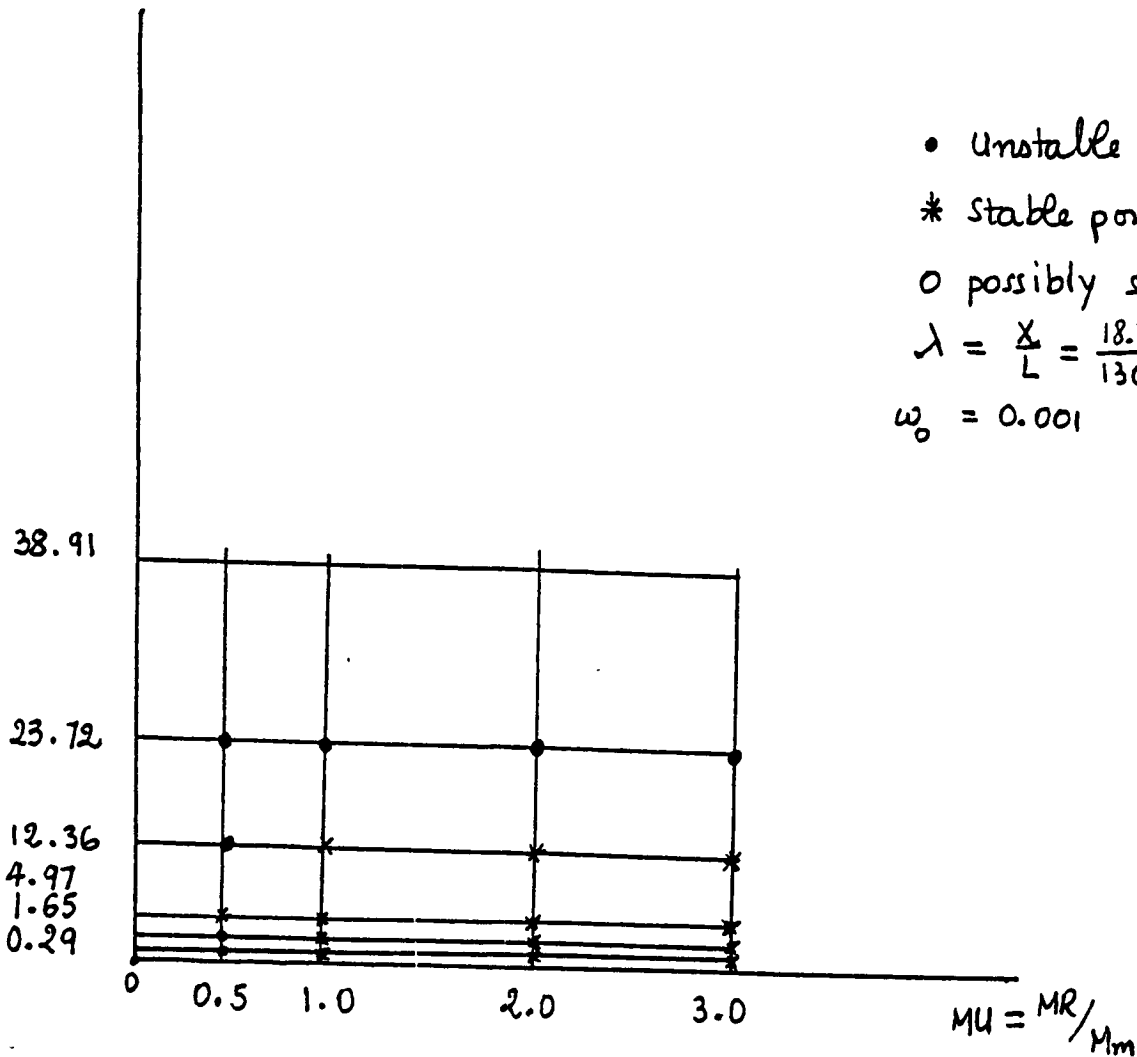
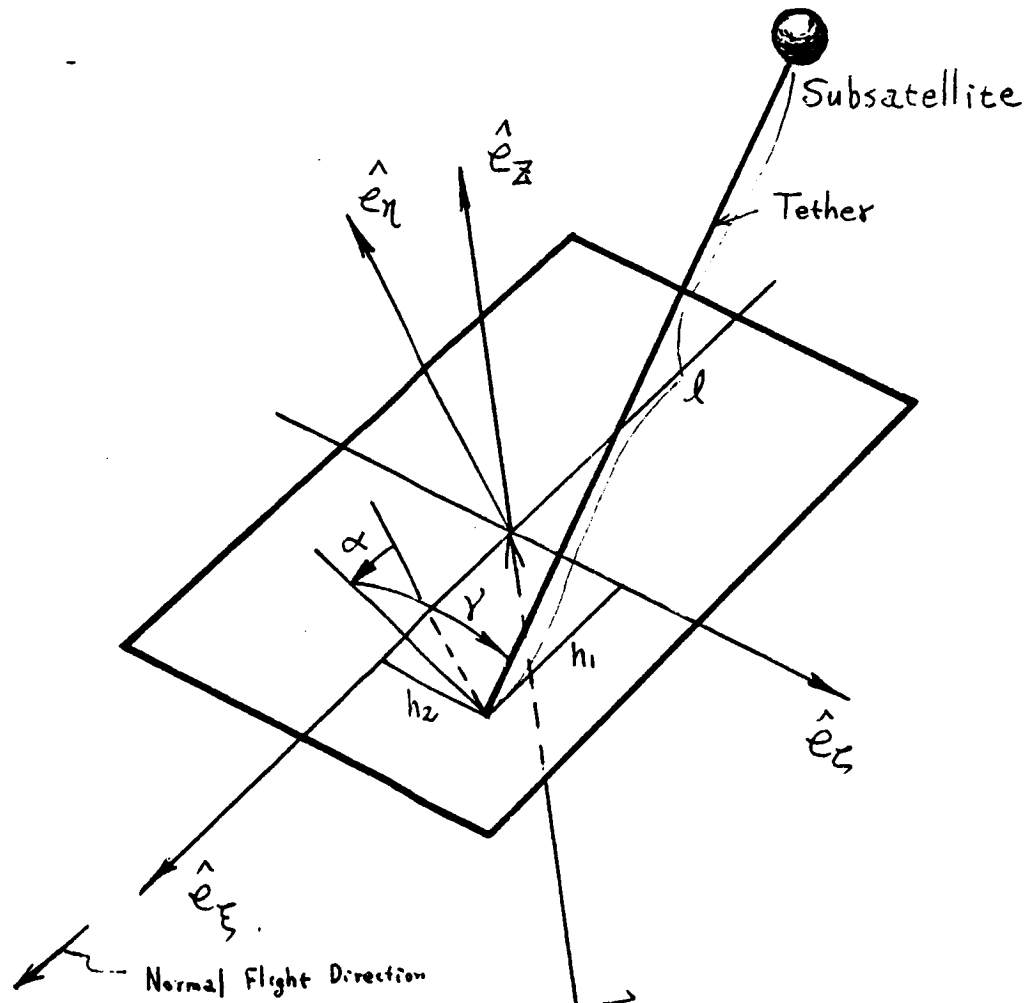


Fig 2-9 Floquet Stability diagram - SCOLE Configuration  
No Gravity Gradient.

C-3

## WHAT CAN WE LEARN ABOUT THE OPEN-LOOP SYSTEM?

- (1) Linearization of 2-D Equations (Torque-Free)
- (2) Stability Analysis -
  - (2a) Assume appendage is vibrating at only one of its flexible modes
  - (2b) System can be described by periodic coefficients
  - (2c) Floquet analysis can be used to determine system parametric instabilities - quasi-analytic results obtained for cases of (i) No gravity-gradient, no offset of mast interface point on reflector, (ii) with offset of mast interface point, but not gravity-gradient.
  - (2d) For general case, a numerical implementation of the Floquet analysis is required.
- (3) Relation between this system and other systems involving geometric offset
  - ✓ (3a) The dynamics of orbiting tethered platform systems  
2-D analysis, Stanley Woodard LSSI  
3-D analysis (in-progress), Fan Ruying - Visiting Scholar, Beijing Inst. of Control Engineering
  - (3b) The dynamics of the Wrap-Rib Antenna system - any published results?



ASSUMED:

- massless tether and fault
- $h_1, h_2$  are offset from the platform's mass center
- $m$  the subsatellite mass is significantly less than that of platform
- $I_x, I_y$  and  $I_z$  are the platform roll, pitch and yaw principal moments of inertia
- $l_c$  is the nominal reference length of tether

Fig. 1

SYSTEM GEOMETRY

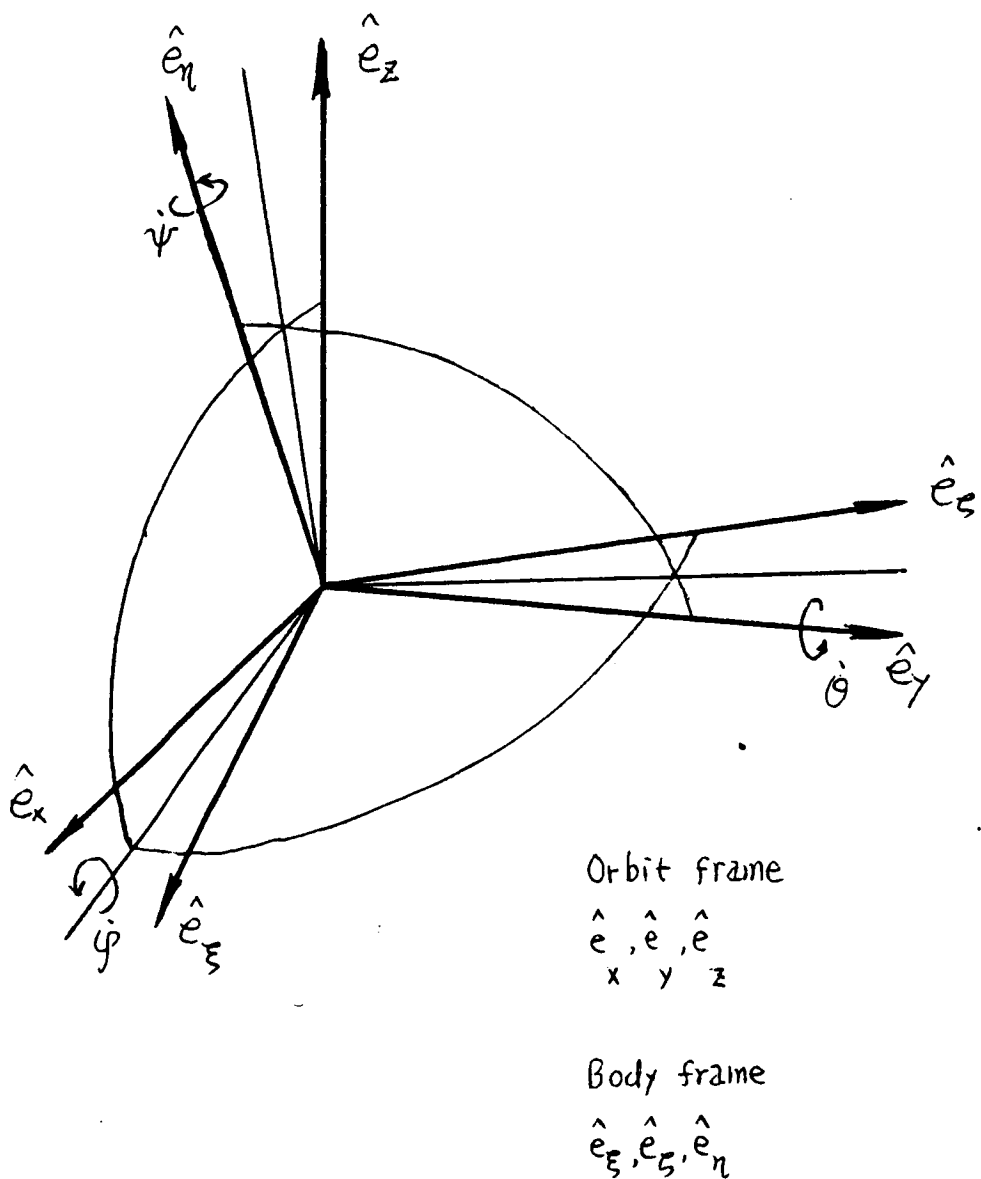


Fig. 2 RELATIONSHIP BETWEEN COORDINATE SYSTEMS

$$\dot{X} = AX + BU$$

$$X = (\epsilon \ \theta \ \varphi \ \alpha \ \gamma \ \epsilon' \ \theta' \ \varphi' \ \alpha' \ \alpha'')^T$$

$$\epsilon = \frac{\dot{\alpha} - \dot{\alpha}_c}{\dot{\alpha}_c}$$

$$A = \begin{pmatrix} 0 & 0 & 0 & 0 & 0 & 0 & 0 & 0 & 0 & 0 \\ 0 & 0 & 0 & 0 & 0 & 0 & 0 & 0 & 0 & 0 \\ 0 & 0 & 0 & 0 & 0 & 0 & 0 & 0 & 0 & 0 \\ 0 & 0 & 0 & 0 & 0 & 0 & 0 & 0 & 0 & 0 \\ 0 & 0 & 0 & 0 & 0 & 0 & 0 & 0 & 0 & 0 \\ 0 & 0 & 0 & 0 & 0 & 0 & 0 & 0 & 0 & 0 \\ 0 & 0 & 0 & 0 & 0 & 0 & 0 & 0 & 0 & 0 \\ 0 & 0 & 0 & 0 & 0 & 0 & 0 & 0 & 0 & 0 \\ 0 & 0 & 0 & 0 & 0 & 0 & 0 & 0 & 0 & 0 \\ 0 & 0 & 0 & 0 & 0 & 0 & 0 & 0 & 0 & 0 \end{pmatrix}$$

$$B = \begin{pmatrix} 3\beta_1 \frac{I_4 - I_3 - I_1}{I_3} + 4\beta_2 \frac{I_3 + I_4 - I_1}{I_3} & \beta_1^2 \beta_2 A_1 & 5\beta_1 \beta_2 A_1 & 0 & 0 & 0 & 0 & 0 & 0 & 0 \\ -3 \frac{I_3 - I_1}{I_3} & \beta_1 \beta_2 A_1 & 5\beta_1 \beta_2 A_1 & 0 & -\beta_1 \beta_2 A_1 & 0 & 0 & -\beta_2 A_1 & 0 & 0 \\ 0 & 0 & 0 & 0 & 0 & 0 & 0 & 0 & 0 & 0 \\ 0 & 0 & 0 & 0 & 0 & 0 & 0 & 0 & 0 & 0 \\ 0 & 0 & 0 & 0 & 0 & 0 & 0 & 0 & 0 & 0 \\ 0 & 0 & 0 & 0 & 0 & 0 & 0 & 0 & 0 & 0 \\ 0 & 0 & 0 & 0 & 0 & 0 & 0 & 0 & 0 & 0 \\ 0 & 0 & 0 & 0 & 0 & 0 & 0 & 0 & 0 & 0 \\ 0 & 0 & 0 & 0 & 0 & 0 & 0 & 0 & 0 & 0 \\ 0 & 0 & 0 & 0 & 0 & 0 & 0 & 0 & 0 & 0 \end{pmatrix}$$

$$\beta_1 = \frac{h_1}{\dot{\alpha}_c}, \quad \beta_2 = \frac{h_2}{\dot{\alpha}_c}, \quad A_1 = \frac{m \ddot{\alpha}_c}{I_3}, \quad A_2 = \frac{m \ddot{\alpha}_c}{I_3}$$

Fig. 3 LINEARIZED EQUATION OF MOTION

### Fig. 3 LINEARIZED EQUATION OF MOTION

$$\begin{pmatrix} \xi' \\ \theta' \\ \alpha' \\ \xi'' \\ \theta'' \\ \alpha'' \end{pmatrix} = \begin{pmatrix} 0 & 0 & 0 & 1 & 0 & 0 \\ 0 & 0 & 0 & 0 & 1 & 0 \\ 0 & 0 & 0 & 0 & 0 & 1 \\ 3\frac{\beta_1(I_y - I_z - I_x)}{I_z} & 0 & 0 & 2 & 2 & 2 \\ 0 & \frac{3(I_y - I_x)}{I_z} & 0 & 0 & 0 & 0 \\ 0 & 0 & -3 + \frac{3(I_z - I_y)}{I_z} & -3 & -2 & 2\beta_1 \end{pmatrix} \begin{pmatrix} \xi \\ \theta \\ \alpha \\ \xi' \\ \theta' \\ \alpha' \end{pmatrix}$$

Linearized Equation of Motion in Orbit Plane

$$\begin{pmatrix} \varphi' \\ \psi' \\ \gamma' \\ \varphi'' \\ \psi'' \\ \gamma'' \end{pmatrix} = \begin{pmatrix} 0 & 0 & 1 & 0 & 0 & 0 \\ 0 & 0 & 0 & 0 & 1 & 0 \\ 0 & 0 & 0 & 0 & 0 & 1 \\ 4\frac{I_y - I_z}{I_z} & 3\beta_1 A_2 \frac{I_y}{I_z} & 0 & \frac{I_z - I_y - I_x}{I_z} & 0 & \varphi' \\ 0 & \frac{I_z - I_x}{I_x} & 5\beta_1 A_2 & \frac{I_z + I_y - I_x}{I_x} & 0 & \psi' \\ 4\frac{I_z + I_y - I_x}{I_z} & \beta_1 \left( \frac{I_x - I_z - I_y}{I_x} - 4 - 5\beta_1^2 A_2 \right) \frac{I_z - I_y - I_x}{I_x} & 0 & \frac{I_x - I_y - I_z}{I_x} & 0 & \gamma' \end{pmatrix} \begin{pmatrix} \varphi \\ \psi \\ \gamma \\ \varphi' \\ \psi' \\ \gamma' \end{pmatrix} + \begin{pmatrix} 0 & 0 & 0 & 0 & 0 & 0 \\ 0 & 0 & 0 & 0 & 0 & 0 \\ 0 & 0 & 0 & 0 & 0 & 0 \\ 0 & 0 & 0 & 0 & 0 & 0 \\ 0 & 0 & 0 & 0 & 0 & 0 \\ 0 & 0 & 0 & 0 & 0 & 0 \end{pmatrix} \begin{pmatrix} \Delta Q_\xi \\ \Delta Q_\theta \\ \Delta Q_\alpha \\ \Delta Q_\varphi \\ \Delta Q_\psi \\ \Delta Q_\gamma \end{pmatrix}$$

Linearized Equation of Motion out of Orbit Plane

$$A_1 = \frac{m\Omega_c^2}{I_z} \quad A_2 = \frac{m\Omega_c^2}{I_x} \quad \beta_1 = \frac{h_1}{I_z} \quad \beta_2 = \frac{h_2}{I_x}$$

Fig.4 SEPARATED LINEARIZED EQUATION WHEN  $\beta_2 = 0$

## WHAT CAN WE LEARN ABOUT THE OPEN-LOOP SYSTEM?

- (1) Linearization of 2-D Equations (Torque-Free)
- (2) Stability Analysis -
  - (2a) Assume appendage is vibrating at only one of its flexible modes
  - (2b) System can be described by periodic coefficients
  - (2c) Floquet analysis can be used to determine system parametric instabilities - quasi-analytic results obtained for cases of (i) No gravity-gradient, no offset of mast interface point on reflector, (ii) with offset of mast interface point, but not gravity-gradient.
  - (2d) For general case, a numerical implementation of the Floquet analysis is required.
- (3) Relation between this system and other systems involving geometric offset
  - (3a) The dynamics of orbiting tethered platform systems  
2-D analysis, Stanley Woodard LSSI  
3-D analysis (in-progress), Fan Ruying -  
Visiting Scholar, Beijing Inst. of Control Engineering
  - ✓ (3b) The dynamics of the Wrap-Rib Antenna system - any published results?

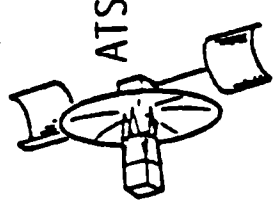
Figure 1

# WRAP-RIB LMASS CONFIGURATION AND MASS PROPERTIES

TOTAL MASS

9695 LBS

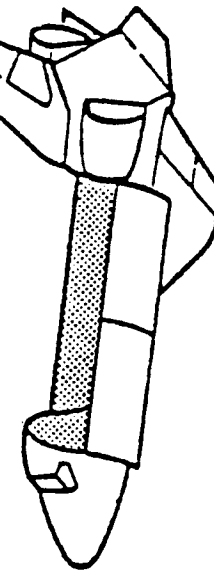
$$\text{MOMENTS OF INERTIA} \quad \left\{ \begin{array}{l} I_x = 2.91 \times 10^6 \text{ SLUG-FT}^2 \\ I_y = 2.64 \times 10^6 \\ I_z = 0.37 \times 10^6 \end{array} \right.$$



PRODUCTS OF INERTIA

$$\left\{ \begin{array}{l} I_{xy} = -3.56 \times 10^3 \\ I_{xz} = -4.22 \times 10^3 \\ I_{yz} = 0.72 \times 10^6 \end{array} \right.$$

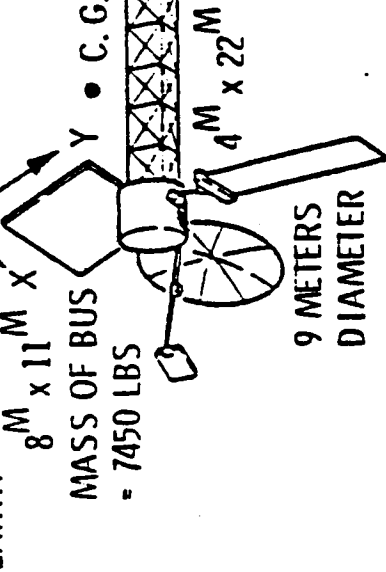
THE SHUTTLE



DISH-HUB MASS  
= 1277 LBS

UPPER BOOM LENGTH = 33.8M

MASS = 90 LBS



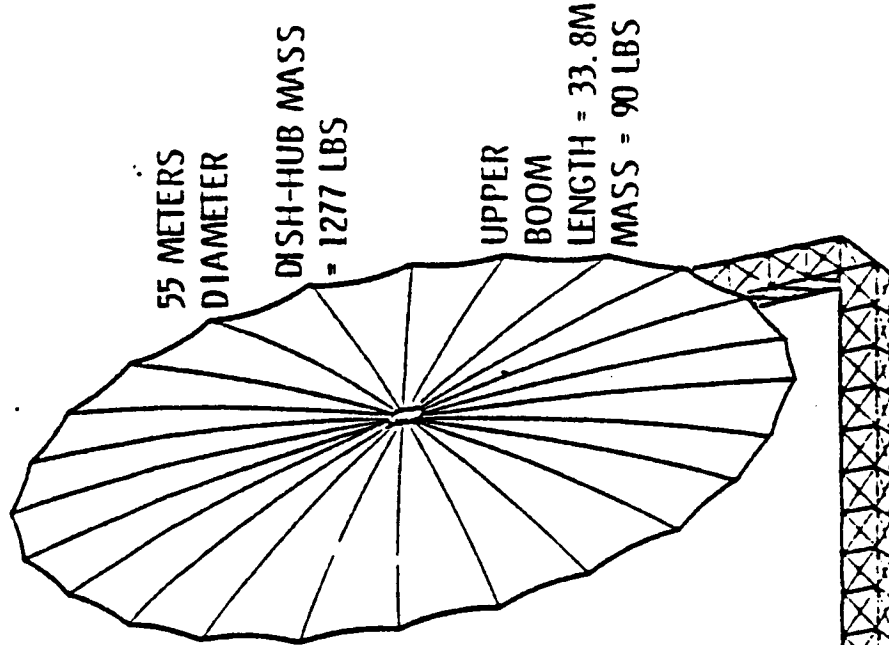
EARTH

8M x 11M

MASS OF BUS • C.G. FOCAL LENGTH 82.5 METERS

= 7450 LBS

LOWER BOOM LENGTH = 80 METERS  
MASS = 210 LBS



## II. ISSUES IN CONTROLLING THE SCOLE CONFIGURATION

- SHOULD CONTROLS ANALYSIS PROCEED IN TWO STEPS,  
FIRST USING A 2-D MODEL?
- WHAT IS THE EFFECT OF A TIME DELAY IN THE CONTROL?

## Systems with delay in Control

### Stability:

In Literature:

$$\dot{x}(t) = Ax(t) + Bx(t-\tau)$$

A is a stable matrix  
stability of combined system is  
analyzed as a function of stability  
parameters of A and B matrices

### Control:

In Literature:

$$\dot{x}(t) = Ax(t) + Bx(t-\tau) + Cu(t)$$

$$u(t) = -\hat{A} x(t) - \hat{B} x(t-\tau)$$

or

$$\dot{x}(t) = Ax(t) + Bu(t-\tau)$$

$$u(t) = kx(t+\tau)$$

Present Problem:

$$\dot{x}(t) = Ax(t) + Bu(t)$$

$$u(t) = kx(t-\tau)$$

A is marginally stable

Design K such that controlled  
plant is stable.

# Control of large Space Structures with delay in control :

$$\dot{X}(t) = A X(t) + B U(t)$$

$$U(t) = K X(t - \tau)$$

Design  $K$  such that above system  
is stable :

### B. Effect of Delay on Control System Stability

The control law of the form  $U = -KX$  is designed for a system represented by

$$\dot{X} = AX + BU \quad (B.1)$$

and a delay  $\tau$  is incorporated into the state variable,  $X$ , and its effect on control system stability is analyzed numerically.

To start with, a second order differential equation representing the vibration of a structure in a particular mode is considered.

The system equation used for numerical analysis is given as

$$\frac{d^2x}{dt^2} + \omega^2 x = u \quad (B.2)$$

The control  $U$  is a rate feedback given by

$$u = -2\zeta\omega \frac{dx}{dt} \quad (B.3)$$

and the closed loop equation with control is written as:

$$\frac{d^2x}{dt^2} + 2\zeta\omega \frac{dx}{dt} + \omega^2 x = 0 \quad (B.4)$$

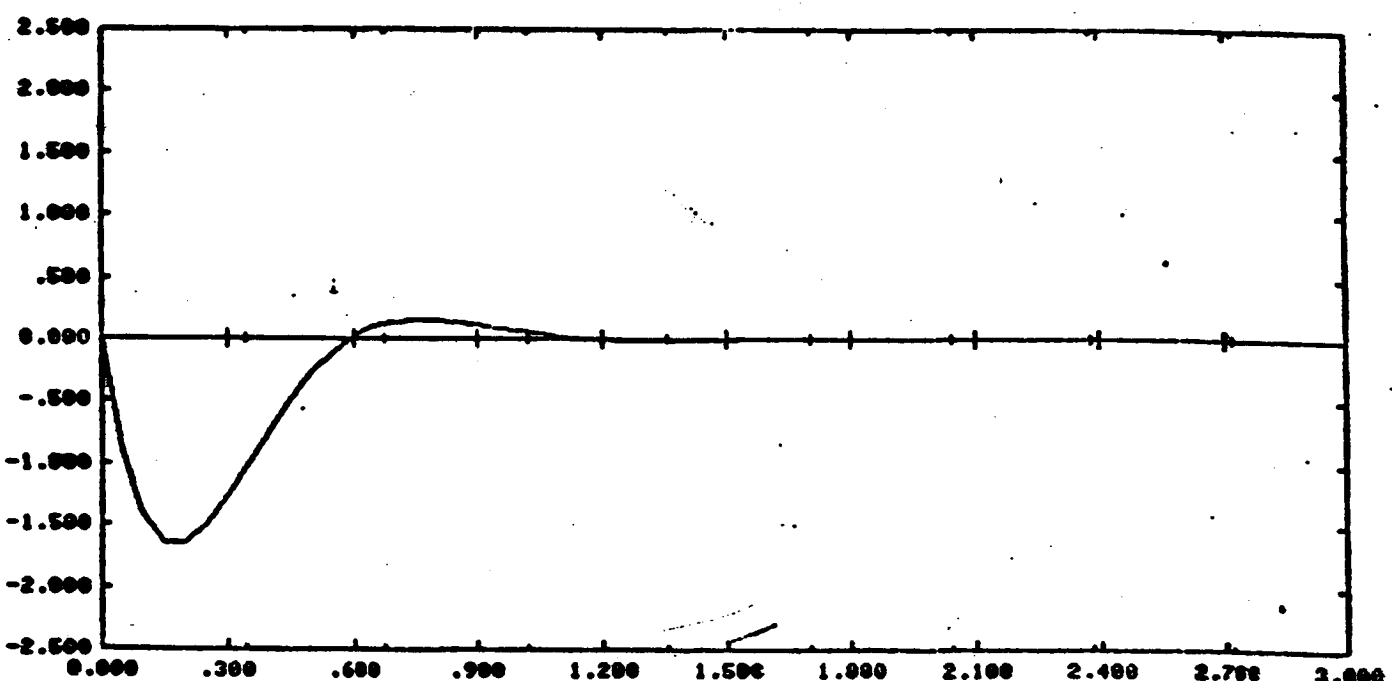
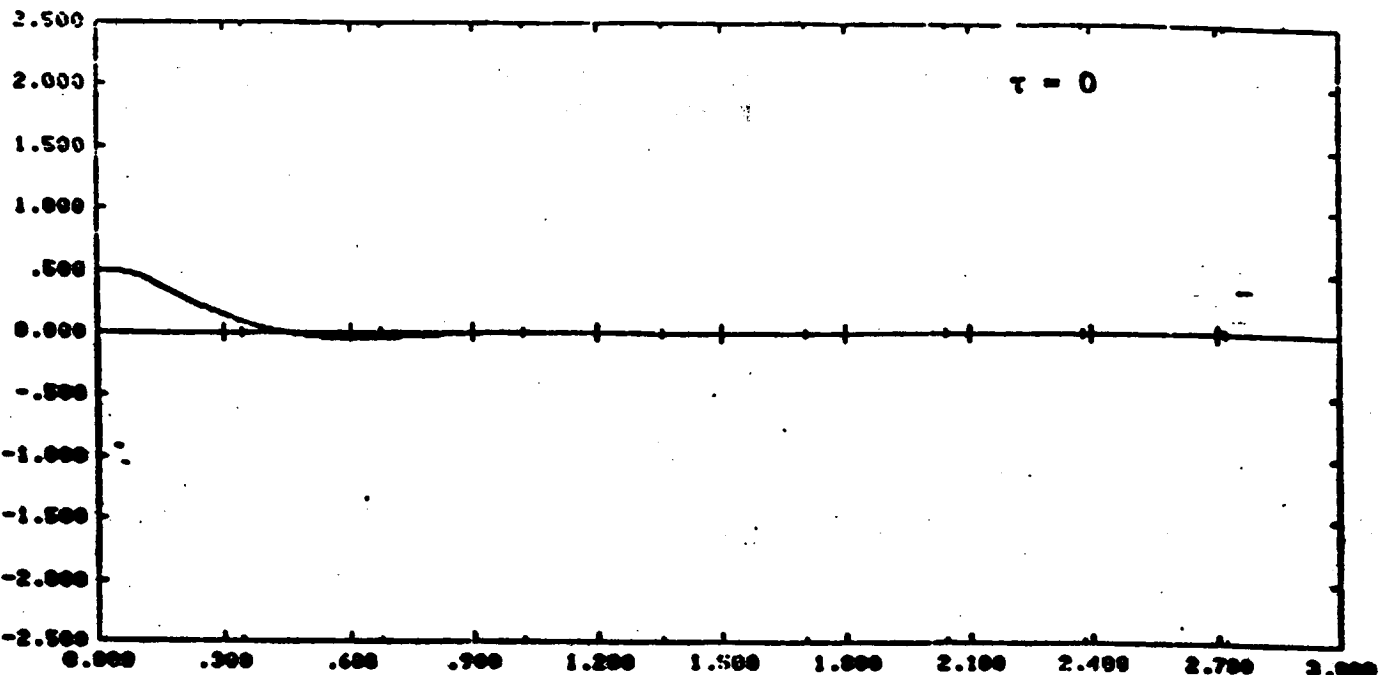
The numerical values selected for numerical simulation are arbitrary and are:

$$\omega = 6.0$$

$$\zeta = 0.5$$

$$x(0) = 0.5$$

$$\dot{x}(0) = 0.0$$



B.1 Transient Response of Second Order System without Time Delay.

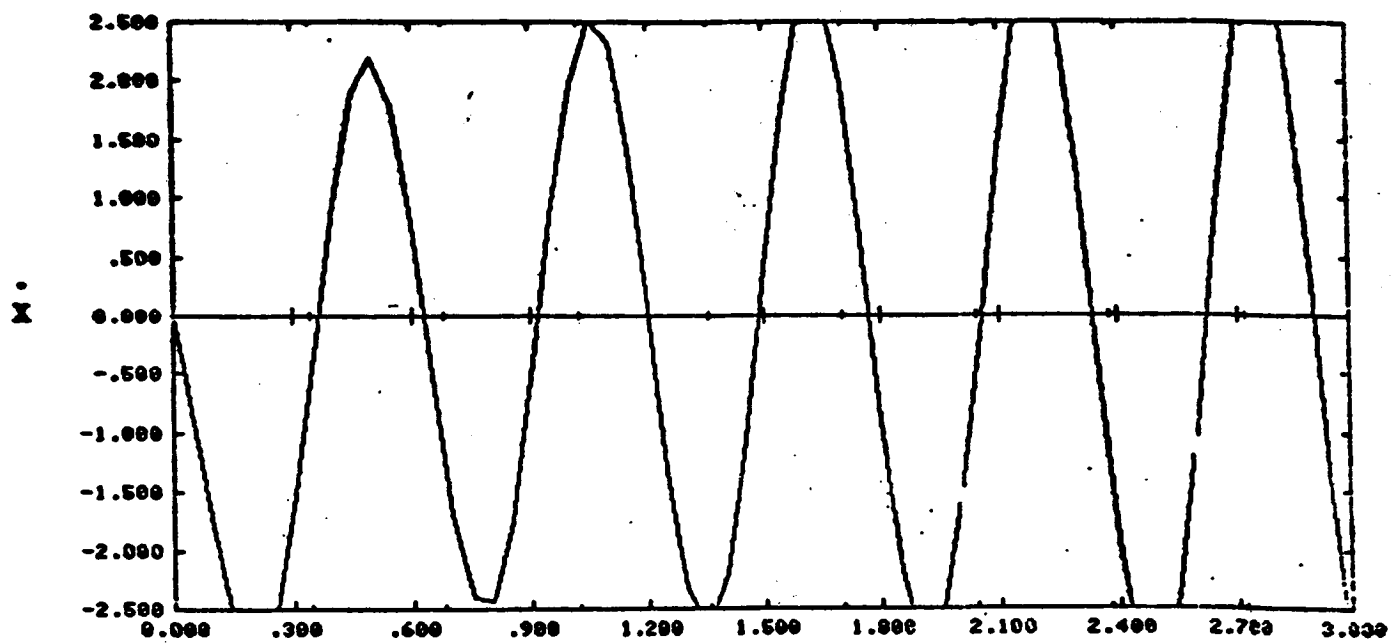
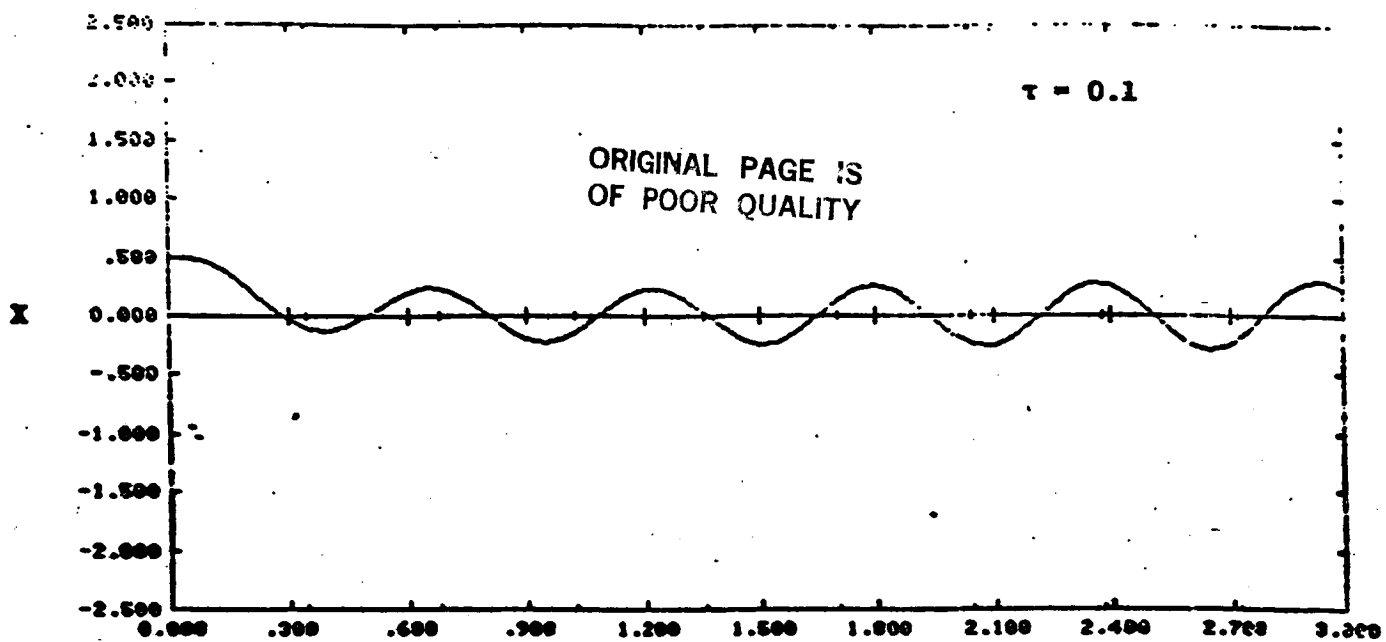
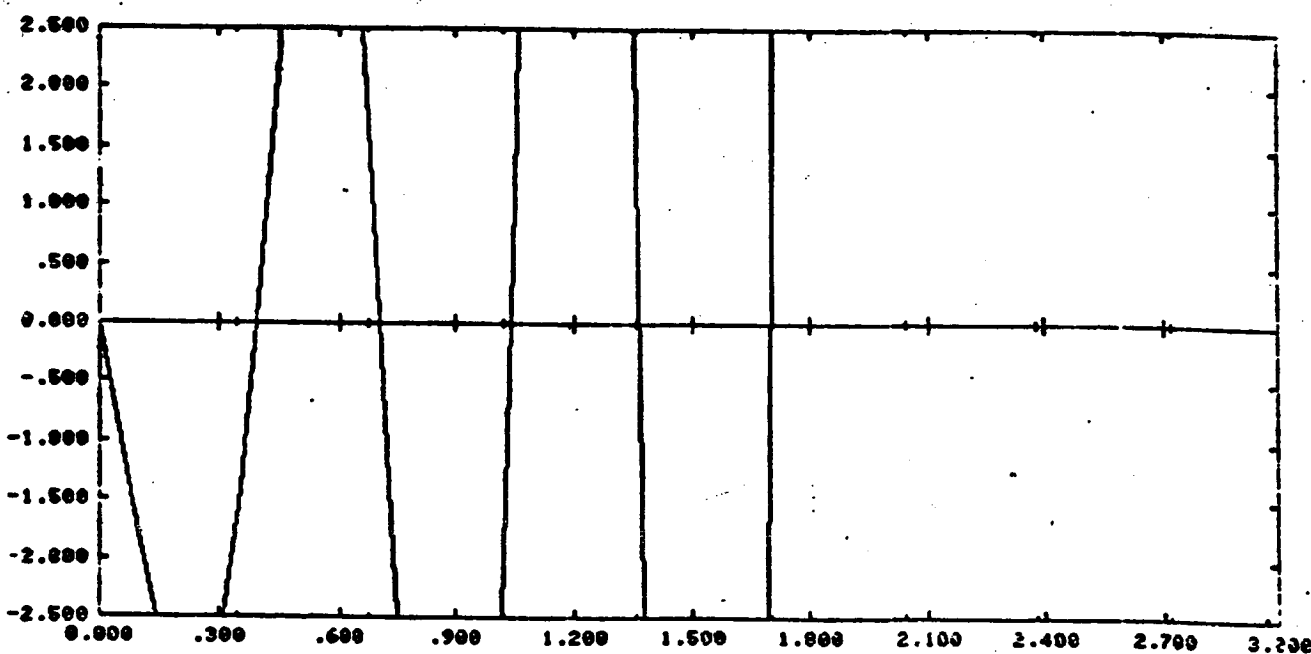
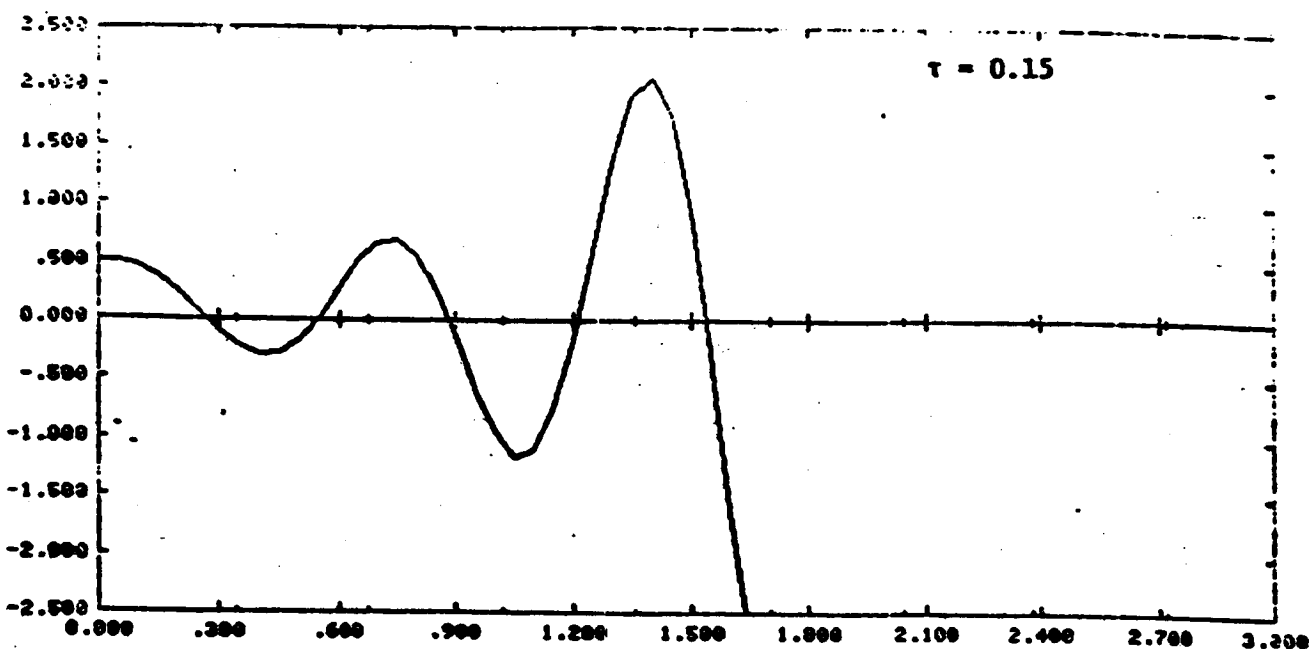


**Figure 5.2** Transient Response of Second Order System with Time Delay  
 $\tau = 0.1$  secs.



B.3 Transient Response of Second Order System with Time Delay  
 $\tau = 0.15$  secs.

System Dynamics :

$$\dot{X}(t) = AX(t) + BU(t) \quad (1)$$

Control Law :

$$U(t) = K X(t) \quad (2)$$

control law (with delay) :

$$U(t) = K X(t-\tau) \quad (3)$$

DISCRETIZATION - EULER'S METHOD :

$$\dot{X}(t) = \frac{X(I+1) - X(I)}{\Delta} ; \quad t = I\Delta \quad (4)$$

without delay :

$$X(I+1) = [I_n + (A+BK)\Delta] X(I) \quad (5)$$

Matrix  $A_c = (A+BK)$  has stable

Eigenvalues  $\lambda_1, \lambda_2, \dots, \lambda_n$  in continuous

time case.

Lyapunov Stability : (Eqn 5)\*

$$V(X(I)) = \frac{1}{2} X^T(I) P X(I) \quad (6)$$

$P$  = Positive definite

$P$  is a solution of the Lyapunov's Equation

$$PA_c + A_c^T P + Q = 0 \quad (7)$$

where  $Q$  = positive definite

$$\begin{aligned} \Delta V(X(I)) &= V(X(I+1)) - V(X(I)) \\ &= \frac{1}{2} [X^T(I+1) P X(I+1) - X^T(I) P X(I)] \\ &= -\frac{1}{2} \Delta X^T(I) [Q - \Delta A_c^T P A_c] \end{aligned} \quad (8)$$

$$\Delta V < 0 \quad \text{if } \Delta < \frac{\lambda_{\min}(Q)}{\lambda_{\max}(A_c^T P A_c)} \quad (9)$$

\* Balas, M. J.; Discrete Time Stability of Continuous Time Controller Design for Large Space Structures; J. Guidance, Control and Dynamics; Sept-Oct 1982, pp 541-543.

# Stability Analysis through Transformation :

DISCRETE SYSTEM Dynamics :

$$X(I+1) = (I_n + \Delta A_c) X(I) \quad (5) \rightarrow (10)$$

Transformation :

$$X(I) = T f(I) \quad (11)$$

$$f(I+1) = T^{-1} (I_n + \Delta A_c) T f(I)$$

$$f(I+1) = (I_n + \Delta \Lambda) f(I) \quad (12)$$

where  $\Lambda = \text{diag} [\lambda_1, \lambda_2, \dots, \lambda_n]$

For System (12) to be stable all the eigen values of the matrix  $(I_n + \Delta \Lambda)$  must lie within unit circle.

$$\text{Let } \lambda_j = \tilde{\sigma}_j + i \tilde{\omega}_j \\ 1 \leq j \leq n$$

$$|1 + \Delta(\bar{\sigma}_j + i\omega_j)| < 1$$

$$(1 + \Delta\bar{\sigma}_j)^2 + \omega_j^2 \Delta^2 < 1$$

$$\Delta(2\bar{\sigma}_j + \Delta(\bar{\sigma}_j^2 + \omega_j^2)) < 0$$

$$\Delta > 0$$

$$2\bar{\sigma}_j + \Delta(\bar{\sigma}_j^2 + \omega_j^2) < 0$$

$$\Delta_j < \frac{-2\bar{\sigma}_j}{\bar{\sigma}_j^2 + \omega_j^2}$$

$$\Delta = \min(\Delta_j) \quad 1 \leq j \leq n$$

Example :

$$\begin{bmatrix} \dot{x}_1(t) \\ \dot{x}_2(t) \end{bmatrix} = \begin{bmatrix} 0 & 1 \\ -36 & -6 \end{bmatrix} \begin{bmatrix} x_1(t) \\ x_2(t) \end{bmatrix}$$

$$\lambda_1 = -3 + i 5.2$$

$$\lambda_2 = -3 - i 5.2$$

$$\Delta_1 = \Delta_2 < \frac{b}{9 + 27.04} < 0.167 \text{ Seconds.}$$

$$\text{Natural period of system} = \frac{2\pi}{6} = 1.04 \text{ Sec.}$$

$$\text{damped natural frequency} = \frac{2\pi}{5.2} = 1.21 \text{ Sec.}$$

Control with delay :

$$\tau = K\Delta ; t = I\Delta$$

$$\dot{X}(t) = AX(t) + BKX(t-\tau)$$

$$X(I+1) = (I_n + \Delta A) X(I) + \Delta BK X(I-K)$$

Augmented System :

$$\begin{bmatrix} X(I+1) \\ X(I) \\ \vdots \\ X(I-K+1) \end{bmatrix} = \underbrace{\begin{bmatrix} I_n + \Delta A & 0 & 0 & \dots & 0 & \Delta BK \\ I_n & 0 & 0 & \dots & 0 & 0 \\ \vdots & & & & \vdots & \vdots \\ 0 & 0 & 0 & \ddots & 0 & 0 \end{bmatrix}}_{\tilde{A}} \begin{bmatrix} X(I) \\ X(I-1) \\ \vdots \\ X(I-K) \end{bmatrix}$$

$$\tilde{X}(I+1) = \tilde{A} \tilde{X}(I)$$

Analytical relation between Eigen values of continuous time System and Sampling period is not established.

Stability with Sampled data Feed back : (THONSEN, 1982)

System dynamics :

$$\dot{X}(t) = AX(t) + BX(t-h) + C U(t)$$

$$U(t) = -\hat{A} X(g(t)) - \hat{B} X(g(t)-h)$$

$$g(t) \triangleq r\Delta \quad t \in [r\Delta, (r+1)\Delta]$$

$$r = \dots -1, 0, 1, \dots$$

$$\Delta < h$$

$$\dot{X}(t) = AX(t) - C\hat{A} X(g(t)) + BX(t-h) - C\hat{B} X(g(t)-h)$$

with

$$C\hat{A} = A - A_0$$

$$\dot{X}(t) = A_0 X(t) + (A - A_0)[X(t) - X(g(t))]$$

$$+ (B - C\hat{B}) X(t-h) + C\hat{B}[X(t-h) - X(g(t)-h)]$$

$A_0$  = Stability matrix

$$\|e^{A_0 t}\| \leq k e^{-\eta t} \quad t \geq 0$$

defining  $W(t) = \begin{cases} k X_0 e^{-\beta t} & t \geq 0 \\ k X_0 & t < 0 \end{cases}$

$$\|X(t)\| \leq W(t) \quad \text{for all } t \geq 0$$

iff

$$\gamma - \beta - k \left\{ \|B - C\hat{B}\| e^{\beta h} + \Delta I e^{\beta \Delta} (\|A - A_0\| + \|C\hat{B}\| e^{\beta h}) \right\} > 0$$

where  $\tau \triangleq \|\Delta\| + \|A - A_0\| e^{\beta \Delta} + \|R\| e^{\beta h} + \|C\hat{B}\| e^{\beta(\Delta+h)}$

Example:

$$\dot{X}(t) = \begin{bmatrix} 1 & 1.5 \\ 0.3 & -2 \end{bmatrix} X(t) + \begin{bmatrix} 0 & -1 \\ 0 & 0 \end{bmatrix} X(t-h) + \begin{bmatrix} 10 \\ 1 \end{bmatrix} U(t)$$

$$A_0 = \begin{bmatrix} -2 & 0 \\ 0 & -2.15 \end{bmatrix} \quad (\text{unstable})$$

$$K=1, \gamma=2, h=0.1, \Delta < 0.037 \quad (\Delta=0.035)$$

$$\hat{B} = [0, -0.1] ; \hat{A} = [0.3, 0.15]$$

$$U(t) = -[0.3, 0.15] \begin{bmatrix} X_1(g(t)) \\ X_2(g(t)) \end{bmatrix} + [0, -1] \begin{bmatrix} X_1(g(t)-0.1) \\ X_2(g(t)-0.1) \end{bmatrix}$$

For large Space Structures :

$$\dot{X}(t) = A X(t) + C^T J(t)$$

$$J(t) = -\hat{B}^T X(t-h)$$

$$\text{i.e.: } \hat{A} = 0$$

$$\hat{B} = 0$$

A. THOWSEN: Stable Sampled data Feedback Control  
of dynamic systems with time delays:

Int. J. of. System Science, 1982, vol. 13, NO. 12;

# Single input - Single output Systems:

$$\dot{X}(t) = AX(t) + BU(t-h)$$

$$Y(t) = CX(t)$$

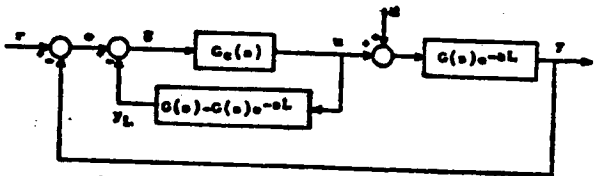


Fig. 1. Smith predictor control system.

$$G(s) = C(SI-A)^{-1}B$$

$$\frac{y(s)}{r(s)} = \frac{G_c(s) G(s) e^{-sL}}{1 + G_c(s) G(s)}$$

characteristic Equation is independent of delay:

- 1) O. J. M. Smith : "A Controller to overcome dead Time"; ISA J; Vol.6, NO.2 pp 28-33; 1955
- 2) K. Watanabe; M. Ito; "A process model control for Linear Systems with delay"; IEEE Trans on AC; Vol 26, NO. 6, Dec 1981; pp 1261-1269.

## Journals

1. IEEE Trans. on Automatic Control ;  
1957 - 1985
2. Int. J. of Control  
- 1985
3. Int. J. of System Science  
- 1985
4. Automatica  
- 1985
5. SIAM J. on optimization and Control  
- 1985
6. J. Guidance, Control and Dynamics  
- 1985.

# **Decentralized Control Experiments on a Flexible Grid**

**by**

**U. Ozguner**

**S. Yurkovich**

**Ohio State University  
Columbus, OH**

## 1. INTRODUCTION

In recent years much attention in the controls community has centered on problems posed by large space structures. These problems include the need to provide active-damping structural control for many, often densely packed, modal frequencies, and the need for distribution of actuation and sensing equipment over and throughout the large, lightweight structure. In the analysis and control synthesis of such problems, integral parts are played by the level of accuracy of the system model and the robustness of the controller. Properly done, the control design should provide damping to the vibrational modes within the controller bandwidth.

This report accounts the progress made on control experiments for NASA's flexible grid experimental apparatus [1,2]. The grid is a 7-ft by 10-ft lattice constructed of overlayed aluminum bars of rectangular cross-section 2-in by 1/8-in, centered at one-foot intervals, and is suspended on cables at two locations across the top bar. This design admits appreciable low-frequency structural dynamics, and allows for implementation of distributed computing components, inertial sensors, and actuation devices. Figure 1 depicts the apparatus. Instrumentation includes non-contacting displacement sensors mounted on a separate rigid structure behind the grid, six rate gyros, and six inertia wheel actuators allowing application of torques up to 20 oz.-in.

A finite-element analysis of the grid provides the model for control system design and simulation. The motions of the grid perpendicular to its plane are of interest in this study, so that in the modeling analysis 88 nodes are utilized with four degrees of freedom.

The control strategy for this study involves a decentralized model reference adaptive approach using a variable structure control [3]. Local models are formulated based on desired damping and response time in a model-following scheme for various modal configurations. Variable structure controllers are then designed employing co-located angular rate and position feedback. In this scheme local control forces the system to move on a local sliding mode in some local error space. An important feature of this approach is that the local subsystem is made insensitive to dynamical interactions with other subsystems once the sliding surface is reached.

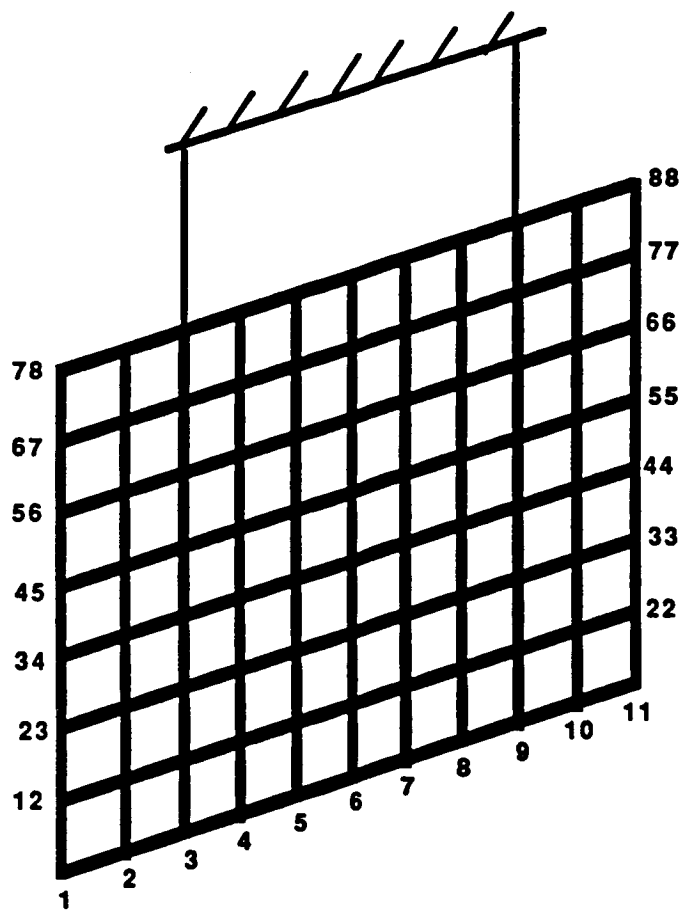


**Figure 1 LRC's Experimental Grid Apparatus;  
grid node points numbered as shown.**

## 2. PROBLEM STATEMENT AND PROGRESS REPORT

The overall experimental process for purposes of this study consists of three basic stages. First, the finite-element analysis is done for the grid apparatus on the Cyber 175 network computing system at NASA's Langley Research Center. The vehicle by which this is done is the SPAR analysis software package. Next, data generated by SPAR is used in a modal dynamics simulator, either on the Cyber 175 system or, as in the case of the results reported on here, on the Electrical Engineering Department's VAX 11/785 system at The Ohio State University. It is within this simulation software that the control algorithm is implemented. The final stage of the process involves actual on-site testing of the design. The overall process is depicted in Figure 2.

### Modeling

Assume that a general mathematical description of the grid structure takes the form

$$\ddot{M}\dot{X} + KX = F ,$$

where the matrix  $X$  contains incremental displacement variables for the 96 grid points (88 for the grid, 8 for the cables) in each of the 6 degrees of freedom (3 axes, rotation about each axis). As noted above, typical modeling exercises involve only four degrees of freedom, where rotation about the axis perpendicular to the plane and translation along the horizontal grid axis are constrained. Also,  $M$  and  $K$  are the mass and stiffness matrices of the structure, respectively, and  $F$  is the vector of forces used in control. Since applications and environments of large space structures dictate the lack of any appreciable natural damping, the model excludes any damping. By employing the unitary transformation

$$X = \Phi W ,$$

where  $\Phi$  is the mode shape matrix and  $W$  contains generalized coordinate modal displacements, a set of uncoupled equations results, namely,

$$(\Phi^T M \Phi) \ddot{W} + (\Phi^T K \Phi) W = \Phi^T F = u .$$

In this expression,  $\Phi^T M \Phi$  is the diagonal modal mass matrix,  $\Phi^T K \Phi$  is the diagonal stiffness matrix, and  $u$  represents the generalized forces (control inputs). In a truncation approximation from the finite-element

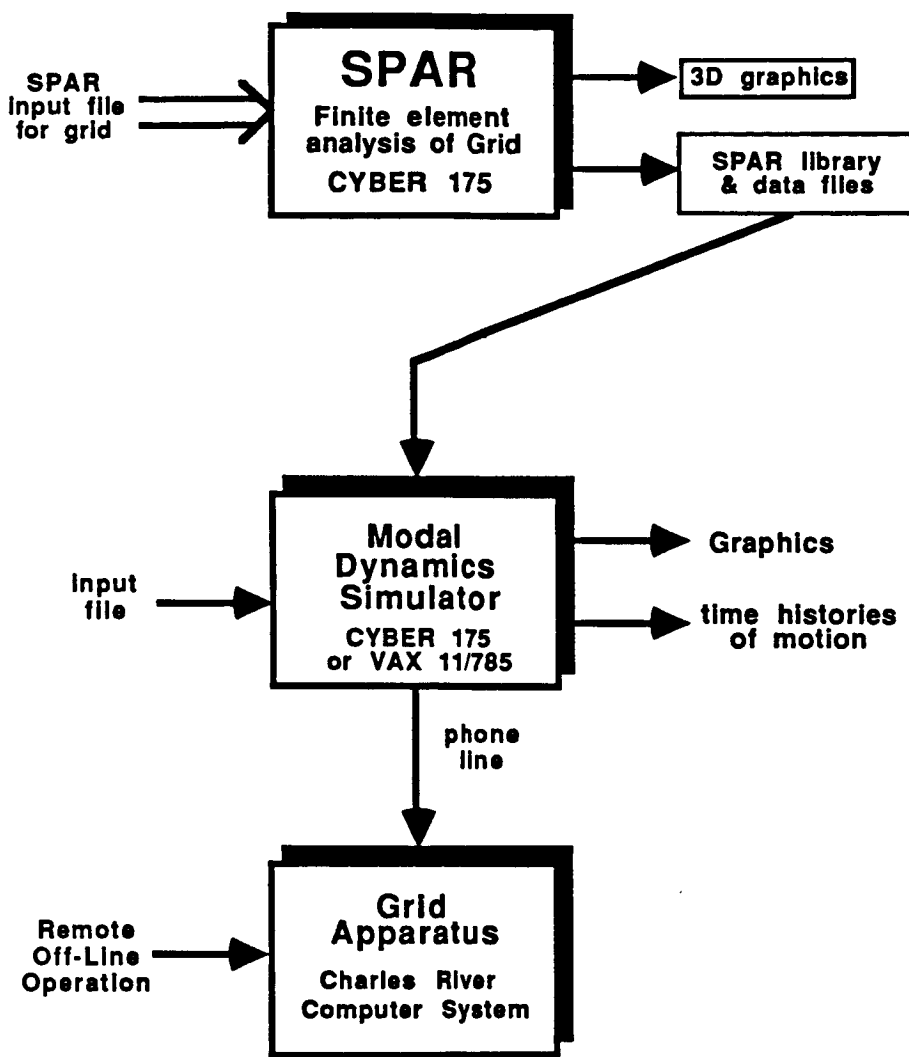


Figure 2 Three stages of overall process

procedure,  $n$  modes are retained, implying that  $\Phi^T M \Phi$  and  $\Phi^T K \Phi$  are  $n \times n$  in size. In a decentralized setting,

$$\dot{w}_i = \begin{bmatrix} 0 & 1 \\ -\omega_i^2 & 0 \end{bmatrix} w_i + \begin{bmatrix} 0 \\ 1 \end{bmatrix} u_i ,$$

where  $\omega_i$  represents the  $i$ -th modal frequency. The development of the control algorithm relative to this viewpoint is given in the next section.

The modal coefficients for this analysis (at gyro and actuator locations) are taken from the SPAR program output, for a model retaining the first 10 modes.

### Software and Simulation Testing

Simulation tests reported on in this study are all products of software implemented on the VAX 11/785 in the EE Dept. at OSU. The first stage of the code serves the purpose of transferring the modal coefficients from the SPAR output data set and formulating the proper mode shape matrix. Initial tests use one-mode models, resulting in a two-state grid model, and later simulations use the full ten-mode model, resulting in a twenty-state system. Next in the simulation code is the measurement, or sensor subroutine, from which the rate gyro feedback is obtained. Angular displacement is computed from these measurements with a simple numerical integration routine. After initial conditions are applied, integration is completed prior to updating of the computed control law.

The grid is initially perturbed in the software by way of initial conditions on the angular displacements and their velocities; future studies will involve a sinusoidal excitation of the grid before control is applied. These initial conditions are introduced through the local reference models, which are in all cases simple two-state (angle and angular velocity) systems. Various other segments were added to the code as needed, such as feedback of Kaman probe output and clipping constraints on the magnitudes of the applied torques. Primary output of the software is in the form of time-scale plots of linear displacement, rate gyro output, estimates of the angular displacements, and the applied torques, all at various grid node-points. Discussion of several tests is included in the next section.

### 3. DETAILS OF RECENT RESULTS

#### Algorithm Development

The Decentralized Model Reference Adaptive Controller with Variable Structure Control has evolved through four stages, the last stage specifically for this application:

##### (1) Variable Structure Control (Utkin, Itkis and others in USSR)

Basically, the standard variable structure controller first drives a system's state trajectory to a given plane in state space and then, ideally, slides along this plane to the origin. The system can be shown to have excellent sensitivity properties while in the sliding mode. The control algorithm essentially checks on which side of the plane the states are and varies the feedback structure accordingly to orient the trajectories towards the plane. In actual implementation, the trajectories may "chatter" while sliding to the origin along the plane.

##### (2) Model Reference Adaptive Control Using Variable Structure Feedback (Young)

D. Young was one of the first to use variable structure controllers in driving the error signal to zero while doing model reference adaptive control. The approach retains all the advantages and disadvantages of variable structure controllers.

##### (3) Variable Structure Controllers for Decentralized Model Reference Adaptive Control for Interconnected Systems (Özguner, Morgan, Al-Abbass)

A recent development has been the application of variable structure controllers for model reference adaptive control of interconnected systems with local state information availability. We summarize this approach briefly in the following.

Consider the system

$$S_i : \dot{x}_i = A_i x_i + B_i u_i + \sum_{j=1}^N A_{ij} x_j$$

$$y_i = D_i x_i ,$$

for  $i = 1, 2, \dots, N$ , where

$$x_i \in R^{n_i} , \quad A_i \in R^{n_i \times n_i} ,$$

$$y_i \in R^1 , \quad B_i \in R^{n_i \times 1} ,$$

$$u_i \in R^1 , \quad D_i \in R^{1 \times n_i} .$$

Given the model, the problem is to design a decentralized adaptive controller such that the states of each local subsystem are regulated to zero or track the states of a reference model. Each local controller is dependent only on the local subsystem, and is not allowed to communicate with the other local controllers. The only information provided for the local controller is the upper bound on the size of the dynamic interactions  $[\sum A_{ij} x_j]_{\max}$ .

Let the local reference model for the  $i$ -th subsystem be given as

$$\begin{aligned}\dot{\hat{x}}_i &= \hat{A}_i \hat{x}_i + \hat{B}_i r_i \\ \hat{y}_i &= \hat{x}_i ,\end{aligned}$$

with  $\hat{x}_i$  in  $R^{n_i}$ ,  $r_i$  the reference input,  $\hat{B}_i$  in  $R^{n_i \times 1}$ , and  $\hat{A}_i$  in  $R^{n_i \times n_i}$ . Furthermore, let

for  $C_i$  in  $R^{1 \times n_i}$ , specify the sliding surface, where

$$e_i = \hat{x}_i - x_i$$

and

$$\dot{e}_i = \hat{A}_i e_i + (\hat{A}_i - A_i)x_i + \hat{B}_i r_i - B_i u_i - \sum_{\substack{j=1 \\ j \neq i}}^N A_{ij} x_j .$$

The control law is obtained from this last expression as

$$u_i = K_p^i e_i + K_p^i x_i + K_r^i r_i + \delta_i ,$$

where  $K_r$  in  $R^1$ ,  $K_p$  in  $R^{1 \times n_i}$ , and  $K_\bullet$  in  $R^{1 \times n_i}$  can be specified [3] in regions of the state space, and where  $\delta_i$  is a constant picked according to the norm of the interactions. The elements  $K_r$ ,  $K_p$ ,  $K_\bullet$ , and  $\delta_i$  are a function of the sliding surface and the coefficients of system and reference model state equations.

Another development used in the above is the idea of time varying sliding surfaces, which aide in smoothing of the chattering.

#### (4) Multi-modeling for Decentralized Model Reference Adaptive Control using Variable Structure Controllers.

Two developments were required to use the above approach for the control of flexible structures. The first was the incorporation of output instead of state feedback into the interconnected system model. The second and more crucial development was the expansion of the essentially general decentralized structure with multimodeling into an interconnected system. As an illustration, consider the two channel case

$$\begin{aligned}\dot{x} &= Ax + B_1 u_1 + B_2 u_2 \\ y_1 &= D_1 x \\ y_2 &= D_2 x\end{aligned}$$

We would like to consider two separate systems,

$$\{ A, B_1, D_1 \}, \quad \{ A, B_2, D_2 \}$$

for designing the controllers. The system model used is

$$\{ \begin{bmatrix} A & * \\ * & A \end{bmatrix}, \begin{bmatrix} B_1 & 0 \\ 0 & B_2 \end{bmatrix}, \begin{bmatrix} D_1 & 0 \\ 0 & D_2 \end{bmatrix} \},$$

where the "interconnection matrices" are not specified. This type of expansion has been previously utilized by Siljak in a different context. In the present context the specification of the fictitious interconnections are not required since the only information needed is an extra dominant term in the local control to suppress interactions.

### Simulation Test Results

In the following pages the results for two of several simulations testing the decentralized control algorithm are presented. For each case the group of output plots is preceded by a short summary depicting the number and location of inputs and outputs (for the numbering of the nodes, see Figure 1), program parameters (such as initial conditions, algorithm scale factors, and so on), and the structure of the reference model. Both simulations shown here are for the full 10-mode grid model. Note that the second of these tests represents results of sampled systems.

#### SIMULATION TEST #4

10 modes

6 inputs, 6 outputs,

- \* co-located rate gyros and actuators located at nodes 25, 31, 52, 61
- \* Kaman probe 2 with actuator 1 (output feedback)  
Kaman probe 7 with actuator 4 (output feedback)

Program parameters: ( $w_i(0)$  and  $\dot{w}_i(0)$  not listed are 0)

$w_1(0) = 0.1$   
 $w_3(0) = 0.1$   
 $w_5(0) = 0.1$   
 $w_7(0) = 0.1$   
 $w_9(0) = 0.1$   
 $\dot{w}_2(0) = 0.2$   
 $\dot{w}_4(0) = 0.2$   
 $\dot{w}_6(0) = 0.2$   
 $\dot{w}_8(0) = 0.2$   
MAX = 1  
 $\alpha_1 \rightarrow \alpha_5 = 2$

Reference model eigenvalues:

$$\lambda_1 = -0.5 ; \lambda_2 = -0.5$$

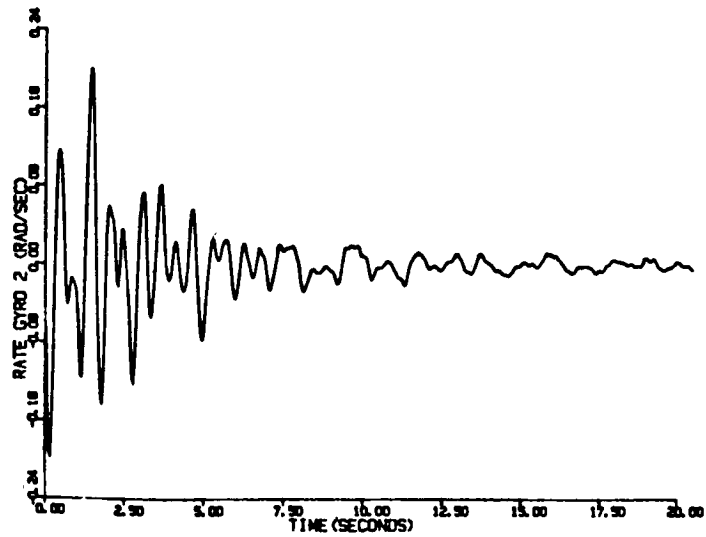
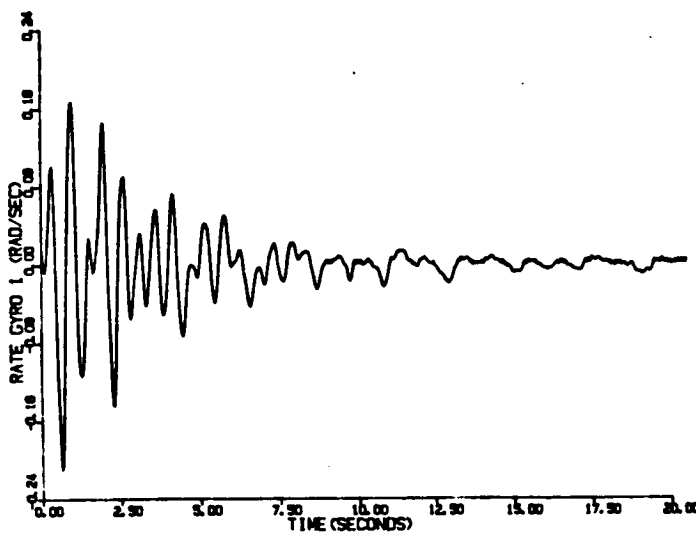
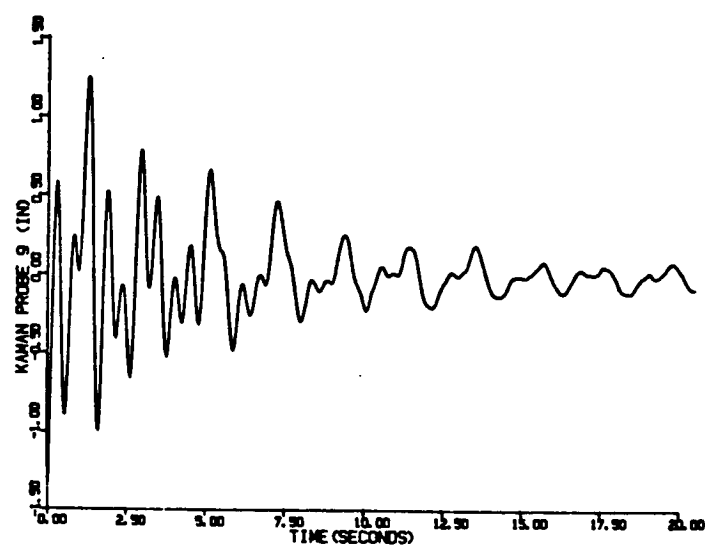
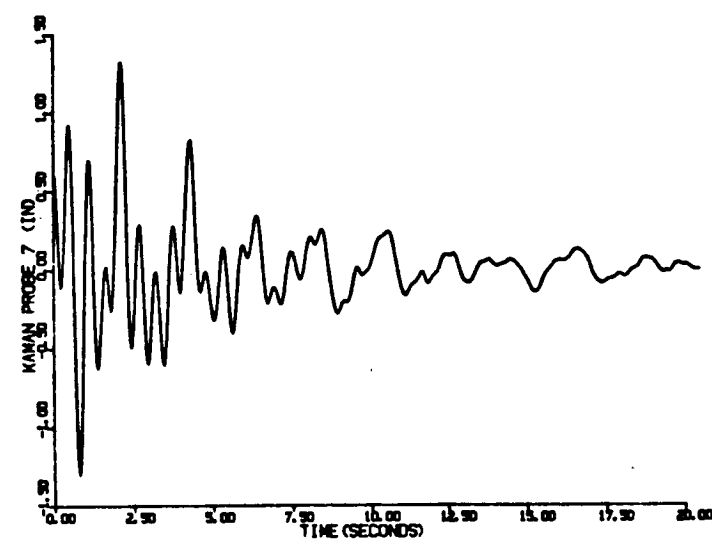
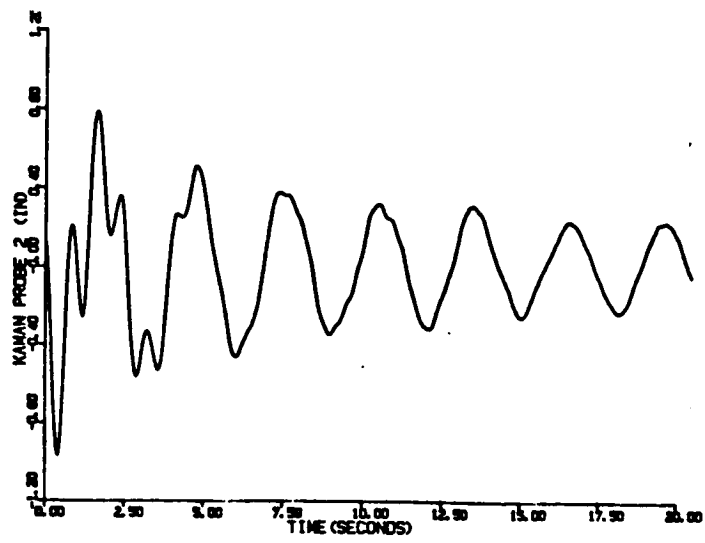
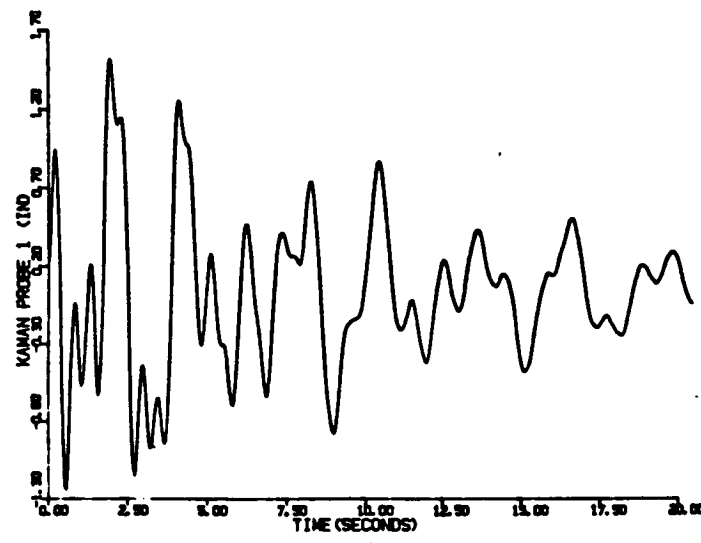
Comments:

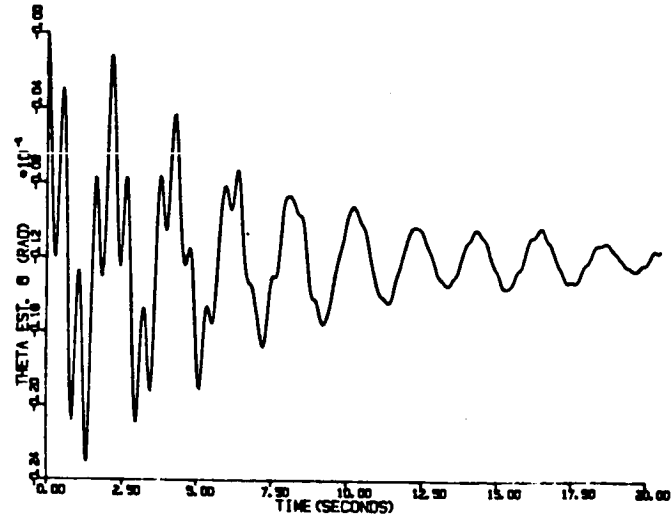
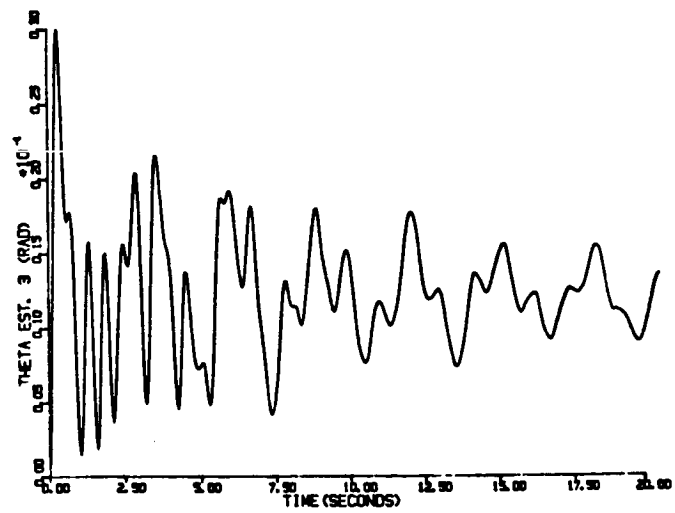
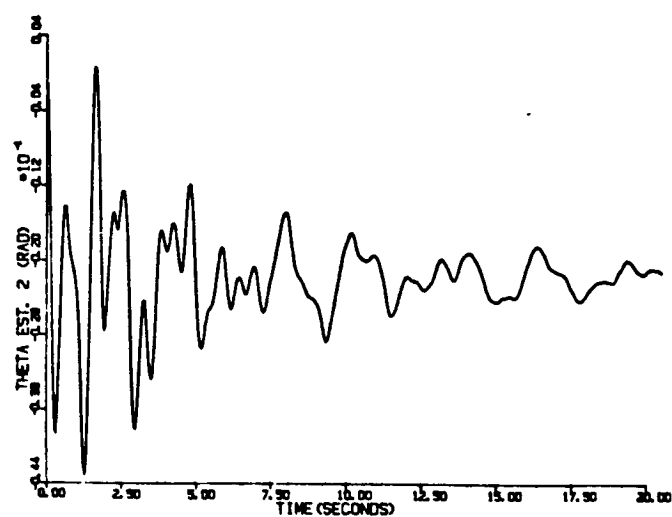
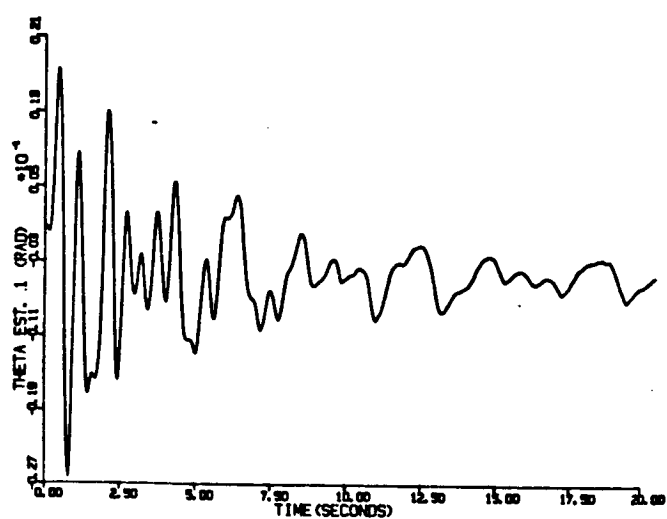
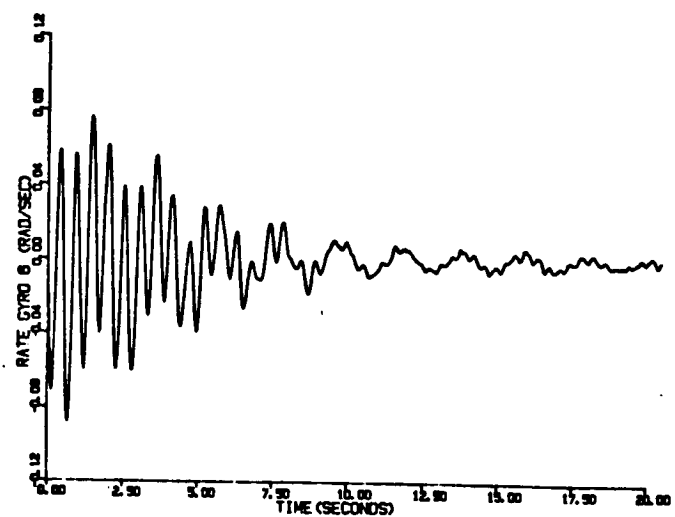
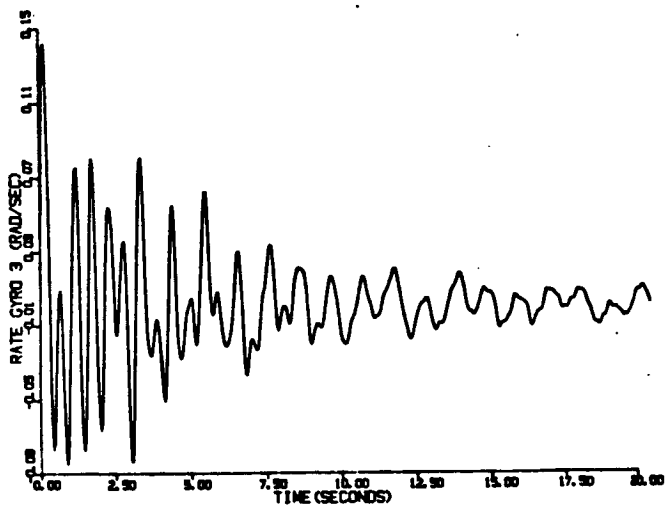
Full model (ten modes) is used with position output feedback, and reference model has critically damped modes.

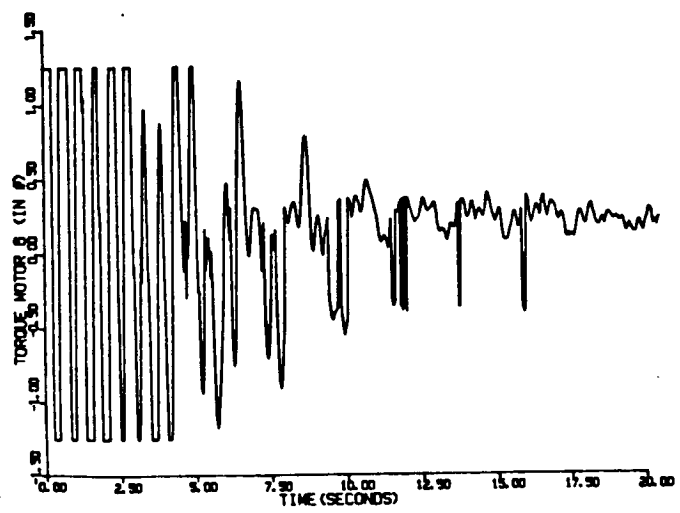
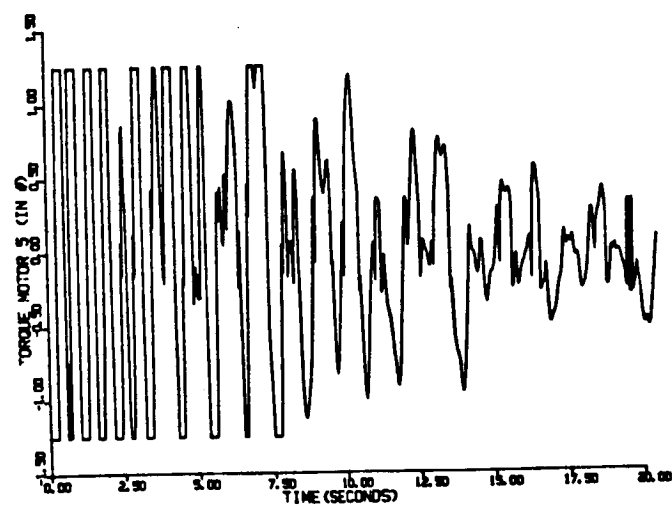
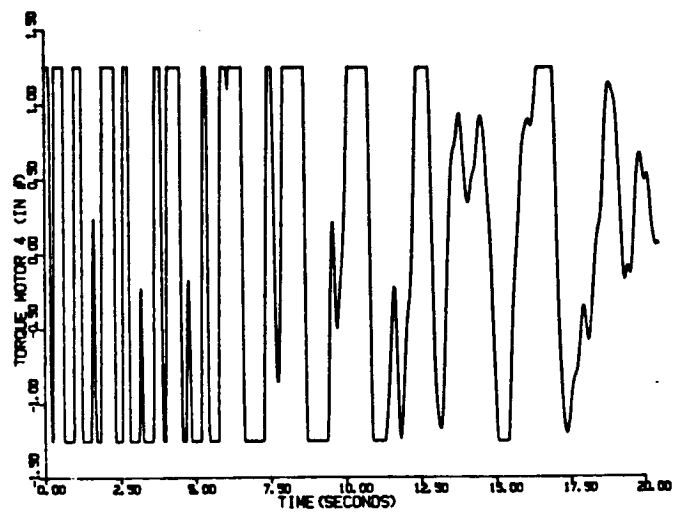
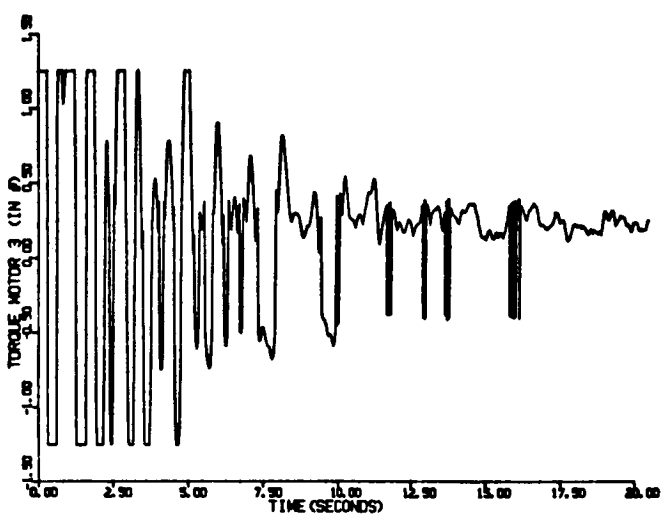
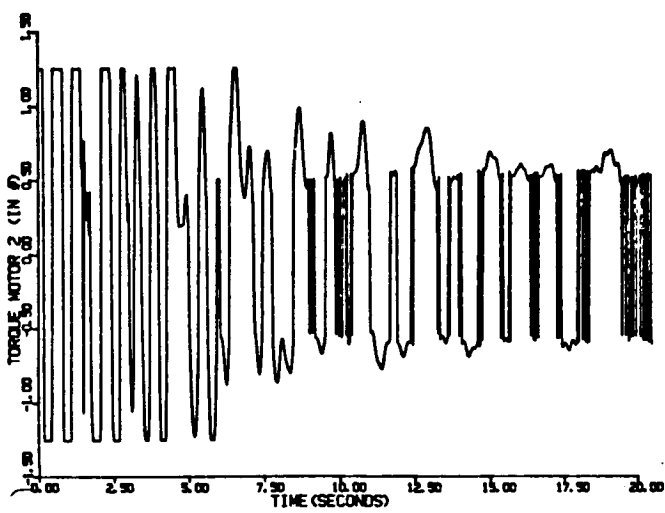
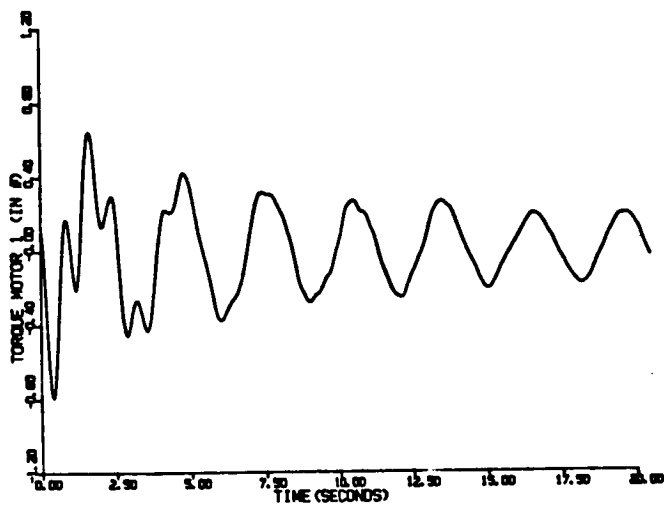
\*\*\* NOTE \*\*\*

The applied torques are clipped (constrained) as

$$|\text{applied torques}| \leq 1.25 \text{ in-lb}$$







## SIMULATION TEST #6

10 modes

6 inputs, 6 outputs,

- \* co-located rate gyros and actuators located at nodes 25, 31, 52, 61
- \* Kaman probe 2 with actuator 1 (output feedback)  
Kaman probe 7 with actuator 4 (output feedback)

Program parameters: ( $w_i(0)$  and  $\dot{w}_i(0)$  not listed are 0)

$w_1(0) = 0.1$   
 $w_3(0) = 0.1$   
 $w_5(0) = 0.1$   
 $w_7(0) = 0.1$   
 $w_9(0) = 0.1$   
 $\dot{w}_2(0) = 0.2$   
 $\dot{w}_4(0) = 0.2$   
 $\dot{w}_6(0) = 0.2$   
 $\dot{w}_8(0) = 0.2$   
MAX = 1  
 $\alpha_1 \rightarrow \alpha_5 = 2$

Reference model eigenvalues:

$$\lambda_1 = -0.5 ; \lambda_2 = -0.5$$

Comments:

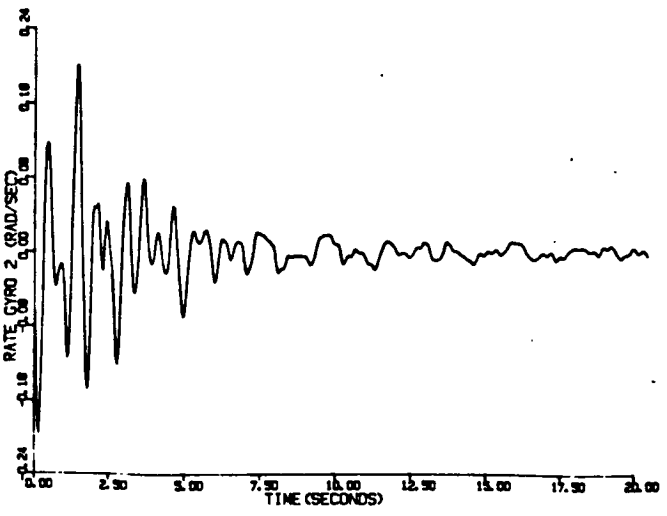
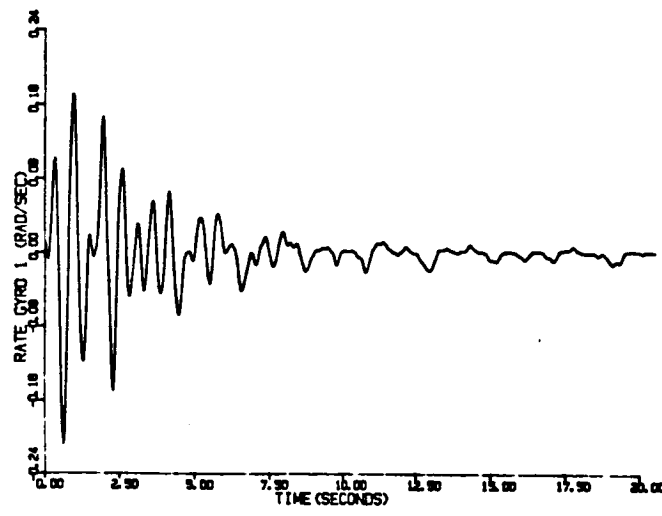
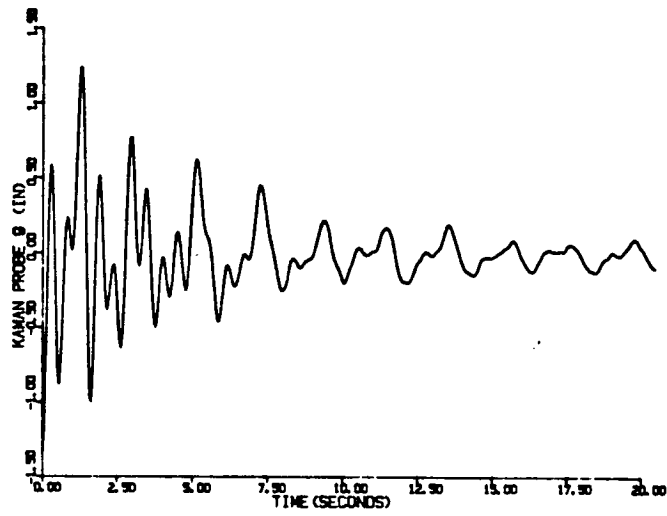
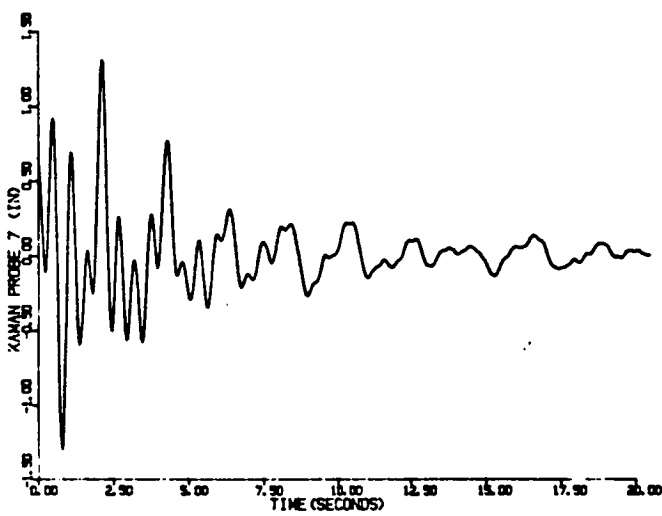
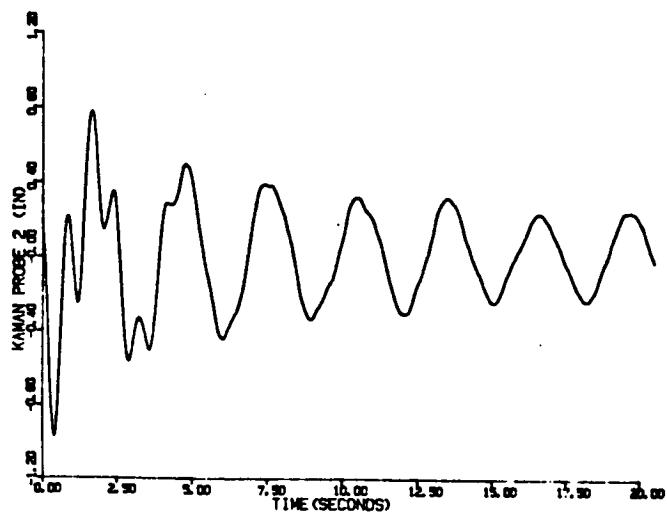
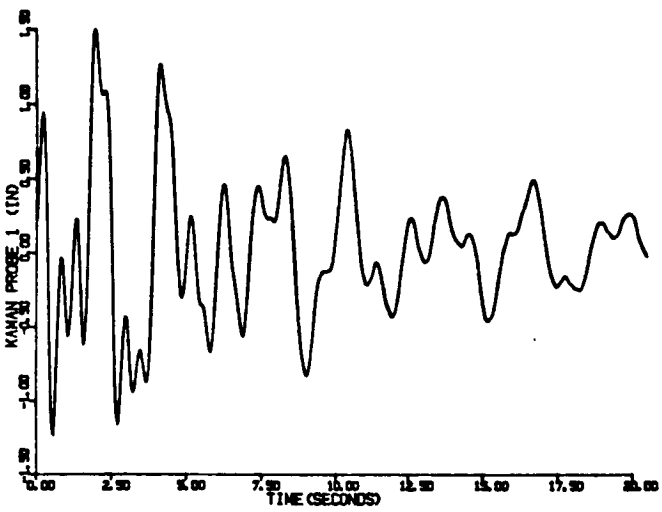
Again, full model (ten modes) is used with position output feedback.

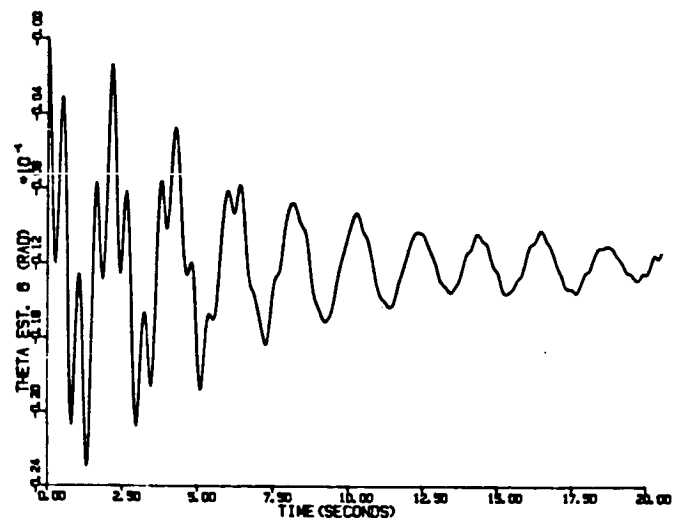
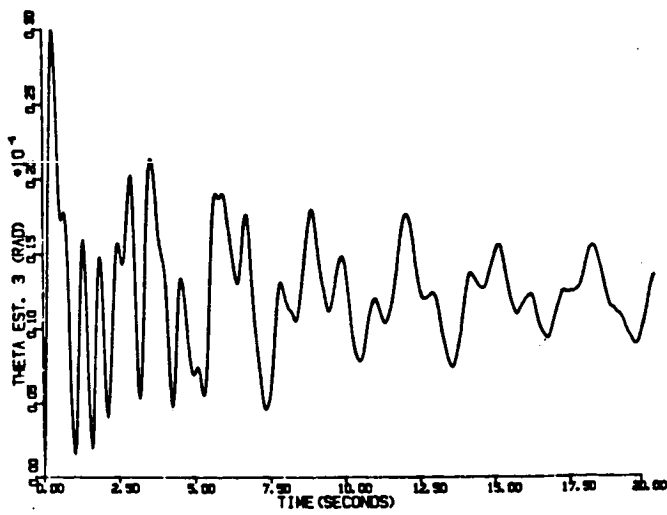
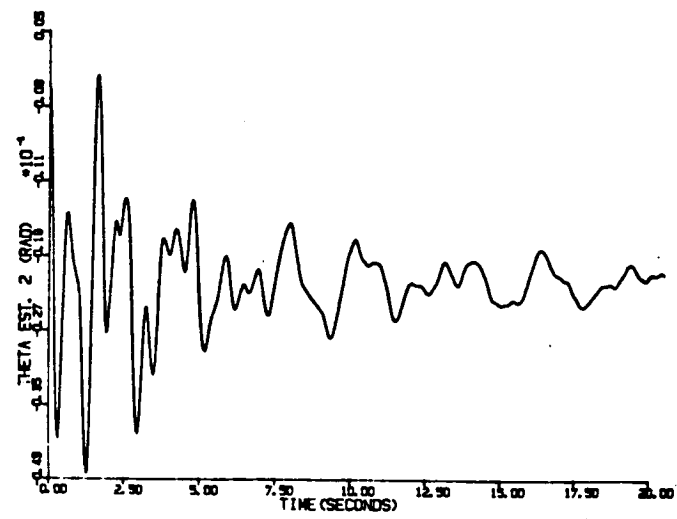
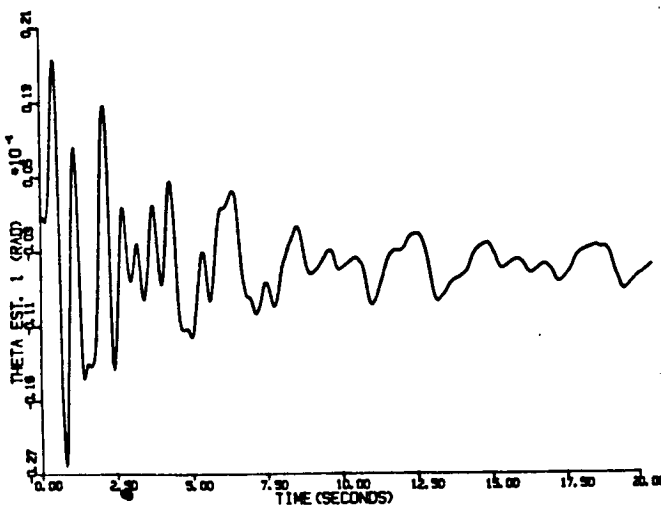
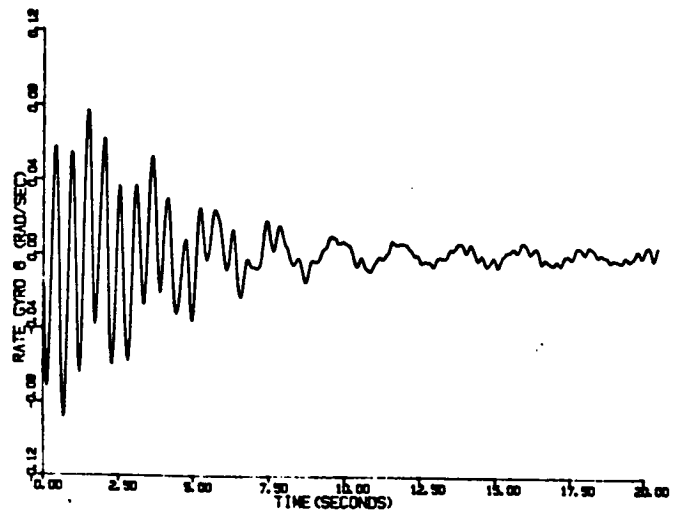
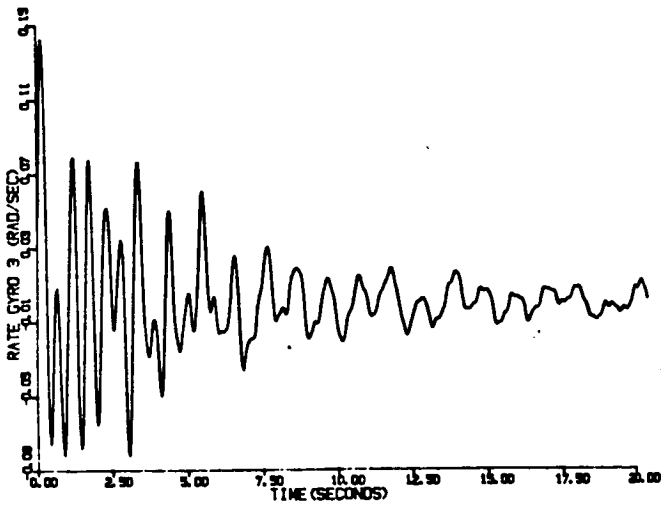
\*\*\* NOTE \*\*\*

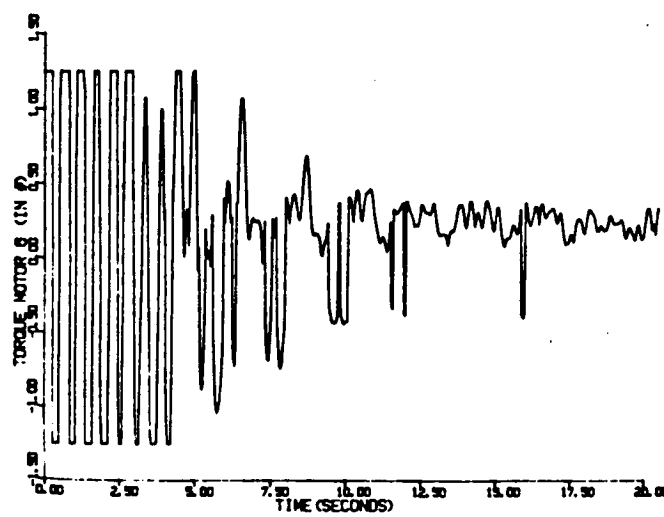
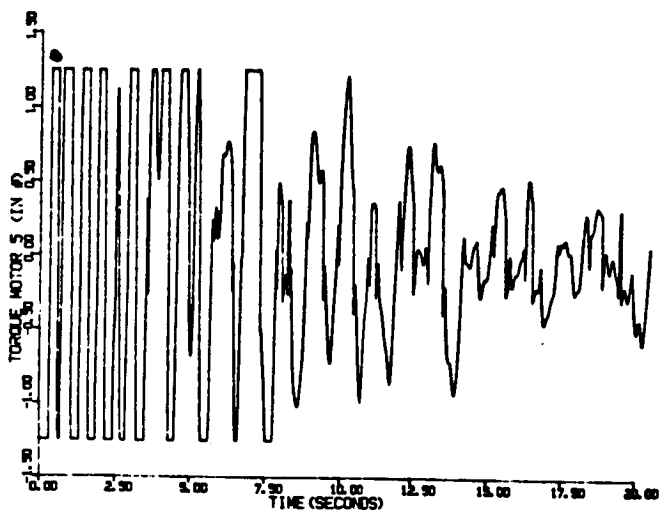
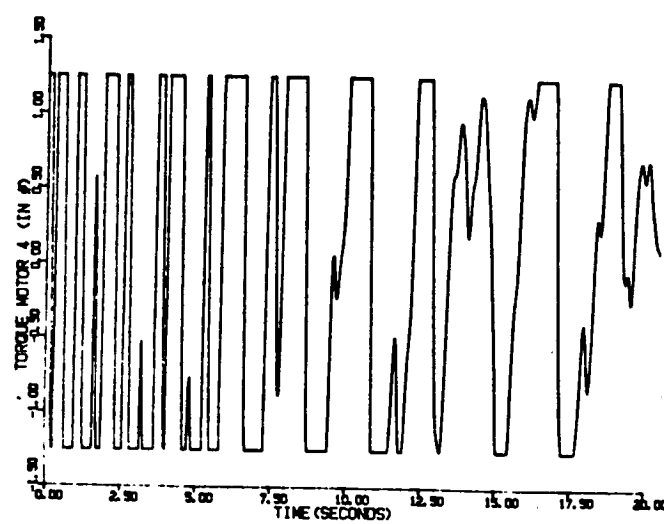
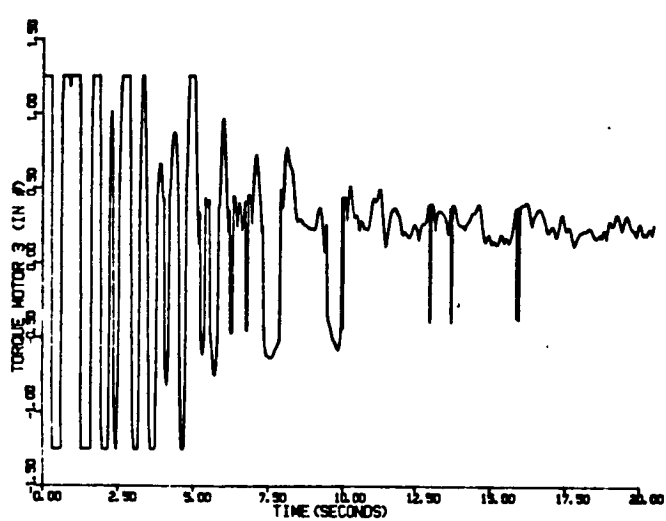
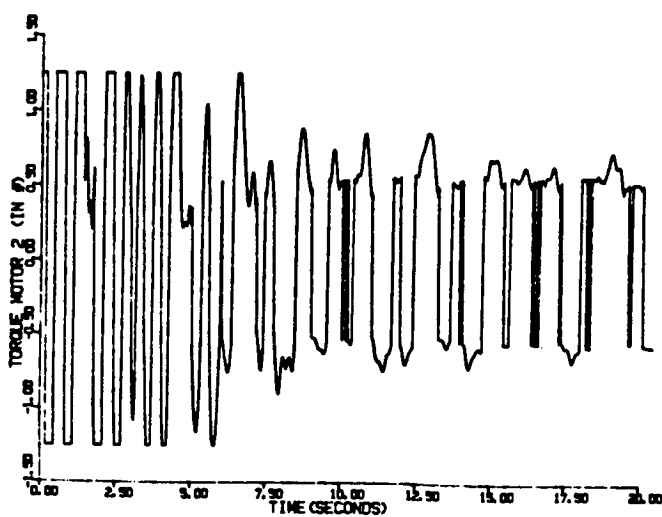
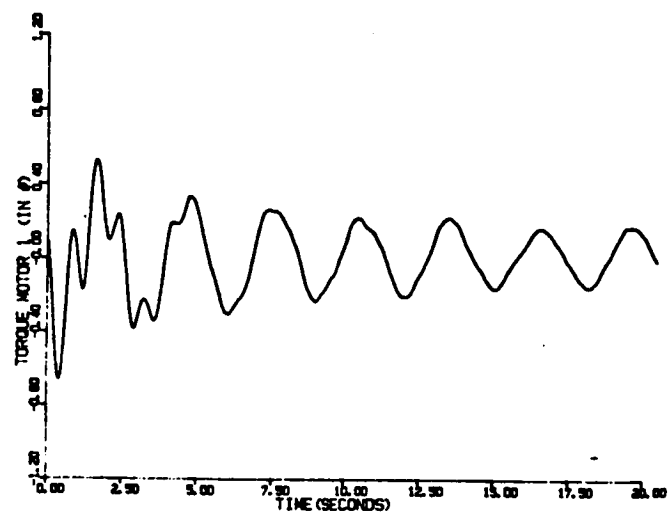
This test represents the sampled version of the algorithm; sampling period here is 32 ms.

Again, the applied torques are clipped (constrained) as

$$|\text{applied torques}| \leq 1.25 \text{ in-lb}$$







#### IV. REMAINING WORK AND SUGGESTIONS FOR FUTURE STUDIES

At the time of writing the present report a number of tests were completed on the ten-mode simulation model of the grid. In considering these results one can express confidence in the successful outcome of the application onto the real system. Both on-site and off-site (remote) experiments are to be performed during which the feedback control algorithms will be implemented on the Charles River Microcomputer system connected to the sensing and actuation on the grid. The gain values which gave satisfactory results on the simulation model are to be tried.

A number of follow up studies can be envisaged using the software and hardware that is now available, and particularly using the expertise obtained. These include both theoretical studies which are required to answer some natural questions that arose during the tenure of the present project, and practical studies to test out some other reasonable algorithms on the grid problem and the results of the above mentioned theoretical studies.

Specifically, further work is required to understand the implications of the multimodeling approach used in the present application. This model is especially suitable for local reduced order modeling. That is, one could try using only some of the modes to be controlled in one channel's model and some in the other, while some have to appear in both. The stabilizability implications and the spillover effects in using such an approach must be analyzed. An algorithm should be obtained for generating such different multiple models.

#### V. REFERENCES

1. R.C. Montgomery and N. Sundararajan, "Identification of the dynamics of a two-dimensional grid structure using least square lattice filters," 1984 American Control Conference, June 6-8, 1984.
2. N. Sundararajan, R.C. Montgomery, and J.P. Williams, "Adaptive identification and control of structural dynamics systems using recursive lattice filters," NASA Technical Paper 2371, 1985.
3. F. Al-Abbass and U. Ozguner, "Decentralized Model Reference Adaptive System Using A Variable Structure Control," 24th Decision and Control Conference, December 1984.

JUNE 1984

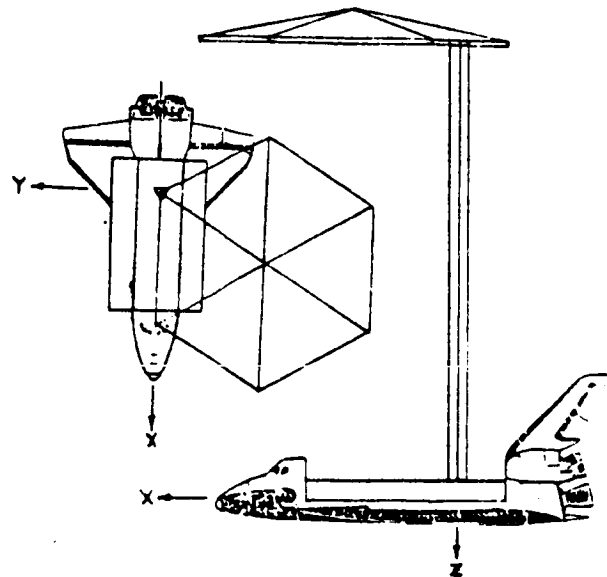
A MATHEMATICAL PROBLEM AND A SPACECRAFT CONTROL LABORATORY  
EXPERIMENT (SCOPE) USED TO EVALUATE CONTROL LAWS FOR  
FLEXIBLE SPACECRAFT... NASA/IEEE DESIGN CHALLENGE

by

Lawrence W. Taylor, Jr.  
Spacecraft Control Branch  
NASA Langley Research Center  
Hampton, VA 23665

and

A. V. Balakrishnan  
Chairman, IEEE Subcommittee on Large Space Structures, COLSS  
System Sciences Department  
University of California at Los Angeles  
Los Angeles, CA



NASA

IEEE

A MATHEMATICAL PROBLEM AND A SPACECRAFT CONTROL LABORATORY  
EXPERIMENT (SCOPE) USED TO EVALUATE CONTROL LAWS FOR  
FLEXIBLE SPACECRAFT... NASA/IEEE DESIGN CHALLENGE

by

Lawrence W. Taylor, Jr.  
Spacecraft Control Branch  
NASA Langley Research Center  
Hampton, VA 23665

and

A. V. Balakrishnan  
Chairman, IEEE Subcommittee on Large Space Structures, COLSS  
System Sciences Department  
University of California at Los Angeles  
Los Angeles, CA

SUMMARY

The problem of controlling large, flexible space systems has been the subject of considerable research. Many approaches to control system synthesis have been evaluated using computer simulation. In several cases, ground experiments have also been used to validate system performance under more realistic conditions. There remains a need, however, to test additional control laws for flexible spacecraft and to directly compare competing design techniques. In this paper an NASA program is discussed which has been initiated to make direct comparisons of control laws for, first, a mathematical problem, then an experimental test article is being assembled under the cognizance of the Spacecraft Control Branch at the NASA Langley Research Center with the advice and counsel of the IEEE Subcommittee on Large Space Structures. The physical apparatus will consist of a softly supported dynamic model of an antenna attached to the Shuttle by a flexible beam. The control objective will include the task of directing the line-of-sight of the Shuttle/antenna configuration toward a fixed

target, under conditions of noisy data, limited control authority and random disturbances. The open competition started in the early part of 1984. Interested researchers are provided information intended to facilitate the analysis and control synthesis tasks. A workshop is planned for early December at the NASA Langley Research Center to discuss and compare results.

#### INTRODUCTION

Many future spacecraft will be large and consequently quite flexible. As the size of antennae is increased, the frequencies of the first flexible modes will decrease and overlap the pointing system bandwidth. It will no longer be possible to use low gain systems with simple notch filters to provide the required control performance. Multiple sensors and actuators, and sophisticated control laws will be necessary to ensure stability, reliability and the pointing accuracy required for large, flexible spacecraft.

Control of such spacecraft has been studied with regard given to modeling, order reduction, fault management, stability and dynamic system performance. Numerous example applications have been used to demonstrate specific approaches to pertinent control problems. Both computer simulations and laboratory experiment results have been offered as evidence of the validity of the approaches to control large, flexible spacecraft. Concerns remain, however, because of the chronic difficulties in controlling these lightly damped large-scale systems. Because of these concerns and because of the desire to offer a means of comparing technical approaches directly, an NASA/IEEE Design Challenge is being offered. An

experimental test article is being assembled under the cognizance of the Spacecraft Control Branch at the NASA Langley Research Center with the advice and counsel of the IEEE (COLSS) Subcommittee on Large Space Structures. This Spacecraft Control Laboratory Experiment (SCOLE) will serve as the focus of a design challenge for the purpose of comparing directly different approaches to control synthesis, modeling, order reduction, state estimation and system identification.

The configuration of the SCOLE will represent a large antenna attached to the Space Shuttle orbiter by a flexible beam. This configuration was chosen because of its similarity to proposed space flight experiments and proposed space-based antenna systems. This paper will discuss the "Design Challenge" in terms of both a mathematical problem and a physical experimental apparatus. The SCOLE program is not part of any flight program.

#### SYMBOLS

a	acceleration vector ft/sec <sup>2</sup>
A	beam cross section area
c	observation matrix
d	noise contaminating direction cosine matrix measurements
e	line-of-sight error
E	modulus of elasticity
f	concentrated force expressions
F <sub>4</sub>	force vector
g	concentrated moment expressions
GI	torsional rigidity
I	moment of inertia matrix for entire Shuttle/antenna configuration

$I_1$	moment of inertia matrix, Shuttle body
$I_4$	moment of inertia matrix, reflector body
$I_\phi$	beam cross section moment of inertia, roll bending
$I_\theta$	beam cross section moment of inertia, pitch bending
$I_\psi$	beam polar moment of inertia, yaw torsion
$L$	length of the reflector mast, beam
$M_1$	control moment applied to the Shuttle body
$M_4$	control moment applied to the reflector body
$M_D$	disturbance moment applied to the Shuttle body
$m$	mass of entire Shuttle/antenna configuration
$m_1$	mass of Shuttle body
$m_4$	mass of reflector body
$\rho$	mass density of beam
$s$	beam position variable
$T_1$	direction cosine matrix, Shuttle body () <sub>earth</sub> = $T_1()$ <sub>Shuttle body</sub>
$T_4$	direction cosine matrix, reflector body () <sub>earth</sub> = $T_4()$ <sub>reflector body</sub>
$v_1$	inertial velocity, Shuttle body
$v_4$	inertial velocity, reflector body
$u_\phi$	lateral deflection of beam bending in y-z plane
$u_\theta$	lateral deflection of beam bending in x-z plane
$u_\psi$	angular deflection of beam twisting about z axis
X,Y,Z	position variables
$\Delta$	displacement of proof-mass actuator
$\delta$	line-of-sight pointing requirement
$\epsilon$	noise contaminating angular velocity measurements

$\theta, \phi, \psi$  pitch, roll, heading  
 $\zeta$  damping ratio  
 $\tau$  noise contaminating acceleration measurements  
 $\omega_1$  angular velocity of Shuttle body  
 $\omega_4$  angular velocity of reflector body

## DISCUSSION

The objective of the NASA-IEEE Design Challenge concerning the control of flexible spacecraft is to promote direct comparison of different approaches to control, state estimation and systems identification. The design challenge has principal parts, the first using a mathematical model, and the second using laboratory experimental apparatus. The specific parts of the Spacecraft Control Laboratory Experiment (SCOLE) program will be discussed in detail.

### Control Objectives

The primary control task is to rapidly slew or change the line-of-sight of an antenna attached to the space Shuttle orbiter, and to settle or damp the structural vibrations to the degree required for precise pointing of the antenna. The objective will be to minimize the time required to slew and settle, until the antenna line-of-sight remains within the angle  $\delta$ . A secondary control task is to change direction during the "on-target" phase to prepare for the next slew maneuver. The objective is to change attitude and stabilize as quickly as possible, while keeping the line-of-sight error less than  $\delta$ .

### Math Model Dynamics

The initial phase of the design challenge will use a mathematical model of the Shuttle orbiter/antenna configuration. It is necessary to obtain a balance, of course, between complex formulations which might be more accurate and simplified formulations which ease the burden of analysis.

The dynamics are described by a distributed parameter beam equation with rigid bodies, each having mass and inertia at either end. One body represents Space Shuttle orbiter; the other body is the antenna reflector. The equations for the structural dynamics and Shuttle motion are formed by adding to the rigid-body equations of motion, beam-bending and torsion equations. The boundary conditions at the ends of the beam contain the forces and moments of the rigid Shuttle and reflector bodies. The nonlinear kinematics couples the otherwise uncoupled beam equations. Additional terms represent the action of two, 2-axis proof-mass actuators at locations on the beam chosen by the designer.

The rigid-body equations of motion for the Shuttle body are given by:

$$\dot{\omega}_1 = - I_1^{-1} (\tilde{\omega}_1 I_1 \omega_1 + M_1 + M_D + M_{B,1})$$

$$\dot{v} = \frac{F_{B,1}}{m_1}$$

Similarly, for the reflector body,

$$\dot{\omega}_4 = -I_4^{-1}(\tilde{\omega}_4 I_4 \omega_4 + M_4 + M_{B,4})$$

$$\dot{v}_4 = \frac{F_4 + F_{B,4}}{m_4}$$

The direction cosine matrices defining the attitudes of the Shuttle and reflector bodies are given by:

$$\dot{T}_1^T = -\tilde{\omega}_1 T_1^T$$

$$\dot{T}_4^T = -\tilde{\omega}_4 T_4^T$$

The direction cosine matrices defining the attitudes of the Shuttle and the reflector bodies are related to the beam end conditions.

$$T_4 = \begin{bmatrix} 1 & 0 & 0 \\ 0 & \cos\Delta\phi & -\sin\Delta\phi \\ 0 & \sin\Delta\phi & \cos\Delta\phi \end{bmatrix} \begin{bmatrix} \cos\Delta\theta & 0 & \sin\Delta\theta \\ 0 & 1 & 0 \\ -\sin\Delta\theta & 0 & \cos\Delta\theta \end{bmatrix} \begin{bmatrix} \cos\Delta\Psi & -\sin\Delta\Psi & 0 \\ \sin\Delta\Psi & \cos\Delta\Psi & 0 \\ 0 & 0 & 1 \end{bmatrix} T_1$$

where:

$$\Delta\Psi = u_\Psi \Big|_{s=L} - u_\Psi \Big|_{s=0}$$

$$\Delta\theta = \frac{\partial u_\theta}{\partial s} \Big|_{s=L} - \frac{\partial u_\theta}{\partial s} \Big|_{s=0}$$

$$\Delta\phi = \frac{\partial u_\phi}{\partial s} \Big|_{s=L} - \frac{\partial u_\phi}{\partial s} \Big|_{s=0}$$

The equations of motion for the flexible beam-like truss connecting the reflector and Shuttle bodies consist of standard beam bending and torsion partial differential equations with energy dissipative terms which enable damped modes with constant characteristics for fixed, though dynamic, end conditions. The system of equations can be viewed as driven by changing end conditions and forces applied at the locations of the proof-mass actuators.

ROLL BEAM BENDING:

$$PA \frac{\partial^2 u_\phi}{\partial t^2} - 2\zeta_\phi \sqrt{PA EI_\phi} \frac{\partial^3 u_\phi}{\partial s^2 \partial t} + EI_\phi \frac{\partial^4 u_\phi}{\partial s^4} = \sum_{n=1}^4 [f_{\phi,n} \delta(s-s_n) + g_{\phi,n} \frac{\partial \delta}{\partial s} (s-s_n)]$$

PITCH BEAM BENDING:

$$PA \frac{\partial^2 u_\theta}{\partial t^2} - 2\zeta_\theta \sqrt{PA EI_\theta} \frac{\partial^3 u_\theta}{\partial s^2 \partial t} + EI_\theta \frac{\partial^4 u_\theta}{\partial s^4} = \sum_{n=1}^4 [f_{\theta,n} \delta(s-s_n) + g_{\theta,n} \frac{\partial \delta}{\partial s} (s-s_n)]$$

YAW BEAM TORSION:

$$PI_\Psi \frac{\partial^2 u_\Psi}{\partial t^2} + 2\zeta_\Psi I_\Psi \sqrt{GP} \frac{\partial^3 u_\Psi}{\partial s^2 \partial t} + GI_\Psi \frac{\partial^2 u_\Psi}{\partial s^2} = \sum_{n=1}^4 g_{\Psi,n} \delta(s - s_n)$$

where:

$$f_{\phi,1} = m_1 \left. \frac{\partial^2 u_\phi}{\partial t^2} \right|_{s=0} \quad \{ \text{SHUTTLE BODY FORCE} \}$$

$$f_{\phi,2} = m_2 \left. \frac{\partial^2 u_\phi}{\partial t^2} \right|_{s=s_2} + m_2 \left. \frac{\partial^2 \Delta_{\phi,2}}{\partial t^2} \right|_{s=s_2} \quad \{ \text{PROOF-MASS ACTUATOR FORCE} \}$$

$$f_{\phi,3} = m_3 \frac{\partial^2 u_\phi}{\partial t^2} \Bigg|_{s=s_3} + m_3 \frac{\partial^2 \Delta_{\phi,2}}{\partial t^2}$$

{PROOF-MASS ACTUATOR}

$$f_{\phi,4} = m_4 \frac{\partial^2 u_\phi}{\partial t^2} \Bigg|_{s=130} - I_{zz,4} \frac{\partial^2 u_\psi}{\partial t^2} / 32.5 + F_y$$

{REFLECTOR BODY FORCE}

$$f_{\theta,1} = m_1 \frac{\partial^2 u_\theta}{\partial t^2} \Bigg|_{s=s_1}$$

{SHUTTLE BODY FORCE}

$$f_{\theta,2} = m_2 \frac{\partial^2 u_\theta}{\partial t^2} \Bigg|_{s=s_2} + m_2 \frac{\partial^2 \Delta_{\theta,2}}{\partial t^2}$$

{PROOF-MASS ACTUATOR FORCE}

$$f_{\theta,3} = m_3 \frac{\partial^2 u_\theta}{\partial t^2} \Bigg|_{s=s_3} + m_3 \frac{\partial^2 \Delta_{\theta,2}}{\partial t^2}$$

{PROOF-MASS ACTUATOR FORCE}

$$f_{\theta,4} = m_4 \frac{\partial^2 u_\theta}{\partial t^2} \Bigg|_{s=130} - I_{zz,4} \frac{\partial^2 u_\psi}{\partial t^2} / 18.75 - F_x$$

{REFLECTOR BODY FORCE}

$$\begin{pmatrix} g_{\phi,1} \\ g_{\theta,1} \\ g_{\psi,1} \end{pmatrix} = I_1 \dot{\omega}_1 + \omega_1 I_1 \omega_1 + M_1 + M_D \quad \{ \text{SHUTTLE BODY, MOMENTS} \}$$

$$\begin{pmatrix} g_{\phi,2} \\ g_{\theta,2} \\ g_{\psi,2} \end{pmatrix} = 0 \quad \{ \text{PROOF-MASS ACTUATOR, MOMENT} \}$$

$$\begin{pmatrix} g_{\phi,3} \\ g_{\theta,3} \\ g_{\psi,3} \end{pmatrix} = 0 \quad \{ \text{PROOF-MASS ACTUATOR, MOMENT} \}$$

$$\begin{pmatrix} g_{\phi,4} \\ g_{\theta,4} \\ g_{\psi,4} \end{pmatrix} = I_4 \dot{\omega}_4 + \omega_4 I_4 \omega_4 + M_4 + \tilde{R}_B F_{B,4} \quad \{ \text{REFLECTOR BODY, MOMENT} \}$$

The angular velocity of the reflector body is related to the Shuttle body by:

$$\omega_4 = \left( \begin{array}{c} \frac{\partial^2 u_\phi}{\partial s \partial t} \Big|_{s=L} \\ \frac{\partial^2 u_\theta}{\partial s \partial t} \Big|_{s=L} \\ \frac{\partial u_\psi}{\partial t} \Big|_{s=L} \end{array} \right) - \left( \begin{array}{c} \frac{\partial^2 u_\phi}{\partial s \partial t} \Big|_{s=0} \\ \frac{\partial^2 u_\theta}{\partial s \partial t} \Big|_{s=0} \\ \frac{\partial u_\psi}{\partial t} \Big|_{s=0} \end{array} \right) + \omega_1 \quad \tilde{R}_B = \begin{pmatrix} 0 & 130 & 0 \\ -130 & 0 & 0 \\ 0 & 0 & 0 \end{pmatrix}$$

The line-of-sight error described in figure 2 is affected by both the pointing error of the Shuttle body and the misalignment of the reflector due to the deflection of the beam supporting the reflector. The line-of-sight is defined by a ray from the feed which is reflected at the center of the reflector. Its direction in the Shuttle body coordinates is given by:

$$R_{LOS} = \frac{-R_R + R_F + 2 \left[ R_A^T (R_R - R_F) \cdot R_A \right]}{\left\| R_R - R_F - 2 \left[ R_A^T R_R - R_F \right] \cdot R_A \right\|}$$

where:

$R_F$  is the feed location (3.75, 0, 0)

$R_R$  is the location of the center of the reflector (18.75, -32.5, -130)

$R_A$  is a unit vector in the direction of the reflector axis in Shuttle body coordinates

The vector  $R_A$  can be related to the direction cosine attitude matrices for the Shuttle body,  $T_1$ , and the reflector body,  $T_4$ , by

$$R_A = \begin{bmatrix} T_1^T \\ T_4^T \end{bmatrix} \begin{pmatrix} 0 \\ 0 \\ 1 \end{pmatrix}$$

The relative alignment of the reflector to the Shuttle body is given by  $T_1^T T_4$  which is a function of the structural deformations of the beam.

The line-of-sight error,  $e$ , is the angular difference between the target direction, given by the unit vector,  $D_T$ , and the line-of-sight direction in Earth axes,  $T_1 R_{LOS}$ .

$$e = \text{ARCSIN } |D_T \times T_1 R_{LOS}| \quad \text{or} \quad \text{ARCSIN } |\tilde{D}_T T_1 R_{LOS}|$$

Computer programs are available which generate time histories of the rigid body and the mode shapes and frequencies for the body-beam-body configuration for "pitch" bending, "roll" bending and "yaw" twisting. Since the modes are based on solving explicitly the distributed parameter equations (without damping and without kinematic coupling) there is no limit to the number of modal characteristic sets that can be generated by the program. It will be the analyst's decision as to how many modes need to be considered.

#### Laboratory Experiment Description

The second part of the design challenge is to validate in the laboratory, the system performance of the more promising control system designs of the first part. The experimental apparatus will consist of a dynamic model of the Space Shuttle orbiter with a large antenna reflector attached by means of a flexible beam. The dynamic model will be extensively instrumented and will have attached force and moment generating devices for control and for disturbance generation. A single, flexible tether will be used to suspend the dynamic model, allowing complete angular freedom in yaw, and limited freedom in pitch and roll. An inverted position will be used to let the reflector mast to hang so that gravity effects on mast bending will be minimized. The dynamics of the laboratory model will of necessity be different from the mathematical model discussed earlier.

### Design Challenge, Part One

For part one of the design challenge, the following mathematical problem is addressed. Given the dynamic equations of the Shuttle/antenna configuration, what control policy minimizes the time to slew to a target and to stabilize so that the line-of-sight (LOS) error is held, for a time, within a specified amount,  $\delta$ . During the time that the LOS error is within  $\delta$ , the attitude must change  $90^\circ$  to prepare for the next slew maneuver. This was previously referred to as the secondary control task. The maximum moment and force generating capability will be limited. Advantage may be taken of selecting the most suitable initial alignment of the Shuttle/antenna about its assigned initial RF axis, line-of-sight. Random, broad band-pass disturbances will be applied to the configuration. Two proof-mass, force actuators may be positioned anywhere along the beam. The design guidelines are summarized below:

1. The initial line-of-sight error is 20 degrees.

$$e(0) = 20 \text{ degrees}$$

2. The initial target direction is straight down.

$$D_T = \begin{pmatrix} 0 \\ 0 \\ 1 \end{pmatrix}$$

3. The initial alignment about the line-of-sight is free to be chosen by the designer. Advantage may be taken of the low value of moment of inertia in roll. The Shuttle/antenna is at rest initially.
4. The objective is to point the line-of-sight of the antenna and stabilize to within 0.02 degree of the target as quickly as possible.

$$\delta = 0.02 \text{ degree}$$

5. Control moments can be applied at 100 Hz sampling rate to both the Shuttle and reflector bodies of 10,000 ft-lb for each axis. The commanded moment for each axis is limited to 10,000 ft-lb. The actual control moment's response to the commanded value is first-order with a time constant of 0.1 second.

For the rolling moment applied to the Shuttle body:

$$-10^4 \leq M_{X,1,\text{command}} \leq 10^4$$

$$M_{X,1}(n+1) = e^{-0.1} M_{X,1}(n) + (1 - e^{-0.1}) M_{X,1,\text{command}}(n)$$

Equations for other axes and for the reflector body are similar.

6. Control forces can be applied at the center of the reflector in the X and Y directions only. The commanded force in a particular direction is limited to 800 lbs. The actual control force's response to the commanded value is first-order with a response time of 0.1 second.

For the side force applied to the reflector body:

$$-800 \leq F_{Y,\text{command}} \leq 800$$

$$F_Y(n+1) = e^{-0.1} F_Y(n) + (1 - e^{-0.1}) F_{Y,\text{command}}(n)$$

Equations for X-axis are similar.

7. Control forces using two proof-mass actuators (each having both X and Y axes) can be applied at two points on the beam. The strokes are limited to  $\pm 1$  ft, and the masses weight 10 lbs each. The actual stroke follows a first-order response to limited commanded values.

For the X-axis of the proof-mass actuator at  $s_2$ :

$$-1 \leq \Delta_{X,2,\text{command}} \leq 1$$

$$\Delta_{X,2}(n+1) = e^{-0.1} \Delta_{X,2}(n) + (1 - e^{-0.1}) \Delta_{X,2,\text{command}}(n)$$

Equations for other axes and locations are similar.

8. The inertial attitude direction cosine matrix for the Shuttle body lags in time the actual values by 0.01 second and are made at a rate of 100 samples per second. Each element of the direction cosine measurement matrix is contaminated by additive, uncorrelated Gaussian noise having an rms value of 0.001. The noise has zero mean.

$$T_{s,\text{measured}}(n+1) = T_{s,\text{true}}(n) + \begin{bmatrix} d_{11}(n) & d_{12}(n) & d_{13}(n) \\ d_{21}(n) & d_{22}(n) & d_{23}(n) \\ d_{31}(n) & d_{32}(n) & d_{33}(n) \end{bmatrix}$$

where:

$$E\{d_{ij}(n)\} = 0$$

$$E\{d_{ij}(n)d_{kL}(n)\} = 0 \quad \text{for } i \neq k \text{ or } j \neq L$$

$$E\{d_{ij}(n)d_{ij}(n+k)\} = 0 \quad \text{for } k \neq 0$$

$$= [0.001]^2 \quad \text{for } k = 0$$

9. The angular velocity measurements for both the Shuttle and reflector bodies pass through a first-order filter with 0.05 sec time constant and lag in time the actual values by 0.01 second and are made at a rate of 100 samples per second. Each rate measurement is contaminated by additive, Gaussian, uncorrelated noise having an rms value of 0.02 degree per second. The noise has zero mean.

For example:

$$\omega_{1,X,\text{measured}}^{(n+1)} = \omega_{1,X,\text{filtered}}^{(n)} + \epsilon_{1,X}^{(n)}$$

$$E\{\epsilon_{1,X}^{(n)} \epsilon_{1,X}^{(n+k)}\} = 0 \quad \text{for } k \neq 0$$

$$= (.02)^2 \quad \text{for } k = 0$$

where

$$\dot{\omega}_{1,X,\text{filtered}} = -20 \omega_{1,X,\text{filtered}} + 20 \omega_{1,X,\text{true}}$$

10. Three-axis accelerometers are located on the Shuttle body at the base of the mast and on the reflector body at its center. Two-axes (X and Y) accelerometers are located at intervals of 10 feet along the mast. The acceleration measurements pass through a first-order filter with a 0.05 second time constant and lag in time the actual values by 0.01 second, and are made at a rate of 100 samples per second. Each measurement is contaminated by Gaussian additive, uncorrelated noise having an rms value of 0.05 ft/sec<sup>2</sup>.

For example:

$$a_{1,X,\text{measured}}(n+1) = a_{1,X,\text{filtered}}(n) + \tau_{1,X}(n)$$

$$E\{\tau_{1,X}(n) \tau_{1,X}(n+k)\} = 0 \quad \text{for } k \neq 0$$

$$= (.05)^2 \quad \text{for } k = 0$$

where:

$$\dot{a}_{1,X,\text{filtered}} = -20 a_{1,X,\text{filtered}} + 20 w_{1,X,\text{true}}$$

11. Gaussian, uncorrelated step-like disturbances are applied 100 times per second to the Shuttle body in the form of 3-axes moments, having rms values of 100 ft-lbs. These disturbances have zero mean.

For example:

$$E\{M_{D,X}(n) M_{D,X}(n+k)\} = 0 \quad \text{for } k \neq 0$$

$$= (100)^2 \quad \text{for } k = 0$$

In summary, the designer's task for part one is to: (1) derive a control law for slewing and stabilization, coded in FORTRAN; (2) select an initial attitude in preparation for slewing 20 degrees; and (3) select two positions for the 2-axes proof-mass actuators. An official system performance assessment computer program will be used to establish the time required to slew and stabilize the Shuttle/antenna configuration.

### Design Challenge, Part Two

As in part one, the task is to minimize the time to slew and stabilize a Shuttle/antenna configuration. The difference is that in part two of the design challenge, a physical laboratory model will be used instead of the dynamic equations of part one. The constraints on total moment and force generation capability will apply to part two, as for part one. Again, the analyst may select the initial alignment about the assigned initial RF line-of-sight. Disturbances will be injected into the Shuttle/antenna model. The designer's task will be similar to that for part one.

### CONCLUDING REMARKS

A Design Challenge, in two parts, has been offered for the purpose of comparing directly different approach to controlling a flexible Shuttle/antenna configuration. The first part of the design challenge uses only mathematical equations of the vehicle dynamics; the second part uses a physical laboratory model of the same configuration. The Spacecraft Control Laboratory Experiment (SCOLE) program is being conducted under the cognizance of the Spacecraft Control Branch at the NASA Langley Research Center. The NASA/IEEE Design Challenge has the advice and counsel of the IEEE-COLSS Subcommittee on Large Space Structures. Workshops will be held to enable investigators to compare results of their research.

## MASS CHARACTERISTICS

	CG LOCATION, FT X Y Z	WEIGHT, LB	$I_{XX}$ SLG-FT <sup>2</sup>	$I_{YY}$ SLG-FT <sup>2</sup>	$I_{ZZ}$ SLG-FT <sup>2</sup>	$I_{XY}$ SLG-FT <sup>2</sup>	$I_{XZ}$ SLG-FT <sup>2</sup>	$I_{YZ}$ SLG-FT <sup>2</sup>
SHUTTLE	0 0 0	205,000	905,443	6,789,100	7,086,601	0	145,393	0
MAST, CG	0 0 -65.	400	17,495	17,495	0	0	0	0
REFLECTOR, CG	18.75 -32.5 -130.	400	4,969	4,969	9,938	0	0	0
REFLECTOR, ATTACHMENT POINT			18,000	9,336	27,407	-7,570	0	0
TOTAL	.036 -.063 -.379	205,800	1,132,508	7,007,447	7,113,962	-7,555	115,202	52,293

The moment of inertia becomes:

$$I = \begin{bmatrix} I_{xx} & -I_{xy} & -I_{xz} \\ -I_{xy} & I_{yy} & -I_{yz} \\ -I_{xz} & -I_{yz} & I_{zz} \end{bmatrix} = \begin{bmatrix} 1,132,508 & 7,555 & -115,202 \\ 7,555 & 7,007,447 & -52,293 \\ -115,202 & -52,293 & 7,113,962 \end{bmatrix}$$

$$I_1 = \begin{bmatrix} 905,443 & 0 & -145,393 \\ 0 & 6,789,100 & 0 \\ -145,393 & 0 & 7,086,601 \end{bmatrix}$$

$$I_4 = \begin{bmatrix} 4,969 & 0 & 0 \\ 0 & 4,969 & 0 \\ 0 & 0 & 9,938 \end{bmatrix}$$

$$m = 6391.30 \text{ slugs}$$

$$m_1 = 6366.46 \text{ slugs}$$

$$m_2 = 0.3108 \text{ slugs}$$

$$m_3 = 0.3108 \text{ slugs}$$

$$m_4 = 12.42 \text{ slugs}$$

$$PA = 0.09556 \text{ slugs/ft}$$

$$EI_\phi = 4.0 \times 10^7 \text{ lb-ft}^2$$

$$\zeta_\phi = .003$$

$$PA = 0.09556 \text{ slugs/ft}$$

$$EI_\theta = 4.0 \times 10^7 \text{ lb-ft}^2$$

$$\zeta_\theta = .003$$

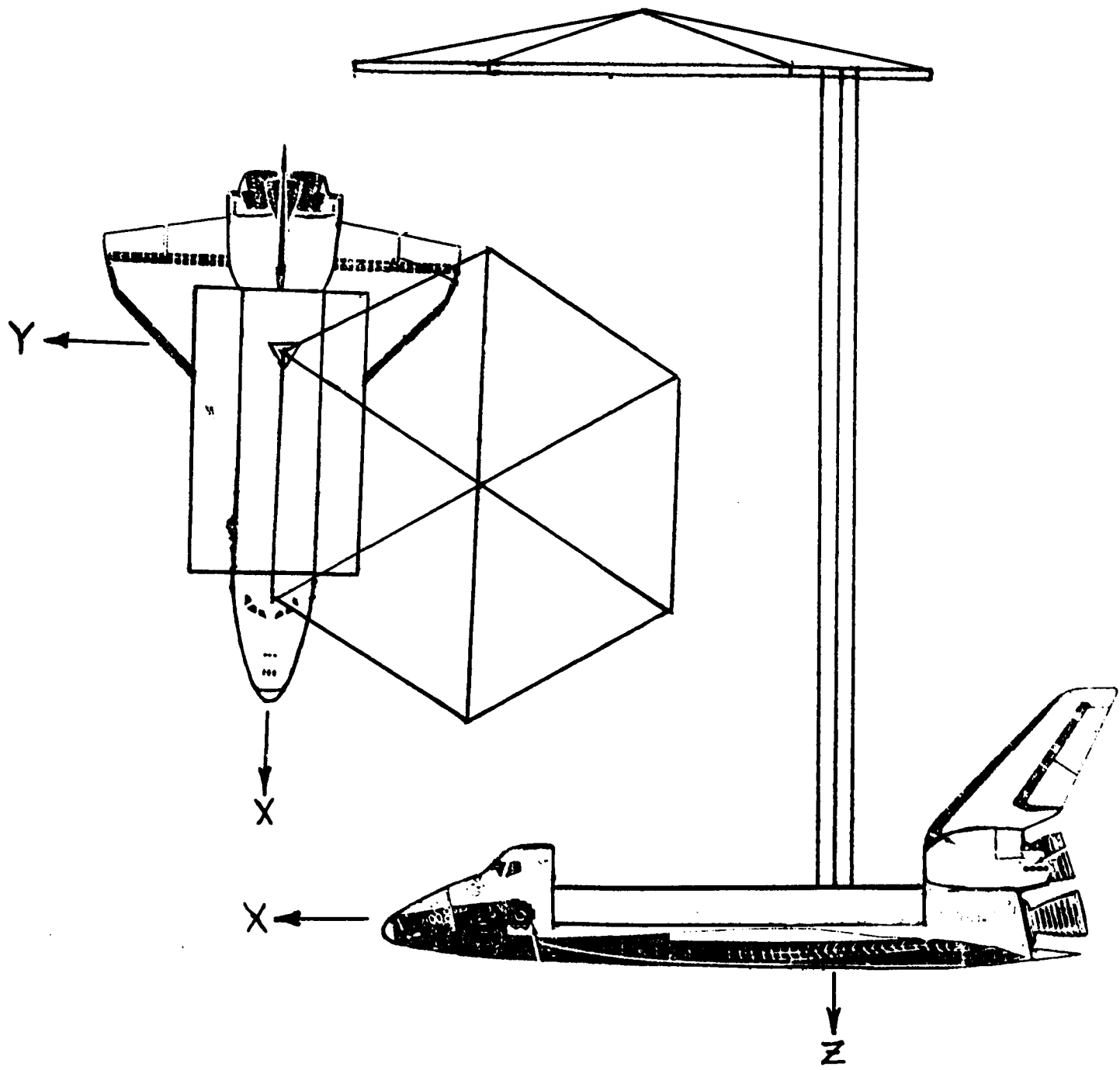
$$PI_\psi = 0.9089 \text{ slug-ft}$$

$$GI_\psi = 4.0 \times 10^7 \text{ lb-ft}^2$$

$$\zeta_\psi = .003$$

Figure 1. Drawing of the Shuttle/Antenna Configuration.

# SPACECRAFT CONTROL LAB EXPERIMENT (SCOLE)



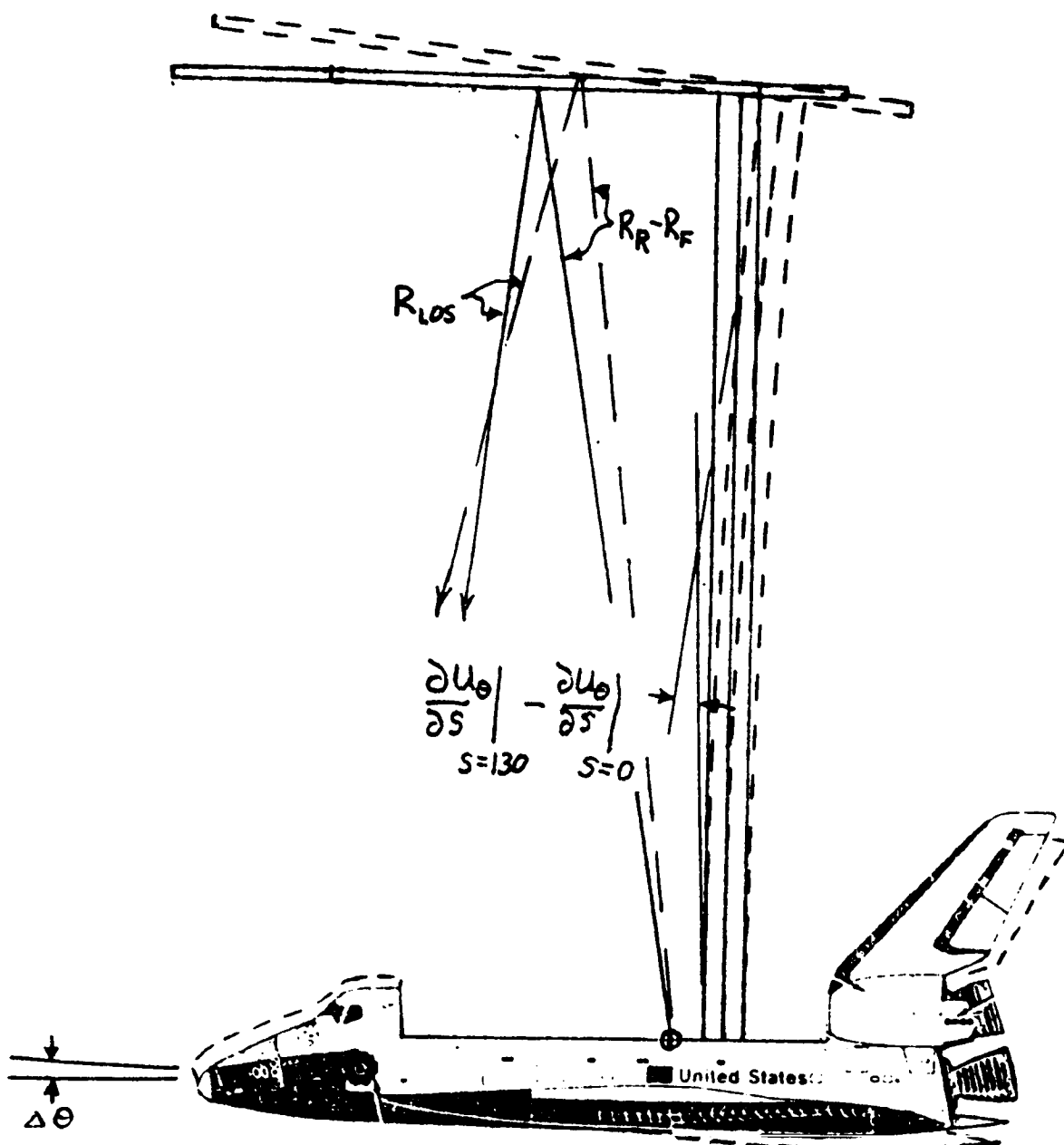


Figure 2.- Schematic of the effect of bending on the line-of-sight pointing error.

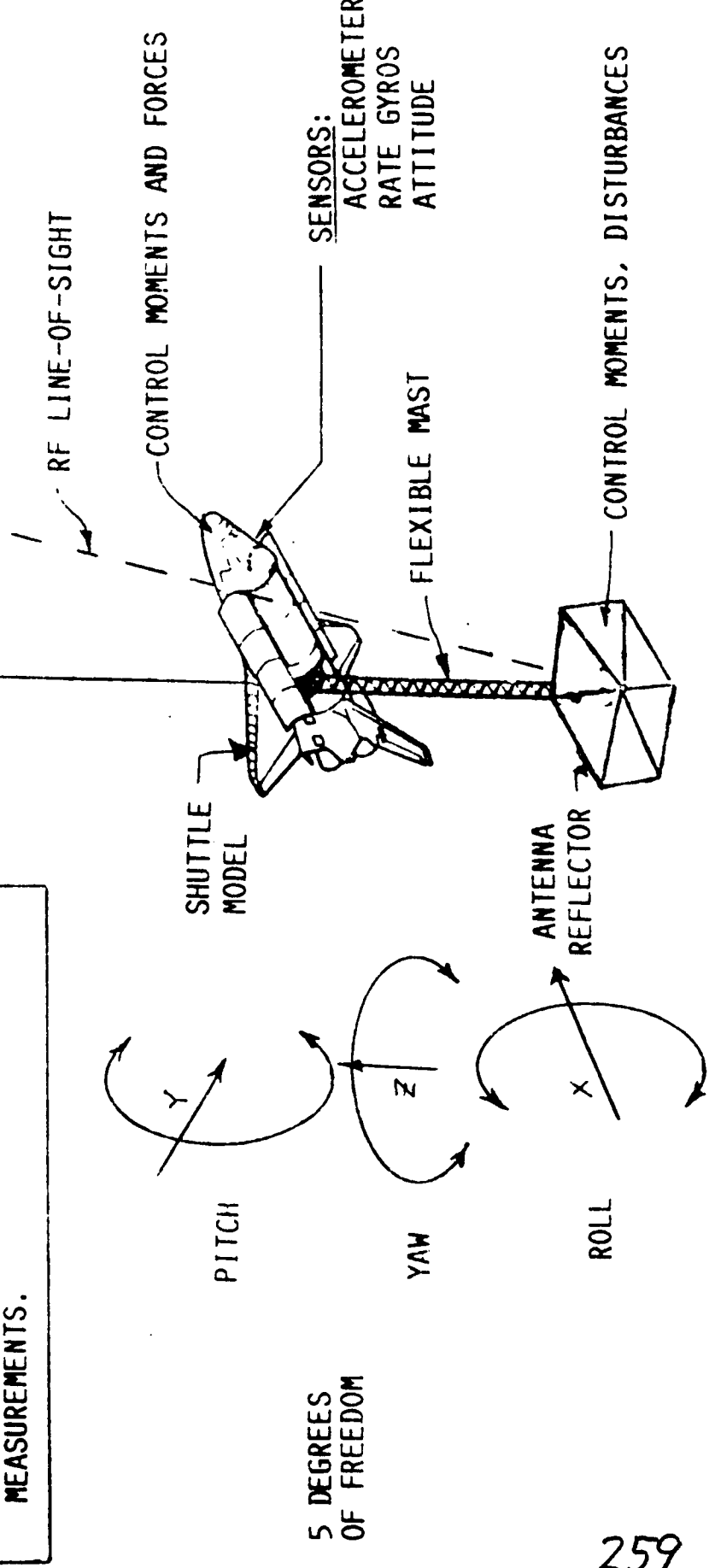
Figure 3. SPACECRAFT CONTROL LABORATORY\* EXPERIMENT (SCOLE)

CONTROL OBJECTIVE:  
TO SLEW, POINT, AND STABILIZE THE RF  
LINE-OF-SIGHT OF A FLEXIBLE, SHUTTLE  
ATTACHED ANTENNA, IN MINIMUM TIME.

SYSTEMS IDENTIFICATION:  
TO CREATE CONTROL INPUTS, THEN MODEL  
THE DYNAMIC SYSTEM FROM RESPONSE  
MEASUREMENTS.

\*SPACECRAFT CONTROL LABORATORY  
OF THE FLIGHT DYNAMICS AND  
CONTROL DIVISION  
BUILDING 1232

45°  
TARGET



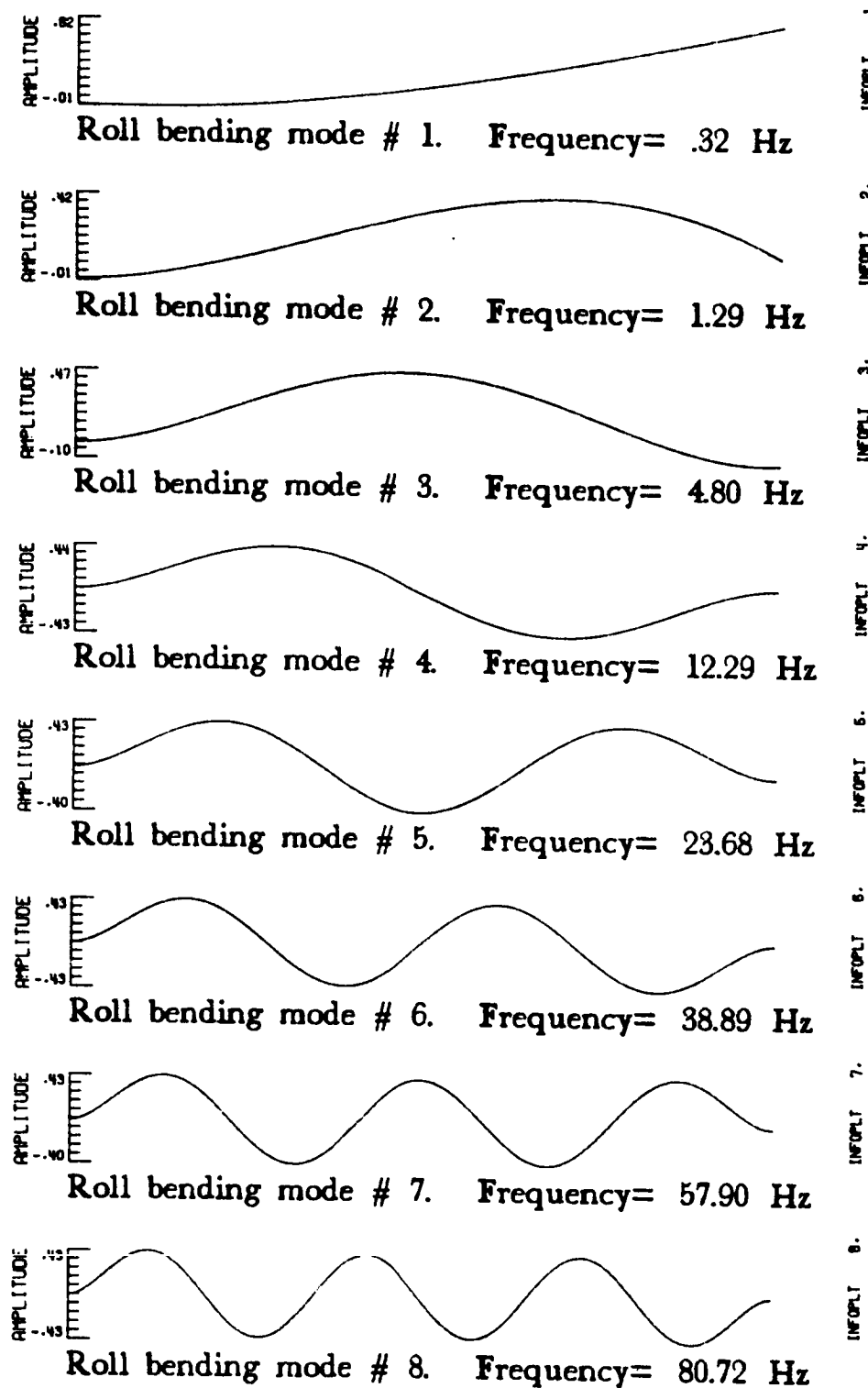


Figure 4a.- Plots of normalized roll bending mode shapes  
for SCOLE configuration.

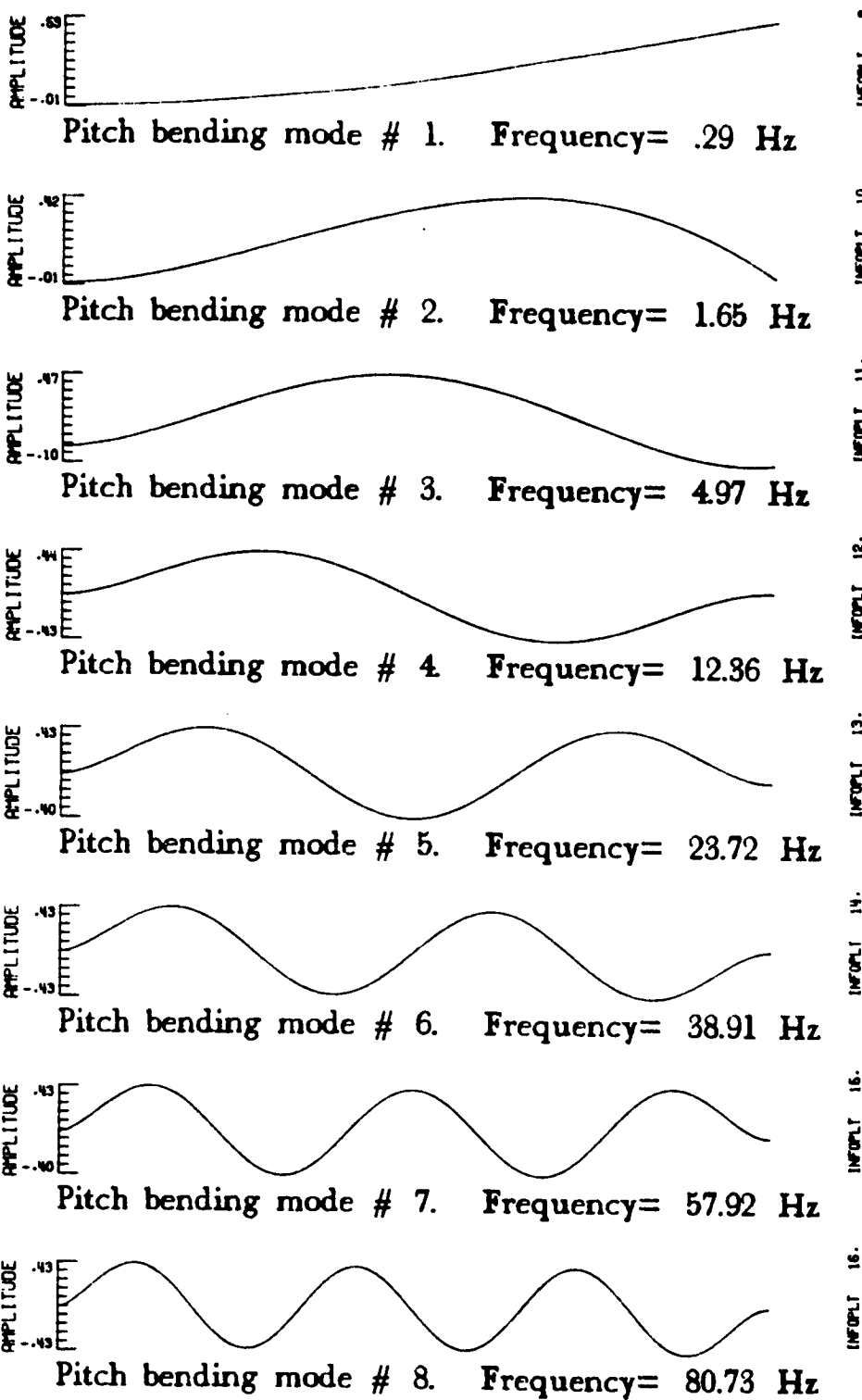


Figure 4b.- Plots of normalized pitch bending mode shapes for SCOLE configuration.

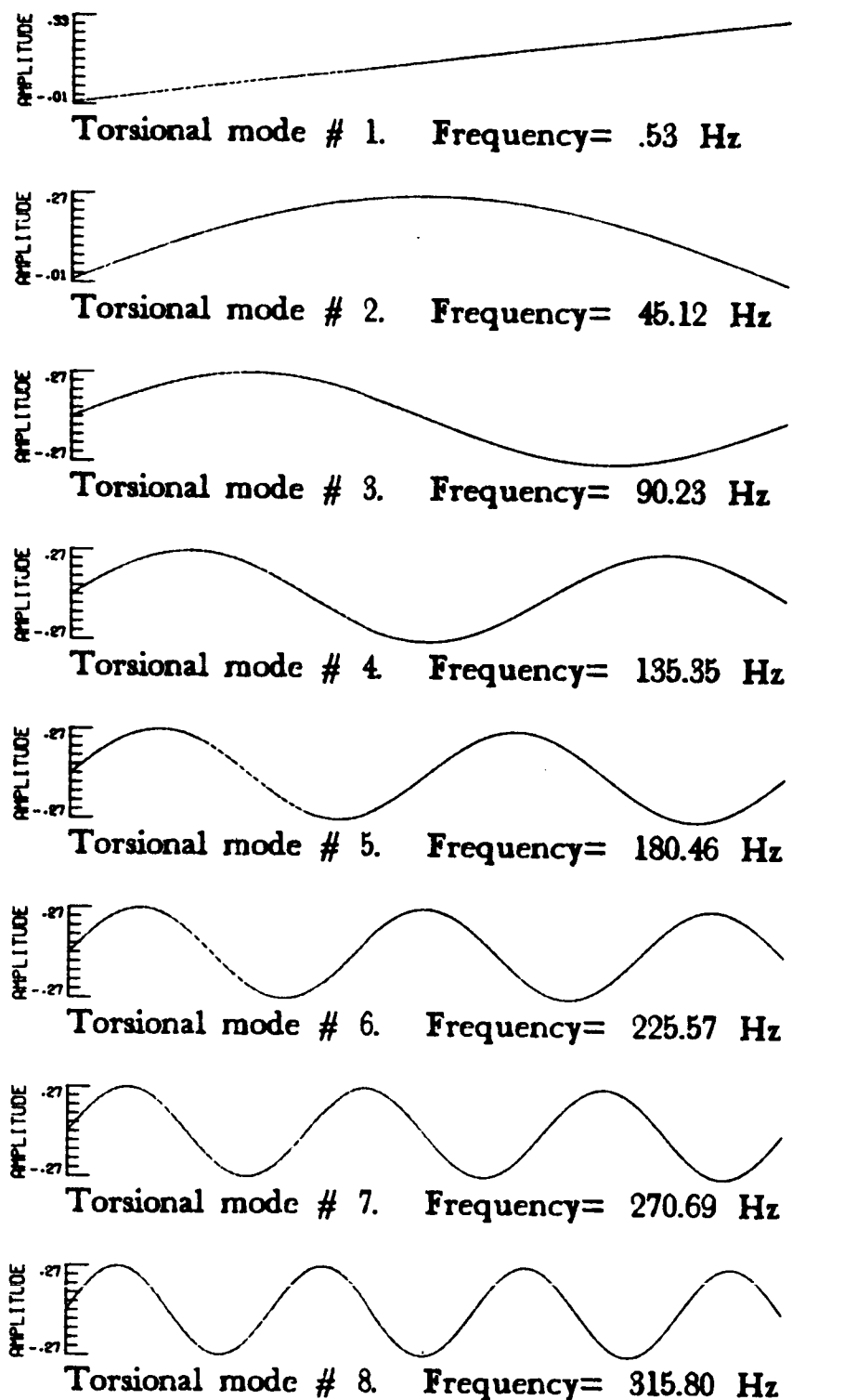


Figure 4c.- Plots of normalized torsional mode shapes for SCOLE configuration.

**LIST OF ATTENDEES**

<u>NAME</u>	<u>ORGANIZATION</u>	<u>ADDRESS</u>	<u>PHONE</u>
Claude R. Keckler	NASA-LaRC	MS 161 Hampton, VA 23665	(804) 865-4591
George Clawson	Honeywell	7900 Westpark Dr. McLean VA 22102	(703) 448-2069
John Breakwell	Lockheed	3251 Havover St. Palo Alto, CA 94304	(415) 424-2736
Al Schy	NASA-LaRC	MS 489 Hampton, VA 23665	(804) 865-2121
Anthony Fontana	NASA-LaRC	MS 161 Hampton, VA 23665	(804) 865-4591
Shalom Fisher	NRL	Code 7735 NRL Wash, DC 20375	(202) 767-3914
Steve Young	Honeywell	2600 Ridgway Pkwy Minneapolis, MN 55440	(612) 378-4126
K. W. Lips	Honeywell	MS 736-S Clearwater, FL	(813) 539-3924
Dave Morris	Honeywell	13350 U. S. Highway 19S Clearwater, FL 33546	(813) 539-4377
Mike Barrett	Honeywell	2600 Ridgway Pkwy Minneapolis, MN 55436	(612) 782-7286
Dave Olkowski	AFRPL/DYS	Edwards AFB Los Angeles, CA 93523	(805) 277-5483
Dan Minnick	RPI	36 Brinsmade Terrace Troy, NY 12180	(518) 271-5655
Brantley Hanks	NASA-LaRC	MS 230 Hampton, VA 23665	(804) 865-3054
Sahjendra Singh	NASA-LaRC	MS 161 Hampton, VA 23665	(804) 865-4591
Jer-nan Juang	NASA-LaRC	MS 230 Hampton, VA 23665	(804) 865-2881
R. C. Montgomery	NASA-LaRC	MS 161 Hampton, VA 23665	(804) 865-4591
N. Sundarajan	NASA-LaRC	MS 161 Hampton, VA 23665	(804) 865-4591
S. M. Joshi	NASA-LaRC	MS 161 Hampton, VA 23665	(804) 865-4591

<u>NAME</u>	<u>ORGANIZATION</u>	<u>ADDRESS</u>	<u>PHONE</u>
J. G. Lin	CRC	6 Churchill Lane Lexington, MA 02173	(617) 863-0889
J. L. Williams	NASA-LaRC	MS 161 Hampton, VA 23665	(804) 865-4591
Steve Yurkovich	OSU	2015 Neil Ave. Columbus, OH 43214	(614) 422-2586
E. S. Armstrong	NASA-LaRC	MS 161 Hampton, VA 23665	(804) 865-4591
Jeff Williams	NASA-LaRC	MS 161 Hampton, VA 23665	(804) 865-4591
Pamela Wolcott	NASA-LaRC	MS 161 Hampton, VA 23665	(804) 865-4591
Eiken Elkins	WPAFB	FIGC	(513) 255-3734
Atit K. Choudiwy	Howard U.	Washington, DC	(202) 636-6593
A. S. S. R. Reddy	Howard U.	Washington, DC	(202) 636-6593
Passeron Lionel R.	Aerospatiale	Cannes France	93 93 93 45
Anthony F. Hotz	Purdue U.	W. Lafayette, IN	(317) 494-5140
A. Balakrishnan	UCLA	Los Angeles, CA	(213) 825-2180
Yogendra P. Kakad	UNCC	Charlotte, NC	(704) 597-2302
Peter M. Bainum	Howard U.	Washington, DC	(202) 636-6612
L. Meirovitch	VPI&SU	Blacksburg, VA	(703) 961-5146
L. W. Taylor	NASA LaRC	MS 161 Hampton, VA 23665	(804) 865-4591

**Standard Bibliographic Page**

1. Report No. NASA TM-89048	2. Government Accession No.	3. Recipient's Catalog No.	
4. Title and Subtitle <b>Proceedings of the 2nd Annual SCOLE Workshop</b>		5. Report Date October 1986	
7. Author(s) <b>Lawrence W. Taylor, Jr. (Compiler)</b>		6. Performing Organization Code <b>506-46-11-01</b>	
9. Performing Organization Name and Address <b>NASA Langley Research Center Hampton, VA 23665</b>		8. Performing Organization Report No.	
12. Sponsoring Agency Name and Address <b>National Aeronautics and Space Administration Washington, DC 20546</b>		10. Work Unit No.	
		11. Contract or Grant No.	
15. Supplementary Notes		13. Type of Report and Period Covered <b>Technical Memorandum</b>	
		14. Sponsoring Agency Code	
16. Abstract  <b>Proceedings of the Second Annual Spacecraft Control Laboratory Experiment (SCOLE) Workshop held at the NASA Langley Research Center, Hampton, VA December 9-10, 1985.</b>			
17. Key Words (Suggested by Authors(s)) <b>Large Flexible Spacecraft Control Structural Dynamics</b>		18. Distribution Statement  <b>Unclassified-Unlimited Subject Category-18</b>	
19. Security Classif.(of this report) <b>Unclassified</b>	20. Security Classif.(of this page) <b>Unclassified</b>	21. No. of Pages 268	22. Price A12